Adhesion Study of Thermoplastic Polyimides with Ti-6Al-4V alloy and PEEK-graphite composites

by

Tae-Ho Yoon

Dissertation submitted to the Faculty of the

Virginia Polytechnic Institute and State University

in partial fulfillment of the requirements for the degree of

Doctor of Philosophy

in

Materials Engineering Science

APPROVED:

J. E. McGrath, Chairman

T. C. Ward

J. P. Wightman

N. S. Eiss

J. S. Riffle

June, 1991

Blacksburg, Virginia

Adhesion Study of Thermoplastic Polyimides with Ti-6Al-4V alloy and PEEK-graphite composites

by

Tae-Ho Yoon

J. E. McGrath, Chairman

Materials Engineering Science

(ABSTRACT)

High glass transition (eg. 360 °C) melt processsable thermoplastic polyimide homopolymers and poly(imide-siloxane) segmented copolymers were prepared from a number of diamines and dianhydrides via solution imidization, polydimethylsiloxane segment incorporation and molecular weight control with non-reactive phthalimide end-groups. The adhesive bond performance of these polyimides was investigated as a function of molecular weight, siloxane incorporation, residual solvent, test temperature, and polyimide structure via single lap shear samples prepared from treated Ti-6Al-4V alloy adherends and compression molded film adhesives or scrim cloth adhesives. The adhesive bond strengths increased greatly with siloxane segment incorporation at 10, 20 and 30 weight percent, and decreased slightly with total polymer molecular weight. As the test temperature was increased, adhesive bond strength increased, decreased or showed a maximum at some temperatures depending on the polyimide structure and siloxane content. The presence of residual solvent increased adhesive bond strength at ambient temperature but decreased the strength at the elevated temperatures. The variation of adhesive bond strength with residual solvent, siloxane and test temperature was attributed to the influence of these parameters on the brittle-ductile transition behavior of the polyimide system. This conclusion was supported by stress-strain measurements which indicated that tensile strength and modulus decreased with siloxane concentration and test temperature, demonstrating that there was an optimum combination of strength and strain for maximum adhesive bond strength. A model was developed to describe this behavior. The poly(imide-30%siloxane) segmented copolymer and a miscible poly(ether-imide) also demonstrated excellent adhesive bond strength with poly(arylene ether

ketone) *PEEK*®-graphite composites. Oxygen or ammonia gas plasma treatment was very effective in further improving adhesive bond strength of melt laminated *PEEK*®-graphite composites.

To

my Grandmother

Chung Ha Choi-Yoon

for

her unending love and support

Acknowledgements

The author would like to express his gratitude to Dr. J. E. McGrath for his support and supervision throughout this research effort, and for the opportunity to attend meetings to gain new knowledge. In particular, support from the Virginia Institute for Materials System (VIMS) and Center for Adhesive and Sealant Science (CASS) is greatfully acknowledged.

The author would also like to extend his thanks to Dr. T. C. Ward, Dr. J. P. Wightman, Dr. N. S. Eiss and Dr. J. S. Riffle for helpful suggestions and for serving on his committee. The author wishes to acknowledge Dr. C. A. Arnold, Dr. E. S. Moyer, Dr. D. Waldbauer Dr. A. Gungor and Ms. B. E. McGrath for precious polymer samples. The author would like express thanks to F. Cromer for XPS and SEM data.

The author would like to express sincere thanks to his wife, Regina for her love and encouragement. He also wish to thank his grandmother, Chung Ha Choi-Yoon, parents, Mr. & Mrs. Yoon, uncle and aunt, Mr. & Mrs. Lee, and in-laws, Dr. & Mrs. Kim.

Table of Contents

Chapter I. Introduction 1

Chapter II. Literature Review 5

2-1 Adhesion and adhesive bonding 5

2-1-1 Mechanisms of adhesion 8

2-1-1-1 Mechanical interlocking 8

2-1-1-2 Diffusion theory 9

2-1-1-3 Electronic theory 9

2-1-1-4 Adsorption theory 10

2-1-1-5 Weak boundary Layer 12

2-1-2 Thermodynamics of adhesion 12

2-1-3 Design of adhesive bonds 15

2-1-4 Testing of adhesive bonds 19

2-1-4-1 Lap shear tests 24

2-1-4-2 Peel and cleavage tests 27

2-1-4-3 Durability tests 29

2-1-4-4 Non-destructive testing 29

2-1-5 Fracture mechanics of adhesive bonds 31
2-1-5-1 Tension mode 32
2-1-5-2 Shear mode 34
2-1-5-3 Cleavage mode 36
2-1-6 Energy dissipation and viscoelasticity 37
2-2 High temperature structural adhesives 38
2-2-1 Historical background 38
2-2-2 Classifications 41
2-2-3 Epoxy-based Adhesives 42
2-2-4 Polyimides 44
2-2-5 Polybenzimidazole 45
2-3 Factors governing polyimide adhesion 47
2-3-1 Molecular weight control 48
2-3-2 Scrim cloth adhesives; influence of drying conditions 48
2-3-3 Bonding conditions 50
2-3-4 High temperature aging 53
2-3-5 Scrim cloth characteristics 54
2-4 Composite materials 55
2-4-1 Fibers 57
2-4-2 Matrix resins 57
2-4-3 Fabrication 60
2-4-4 Surface treatment of composite materials 62
2-4-4-1 Solvent cleaning 63
2-4-4-2 Grit blasting 63
2-4-4-3 Plasma treatment 63
2-4-5 Joining techniques for composites 64
2-4-5-1 Adhesive bonding 65
2-4-5-2 Welding 65

2-5 Titanium alloy adherend 66
2-5-1 Titanium and its alloys 66
2-5-2 Surface treatment of titanium alloys 68
2-5-3 Joining of titanium alloys 70

Chapter III. Experimental 71
3-1 Synthesis and characterization of polyimide homopolymers and segmented copolymers 72
3-1-1 Reagents and solvents 72
3-1-2 Purification of reagents and solvents 73
3-1-3 Calculation of PA concentration for molecular weight control 76
3-1-3-1 Model calculation for a homopolyimide 77
3-1-3-2 Model calculation for a poly(imide-siloxane) segmented copolymers 80
3-1-4 Synthesis of poly(amic-acid) homopolymers 83
3-1-5 Synthesis of poly(amic-acid-siloxane) segmented copolymers 83
3-1-6 Solution Imidization 86
3-1-7 Characterization 88
3-2 Adhesion investigation with polyimides 90
3-2-1 Materials 90
3-2-2 Adherend preparation 92
3-2-2-1 Surface treatment of Ti-6Al-4V alloys 92
3-2-2-2 Surface treatment of PEEK-graphite composites 93
3-2-3 Adhesive preparation 94
3-2-3-1 Compression molded film adhesives 94
3-2-3-2 Scrim cloth adhesives 94
3-2-4 Bonding preparation of single lap shear samples 95
3-2-4-1 Ti-6Al-4V alloy adherend 95
3-2-4-2 PEEK-graphite composite adherend 98

3-2-5 Testing of single lap shear samples 98
3-3 Stress-strain analysis 99
3-3-1 Materials 99
3-3-2 Sample preparation 99
3-3-3 Testing 99
3-4 Surface characterization of PEEK-graphite composites 101
3-4-1 X-ray photoelectron spectroscopy (XPS) 101
3-4-2 Scanning electron microscopy 102
3-4-3 Contact angle measurement 102

Chapter IV. Results and Discussions 103
4-1 Characterization of polyimide homopolymers and poly(imide- siloxane) segmented copolymers 103
4-1-1 FT-IR study 103
4-1-2 Intrinsic viscosity measurement 105
4-1-3 Glass transition temperature determination 107
4-1-4 Thermal Stability 109
4-1-5 Thermo-mechanical analysis 112
4-1-6 Compression molding temperature 114
4-1-7 Effect of polyimide structure 115
4-2 Mechanical properties of polyimides 118
4-2-1 Effect of molecular weight 118
4-2-2 Effect of polydimethylsiloxane segment incorporation 119
4-2-3 Effect of test temperature 124
4-2-4 Polyimide structure 127
4-3 Adhesion study of Ti-6Al-4V alloys 132
4-3-1 Ti-6Al-4V alloy adherend 132
4-3-2 Bonding condition optimization 134

4-3-3 Effect of molecular weight 135
4-3-4 Polyimide-siloxane segmented copolymers 139
4-3-5 Effect of test temperature 142
4-3-6 Comparison with previous literature studies 146
4-4 Effect of residual solvent on adhesion behavior 147
4-4-1 Residual solvent determination 147
4-4-2 Flow behavior of scrim cloth adheives 151
4-4-3 Bonding temperature optimization 151
4-4-4 Influence of scrim cloth adhesives drying temperature 155
4-4-5 Effect of siloxane incorporation on adhesive bond strength 158
4-4-6 Comparison of scrim cloth adhesives with film adhesives 161
4-5 Effect of polyimide structure on adhesion behavior 164
4-5-1 Bonding condition optimization 164
4-5-2 Adhesive bond strength of high Tg polyimides 165
4-5-3 Effect of residual solvent on the adhesive bond strength 168
4-6 Failure mode analysis of adhesive bonds 170
4-6-1 Failure modes of polyimide film adhesives from BTDA-mDDS 171
4-6-2 Failure mode of polyimide scrim cloth adhesives 176
4-6-3 Effect of polyimide structure on failure mode 179
4-7 Proposed model 179
4-8 Adhesion study of PEEK-graphite composite 184
4-8-1 Bonding temperature optimization 184
4-8-2 Effect of surface treatment on adhesive bond strength 186
4-8-3 Surface analysis of treated PEEK-graphite composite 191
4-8-4 Topology change by surface treatment 196
4-8-5 Contact angle measurement 198

Chapter V. Summary and Conclusions 202

Chapter VI. Suggested future studies 207

Bibliography 210

Appendix A. Complexity of adhesive bond formation using ill-defined polyimides 220

Vita 223

List of Illustrations

Figure 1. A liquid drop resting at equilibrium on a solid surface 13

Figure 2. Types of stress in a adhesive joints [71] 17

Figure 3. Joint stress evaluation [71] 18

Figure 4. Types of adhesive joints used in adhesive bonding of flat adherend ends [71] 20

Figure 5. Adhesive shear stress distribution of Al-Al lap joint [77] 21

Figure 6. Stress in a single lap shear joint [77] 22

Figure 7. Single lap shear shear sample (ASTM D-1002) 25

Figure 8. Deformation of Lap shear sample in tension [77] 26

Figure 9. Double cantilever beam test specimens 28

Figure 10. Commonly used durability test methods 30

Figure 11. Thin and thick adhesive layers in tension and in shear test 33

Figure 12. Cleavage test with stiff and flexible detaching portion 35

Figure 13. Effect of test rate on stress-strain behavior of polymers [107] 39

Figure 14. Effect of test temperature on stress-strain behavior of polymers [107] 40

Figure 15. Relationships between molecular weight and physical properties and viscosity. 49

Figure 16. Effect of plasticizer on mechanical behavior of polymers [107] 51

Figure 17. Comparison between conventional monolithic materials and composites [74] 56

Figure 18. Monomers used for polyimides synthesis 74

Figure 19. Apparatus used for poly(amic-acid) homopolymer synthesis 84

Figure 20. Synthetic scheme for polyimide homopolymer 85

Figure 21. Synthetic scheme for poly(imide-siloxane) segmented copolymer 87

Figure 22. Apparatus used for solution imidization 89

Figure 23. Preparation of single lap shear sample 96

Figure 24. Bonding procedure for polyimides 97

Figure 25. Dimensions of stress-strain samples 100

Figure 26. FTIR of polyimide homopolymer form BTDA-mDDS (20,000 g/mole) 104

Figure 27. DSC of polyimide homopolymer and poly(imide-siloxane) copolymers (20,000 g/mole) 108

Figure 28. Isothermal TGA of polyimide homopolymer and poly(imide-siloxane) copolymers from BTDA-mDDS (30,000 g/mole) at 360 °C 110

Figure 29. Dynamic TGA of polyimide homopolymer and poly(imide-siloxne) copolymers (20,000 g/mole) 111

Figure 30. TMA of polyimide homopolymers and poly(imide-siloxane) copolymers 113

Figure 31. FTIR spectrum of polyimide from 6FDA-pPD 116

Figure 32. DMTA of polyimide from 6FDA-pPD (20,000 g/mole) 117

Figure 33. Effect of molecular weight on stress-strain behavior of homopolyimide 120

Figure 34. Stress-strain behavior of polyimide homopolymer and poly(imide-siloxane) copolymers (30,000 g/mole) at ambient temperature 122

Figure 35. Effect of siloxane block ($<Mn> = 1550$ g/mole) incorporation on the stess-strain behavior of polyimides 123

Figure 36. Stress-strain behavior of polyimide homopolymer and poly(imide-30%siloxane) copolymers as a function of temperature 125

Figure 37. Effect of test temperature on the stress-strain behavior of polyimides homopolymer and poly(imide-siloxane) copolymers 126

Figure 38. Effect of test temperature and molecular weight on the stress-strain behavior of poly(imide-10% siloxane) copolymers 128

Figure 39. Stress-strain behavior of polyimide from 6FDA-pPD, Ultem and Kapton as a function of temperature 130

Figure 40. SEM micrographs of as-received and sand blated/Pasa Jell 107 treated Ti-6Al-4V alloy adherends 133

Figure 41. Effect of bonding temperature on the adhesive bond strength of polyimide homopolymers and poly(imide-siloxane) segmented copolymers 136

Figure 42. Effect of molecular weight on the adhesive bond strength of polyimide homopolymers and poly(imide-siloxane) copolymers (BTDA-mDDS) 138

Figure 43. Effect of siloxane incorporation on the adhesive bond strength of polyimide 140

Figure 44. Effect of test temperature on the adhesive bond strength of polyimides ... 143

Figure 45. Effect of scrim cloth adhesive drying temperature on the residual solvent measured by TGA ... 150

Figure 46. Effect of scrim cloth adhesive drying temperature and siloxane incorporation on the flow behavior of scrim cloth adhesives ... 152

Figure 47. Effect of bonding temperatures on the adhesive bonding of scrim cloth adhesives ... 154

Figure 48. Effect of scrim cloth drying temperatures on the adhesive bond strength ... 156

Figure 49. Effect of siloxane on the adhesive bond strength of polyimide with scrim cloth adhesives ... 159

Figure 50. Comparison of adhesive bond strength from scrim cloth adhesive with that from film adhesives ... 162

Figure 51. Effect of polyimide structure on the adhesion behavior of polyimides ... 167

Figure 52. Effect of scrim cloth adhesive on the adhesive bond strength of high Tg polyimides ... 169

Figure 53. Examples of failure mode of film adhesive from BTDA-mDDS polyimide ... 175

Figure 54. Examples of failure mode of scrim cloth adhesive of homopolyimide ... 178

Figure 55. A possible model for the relationship between strength, ductility and bond strength at a given strain rate ... 181

Figure 56. Proposed model for adhesive bond strength variation with test temperature at a given strain rate ... 182

Figure 57. Effect of surface treatment on the adhesive bond strength of PEEK-graphite composite with poly(imide-30%siloxane) copolymer and Ultem 1000 ... 187

Figure 58. Effect of treatment time of gas plasma and a combination of gas plasma and grit blasting on adhesive bond strength with polyimide copolymer ... 189

Figure 59. Effect of treatment time of gas plasma and a combination of gas plasma and grit blasting on adhesive bond strength of Ultem 1000 ... 190

Figure 60. Atomic concentration ratio change by surface treatments in XPS analysis ... 193

Figure 61. Deconvolution of C1s peaks of surface treated PEEK-graphite composite ... 195

Figure 62. O1s peaks of surface treated PEEK:-graphite composites ... 197

Figure 63. SEM micrographs of PEEK-graphite composites ... 199

Figure 64. Effect of surface treatment on the water contact angle of PEEK-graphite composites ... 200

List of Tables

Table 1. Advantages and disadvantages of adhesion [32] 6

Table 2. Definitions in adhesion science (ASTM standard V15.06, 1989) 7

Table 3. Bond type and typical bond energies [35] 11

Table 4. Testing methods (ASTM Standard) 23

Table 5. Mechanical properties of selected polyimides[140] 46

Table 6. Effect of scrim cloth drying conditions on volatiles, flow and bond strength [12] 52

Table 7. Characteristics of fibers [168] 58

Table 8. Mechanical properties of polymeric matrix materials [168] 59

Table 9. Composite fabrication routes [167] 61

Table 10. Mechanical properties of selected metals [168] 67

Table 11. Classification of surface pretreatment for adhesive bonding of Titanium [194] . 69

Table 12. Reagents and solvents used for polyimide synthesis 75

Table 13. Incorporated mole percent of phthalic anhydride utilized for molecular weight control with non-reactive end-groupd 78

Table 14. Materials for adhesion study 91

Table 15. Characteristics of polyimide adhesives 106

Table 16. Mechanical properties of polyimide by stress-strain. 131

Table 17. Nomenclature of scrim cloth adhesives as a function of drying condition 149

Table 18. Effect of bonding temperature and pressure on the adhesive bond strength of 6FDA-pPD and 6FDA-pDDS polyimides 166

Table 19. XPS results of failure analysis 172

Table 20. Summary of failure mode of film adhesive from BTDA-mDDS polyimide 174

Table 21. Summary of failure mode of scrim cloth adhesive from BTDA-mDDS polyimide 177

Table 22. Bonding temperature optimization of PEEK-graphite composite 185

Table 23. Summary of surface analysis of PEEK-graphite composites 192

Table 24. Characteristics and adhesive bond strength of ill-defined polyimide adhesives 222

Chapter I. Introduction

A strong demand for high temperature polymers for military, aerospace and electronic applications has led to a tremendous research effort to develop new polymeric materials which meet the rigorous requirements. Polyimides are one of the best high temperature aromatic polymers and have received a great deal of attention due to their excellent properties. These include their thermal and mechanical properties, thermo-oxidative stabilities and high glass transition temperature. However, their utilization has been limited due to poor processability and/or the production of water during the standard in situ poly(amic-acid) to polyimide transformation. Consequently, instead of employing fully cyclized polyimide, poly(amic-acid) (which cyclizes upon processing) supported on scrim cloth (E-glass fabric) has been nearly exclusively utilized in the adhesion field.

Although utilization of poly(amic-acid) intermediates enhanced processability, scrim cloth based adhesives still have unsolved problems such as unremoved solvent and water evolution upon cyclization. This might be expected to have a very strong influence on the adhesive bond performance, especially at elevated temperatures. A number of approaches to enhance

the processability of fully imidized polyimides, such as incorporation of flexible bridging units into polyimide backbone [1-3] and bulky side groups [4], and utilization of diamines containing meta linkages [5], were somewhat successful in developing soluble and processable high Tg polyimides. Recently, our laboratory has succeeded in synthesizing soluble and processable thermoplastic high Tg polyimides without detracting from their excellent proerties by utilizing newly developed techniques such as solution imidization, siloxane incorporation, and molecular weight control with non-reactive end groups [6-9].

Although there has been a great amount of research on the development of high Tg structural adhesives, the major variables affecting their adhesive properties have not been fully investigated in detail, but only confined to preliminary studies. The major requirements for optimal adhesive performance are good bond consolidation and good mechanical properties. The molecular weight should be high enough to afford chain entanglements which yield good mechanical properties, but low enough to provide good melt flow under bonding conditions. Earlier studies [10,11] have shown that the bond strength as well as other mechanical properties certainly depend on the polyimide molecular weight. However, the range of molecular weight used in those studies was fairly narrow and melt stability issues were not addressed.

Scrim cloth adhesives coated with poly(amic-acid) have been exclusively used in adhesion studies of polyimides. However, only few studies have been conducted to study the effect of scrim cloth adhesives on the adhesive bond strength, as well as the behavior of scrim cloth adhesives themselves. Dezern and Young [12] have found that scrim cloth adhesives contained quite an amount of residual solvent and unconverted poly(amic-acid), unless dried at very high temperature. They also reported that the adhesive bond strength of scrim cloth adhesives is a function of scrim cloth drying temperature and bonding temperature, which controlled flow and thus bond consolidation.

Adhesive bond strengths vary with test temperatures and some studies [12-17] have shown decreased bond strength of scrim cloth adhesives while others [18-19] have shown slightly

increased bond strength with test temperature. It has also been observed [12,20] that aging of adhesive bonds from scrim cloth adhesives at elevated temperatures decreased bond strength at room temperature, but increased it at the elevated test temperatures. However, no clear explanation has been provided yet. In addition, no comparison of adhesive bond strength of a scrim cloth adhesive with that of a melt fabricated film has been made, although some polyimides have been claimed to be thermoplastic.

Due to advantages such as high specific strength and specific modulus and other advantages such as high corrosion resistance and design flexibilities, polymeric composite materials have been used increasingly for aerospace, electronic materials, biomaterials, sporting goods and automobile applications. However, a number of obstacles, such as joining difficulty, high cost and processing limitations have to be overcome before high volume applications will be feasible. Adhesive bonding, as opposed to mechanical fastening, has been increasingly utilized for composite joining. A number of bonding techniques such as resistance heating, ultrasonic welding, focused infrared heating [21] as well as microwave processing [22] have been introduced. In order to achieve strong and durable adhesive bonding, proper surface treatments and good adhesives have also been demonstrated to be vital requirements. Various papers have indicated that gas plasma treatment is a promising technique to enhance bond strength of polymers [23-26], polymeric composites [27-30] and metals [31]. The nature of the polymeric adhesive also plays a very important role on the bond performance [28].

In this thesis, the adhesive bond strength of polyimides was investigated as a function of molecular weight, siloxane incorporation, test temperature and polyimide molecular structure using compression molded film adhesives, as well as scrim scrim cloth adhesives. Secondly, an extensive study has been conducted on the effect of residual solvent on adhesive bond performance with scrim cloth adhesive and fully imidized thermoplastic polyimide, as a function of scrim cloth drying temperature, bonding and testing temperature. Adhesive bond strengths of the film adhesive were also compared with those of the scrim cloth adhesive. Thirdly, it was attempted to correlate adhesive bond strength with mechanical properties

measured by stress-strain tests. Finally, adhesive bond performance of *PEEK*®-graphite composite with poly(imide-30%siloxane) copolymer and poly(ether-imide) *Ultem*® 1000 was investigated as a function of surface treatments such as acetone/distilled water washing, grit blasting and gas plasma treatment (oxygen, ammonia, nitrogen and argon).

Chapter II. Literature Review

2-1 Adhesion and adhesive bonding

Although adhesion has been utilized for a long time as a means of joining materials, systematic investigation of adhesion did not begin until the middle of 20th century. The recognition of the many advantages of adhesive bonding (Table 1) over mechanical fastening [32], has accelerated attempts to understand adhesive joints. A major objective has been to achieve strong and durable adhesive bonds.

Adhesion may be defined [33] as the state in which two surfaces are held together by interfacial forces which may consist of valence forces, mechanical interlocking forces or both. Other commonly accepted terminologies of adhesion science are listed in Table 2. The adhesive bonds derive their strength from interactions of molecules, atoms and ions at the surface [32,34]. The magnitude of these attractive forces varies from strong chemical bonds to weak van der Waals dispersion forces, and is a function of distance between the two materials. Therefore, intimate contact which is often termed good "wetting" is essential for good adhesion.

Table 1. Advantages and disadvantages of adhesion [32]

Advantages

1. Ability to join dissimilar materials, eg. metal to composite
2. Ability to join thin sheet materials
3. Improved stress distribution of bonded joints
4. Convenient and cost effectve
5. Increased design flexibility
6. Improved appearance-smooth, blemish free
7. Improved corrosion resistance

Disadvantages

1. Elaborate surface treatment may be required
2. Limited upper service temperature
3. Mechanical strength may be limited in tension and shear
4. Difficult to repair and inspect
5. Health hazard (for solvent processing)
6. May require long process time

Table 2. Definitions in adhesion science (ASTM standard V15.06, 1989)

Adherend	A body which is held to another body by an adhesive
Adhesive	A substance capable of holding materials together by surface attachment
Structural adhesive	A bonding agent used for transferring loads between adherends, exposed to service environments typical for the structuring loads between adherends
Bond	The union of materials by adhesive joint: The location at which two adherend are held together with a layer of adhesive
Bond strength	The unit load applied in tension, compression, flexure, peel, impact, cleavage or shear, required to break an adhesive assembly with failure occuring in or near the plane of the bond
Adhesive failure	Rupture of an adhesive bond, such that the separation appears to be at the adhesive and adherend

The science of adhesion includes two major fields; chemistry and physics of surfaces and interfaces, and fracture mechanics of adhesive bonds under various environments. The former deals with bond formation and attempts to predict the magnitude of the intrinsic adhesive bond strength. The latter includes mechanical analysis of adhesive bonds and the development of reproducible and representative test methods. Although there has been a tremendous effort to explain the existing adhesion phenomena and to elucidate the mechanisms of adhesion, adhesion science is still a somewhat primative area of research. Therefore, better theories, materials and processing advances are needed.

2-1-1 Mechanisms of adhesion

In addition to the intimate contact between adhesive and adherend, the nature and magnitude of the adhesion forces are also mportant for a strong, durable adhesive bond. The intrinsic adhesion forces operating across the adhesive/adherend interface are critical to the mechanisms of adhesion and may involve physical (mechanical interlocking, adsorption, or diffusion) and chemical bonding (covalent, hydrogen or ionic bonds). Although, there are many widely accepted theories on the mechanisms of adhesion, such as mechanical interlocking, electronic (eg. acid-base), adsorption, diffusion and weak boundary layer theory, none can satisfactorily explain all of the existing important adhesion phenomena [35-39]. Several of these these theories are reviewed in the following sections.

2-1-1-1 Mechanical interlocking

This theory proposes that adhesive bond strength arises mainly from the mechanical interlocking of the adhesive onto the substrate. Thus, an "Ink-bottle" type pit present on the adherend is considered to be the ideal case for this theory but is practically seldom encountered. However, anodization of aluminium alloy usually results in deep cylindrical pores which

may lead to mechanical interlocking [40]. Surface preparation methode such as grit blasting, on the other hand, increases surface roughness rather than creating "pits" per se and thus is less likely to result in mechanical interlocking. Although there are some good examples [40-43] in which mechanical interlocking is the main mechanism for adhesive bond strength, other cases also exist where perfectly smooth mica [44] and optically smooth rubber result in good adhesion [45]. Therefore, adhesion phenomena can not be attributed solely to mechanical interlocking

2-1-1-2 Diffusion theory

The diffusion theory of adhesion, proposed by Voyutskii [46], states that intrinsic polymer-polymer adhesion is due to the mutual diffusion of polymer molecules across the interface. Therefore, this theory is applicable only to those polymers whose chain mobility and mutual solubility are high enough for inter diffusion. These conditions are met usually in the autohesion of elastomers and in the solvent welding of compatible amorphous polymers. However, diffusion is unlikely to occur in polymers which have dissimilar solubility parameters, or where they are highly crosslinked, crystalline or below the glass transition temperature.

2-1-1-3 Electronic theory

When two substrates have different electronic band structure, there is likely to be some electron transfer upon contact to balance the Fermi levels, resulting in the formation of electrical double layer. An electrostatic forces arising from the electrical double layer could be the main source of adhesive bond strength. The electronic theory of adhesion was proposed by Deryaguin and co-workers [47]. Although it has been demonstrated in some cases that

electrostatic forces from electrical double layer are the major source of adhesion strength [48-50], it is not a general phenomenon and has not been proven in other cases.

2-1-1-4 Adsorption theory

The adsorption theory of adhesion is the most widely applicable one among those proposed and has been studied in depth [51-54]. According to this theory, the adhesive bond strength arises from the interatomic and intermolecular forces between the atoms and molecules at the interface of the adhesive/substrate, provided that there is a good interfacial contact. The reacting forces are divided into three groups (Table 3)[35]; primary bond, secondary bond and donor-acceptor interaction. The first category includes ionic, covalent and metallic bonds. Van der Waal's forces are the most common forces in adhesion and belong to the secondary bond which also includes hydrogen bonds. The acid-base interaction pioneered by Fowkes [55.56] has strength falling between secondary and primary bonds. A number of studies indicate the importance of acid-base interaction [57-59]

One of the main advantages of this theory is that the the adhesive bond strength can be deduced from the measured work of adhesion employing the Young-Dupre equation. Thus, the adhesive bond strength is thought to stem from two components; the dispersion and acid-base interaction forces. In general, the theoretical calculations predict a much lower adhesive bond strength strength than the experimental value due to energy dissipation.

It is obvious that the introduction of active chemical groups into the surface of adhesive and adherend will improve the adhesive bond strength as well as durability [60-62]. This might be achieved by proper surface treatments or by applying coupling agents.

Table 3. Bond type and typical bond energies [35]

Bond Type	Bond Energy (kJ/mol)
Primary bonds	
Ionic	600-1100
Covalent	60-700
Metallic	110-350
Donor-acceptor bonds	
Bronsted acid-base interactions (i.e. up to a primary ionic bond	Up to 1000
Lewis acid-base interactions	Up to 80
Secondary bonds	
Hydrogen bonds	
Hydrogen bonds involving fluorine	Up to 40
Hydrogen bonds excluding fluorine	10-25
Van der Waals bonds	
Permanant dipole-dipole interactions	4-20
Dipole-induced dipole interactions	Less than 2
Dispersion (London) forces	0.08-40

2-1-1-5 Weak boundary Layer

Weak boundary layers (WBL) certainly can form on the adherend surface via the presence of adsorbed water, lubricating oils, oxide layers, etc., and thus has paramount effect (generally adverse) on adhesive bond performance [63]. WBL is also common in polymers and polymeric composites due to their tendency to reject foreign substances, which would include additives as well as low molar mass polymers. As a result, the removal or prevention of WBL is very important for strong and durable adhesive bonds [64] and could be achieved by proper surface preparations such as abrasion and solvent cleaning. Gas plasma treatment is widely applied not only to remove the WBL but also to induce the active functional groups for chemical bonding. However, not all interfacial layers are detrimental to adhesion. For example, stearic acid on aluminium oxide improves adhesion to polyethylene [65], while silane on glass [66,67], steel [68], and silicon oxide [69] also has a favorable effect.

2-1-2 Thermodynamics of adhesion

As Young proposed, the force balance equation of a liquid droplet (Figure 1) can be expressed by

$$\gamma_{sv} = \gamma_{sl} + \cos\theta\gamma_{lv} \qquad [2-1]$$

$$\cos\theta\,\gamma_{lv} = \gamma_{sv} - \gamma_{sl}$$

where;

γ_{sv} = surface tension of solid-vapor

γ_{sl} = surface tension of solid-liquid

γ_{lv} = surface tension of liquid-vapor

θ = contact angle.

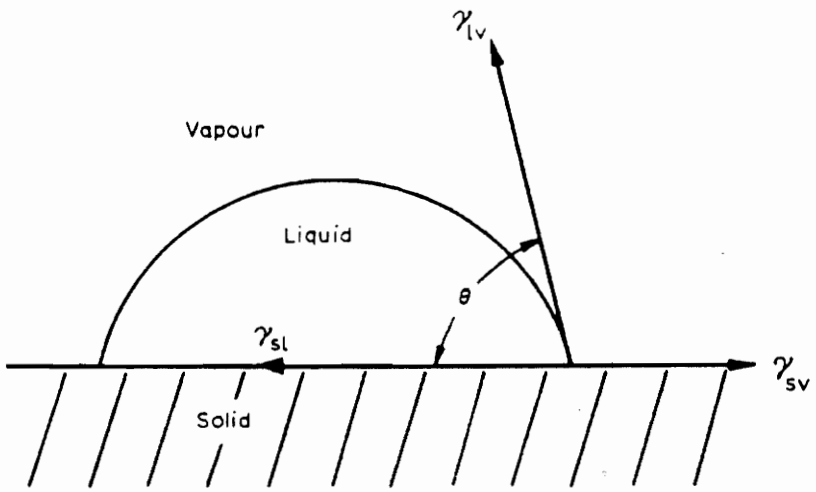

Figure 1. A liquid drop resting at equilibrium on a solid surface

As the contact angle decreases, the liquid droplet will spread and thus the larger contact area. At zero degree, spontaneous spreading or complete wetting occurs. The contact angles are a function of surface roughness and temperature. Wenzel introduced the surface roughness factor R which is the ratio of the true area of the solid to the apparent area,

$$R = \cos\theta'/\cos\theta$$

θ = true contact angle

θ' = measured contact angle.

If the true contact angle is smaller than 90 degrees, the surface roughness would decrease the measured contact angle while the reverse is true for the true contact angle of 90 degrees or greater. A carefully machined or ground surface have values of R from 1.5 to 2 or higher.

The spreading phenomena or wettability of an adhesive plays a critical role in adhesion and can be measured from the contact angle measurement. The work of adhesion (Wa) between two immiscible liquids according to Dupre's is,

$$Wa = \gamma_{sv} + \gamma_{lv} - \gamma_{sl} \qquad [2-2]$$

and the work of cohesion (Wc) for a single liquid is

$$Wc = 2\gamma_{lv} = 2\gamma_l \qquad [2-3]$$

The work of adhesion, Wa, between a solid surface and a liquid droplet can be calculated from the surface tension of the liquid and the contact angle with Young-Dupre equation which is obtained by combining equation 2-1 and 2-2,

$$Wa = \gamma_{sv} + \gamma_{lv} - \gamma_{sl} = \gamma_{lv} + \cos\theta + \gamma_{lv}$$

$$Wa = \gamma_l(1 + \cos\theta) \qquad [2-4]$$

The criterion for spreading is that work of adhesion be greater than that of cohesion, Wa > Wc. The initial spreading coefficient introduced by Harkins and co-workers can be expressed as:

$$S_{l/s} = W_a - W_c$$

$$= \gamma_{sv} + \gamma_{lv} - \gamma_{sl} - 2\gamma_{lv}$$

$$= \gamma_{sv} - (\gamma_{lv} + \gamma_{sl}) \qquad [2-5]$$

If $S_{l/s} > 0$, spontaneous spreading would take place and the spreading coefficient S can be calculated from surface tension, which is usually obtained from the contact angle measurements. With an informative approximation ($\gamma_{sl} = 0$), the condition for spreading is obtained as follows;

$$S_{l/s} = \gamma_{sv} - \gamma_{lv} > 0 \qquad [2-6]$$

thus, $\gamma_s > \gamma_{lv}$

In order for spreading to occur, the surface energy of the solid should be larger than that of the liquid, which is the concept of critical surface tension proposed by Zisman [70].

2-1-3 Design of adhesive bonds

Although no set rules have been established for the design of adhesive bonds due to their complexity, several general principles have been introduced [38, 71-73]. The primary goal of joint design is to obtain a maximum bond performance; strength and service life, which are dictated by 1) mechanical properties of adhesive and adherend, 2) bond geometry, 3) residual internal stress, 4) degree of true interfacial contact and 5) service environments. The major factors in adhesive bond design to be considered for maximum performance are as follows;

1. stress in the the direction of maximum strength
2. maximum bond area
3. uniform, thin and continuous adhesive layer
4. no stress concentration points

There are five types of stress found in the adhesive joint as illustrated in Figure 2; compression, tension, shear, cleavage and peel stresses. Any combination of these stresses may be encountered in adhesive applications. Most structural adhesives are highly resistant to compression and shear as opposed to peel or cleavage stresses [32]. Therefore, this fact should be considered in placing the adhesive in shear or compression to prevent or minimize the peel or cleavage stresses. One of the difficulties in tension testing is that a small misalignment of the substrate will result in cleavage or peel stresses, unless one of the substrate is highly compliant. However, designing an adhesive joint to operate in compression mode limits its application. The schematic diagram of some joint stresses are shown in Figure 3 [71].

The strength of adhesive bonds, in general, is improved by increasing the length and width of bonded area which has a linear relationship with width but non-linear with length. The thickness of the adhesive layer also plays an important role in adhesive bond strength [74]. Adhesive bond strength of tensile butt joints generally decreases with increasing adhesive layer thickness, while that of shear samples shows either a maximum at the adhesive thickness of around 0.02" or no variation [73, 219]. The dependence of adhesive bond strength on adhesive bond layer thickness is due to the variation of stress distribution in the adhesive with it's thickness. A thick layer would improve the toughness [75] but may increase the creep tendency. The adhesive bond strength also depend on the adherend; yield strength and thickness. One should design the adhesive bond so as not to exceed the yield strength of the adherend.

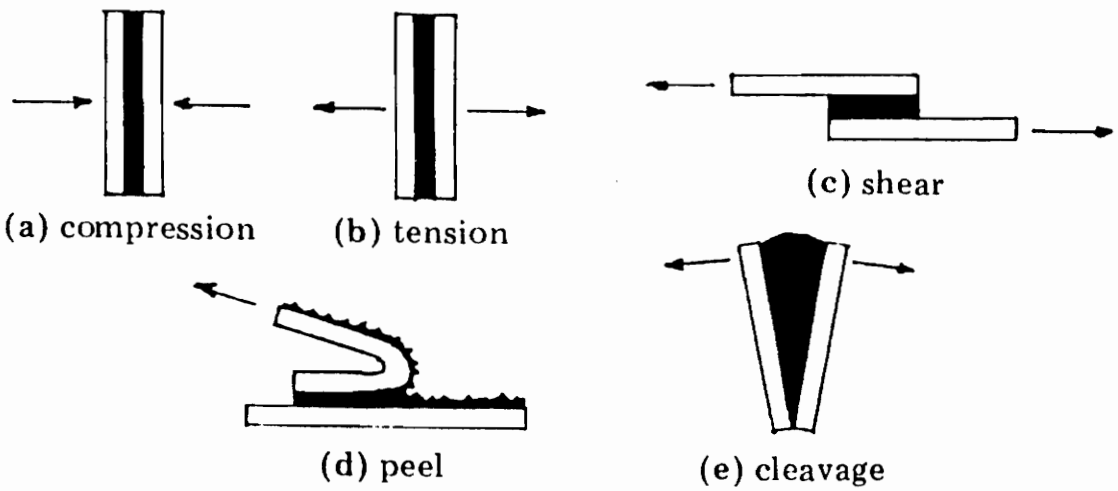

Figure 2. Types of stress in a adhesive joints [71]

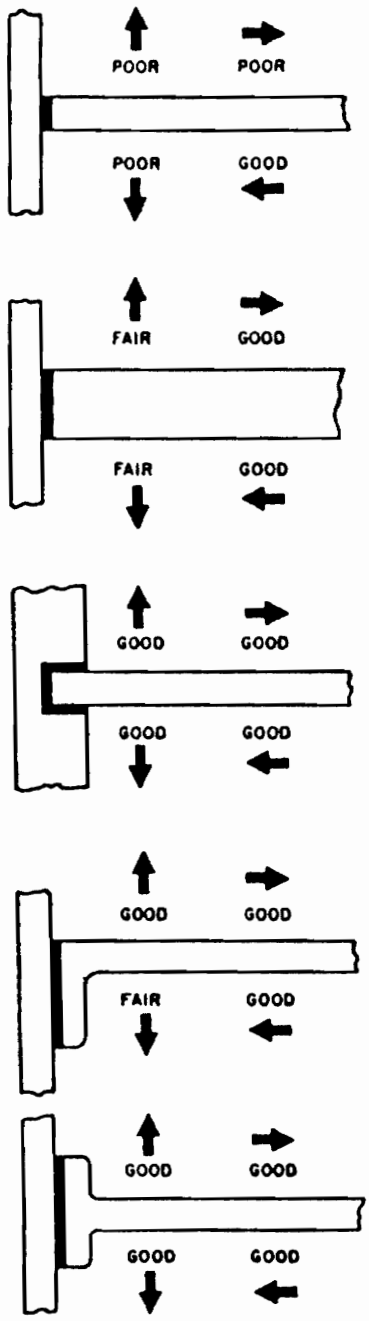

Figure 3. Joint stress evaluation [71]

The voids formed by trapped air or volatiles and any form of discontinuity will act as stress concentration points, initiating the failure of the joint. Consequently, a continuous and void-free adhesive layer is required for good adhesive bond performance. Other sources of stress concentration are residual stress from the thermal expansion mismatch between adherend and adhesive [76], and joint geometry. These sources can be eliminated by the selection of proper adhesive/adherend combination, processing conditions and bond geometry. The most commonly used bond geometries are shown in Figure 4.

The stress distribution of a single lap shear joint is is not uniform (Figure 5) [77] but most of the stress is concentrated at the end of the lap. The excess adhesive (spew fillet) on the edge of adhesive bond also has an effect on the adhesive bond strength since the excess adhesive reduce the edge effect [220]. The stress in the single lap joint is ordinarily a combination of shear and tensile stress, and sometimes peel stress at the end of a joint (Figure 6) [77]. The scarf joint as well as beveled joint demonstrates better stress distribution than single lap joint over the entire bonded area thereby eliminating the stress concentration characteristics of lap joints (Figure 5). Unfortunately, the beveled and scarf joints have some production difficulties.

2-1-4 Testing of adhesive bonds

Numerous test methods have been developed to measure the integrity of adhesive bonds [71,73]. Many have been standardized by American Society for Testing and Materials (ASTM) committee D-14, Society of Automotive Engineers (SAE), government agencies and industries (Table 4). Such test methods evaluate not only the inherent strength of the adhesive joint but also the bonding techniques, surface preparation, application of adhesive, and the curing of the adhesive. Thus, testing measures the adhesive joint strength and also helps in predicting the performance and reliability of an adhesive joint. Since the measured strength will vary considerably depending on the sample geometry and test conditions, it is obviously important to follow the test procedure exactly as described.

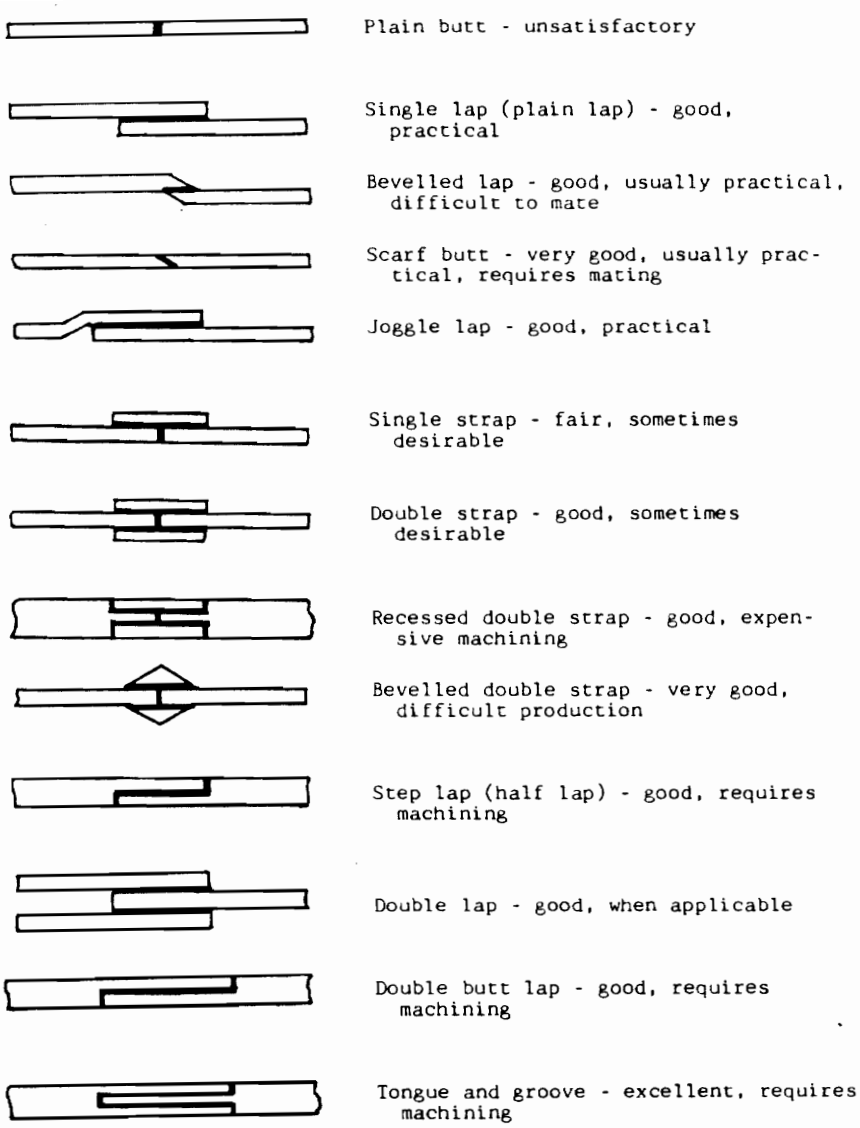

Figure 4. Types of adhesive joints used in adhesive bonding of flat adherend ends [71]

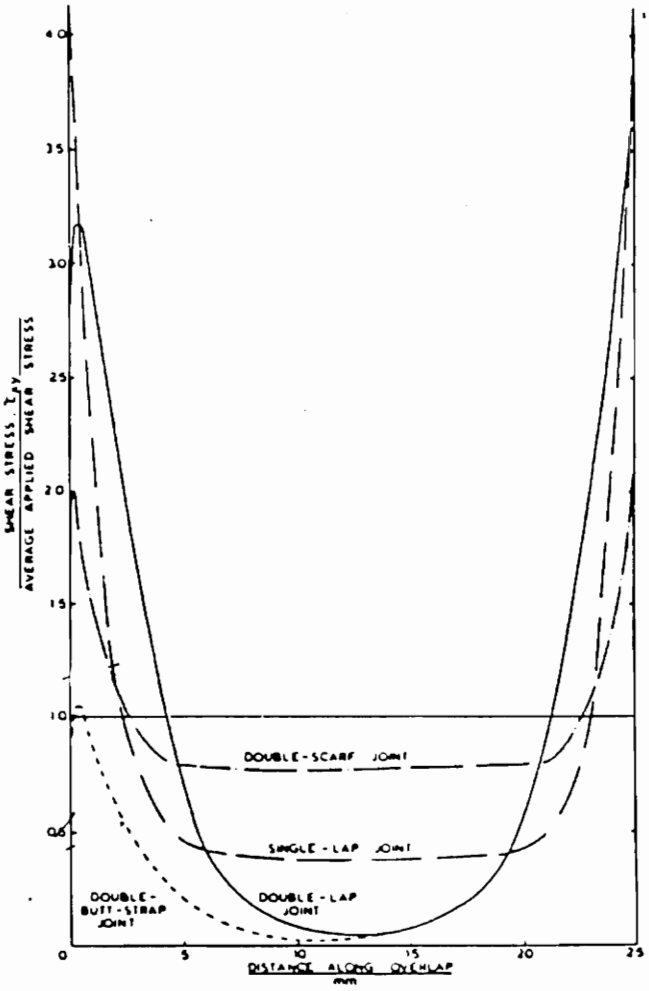

Figure 5. Adhesive shear stress distribution of Al-Al lap joint [77]

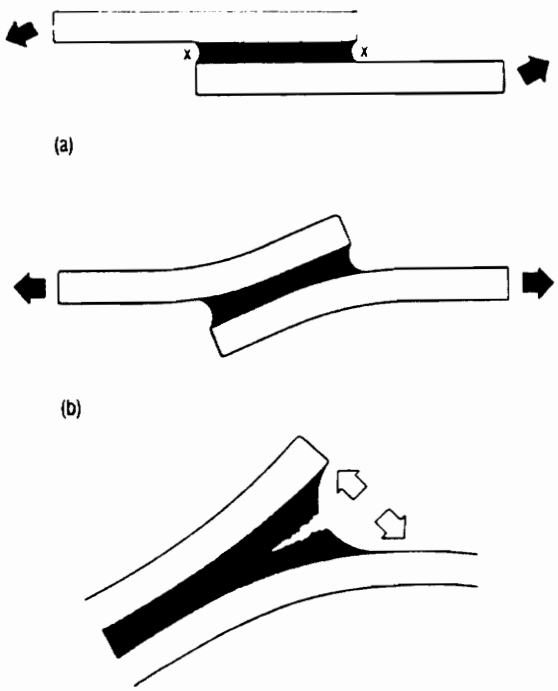

Figure 6. Stress in a single lap shear joint [77]

Table 4. Testing methods (ASTM Standard)

Lap Shear Tests	ASTM D-1002-72	Single Lap Shear in Tension
	D-3163	Single Lap Shear, Rigid Substrate
	D-2295-72	Single Lap Shear, High Temperature
	D-2557-72	Single Lap Shear. Low temperature
	D-905	Single Lap Shear in Compression
	D-3164-73	Double Lap Shear
Peel Tests	ASTM D-3167-76	Floating Roller Test
	D-903-49	180 Peel Test
	D-1876-72	T-Peel Test
	D-1781-76	Climbing Drum Peel Test
	D-2918-71	T-Peel, Durability Test
Impact Test	ASTM D-950-82	
Creep Test	ASTM D-1780-72	Single Lap Shear in Tension
	D-2293-69	Shear by compression loading
Fatigue Test	ASTM D-31166-73	Single Lap Shear in Tension
Cleavage Test	ASTM D-1062-78	
Durability Test	ASTM D-896-84	Chemical Resistance (any ASTM Samples)
	D-904-57	Light(Natural and Artificial)
	D-1183-70	Cyclic Loading
	D-1820-70	Natural Outdoor Aging
	D-1879-70	High Energy Radiation
	D-2918-71	High Stress, Moisture & Temp (Peel only)
	D-2919-71	High Stress, Moisture & Temp (Single Lap in Tension)
	D-3762-79	Wedge Test
	B-117	Salt Spray Test

The test methods can be classified into two major groups; destructive and non-destructive. The former methods are widely applied for the evaluation of adhesive joints since they are relatively well established compared to the latter. The destructive test methods can be grouped into three categories depending on the purpose of the the test; strength measurement (tensile, shear, peel, and impact stress), toughness measurement (peel, double cantilever beam, blister and indentation test), and performance (durability, weathering test). In this review, some representative methods such as shear, peel and a durability test will be discussed together with non- destructive testing mrthodologies.

2-1-4-1 Lap shear tests

Pure shear stresses are those which are imposed parallel to the bond and in its plane (Figure 2). Since pure shear stress is rarely encountered in actual adhesive assemblies, conventional test samples are adequate for most purposes. Among the shear tests (Table 4), single lap shear samples are widely utilized because the samples are simple to fabricate, the geometry and service environments are easy to duplicate, and reproducible and usable results can be easily obtained. The specifications of single lap shear test are described in ASTM D-1002 and test specimen is shown in Figure 7.

The adhesive bond strengths of lap joint are directly proportional to the width of the specimen but not to the overlap length due to the edge effect. Adhesive bond strength of lap shear samples are also a function of mechanical properties, and thickness of adhesive [74] and adherend [78-80]. Shear strength can also be measured by compression loading (ASTM D-905). The major drawback of this test is that the failure mode is not pure shear but a mixture of shear and tensile stress. Furthermore, adherends often experience elastic or plastic deformation (Figure 8) which would induce peeling or cleavage mode due to the stress concentraion at the end of the joint [73,77].

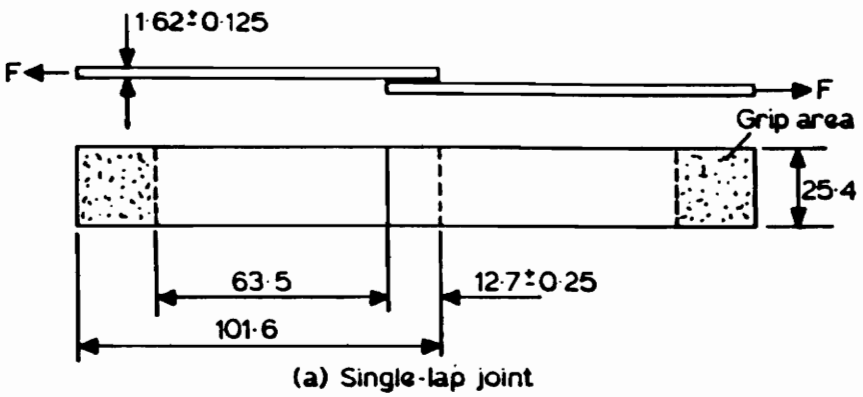

Figure 7. Single lap shear shear sample (ASTM D-1002)

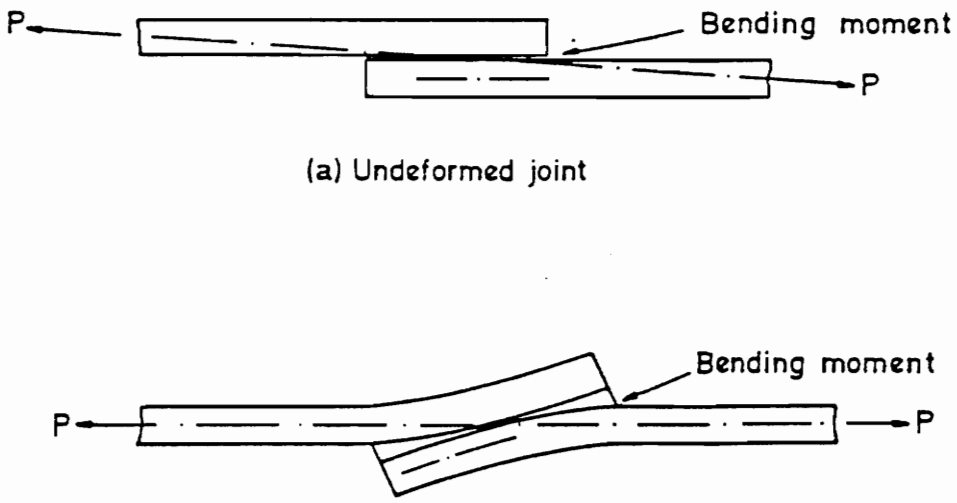

Figure 8. Deformation of Lap shear sample in tension [77]

2-1-4-2 Peel and cleavage tests

The peel test involves the stripping of a flexible member of an assembly that has been bonded with an adhesive to another member that may be flexible or rigid. The test consists of pulling the flexible member at an angle of 90 or 180 degree. Commonly applied peel tests are the floating roller test (D-3167), climbing drum peel test (D-1781), T-peel test (D-1876) and 180 degree peel test (D-903). T-peel test provides the lowest values of any peel test due to the transmission of applied load to the bond [81]. According to Gent and co-workers [82], a 45 degree peel test is better than the 90 or 180 degree test since it minimizes the deformation of the adherends and thus the energy dissipation. The major problem of the peel test is its high sensitivity to the adherend and adhesives. A small change in the adhesive strength or thickness of the adherend would result in a large variation of peel strength [83 ,84]. Therefore, it is suggested that the average force of a 5 to 6 inch length pull be taken as an indication of the peel strength and peel forces are reported as linear values; pounds per linear inch (PLI), or comparable SI units.

In a cleavage test, two rigid members are used. Therefore, there should be no peel stress unless the applied force is large enough to deform the adherend or exceed the yield strength of the adherend. The peel test and cleavage tests are used not only to measure the strength of adhesive bond but also to measure fracture toughness. Double cantilever beam (DCB) [85-88], blister tests [89-90] and indentation test [91,92] are also utilized to measure the toughness of the adhesive via measuring the strain energy release rate. The DCB test (Figure 9) is basically similar to the T-peel test while the blister test is similar to the indentation test.

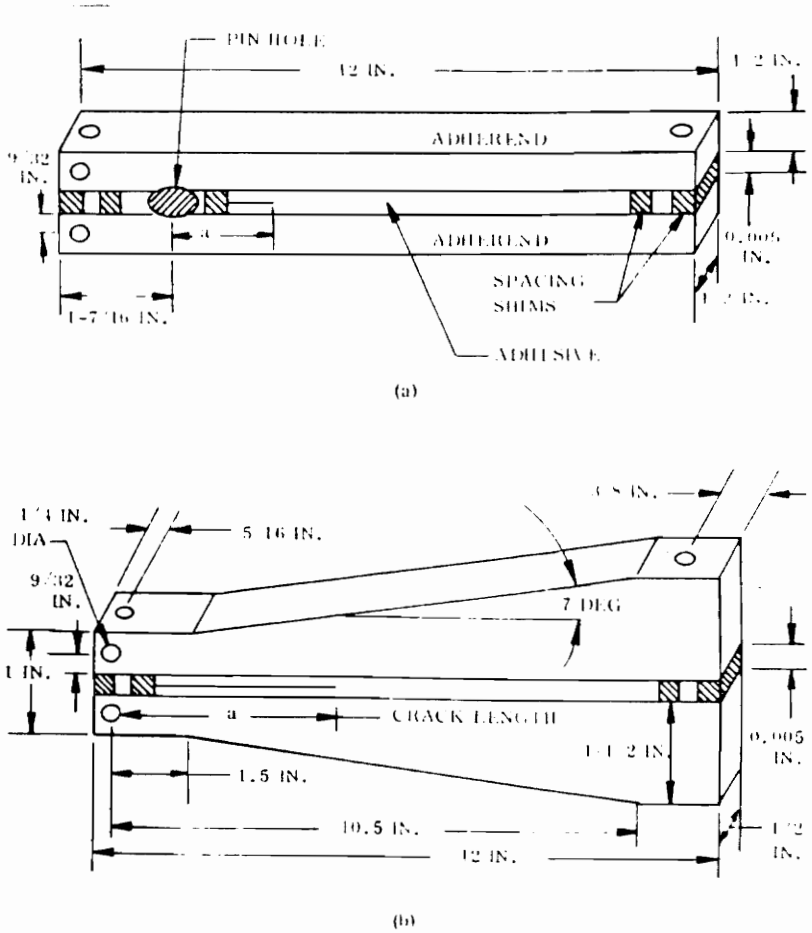

Figure 9. Double cantilever beam test specimens

2-1-4-3 Durability tests

In durability tests, the test specimens are subjected to hostile environments, such as hot/wet, acidic or basic, atomic oxygen, and ultraviolet environments, etc.. Among these environments, hot/wet conditions are the most commonly used [93-96]. If the hostile environment is combined with an applied load, which is up to 50 percent of ultimate adhesive bond strength, it is called the stress-durability test. Stress-durability tests in hot/wet conditions are often conducted to investigate the effectiveness of surface treatments, since most conventional test methods are unable to evaluate the goodness of the surface treatment. The most widely applied stress-durability test methods in structural adhesive testing are the Boeing wedge test, 3M's spring loaded test and the Alcoa stress test (Figure 10), in conjunction with ASTM methods (Table 4). In a stress-durability test, an applied load is adjusted periodically due to the creep of the adhesive during the test. The survival time is recorded together with given conditions such as temperature, humidity and the applied load. However, stress adjustment is not needed for the wedge test and a periodic measurement of crack length is employed.

2-1-4-4 Non-destructive testing

There has been a strong demand for highly reliable non-destructive test methods (NDE) to evaluate and predict bond strength and performance. The simplest and most commonly used technique is tap testing [97]. But, this method is limited to thin layer (less than 1 mm) and a larger unbonded zone (larger than 10mm in diameter). Although a number of NDE techniques have been developed, most of them are used to detect and characterize the unbonded zone rather than measuring or predicting the bond strength. Currently available NDE methods include resonance, pulse- echo, pulse-echo, through-transmission, ultrasonic spectroscopy and Lamb waves (LW, C-scan) [98-100].

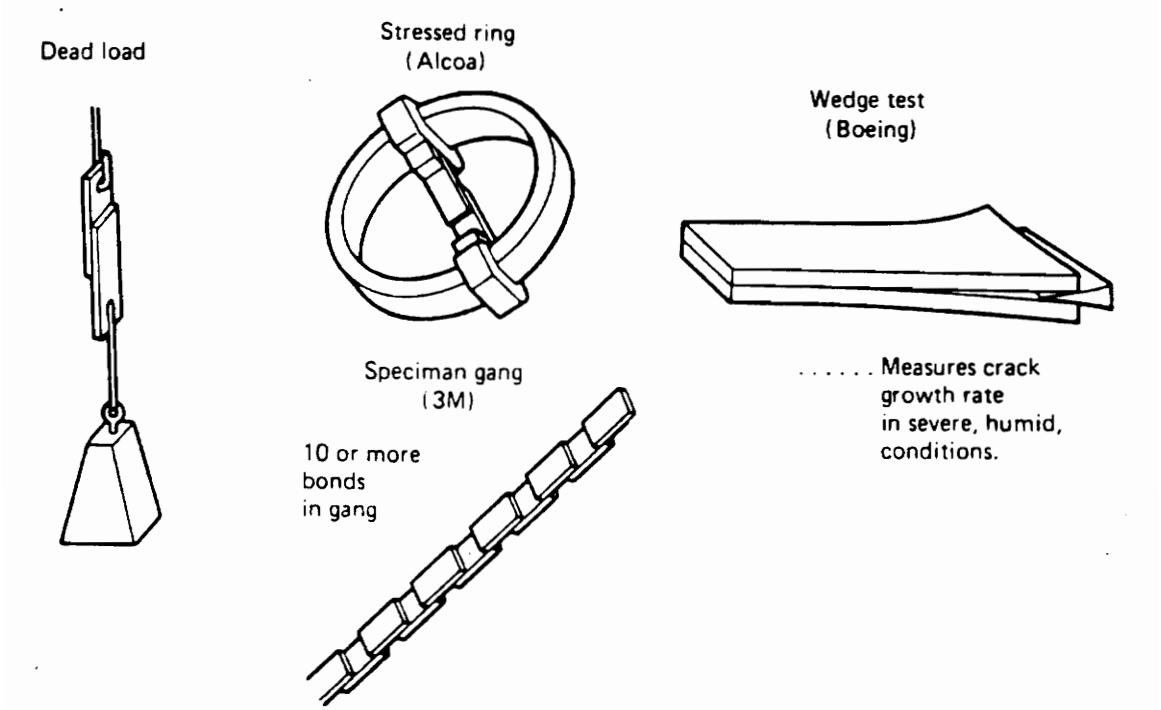

Figure 10. Commonly used durability test methods

The ultimate goal of NDE is to measure the strength of adhesive bonds without breaking the bond. However, the method has not been completely successful due to the following limitations;

1. strength is not a just physical parameter but also is a function of the actual fabricated structure
2. NDE is often not yet sufficiently sensitive to interface characteristics
3. NDE is unable to detect poor surface preparation
4. bond strength may be controlled by the weakest spot, but NDE provides average bond strength

2-1-5 Fracture mechanics of adhesive bonds

There has been a great deal of research to correlate the adhesive bond strength with its governing factors, such as loading mode, dimension and elastic properties of adhesive bond, and intrinsic adhesive strength of the interface. One method of analysis [76] is the utilization of simple energy criterion for fracture of adhesive bonds in terms of work of detachment, Wa, since the detachment initiated by pre-existing flaw and/or debond proceeds with release of mechanical energy, either strain energy or potential energy.

The fracture energy, Wa, is the characteristic energy required for separation of the adherends per unit area of interface and is independent of the methods of measurement. It is thus regarded as the presentative of the adhesive bond strength. However, Wa is not constant but depends on the rate of separation, environment, thickness of the adhesive and test temperature, especially for viscoelastic materials [78,101]. Nevertheless, Wa should be independent of the mode of applied load; tension, shear, or peel [101,102]. Therefore, the energy criterion is widely applied to investigate fracture mechanics of adhesive bonds.

2-1-5-1 Tension mode

Whenever adhesive bonds are under an applied load, the adhesive experiences deformation due to the stored strain energy, which is basically the work of detachment, Wa. The two extreme cases in tension are shown in Figure 11; a thin adhesive layer with a relatively long debonded zone (Case 1) and a thick adhesive layer with a relatively short debonded zone (Case 2). The work of detachment was calculated for the tensile mode based on the relation proposed by Rivlin and Thomas for cohesive rupture of a deformable solid [103].

$$W_a = h_o W_b \quad \text{for Case 1} \qquad [2-7]$$

where h_o is the adhesive layer thickness in the unstrained state and W_b is the strain energy per unit volume of adhesive at the moment of failure. For the second case,

$$W_a = KcW_b \qquad [2-8]$$

where c is the length of debonded zone and K is the numerical factor, approximated by $(\pi + \varepsilon_b)^{-1/2}$, where ε_b is the tensile strain at break.

The limitation of these two extremes can be overcome by a numerical relation which is as follows;

$$\frac{W_a}{h_o W_b} = 1 - \exp\frac{-Kc}{h_o} \qquad [2-9]$$

When the overall strains are small and the adhesive may be regarded as linearly elastic with Young's modulus E, the equations of 2-7 and 2-8 can be rewritten with W_b replaced by $\sigma b^2/2E$ where σb^2 is the applied stress at break and k is approximately equals π;

$$\sigma b = (2EW_a/h_o)^{1/2} \quad \text{for Case 1} \qquad [2-10]$$

$$\sigma b = (2EW_a/\pi c)^{1/2} \quad \text{for Case 2} \qquad [2-11]$$

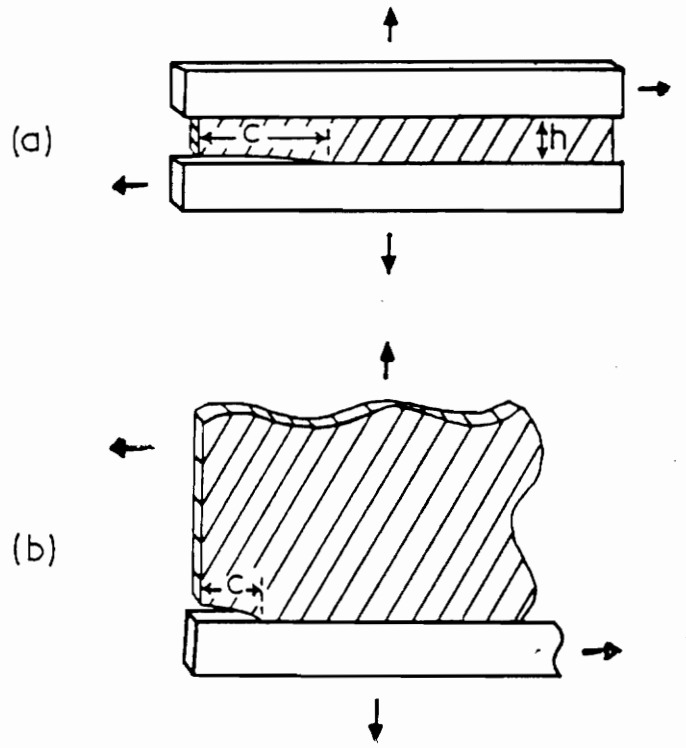

Figure 11. Thin and thick adhesive layer in tension and in shear test

As expected from Equation 2-10, the thickness of the adhesive is an important factor when the adhesive layer is thin and debonded zone is relatively large (Case 1). However, the size of the flaw or debonded zone is the governing factor in Case 2. Therefore, it can be said that smaller the critical dimension, the greater the energy density (Wb) required to cause bond failure.

2-1-5-2 Shear mode

When the adhesive bonds containing a deformable adhesive are subjected to an applied force (Figure 11), the work of detachment or fracture energy can be calculated from the stored strain energy in the adhesive. For incompressible linearly elastic materials, the applied shear stress at break for two extreme cases are given as;

$$T_b = (2GW_a/h_o)^{1/2} = (2EW_a/3h_o)^{1/2} \qquad [2-12]$$

for thin adhesive layer and relatively large debonded zone (Case 1), where G=E/3 stands for shear modulus. For case 2, thick adhesive but small debonded zone ($c << h_o$),

$$T_b = (2GW_a/\pi c)^{1/2} = (2EW_a/3\pi c)^{1/2} \qquad [2-13]$$

Since the effective shear stiffness and the uniformity of strain for Case1 are not sensitive to adhesive thickness, the shear strength for relatively thin layer of adhesive is inversely proportional to $h_o^{1/2}$ (Equation 2-12). However, in general, the size of debonded zone or flaw is much smaller than the adhesive thickness and the shear strength of adhesive bonds will not depend on the adhesive thickness but on the size of debonded zone or flaw (Equation 2-13).

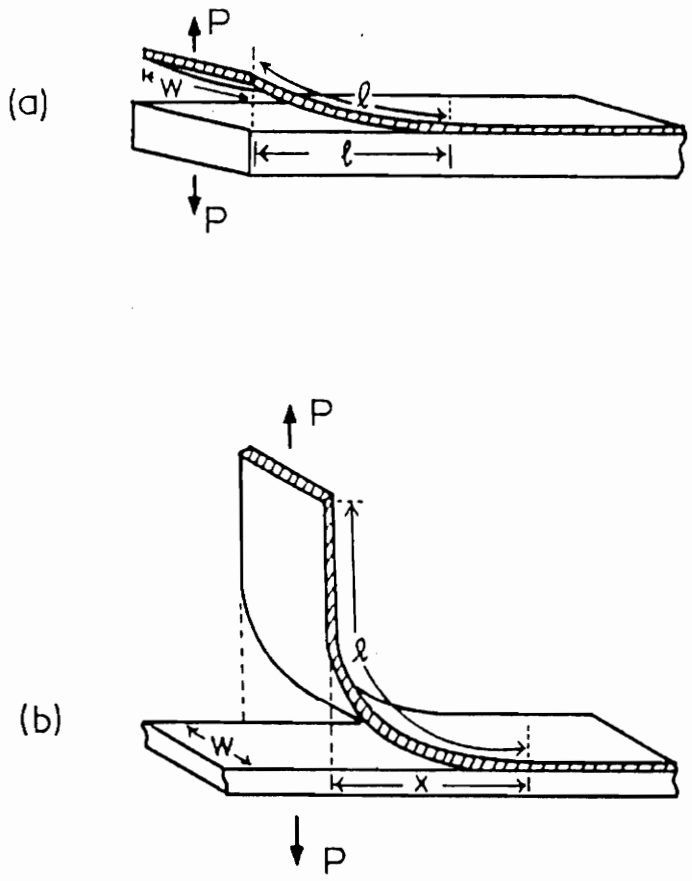

Figure 12. Cleavage test with stiff and flexible detaching portion

2-1-5-3 Cleavage mode

The cleavage mode also has two extreme cases; a very stiff and a very flexible detaching portion as indicated in Figure 12. When the detaching portion is very stiff, the work of detachment is not obtained from strain energy but from stored bending energy in the detached portion which is deformed slightly by the cleavage force P. Based on the analysis by Benbow and Roessler [104] for the the cohesive fracture by cleavage, the work of detachment is calculated for a stiff adherend as;

$$W_a = \frac{P^2 L^2}{2EI\omega} \qquad [2-14]$$

where L is the length of the cleavage portion, equivalent to the length c of the debonded zone, EI is the bending stiffness of the bent strip and ω is the width of test specimen. This equation is only valid for a small degree of bending. When the bending strip is flexible so as to be bent through 90 degree by the cleavage force P, the work of detachment is provided directly by the peel force due to the constant bending energy with separation;

$$W_a = \frac{P}{\omega} \qquad [2-15]$$

From utilization of the empirical relation, it is possible to overcome the problems from the extreme as expressed by;

$$\frac{W_a \omega}{P} = 1 - \exp\left[\frac{-L^2}{K^2}\right] \qquad [2-16]$$

where ω is either the distance between the separation front and the perpendicular plane or hypothetical distance. In either case, K can be expressed by simple bending theory,

$$K^2 = \frac{2EI}{P} \qquad [2-17]$$

Thus , Equation 2-17 allows Equation 2-16 to be much more applicable.

2-1-6 Energy dissipation and viscoelasticity

The adhesive bond strength from mechanical testing is usually larger than the predicted value from equilibrium considerations due to energy dissipation by the adhesive and sometimes by the adherend. The importance of energy dissipation in adhesive bonds can be illustrated by the peeling test [83,105]. During the steady state peeling experiment, the energy balance may be expressed as follows;

$$W_T = E_{TH} + E_{AS} + E_{AD}$$

where;

W_T = work of detachment

E_{TH} = thermodynamic surface detachment energy

E_{AS} = energy dissipated within the adhesive

E_{AD} = energy dissipated within the adherend.

The first term on the right side of the balanced equation is a measure of the intrinsic adhesion force across the interface and is, in principle, independent of peeling rate and test temperature. If the adhesive and adherend are deformed in a perfectly reversible way during the test, the intrinsic adhesion force will be the work of detachment. However, the detachment energy is much higher than the intrinsic adhesion force due to the energy dissipation by the adhesive as well as the adherend. This is true for most adhesive bond systems at normal test rates and temperatures.

Since most adhesives are polymeric materials, the effect of rate and temperature on the energy dissipation, thereby adhesive bond strength is closely related to the viscoelastic behavior of polymers [101,106]. The adhesive bond strength increases as the temperature is decreased

or the test rate is increased. In addition, the locus of failure also depends on the test conditions; cohesive failure tends to be observed at high temperature or low test rates but adhesive failure modes was dominating at low temperatures or high testing rate. The effect of test rate and test temperature on the tensile strength and strain is shown in Figure 13 and 14, respectively.

2-2 High temperature structural adhesives

2-2-1 Historical background

High temperature structural adhesives have become extremely desirable in the aerospace, military and electronic applications where environments are much more severe than those in general usage. Unfortunately, most of the polymers currently available fail to meet the rigors of such usage. As Hergenrother [108] indicated, the requirements for the high temperature structural adhesives are far simpler to describe than to achieve since they must maintain the bond strength under unimaginable conditions such as thousands of hours at 232 °C, hundreds of hours at 316 °C, or minutes at 538 °C. The first structural adhesive developed was a vinyl phenolic resin for the bonding of aircraft fuselage structure during the second world war [109]. Epoxy-based resins, modified and unmodified, have been most widely applied as structural adhesives ever since they were first developed in 1936 by Schlack in Germany [110] due to their ease of application and good performance. However, the application of epoxy resins is limited to relatively a low temperature range (below 200 °C) as a result of their low thermal distortion temperatures. Poor fracture toughness as well as low tensile elongation also limited their use and thus led to improvements by modification with toughening agents and/or curing agents.

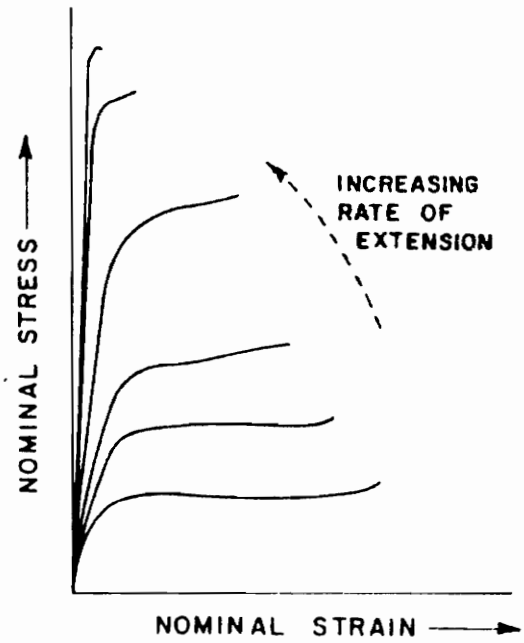

Figure 13. Effect of test rate on stress-strain behavior of polymers [107]

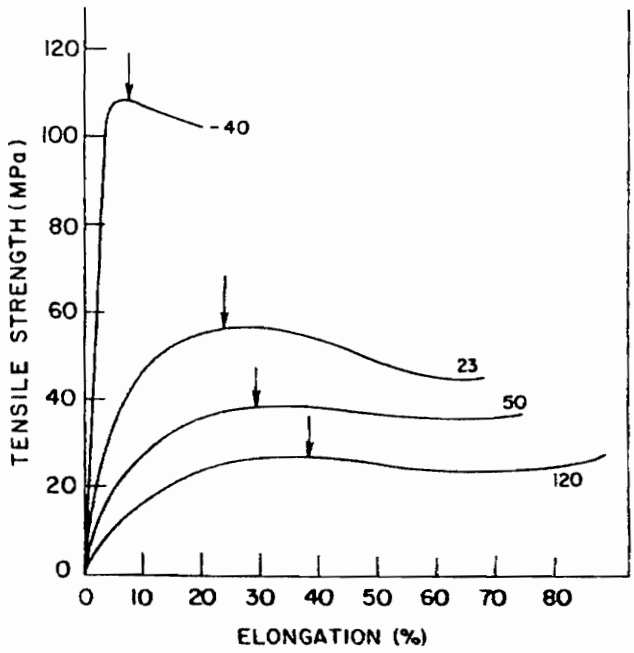

Figure 14. Effect of test temperature on stress-strain behavior of polymers [107]

A strong demand for high temperature adhesives in military and supersonic aircraft applications, which could not be satisfied by some currently available adhesives including epoxy resins has initiated the development of new polymeric adhesives which could be utilized above 200 °C. In the 1960's, several high temperature adhesives were introduced, such as polybenzimidazole (1961) [111], polyquinoxalines (1964) [112,113], polyphenylquinoxalines (1967) [114] and polyimides (1965) [115,116], which could have Tg values above 300 °C. However, the utilization of these polymers were limited again by poor processability and evolution of volatiles, despite their outstanding thermal and mechanical properties. Much research has been conducted to overcome some of these problems.

Currently, in high temperature applications, thermoplastic structural adhesives show significant potential relative to thermoset adhesives due to their versatility in multi-processing, including recycling [117]. The absence of "chemistry" during bonding could improve quality control, etc. In low temperature applications, however, a number of thermoset adhesives are still widely utilized, such as the polyurethanes [118,119], phenolics [120], polyesters [121], and acrylic adhesives [122-124].

2-2-2 Classifications

According to ASTM D-907-82 [33], a structural adhesive is defined as a bonding agent used for transferring required loads between adherends exposed to service environments typical for the structure involved. Therefore, structural adhesives must be able to distribute stress uniformly throughout the bonded area in order to have sufficient cohesive strength to sustain applied loads and to be able to withstand service environments for a period of time much greater than the expected lifetime of the structure.

Millard [125] classified high temperature structural adhesives into two groups based on the application temperature; intermediate temperature resistant adhesive (up to 204 °C) and high

temperature resistant adhesives (204-343 °C). Epoxy- based and phenolic adhesives belong to the former category, while the heterocyclic aromatic polymers such as the polyimides (PIs), polyquinoxlines (PQs) and polybenzimidazoles (PBIs), belong to the latter group. A similar classification was discussed by Lee [126], who considered three groups based on the application temperature.

The adhesives such as PBIs and PQs belonging to Group I are utilized for missiles and advanced weapon systems which need to survive only several minutes in the temperature range of 538-760 °C. The second group of adhesives such as PIs and PPQs are required to provide good adhesive bond strength for hundreds of hours in the temperature range of 288-371 °C. These adhesives are used for advanced aircraft and space vehicles. The adhesives used for military air planes, high speed civil aircraft and advanced helicopters need to provide thousands of hours of service life in the temperature range of 177-232 °C. Obviously, heterocyclic aromatic polymers are the major high temperature structural adhesives despite their shortcomings. In this section, epoxy resins, polyimides and polybenzimidazole are reviewed.

2-2-3 Epoxy-based Adhesives

Ever since their first introduction by P. Schlack in 1936 [110], epoxy-based resins have enjoyed wide popularity due to their outstanding bondability to a number of surfaces owing to their polar nature. Other attractive features include high chemical and corrosion resistance, good mechanical, thermal and electrical properties, low shrinkage upon curing, and good processability under various conditions. The epoxy resins are characterized by a three-membered ring known as the epoxy, epoxide or formally, an oxirane as shown below.

There are a number of epoxy resins used as either resin itself or blends with other polymers. Typical base resins are the cycloaliphatic or diglycidyl ether bisphenol A (DGEBA), Epoxy-novolac, Peracid-resins, and Hydantoin- resins [127]. Commercially available epoxy resins for

adhesion include Nitrile epoxy, epoxy-polyamide, epoxy-phenolic and epoxy-nylon systems [128,129].

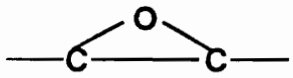

The optimum properties are obtained by curing the epoxy resin into a three-dimensional insoluble and infusible network with a curing agent or hardener. The selection of curing agent depends on the processing method, curing conditions, and physical and chemical properties desired. The curing agents are either catalytic or coreactive. A catalytic curing agent functions as an initiator for epoxy resin homopolymerization, whereas the coreactive agents act as a comonomer in the polymerization process. The final properties of cured adhesives are highly dependent on the cure process and conditions [130-135].

As network or cured materials, the unmodified epoxies are hard and hornlike substances which, depending on the curing system chosen, can be somewhat brittle in nature. To increase the versatility of the epoxy adhesives, modifiers are often utilized, which are diluents, fillers, toughening agents and flexibilizers [130-137]. In general, Tg of cured epoxies fall in the range of 50 to 200 °C [129] with few exceptions, such as phenolic resins [128,138]. It may be possible to achieve high Tg (e.g. 300 °C) but toughness will drastically decrease due to the decreased Mc. It has been reported that epoxy resins chemically modified with polysulfone functional oligomers exhibited excellent fracture toughness owing to the phase separated thermoplastic domains [139].

2-2-4 Polyimides

Polyimides are heterocyclic chain or network polymers which are characterized by the presence of imide functionality, a cyclic nitrogen bound to two carboxylic groups and may contain either aliphatic or aromatic groups in the polymer backbone.

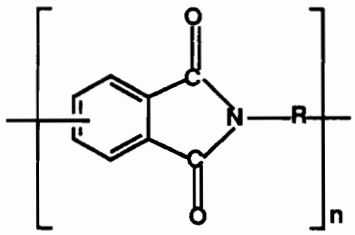

Aromatic, heterocyclic polyimides exhibit outstanding mechanical properties and excellent thermal and oxidative stabilities due to the high electron resonance structure produced by the numerous cyclical chains present in their backbone [140,141]. Polyimides have high glass transition temperatures in general above 300 °C, are briefly stable up to 500 °C in air, and do not dissolve in many solvents except possibly a few polar solvents such as NMP and DMAc.

Aromatic polyimides were first synthesized in 1908 [142] by the self condensation of 4-aminophthalic anhydride. Insolubility and infusibility of early polyimides were partially overcome by Edward [115] and Endry [116] who introduced the two-step process of aromatic polyimides in 1965. The first step involves the preparation of a poly(amic-acid) prepolymer by a condensation reaction. The prepolymers were then converted to polyimides thermally [143] by programed heating to 300 °C, or via chemical dehydration methods [144-145]. Although the two-step process had enhanced processability, it introduced a new problem; the evolution of water during cyclodehydration processing, which often resulted in foams with poor mechanical properties.

In an attempt to circumvent the volatility problem and to improve the processability, numerous research investigations have been conducted, such as the introduction of meta-substituted diamines [145-148], bulky side-groups [4,149], flexible linkage [3,19,20,150] or siloxane oligomer incorporation [151,154]. Although these approaches resulted in some improvements, such as in the commercially successful *Ultem®*, poly(ether-imide) [155], which is a true thermoplastic, many thermoplastic polyimides were not possible until McGrath and co-workers [156-158] refined several important techniques such as solution imidization method and molecular weight control with non-reactive end-groups. The solution imidization was conducted in the presence of an azeotroping agent, such as 20 weight percent of cyclohexylpyrolidinone (CHP) or 10 weight percent of cyclohexylpyrolidinone (CHP) or 10 weight % of dichlorobenzene at around 165 °C for 24 hours. Recently a so-called 'one-pot' process was introduced [158]. A number of polyimides have been developed and some of them are commercially available; Avimid K-III, Avimid-N and *Kapton®* (Du Pont), LARC-TPI (Mitsui-Toatsu), XU-218 (Ciba-Geigy), PI-2080 (Upjohn) and *Ultem®* (GE); only the latter is a true thermoplastic. The mechanical properties of selected polyimides are listed in Table 5.

Another research direction has been the preparation of thermoset polyimides through the use of low molecular weight imide oligomers terminated with acetylenic [159,160] or nadic [161,162] groups. The commercially available additional polyimides are PMR-15, Thermid 600 (National Starch and Chem Co.), Kerimid 601 (Rhone-Poulenc) and LARC-13 (NASA-Langley Res. Center). This approach allows for good processability, while maintaining high Tg and good solvent resistance. However, low fracture toughness was observed, possibly due to their highly crosslinked nature of these rigid networks..

2-2-5 Polybenzimidazole

Polybenzimidazoles (PBI s) are a class of linear heterocyclic aromatic polymer whose repeat unit contains a benzimidazole moiety as shown below. The acronym PBI is commonly used

Table 5. Mechanical properties of selected polyimides[140]

	σ(MPa)	ε(%)	E(MPa)	Tg(°C)
Ultem® 1000	105	60	296	210
PI 2080	111	10	253	310
LARC-TPI	135	4.8	372	260
Kapton®	172	70	296	
PMR-15	55	1.5	324	290

for the poly(2,2′-(m-phenylene)-5,5′-bibenzimidazole), which is commercially available from Hoechst Celanese Corp. The first PBI was prepared in 1959 [163]. Subsequently, fully aromatic PBIs were prepared via melt condensation by Vogel and Marvel in 1961 [164], which exhibited excellent thermo-oxidative stabilities. Due to their insolubility and infusibility, prepolymer techniques were introduced, wherein low molecular weight oligomers were first prepared and then converted to PBI by "curing".

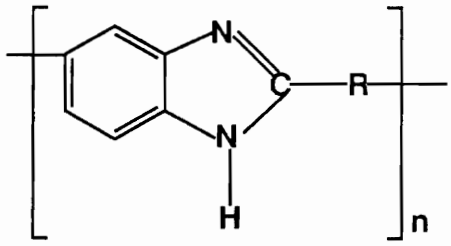

PBIs exhibit glass transition temperature of 430 °C or higher and show excellent short term high temperature stability, non-flamability and high chemical resistance. PBIs are widely utilized in high temperature applications and flame-resistant cloths either by themselves or by blending with other polymers such as Aramid or flame resistant Rayon. However, difficulties in processing and their hydrophilic characteristics remain a major obstacle. For example, the Hoechst-Celanese material sorbs about 16 percent of water.

2-3 Factors governing polyimide adhesion

As discussed previously, poor processability of polyimides has limited their versatility. In an attempt to improve the processability, poly(amic-acid)s have been utilized together with scrim cloth as a carrier, instead of fully cyclized polyimides. Scrim cloth, which is usually E-glass fabric, not only carries the poly(amic-acid) but also provides a path for the water molecules to diffuse from the adhesive bond, without inducing structural weakness. However, problems

still exist from the water evolution which occurs during cyclodehydration. Also, the effects of scrim cloth and residual solvent on the mechanical properties, as well as on the adhesive bond strength has not been fully elucidated. In addition, the effect of molecular weight control with either reactive or non-reactive end-groups has not been studied.

2-3-1 Molecular weight control

It is well recognized that all physical properties including mechanical properties are a function of molecular weight [107]. Above a critical molecular weight often associated with entanglements, most physical properties level off as shown in Figure 15. However, the zero shear viscosity (also concentrated solution viscosity) increases as a power of one of molecular weight up to the chain entanglement point and power of 3.4 thereafter (Figure 15). Therefore,it is suggested that the molecular weight should be in a certain range in order to achieve good physical properties as well as to have low viscosity for good processability.

Molecular weight control of polyimides was attempted by St. Clair and co-workers [13,19], but no details have been reported. Only a few studies have measured the mechanical properties and adhesive bond strength as a function of molecular weight of polyimides [10,11]. However, the range of molecular weight utilized in their studies were too narrow to draw any reasonable conclusions. Recently, controlled molecular weight of LARC-TPI has been marketed by Mitsui Toatsu Chem. Inc., Tokyo, Japan, and has been utilized for adhesion study [164] as well as for composite fabrication [165].

2-3-2 Scrim cloth adhesives; influence of drying conditions

Due to the utilization of poly(amic-acid) and thus scrim cloth (112 E-glass fabric), the drying conditions of scrim cloth adhesives are critical for the adhesive bond strength. In order to

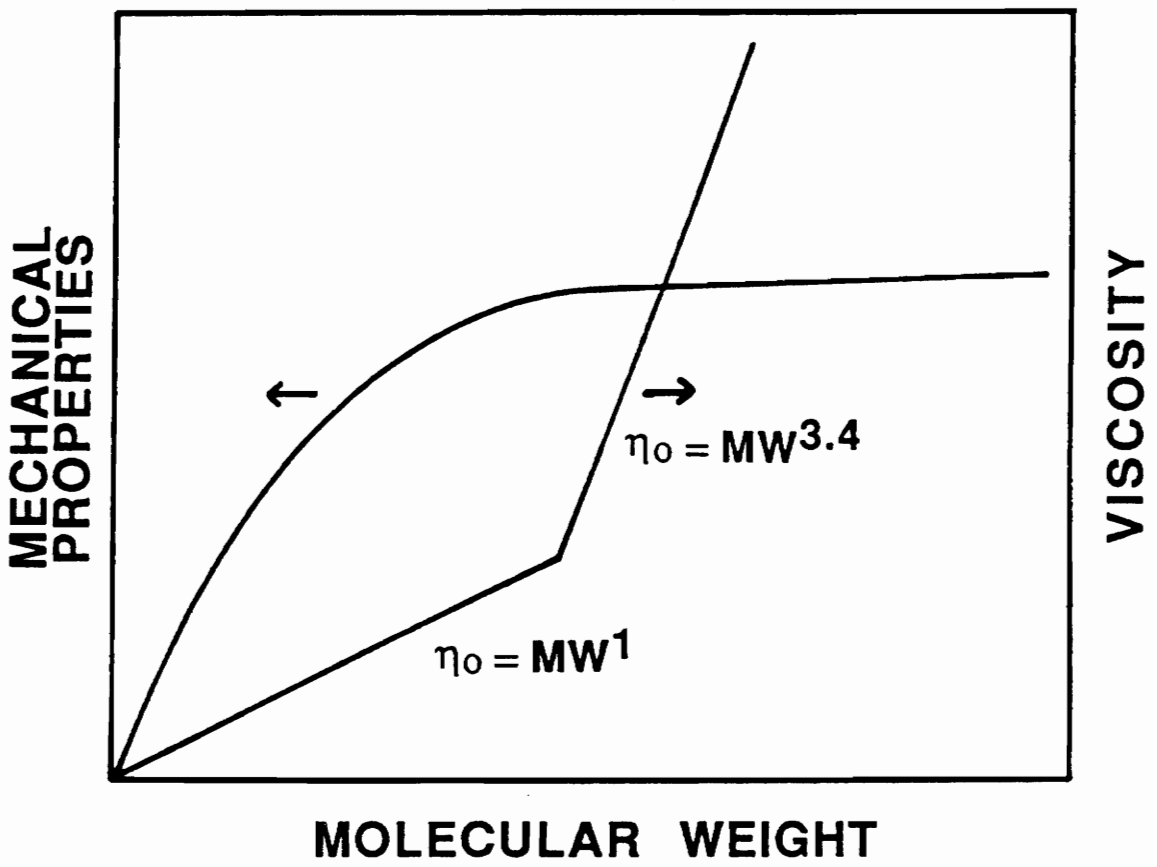

Figure 15. Relationships between molecular weight and physical properties and viscosity.

afford good processability, scrim cloth adhesives are dried at moderate temperatures (150 to 200 °C). This drying process probably leaves a partially imidized adhesive and a small amount of residual solvent in the adhesive, which might actually enhance bond consolidation. Residual solvent as well as trapped water in the scrim cloth adhesives may act as a plasticizer, thus resulting in improved flow and possibly enhanced ductility, but reduced strength and stiffness (Figure 16) [107]. Therefore, it is deemed important to control, if possible, the amount of residual solvent to achieve maximum adhesive bond strength at room temperature as well as at the elevated temperatures.

Studies by Dezern and Young [12] showed that the volatiles (which are presumably a mixture of solvent and water) decreased as scrim cloth adhesive drying temperature increased as shown in Table 6. Consistently, flow properties and room temperature adhesive bond strength decreased as scrim cloth drying temperature increased, while Tg of adhesives increases. Surprisingly, a minimum adhesive bond strength was obtained at 200 °C test from material dried at 175 °C (Table 6), but further explanation of this curious behavior was not provided.

2-3-3 Bonding conditions

In order to achieve maximum adhesive bond strength, there are three obvious variables to control; temperature, holding time and pressure. Bonding temperature has a major influence on the bond consolidation and thus adhesive bond strength, while pressure [18] and holding time [13] have also significant effects. During the bonding process, residual solvent and water molecules may escape from the adhesive bond through the scrim cloth, while bond consolidation and imidization are in progress. Certainly, the presence of residual solvent would promote bond consolidation, but too much would result in bubble formation. Thus, scrim cloth drying conditions are very important. It may not be possible to remove all volatiles by the drying process unless the scrim cloth adhesives are dried above the glass transition temperature of the adhesive. But this itself could induce chain-extension reactions and/or side re-

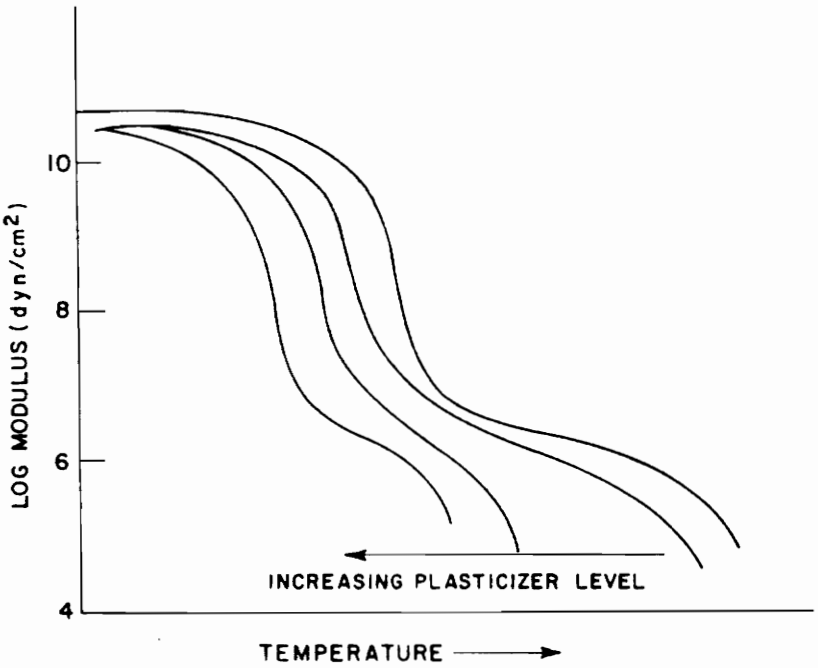

Figure 16. Effect of plasticizer on mechanical behavior of polymers [107]

Table 6. Effect of scrim cloth drying conditions on volatiles, flow and bond strength [12]

* Polyimide from BTDA+mDDS
* 15% solution in dyglyme on 112 E-glass

* Dry conditions
  1. 25 °C → 60 °C hold 30 min.
  2. 60 °C → 100 °C, hold 1 hour
  3. 100 °C → 150 °C, hold 1 hour
  4. 100 °C → 175 °C, hold 0.5 hour
  5. 100 °C → 200 °C, hold 0.5 hour
  6. 100 °C →250 °C, hold 6 hours

S.C.D.C[1].	Volatiles (%)	Tg[2] Be	Af	Flow[3] (%)	B.S.(MPa)[4] R.T.	200 °C
3	12	158	248	140	30	23
4	9	163	248	45	29	16
5	3	210	248	5	21	16
6	<1	210	254	0	18	20

1. Scrim cloth drying conditions
2. Glass transition temperature; before and after bonding
3. Measured at 343 °C, 1.38MPa for 3 min
4. Read from figure

action, resulting in the typical marginally processable adhesive if there are any reactive end-groups. Moreover, degradation of the adhesive can also occur.

Although several papers [13,14,18,19,20] are published in the literature that focus on bonding conditions, it is difficult to compare them since different types of polyimides and pre-conditions were utilized. However, in general, high bonding temperatures resulted in better adhesive bond strengths. These studies [11,14] indicated that the bonding temperatures do not have a major impact on the adhesive bond strength unless the difference is large (e.g. 100 °C). The bonding pressure has a similar effect as bonding temperatures.

One study [13] indicates that the adhesive bond strength at room temperature as well as at 200 °C decreases with holding time while others [19] show decreased bond strength at room temperature, but actually increased values at 200 °C. The difference, which was not elucidated by the authors, may be attributed to variables such as the scrim cloth drying conditions and characteristics of the polyimides, both of which are major governing factors on the bond consolidation, together with the mechanical properties of the adhesives. Also, there is a possibility of solvent degradation during the bonding process, which may also lead to a decrease in the adhesive bond strength.

2-3-4 High temperature aging

Adhesively bonded samples are sometimes exposed to high temperature (eg. 204 or 232 °C) to investigate the thermal stability of adhesive bonds, which is often called "the aging study". It can be carried out in the air convection oven or an environmental chamber. Although the reported aging effect on the adhesive bond strength differ somewhat one from another, the general trend can be summarized as follows [13,14,19,20];

1. increasing Tg

2. decreasing adhesive bond strength at room temperature

3. enhanced adhesive bond strength high temperature (eg. 204 °C)

High temperature aging might have several effects such as chain extension and/or side reactions, removal of residual solvent and trapped water, increasing degree of imidization, and degradation of solvent. Most of these would make adhesives more brittle, resulting in lower adhesive bond strength at room temperature and higher bond strength at elevated temperatures.

2-3-5 Scrim cloth characteristics

In the adhesion study of polyimides, scrim cloth (112 E glass fabric) has been widely utilized as a carrier of poly(amic-acid)s. Scrim cloth also provides a path for the solvent and water molecules to escape from the adhesive bond. Since E-glass is stable far above the Tg of polyimides and flexible, like any other cloth, it should have some effect on the adhesive bond strength, such as a composite effect. However, the effects of these factors have not been systematically studied yet.

Progar and St. Clair [13] showed that the scrim cloth adhesive of 422 polyimide whose Tg is 203 °C exhibited bond strength of 15.6 MPa at 204 °C. Water soluble LARC-TPI poly(amic-acid) [14] whose Tg is 230 °C also showed a similar trend; 18.5 MPa of adhesive bond strength at 232 °C. The adhesive bond strength is very high even at around the Tg of the adhesive, which is somewhat unusual and might be due to the scrim cloth. Since no adhesion study has been conducted on the fully imidized polyimide film adhesive (without the scrim cloth), it is difficult to deduce the effect of scrim cloth at either room temperature or elevated temperatures.

2-4 Composite materials

Composite materials have been known ever since the Israelites used chopped straw to control the residual cracking in bricks ! Asides from the man-made composite materials, there are a number of natural composites such as wood, bamboo, teeth, bones, tissue etc. Since any discussion of composite materials is would be rather be a broad subject, this review will be confined to some aspect of advanced polymeric composites. Because of the variety of existing composite materials, a universally accepted definition is not available, but one due to D. Hull [167] might be appropriate to give a brief idea of composite materials.

1. composites consist of two or more physically distinct and are mechanically separable materials
2. they can be made by mixing the separate materials in such a way that the dispersion of one material in the other can be done in a controlled way to achieve optimum properties
3. the properties are superior and possibly unique in some specific respect, relative to the properties of the individual components.

Polymeric composites have been used increasingly for aerospace, spacecraft and automobiles as well as for other applications [167-169]. The high specific strength and modulus (Figure 17) and other advantages such as high corrosion resistance and design flexibilities afford superior properties to the composite material relative to metallic materials. However, a number of obstacles, such as joining difficulty, high cost and temperature limitations need to be overcome. Advanced polymeric composite materials, in general, consist of two main parts; reinforcing fibers and matrix resin. Thus, the interaction between fibers and thermoplastic or thermosetting matrix resins plays very important role in the properties of composites.

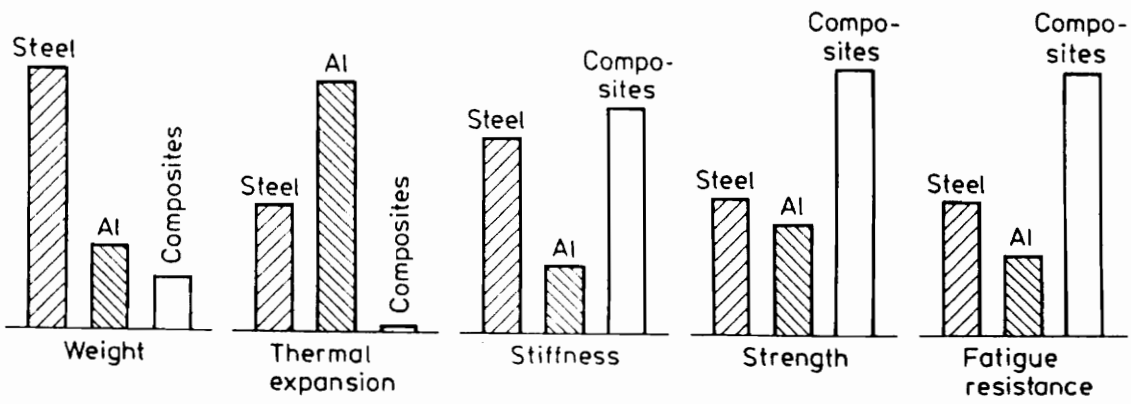

Figure 17. Comparison between conventional monolithic materials and composites [74]

2-4-1 Fibers

In advanced polymeric composite materials, the so-called advanced fibers which possess very high strength (3-4.5 GPa) and very high stiffness (80-550 GPa) coupled with a very low density (1.44-2.7 g/cc) are widely utilized due to the fact that fibrous forms are stronger and stiffer than any other forms such as as particles, flakes, whisker and sheets [169]. Various forms of glass fiber are the most common reinforcement for polymeric composite materials. Kevlar (aramid) fiber developed by Du Pont in the 1960s is much stiffer and lighter than glass fiber. Other high performance fibers are boron, silicon carbide, carbon(graphite) and alumina [167,168]. Some characteristics of these fibers are listed in Table 7. Carbon fibers of extremely high modulus can be made by carbonization of organic precursor fibers at 200-300 °C followed by graphitization at 1000-2500 °C [170-172]. The most commonly used precursor fiber is polyacronitrile (PAN) which was first introduced by Shindo in 1961 [173].

High performance carbon fibers have some physical properties which make them versatile materials for many applications. They are elastic to failure at normal temperature, which render them creep and fatigue resistant and have excellent thermo-physical properties. Carbon fibers are considered chemically inert, except in a strong oxidizing environment or where in contact with certain molten metals. A major drawback is that they are brittle and currently are expensive.

2-4-2 Matrix resins

The role of matrix resin is also critical in achieving the desired mechanical properties associated with polymeric composite materials. The matrix resins maintain fiber orientation and spacing, transmit applied load and protect the fibers from damage. A number of commercial thermoplastic polymers have been already utilized to produce polymeric composites, such as

Table 7. Characteristics of fibers [168]

Property	E-glass	S-glass	HS[b] graphite	HM[c] graphite	Kevlar 29	Kevlar 49
diameter, μm	3–20[d]	9	6–8	7–9	12.1	11.9
density, g/cm^3	2.54	2.49	1.7–1.8	1.85	1.44	1.44
tensile strength, GPa[e]	2.4	4.5	3–4.5	2.4	3.5	3.6
elastic modulus, GPa[e]	72.4	85.5	234–253	345–520	59	124
thermal expansion, 10^{-6}/°C	5.0	5.6	0.5(a)[f]	−1.2(a)[f]	2(a)[f]	2(a)[f]
			7(r)[f]	12(r)[f]	58(r)[f]	59(r)[f]
thermal conductivity, W/(m·K)	1.86	2.55	8–25(a)[f]	105(a)[f]		3.1
cost, $/kg	1.1	22–33	66–110	220–660	11–22	22–33

[a] Data culled from many sources; should not be used for design.
[b] High strength.
[c] High modulus.
[d] Most common roving sizes are 9, 10, and 13 μm.
[e] To convert GPa to psi, multiply by 145,000.
[f] (a) = axial; (r) = radial.

Table 8. Mechanical properties of polymeric matrix materials [168]

	Epoxy	Poly-imide	PEEK	Poly-amide-imide	Poly-ether-imide	Poly-sulfone	Poly-phenylene sulfide	Phenolics
Tensile strength (MPa)	35–85	120	92	95	105	75	70	50–55
Flexural modulus (MPa)	15–35	35	40	50	35	28	40	—
Density (g cm^{-3})	1.38	1.46	1.30	1.38	—	1.25	1.32	1.30
Continuous-service temperature (°C)	25–85	260–425	310	—	170	175–190	260	150–175
Coefficient of thermal expansion (10^{-5} °C^{-1})	8–11	9	—	6.3	5.6	9.4–10	9.9	4.5–11
Water absorption (24 h%)	0.1	0.3	0.1	0.3	0.25	0.2	0.2	0.1–0.2

Source: Adapted with permission from Ref. 3.

polysulfone (*Udel*®), liquid crystal polyester (*Vectra*®), Polyetheretherketone (*PEEK*®), Polyphenylene sulfide, polyetherimide (*Ultem*®), and LARC-TPI. Representative properties of common polymeric matrix materials are listed listed in Table 8 [168]. The thermosetting epoxy resins have been widely used due to their excellent properties and ease of processing. However, a major disadvantage of these polymeric networks is low toughness, which is characteristic of thermoset polymers. There has been a tremendous amount of research to enhance the fracture toughness of these polymers with incorporation of toughening agents such as functionalized rubber or thermoplastics.

Additional type polyimides have been introduced but most of them have not gained wide popularity. However, thermoset bismaleimides or BMIs have developed a siginificant number of applications [3,175]. Recently, there has been an increasing interest in thermoplastic polymeric resins for composites. Although thermoplatics have some drawbacks including high cost and high processing temperatures, they have certain advantages over thermosets, such as high toughness, multi-reforming operation, and possibly semicrystallinity, and possibly semicrystallinity, which allows for good solvent resistance [117].

2-4-3 Fabrication

Although a number of composite fabrication processes have been introduced, care should be exercised in choosing the proper manufacturing process, since this can have a profound effect on the final properties of composite materials. Processing and thermal history can have a major effect on the microstructure, internal stress and morphology. Fabrication processes are sometimes classified into two groups, namely open mold and closed mold process [167]. The major difference is that the former is a two-step process while the latter may be a one step process. Several manufacturing routes are listed in Table 9.

Table 9. Composite fabrication routes [167]

Open Mold Process

1. Hand Lay-up
2. Spray-up
3. Vacuum bag, pressure bag, autoclave
4. Filament winding
5. Centrifugal casting

Closed Mold Process

1. Hot press, compression moulding
2. Injection, transfer moulding
3. Pultrusion
4. Cold press moulding
5. Resin injection
6. Reinforced reaction injection moulding

In the prepregging process, the matrix resins must be either molten or in solution to wet the fibers. Therefore, the low viscosity thermosets have developed more rapidly than thermoplastics. However, the development of of powder prepregging process have great potential to eliminate the melting or preparing the solution of thermoplastic resins [165,166]. Among the processing routes, resin transfer molding (RTM) also shows great potential in reducing the manufacturing cost. Overall, the manufacturing process should be chosen carefully depending on the resin and the shape of the final product to achieve optimum properties.

During processing, mold release agents or release cloth is often utilized to make the final product release easily. The commonly used releasing agents are *Teflon®*, silicones and polyolefins. Since these release agents may transfer to the composite surface, surface treatments may be necessary to remove them so as to improve bondability and adhesion.

2-4-4 Surface treatment of composite materials

It has been recognized for many years that the establishment of intimate molecular contact at the interface of adherend and adhesive is a necessary but insufficient requirement to achieve strong, durable adhesive joints. Therefore, surface treatments of adherends are thought to be a decisive factor for the performance and reliability of adhesive bonding. Surface treatments have often been conducted to remove the weak boundary layer, increase surface area, provide favorable conditions and/or introduce chemical functional groups. Widely applied surface treatment techniques in polymeric composites are solvent cleaning, acid etching, grit blasting, corona discharge and gas plasma treatment.

2-4-4-1 Solvent cleaning

Since solvent cleaning is rather a primitive technique, it has often been utilized as a control process or supportive process. Widely used solvents are Methyl ethyl ketone (MEK) for *PEEK®* composite [29,30,176], and sulfuric acid and methanol for LARC-160 composite [127]. However, no major improvement of adhesive bond strength has been observed. Due to the chemical nature and toxicity of the solvents, care should be exercised for the selection of proper solvent for a given composite system.

2-4-4-2 Grit blasting

Grit or sand blasting, has been widely utilized not only in a cleaning of composite materials but also in metallic materials. Composite surfaces are bombarded by aluminum oxide or silica grit in a support of high pressure air. Thus, this technique is designed to generate a very rough surface. Wu [177] has reported that grit blasting did not improve the adhesive bond strength of *PEEK®* -graphite composite, while Moyer [27] indicated that it enhanced adhesive bond strength as well as wettability of LARC-160 composite. The former result might be due to the improper cleaning after grit blasting process. Thus, proper cleaning and a primer coating is highly recommended after grit blasting in order to preserve the clean surface, as well as to provide bonding of chopped fiber and matrix resin to the composite. Otherwise, it may act as a weak boundary layer.

2-4-4-3 Plasma treatment

Recently, plasma treatments together with corona discharge have been widely applied to improve both the wettability and bondability of many polymers [23-25], polymeric composites [21,27,29,30,176,177] and even metals [178]. A comprehensive review of plasma treatment has

also been published [26]. By definition, plasma is an ionized gas that is spatially neutral and which consists of radicals, excited molecules and atoms, ions and electrons [26,179]. Plasma can exist over an extremely wide range of temperature and pressure. The solar corona, a lightening bolt, a flame and a 'neon' sign are some examples of plasma. However, in a surface modification process, two types of plasmas are mainly utilized; cold plasma and hybrid plasma. Cold plasma, also called glow discharge, is produced under reduced pressure of gas (0.1-1 torr) and applied force (eg. radio frequency). On the other hand, hybrid plasmas are created by corona discharge at atmospheric pressure, and is thus called corona discharge.

In the plasma treatment of materials, all significant reactions are based on free radical chemistry [179]. The surface free radicals are created either by direct attack of gas-phase free radicals, ions, or by photodecomposition of the surface by vacuum-ultraviolet light generated in the primary plasma. The surface free radicals are then able to react either with each other or with species in the plasma environment.

Gas plasma treatments have four major effects on organic substrates four major effects on organic substrates; surface cleaning, ablation (dry micro-etching), crosslinking and surface activation. These effects are occuring simultaneously, and one or more of these effects may predominate depending on the processing conditions, reactor design and type of gas. A number of studies [180-181] have demonstrated that plasma treatment improved wettability as well as bondability even with inert gas due to the induced free radicals, but the effectiveness is a function of gas and other experimental factors. The treatment time should be optimized to achieve maximum bond strength.

2-4-5 Joining techniques for composites

In the joining of composite materials, adhesive bonding [182,183] and mechanical fastening have been widely utilized [182-184]. Attention has been focussed recently, however, to local-

ized welding of thermoplastic polymer matrix composites [21,185]. Adhesive bonding has the advantage of continuous connection which avoids large stress concentration points, resulting from cutting fiber when holes are drilled. However, in many structures, mechanical fasteners are still utilized due to their advantages over adhesive bondings such as ease of inspection, manufacture, maintenance and repair. Hence adhesive bonding and mechanical fastening are important in joining structural components of polymeric composites.

2-4-5-1 Adhesive bonding

Adhesive bonding is very useful in joining thermoplastic as well as thermoset composites which can not be welded. Adhesive bonding offers a number of advantages over mechanical fastening despite its drawbacks [26,179]. Adhesive joints have uniform distribution of applied loads, and high damage tolerance. However, the thermal stability of joined composites is usually limited to that of the adhesive. Adhesive bonding conditions should be carefully chosen so as to achieve good bond consolidation without deforming the composites. For most cases, surface treatment has to be conducted to achieve strong and durable adhesive bonds.

2-4-5-2 Welding

Since a welding process requires flow or "melting" of materials to be joined at the interface, thermoplastic polymers have emerged as a promising composite matrices, due to the fact that they are weldable [185-187]. Depending on how the heat is supplied, welding can be broadly classified as: 1). thermal bonding (hot gas welding, extrusion welding, hot- tool welding and infrared welding); 2). friction welding (spin welding, angular vibration welding, orbital welding, vibration welding and ultrasonic welding); 3). electromagnetic bonding (resistance(implant) welding, induction welding, dielectric heating and microwave heating). Each method has advantages and disadvantages depending on the geometry of the composite and its cost. The

major advantages of welding is that usually no adhesives are required. Therefore, the application temperature may be as high as that of the composite matrix transition temperatures (Tg, Tm, etc.)

2-5 Titanium alloy adherend

2-5-1 Titanium and its alloys

Titanium is ninth most abundant element (0.6%) of the earth's crust in the form of ilmenite ($FeO - TiO_2$), rutile (TiO_2) and others [188]. Titanium and its alloys are very valuable materials in advanced aircraft, military and nuclear power plant applications [189] due to the some outstanding characteristics such as a relatively low density (4.507 g/cc for α and 4.35 g/cc for β at 20 °C), high melting point (1668 °C, estimated boiling point-3260 °C) and good corrosion resistance [188,190,191]. Because of its high cost, it is commonly used only where no other materials can perform adequately. The mechanical properties of some commercial metals are listed in Table 10.

Titanium has two crystalline structures; α-phase below 882.5 °C and β-phase above that [190,191]. The α-phase, close-packed hexagonal structure, has high strength, high toughness, good creep resistance and weldability but has poor formability. On the other hand , the β-phase, body centered cubic, possesses good formability, hot and cold strength, but low creep resistance. In order to combine the good properties of α-and β-phase, numerous titanium alloys have been prepared [191]. Ti-6Al-4V alloy has a mixed phase of α and β over a wide range of temperatures. Vanadium was added to produce the β-phase at low temperatures, while aluminum is added to stabilize α-phase of titanium in the high temperature range and also to strengthen the α-phase by solid solution. The α-β alloys show good fabrication

Table 10. Mechanical properties of selected metals [168]

	E (GPa)	σ_y (MPa)	σ_{max} (MPa)	K_{Ic} (MPa $m^{1/2}$)
Pure (ductile) metals				
Aluminum	70	40	200	100
Copper	120	60	400	to
Nickel	210	70	400	350
Ti-6Al-4V	110	900	1000	120
Aluminum alloys (high strength - low strength)	70	100-380	250-480	23-40
Plain carbon steel	210	250	420	140
Stainless steel (304)	195	240	365	200

characteristics, high strength at ambient temperature and moderate strength at elevated temperature strength, resulting in excellent materials for aerospace applications [192].

The surface of titanium and its alloys is always covered with titanium oxides as a consequence of its high reactivity. There are three oxide forms; rutile, brookite and anatas [185]. Among them, rutile is the most stable and is found in the titanium ore. Rutile is formed at the highest temperatures followed by brookite and anatas. All of the oxides can be prepared synthetically [191].

2-5-2 Surface treatment of titanium alloys

Ever since an alkaline hydrogen peroxide etch (AHP) was developed in early 1970s [193], a number of surface treatment methods have been introduced to achieve strong, durable adhesive bonds even in hot/humid conditions [194]. The various surface preparation techniques developed for improving adhesive bond strength and durability can be broadly classified into four groups depending on the nature of process; mechanical, chemical, mechano-chemical and electrochemical. Table 11 lists the process according to this classification [194]. Among them, chemical (etching) and electrochemical (anodization) process are widely applied. The most common processes are chromic acid anodization (CAA) and sodium hydroxide anodization (SHA). Recently, plasma-spray techniques have been introduced and exhibited great potential [195].

Titanium alloys have traditionally been treated to form a stable oxide at the adherend surfaces for adhesive bonding. This can be achieved by anodizing in acid or basic media or by etching [196-204]. The anodization generally yield rather thick oxides (a few hundred angstroms). A commercially available chemical treatment, Pasa Jell, provides a relatively thin oxide layer (less than 100 anstrom). Pasa Jell, which was introduced in the early 1970s, has been widely utilized as a reference technique. According to Proger [201], the thin oxide seems to provide

Table 11. Classification of surface pretreatment for adhesive bonding of Titanium [35]

Classification	*Process*	*Results*	
		Joint strength	*Joint durability*
Mechanical	Alumina blasting	Good	Adequate
	Mechanical abrasion	Poor	Poor
Chemical	Alkaline cleaners	Poor	Poor
	TURCO 5578	Adequate	Adequate
	Nitric–hydrofluoric acid etch	Adequate	Poor
	Phosphate–fluoride	Adequate	Poor
	Modified phosphate–fluoride	Adequate	Slightly better than the conventional
	Pasa Jell 107	Adequate	Adequate
	Alkaline-peroxide etch	Good	Good
	Activated chemical oxidation	Good	Good
Mechanico-chemical	VAST process	Good	Poor
Electrochemical	Anodising in chromic acid–fluoride mixture	Good	Good
	Anodising in alkaline-peroxide solutions	Good	Good
	Cathodic deposition from non-aqueous solutions of aluminium nitrate	Adequate	Adequate

excellent durability and it is believed that the thinner oxide is more stable than the thicker one at high temperatures (eg. 232 °C).

Studies on the surface treatment of titanium alloys for adhesive bonding have shown that the durability of adhesive bond depends on the morphology, thickness, acidity/basicity, roughness mechanical properties and surface energy of the oxide. Therefore, proper surface treatment is important to provide a favorable oxide surface needed for a strong, durable adhesive bond. Titanium oxide can have either a crystalline or amorphous structure. Most studies have indicated that amorphous titanium oxide is obtained by the chemical and electrochemical surface modifications. However, Allen and co-workers [193,205], and Matz [206] have reported that the crystalline oxide (rutile) was obtained. Since anatas (either amorphous or crystal titanium oxide) change to rutile when subjected to hot/humid environment, the transformation of titanium oxide accompanies oxygen diffusion into titanium alloy and volume contraction, resulting in reduced durability [194,207]. Thus, it is believed that rutile is the best for hot/humid conditions [204].

2-5-3 Joining of titanium alloys

Although a number of methods are available, adhesive bonding is predominantly applied to join the titanium alloy over other methods. It is sometimes difficult to utilize mechanical fastening due to its high strength and high electro potential [191]. If titanium is coupled with less noble materials such as aluminum alloys, carbon steel and magnesium alloys, these less noble materials will suffer severe corrosion problems. Therefore, it is difficult to find proper rivets or bolts and nuts which do not corrode in a coupling with titanium alloys, resulting in wide application of adhesive bonding. Adhesive bonding is also preferred to reduce air-friction especially in supersonic aircraft [208].

Chapter III. Experimental

Although polyimides have outstanding properties and are known to be an excellent candidate for high temperature structural adhesives, the investigation of their adhesive characteristics have been mostly limited to studies with poly(amic-acid) coated scrim cloth adhesives, because of their insolubilities and infusibilities when fully cyclized. The relatively recent development of true thermoplastic polyimides such as the General Electric Material known as *Ultem*® 1000 has offered a new avenue for material development. In our laboratory even higher performance polyimides have been generated via new techniques such as solution imidization, molecular weight control with non-reactive end groups and siloxane incorporation, which have made polyimides even more attractive as high temperature structural adhesives. Hence, it was deemed important to investigate the adhesive properties of fully imidized but thermoplastically processable polyimides with and without the use of the commonly used scrim cloth.

In this chapter, the first topic covered is the synthesis of polyimide homopolymers and poly(imide-siloxane) segmented copolymers prepared via new techniques developed in our laboratory which afford true thermoplastic fully cyclized polyimides. This section is followed by a description of the adhesive property measurement of these polyimides bonded with Ti-6Al-4V alloy and *PEEK*®-graphite composite adherends. The adhesive characteristics were

investigated as a function of test temperaature, residual polymerization or casting solvent, molecular weight control with non-reactive end groups, polyimide structure and poly(dimethyl-siloxane) incorporation. The influence of surface modifications of *PEEK*®-graphite composites on adhesive bond strength was also investigated. The mechanical properties of polyimide homopolymers and poly(imide-siloxane) segmented copolymers were studied via stress -strain measurements and dynamic mechanical behavior. Finally, the surface treated *PEEK*®-graphite composites were characterized by X-ray Photoelectron Spectroscopy (XPS), Scanning Electron Microscopy (SEM) and contact angle measurement.

3-1 Synthesis and characterization of polyimide homopolymers and segmented copolymers

3-1-1 Reagents and solvents

High glass transition, linear, thermoplastic polyimides were synthesized from a number of aromatic diamines and aromatic dianhydrides in a dipolar aprotic solvent. It is also possible to utilize one or more diamines or dianhydrides. A great number of diamines and dianhydrides have been developed [209] and some of them are commercially available. In this research, 3,3′ and 4,4′ diamino-diphenyl-sulfone (m- and p-DDS) and 4,4′ phenylene diamine (p-PD) were chosen as diamine moieties, and 3,3′,4,4′-benzophenone tetracarboxylic dianhydride (BTDA) and hexa-fluoro dianhydride (6FDA) as dianhydrides as shown in Figure 18. Additionally, α-ω-aminopropyl terminated poly(dimethyl-siloxane) (PDMS) oligomers were utilized in combination with m-DDS to enhance the processability and properties. The latter included reduced water up-take, inhanced impact resistance, improved weatherability, and surface modifications. The detailed synthesis of PDMS has been described previously [210].

A mono-functional phthalic anhydride was used as an end-capping agent to control the molecular weight as well as to provide non-reactive end groups which enhanced melt processability and stability.

Due to the highly polar nature of monomers, N-methyl- pyrollidinone(NMP) was exclusively utilized as a solvent for homopolymerizations, while a cosolvent, tetrahydrofuran (THF), was use for copolymerization due to the solubility limitation of siloxane oligomers in NMP. Additional solvents, such as cychlohexyl-pyrollidinone (CHP) or diclorobenzene (DCB) were used as an azeotroping agent in the solution imidization method chosen for the cyclodehydration process. All reagents and solvents utilized in this research are listed in Table 12.

3-1-2 Purification of reagents and solvents

Since the purity of monomers and solvents is a decisive factor for high conversions and high molecular weight, it is very important to have extremely high purity monomers and solvents, and to use proper purification techniques. The dianhydrides, such as BTDA (Allco) and 6FDA (Hoechst Celanese Corp.), were obtained as a white crystalline solids of high pure monomer grade. They were used only after drying at 150 °C for 12 hours in an air convection oven. This treatment is useful to form anhydride moieties from any hydrolyzed diacid functionalities [211].

Diamines such as m-DDS and p-DDS were obtained as a fine white powder (98% purity) and were recrystallized in deoxygenated methanol. A maximum dissolution of diamine was obtained in near boiling point of methanol, followed by cooling to room temperature to achieve a crystal form of the diamine. After filtering and drying at 100 ° C for overnight, the purified diamine was stored in a desiccator until needed. On the other hand, pPD and PA were purified by a sublimation method which was carried out near the melting point of monomer under reduced pressure. White crystals were collected and stored in a desiccator. High purity was further verified by measuring the melting point of the monomers.

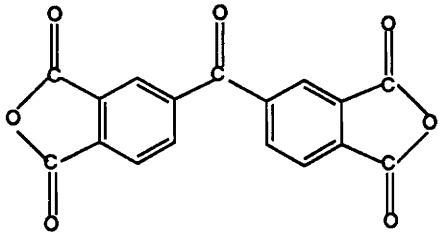

Benzophenone Tetracarboxylic Dianhydride (BTDA)

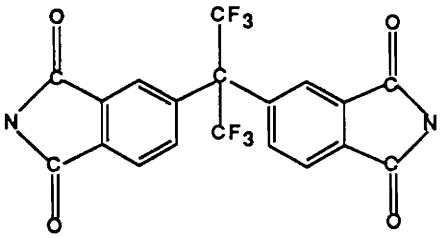

Hexafluoro Dianhydride (6FDA)

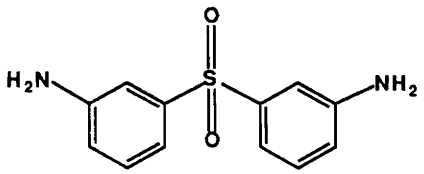

3,3'-Diaminodiphenyl Sulfone (mDDS)

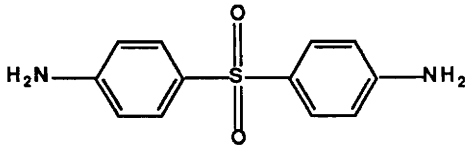

4,4'-Diaminodiphenyl Sulfone (pDDS)

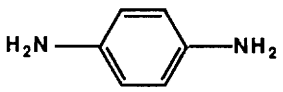

4,4' Phenylene Diamine (pPD)

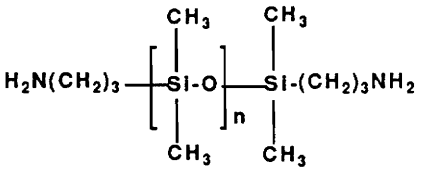

Polydimethylsiloxane (PDMS)

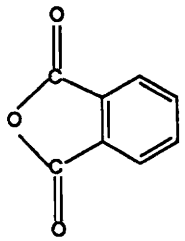

Phthalic anhydride (PA)

Figure 18. Monomers used for polyimides synthesis

Table 12. Reagents and solvents used for polyimide synthesis

Reagent		MW (g/mole)	MP (°C)	BP (°C)	Supplier
Dianhydride	BTDA	322.23	224-226		Allco
	6FDA	444.25	245-246		Hoechst-Celanese
Diamine	mDDS	284.3	167-170		Aldrich
	pDDS	248.3	175-177		Aldrich
	pPD	108.14	143-145		Aldrich
End-capper	PA	148.12	131-134		Aldrich
Solvent	NMP			205	Fisher
	THF			66	Fisher
	CHP			290	Fisher
	DCB			65	Aldrich

All solvents were vacuum distilled after stirring overnight with a drying agent. NMP, CHP and and DCB were distilled under reduced pressure after stirring at least 12 hours over phosphorous pentoxide. THF was distilled at atmospheric pressure under nitrogen flow after stirring with crushed calcium hydride for 12 hours. All distilled solvents were stored in sealed flasks in a desiccator and were transferred by a syringe to minimize the exposure to moisture.

3-1-3 Calculation of PA concentration for molecular weight control

The controlled molecular weight of polymers can be achieved by an addition of a slight excess of one monomer (off-stoichiometry) or a mono-functional agent [107,212]. In this study, a combination of these two approaches was utilized to afford controlled molecular weight with non-reactive end groups. A slight excess of diamine was used to generate amine terminated polymer chains which were capped with the mono-functional phthalic anhydride. The amount of phthalic anhydride needed was calculated based on the Carrothers equation to obtain a polymer having number average molecular weights of 20,000, 30,000 and 40,000 g/mole, with non-reactive end groups. Carrother's equation is given as follows;

$$<Xn> = \frac{(1+r)}{(1+r-2rp)} \qquad [3-1]$$

where:

$<Xn>$ = number average repeat units (2DP)

DP = degree of polymerization

p = fractional % conversion

r = stoichiometric imbalance = Na/Nb < 1

Na = number of moles of dianhydride

Nb = number of moles of diamine

If we assume 100% conversion, Equation 3-1 becomes

$$<Xn> = \frac{(1+r)}{(1-r)} \qquad [3-2]$$

By rewriting Equation 3-2

$$r = \frac{(<Xn> - 1)}{(<Xn> + 1)} = \frac{Na}{Nb} \qquad [3-3]$$

With a given stoichiometric imbalance, r, the molarity of one moiety can be obtained provided the other is known. Thus, it is possible to calculate the required amount of the end-capping agent.

$$N_{EC} = 2(Na - Nb) \qquad [3-4]$$

where:

N_{EC} is the number of moles of end-capping agent.

The reason for the the factor 2 is that each mole of polymer chain needs two moles of end-capping agent to cap both ends. The amount of PA for desired molecular weight is listed in Table 13 and the model calculations are described in the following sections.

3-1-3-1 Model calculation for a homopolyimide

The calculation is based on the BTDA+mDDS polyimide with an end-capping agent PA for a target molecular weight of 20,000 g/mole. By definition, the degree of polymerization, DP, is obtained as follows;

$$DP = \frac{20{,}000}{(248.5 + 322.23)} = 35.033$$

Then, $<Xn> = 2DP = 70.110$.

Table 13. Incorporated mole percent of phthalic anhydride utilized for molecular weight control with non-reactive end-groupd

Polyimide	20K	30k	40k
BTDA+mDDS	2.7735	1.866	1.4062
BTDA+mDDS+10%PDMS	2.749	1.849	1.3937
BTDA+mDDS+20%PDMS	3.314	2.234	1.685
BTDA+mDDS+30%PDMS	3.67	4.497	-
6FDA+pDDS	3.3465	-	-
6FDA+pPD	2.688	-	-

The stoichiometric imbalance, r, is obtained with Equation 3-3

$$r = \frac{(<Xn> - 1)}{(<Xn> + 1)} = 0.9718$$

Since $r = N_{BTDA}/N_{DDS}$,

$$N_{DDS} = N_{BTDA}/\ 0.9718.$$

If we use 25g (0.07758 mole) of BTDA, the amount of DDS needed is as follows;

$$N_{DDS} = 0.07758/0.9718 = 0.07983 \text{ mole}$$

$$\text{DDS} = 0.07983 \times 248.3 \text{ g} = 19.8216 \text{ g}$$

By utilizing Equation 3-4, the amount of PA is calculated as follows;

$$N_{PA} = N_{EC}$$

$$= 2\{[\text{DDS}]\text{-}[\text{BTDA}]\}$$

$$= 2(0.07983\text{-}0.07758)$$

$$= 0.00449 \text{ mole}$$

$$\text{PA} = 0.00449 \times 148.12\text{g} = 0.6651\text{g}$$

Therefore, the amount of reagents needed to synthesize approximately 45g of polyimide having molecular weight of 20,000 g/mole with non-reactive end-groups are 25 g (0.0775 mole) of BTDA, 19.8216 g (0.07983 mole) of mDDS and 0.6651 g (0.00449 mole) of PA.

The accuracy of this calculation is confirmed by the back-calculation of a number of DDS monomer units in a polymer chain which contains two PA units.

$$K = 2\frac{N_{DDS}}{N_{PA}} = \frac{2 \times 0.7983}{0.00449} = 35.55 \ \textit{units}$$

where K is the number of DDS units in one polymer chain. The back-calculated number, 35.55, is very close to DP, 35.05. The discrepancy arises from the the error in rounding out the calculation. However, the actual molecular weight may be lower than the calculated value due to the the loss of water molecules during the imidization process and possible incomplete conversion ($<100\%$).

3-1-3-2 Model calculation for a poly(imide-siloxane) segmented copolymers

The siloxane incorporation resulted in a more complicated calculation compared to the homopolyimide case. Calculation is based on the poly(imide-10%siloxane) from BTDA + mDDS + PDMS having molecular weight of 20,000 g/mole. The molecular weight of PDMS oligomer is 1,551g/mole. Since the siloxane oligomers are amine terminated at both ends, the number of moles of BTDA equals the summation of moles of DDS and PDMS in a stoichiometric reaction.

The amount of DDS needed is calculated by the following equation with a given amount of BTDA, which provides a stoichiometrically balanced amount of monomers since $N_{BTDA} = N_{DDS} + N_{PDMS}$.

$$DDS\ (g) = Z \times BTDA\ (g) \qquad [3-5]$$

where;

DDS = amount of DDS

Z = [1-{(BTDA/(WTxPDMS)}]/[{(BTDAxWT/(1-WT)PDMS} + (BTDA/DDS)]

BTDA = amount of BTDA

PDMS = amount of PDMS

WT = weight % of PDMS incorporated

First, the amount of DDS and PDMS for a stoichiometric reaction are calculated from Equation 3-5 with a given BTDA, 25g (0.07758 mole), resulting in DDS= 17.5608g (0.07072 mole) and PDMS = 10.6402g (0.00686 mole). In order to calculate the degree of polymerization, DP, and the number average degree of polymerization, $<Xn>$, it is assumed that even distribution of PDMS oligomers over the polymer chains. Therefore, a number of monomer units found in one polymer chain can be expressed by relative molarity or relative probability. By letting $P_{BTDA} = 1$, the probability for DDS is 0.9598 and that for PDMS is 0.04015

Based on these probabilities, DP and $<Xn>$ can be obtained for 20,000g/mole molecular weight polymer.

$$\begin{aligned} DP &= 20{,}000 \,/\, (322.23x1 + 248.3x0.9598 + 1551x0.04015) \\ &= 20{,}000 \,/\, 565.39 \\ &= 35.37 \end{aligned}$$

Then, the number average degree of polymerization, $<Xn>$ is

$$<Xn> = 2DP = 70.74$$

The stoichiometric imbalance, r, is obtained as follows;

$$r = \frac{(<Xn> - 1)}{(<Xn> + 1)} = 0.9721 \qquad [3-6]$$

$$r = \frac{N'_{BTDA}}{N_{DDS} + N_{PDMS}} = \frac{N'_{BTDA}}{N_{BTDA}}$$

where;

N_{BTDA} = # of moles of BTDA for stoichiometric reaction

N'_{BTDA} = # of moles of BTDA for molecular weight of 20,000 g/mole.

The reason for varying the amount of BTDA is that the change of DDS results in a change of PDMS, which leads to the change of weight percent of incorporated PDMS. From Equation 3-6, a number of moles of BTDA for the molecular weight of 20,000 g/mole is calculated;

$$N'_{BTDA} = 0.9721 \times N_{BTDA}$$
$$= (0.9721)(0.07758 \text{ mole})$$
$$= 0.07542 \text{ mole}$$

Thus, the amount of PA required for 20,000 g/mole can be calculated from Equation 3-4;

$$N_{PA} = 2(N_{BTDA} - N'_{BTDA})$$
$$= 2(N_{BTDA} - N'_{BTDA})$$
$$= 2(0.07758\text{-}0.07542)$$
$$= 0.004325 \text{ mole}$$
$$PA = N_{PA} \times 148.12 = 0.004352 \times 148.12 = 0.6406 \text{ g}$$

A confirmation of this calculation can be made as did in Section 3-1-3;

$$K = 2(N_{DDS} + N_{PDMS}) / N_{PA}$$
$$= 2(0.07758) / 0.004325 = 35.87$$

The back-calculated value (35.87) is very close to DP, 35.37, which indicates that the calculation is reliable.

3-1-4 Synthesis of poly(amic-acid) homopolymers

Poly(amic-acid)s of homopolyimide were synthesized by a solution condensation reaction with aromatic dianhydrides in a dipolar aprotic solvent, N-methylpyrrolidone (NMP), at room temperature under nitrogen flow. The combinations of diamine and dianhydride for polyimide synthesis were BTDA + mDDS, 6FDA + pDDS, and 6FDA + pPD. Phthalic anhydride (PA) was also added to afford controlled molecular weight and non-reactive end-groups. The apparatus used for polyimide synthesis is shown in Figure 19.

The apparatus was flamed just prior to use via a Bunsen burner under nitrogen purge in order to remove any adsorbed moisture on the glassware. Next, NMP was added by a syringe into a round bottom three neck flask equipped with a nitrogen gas inlet, drying tube, and mechanical overhead stirrer. Carefully weighted diamine via a weighing pan was added while stirring. After complete dissolution of diamine, PA was added followed by the dianhydride. As soon as the dianhydride was added, the mixture turned dark red in color and an exotherm of approximately 10 °C was observed. All weighing pans were rinsed with NMP and the final solids content was controlled to 15% by weight. Approximately half an hour later, the reaction mixture changed to a golden yellow solution and no more exotherm was detected at that stage. The reaction was allowed to continue for 8-12 hours under nitrogen flow and stirring to achieve maximum conversion. The clear golden colored poly(amic-acid) was cyclodehydrated to form a polyimide. The synthetic scheme of polyimide homopolymer is shown in Figure 20.

3-1-5 Synthesis of poly(amic-acid-siloxane) segmented copolymers

Poly(amic-acid-siloxane) segmented copolymers were also synthesized by a solution condensation reaction with aromatic dianhydrides, diamines and additional aminopropyl ter-

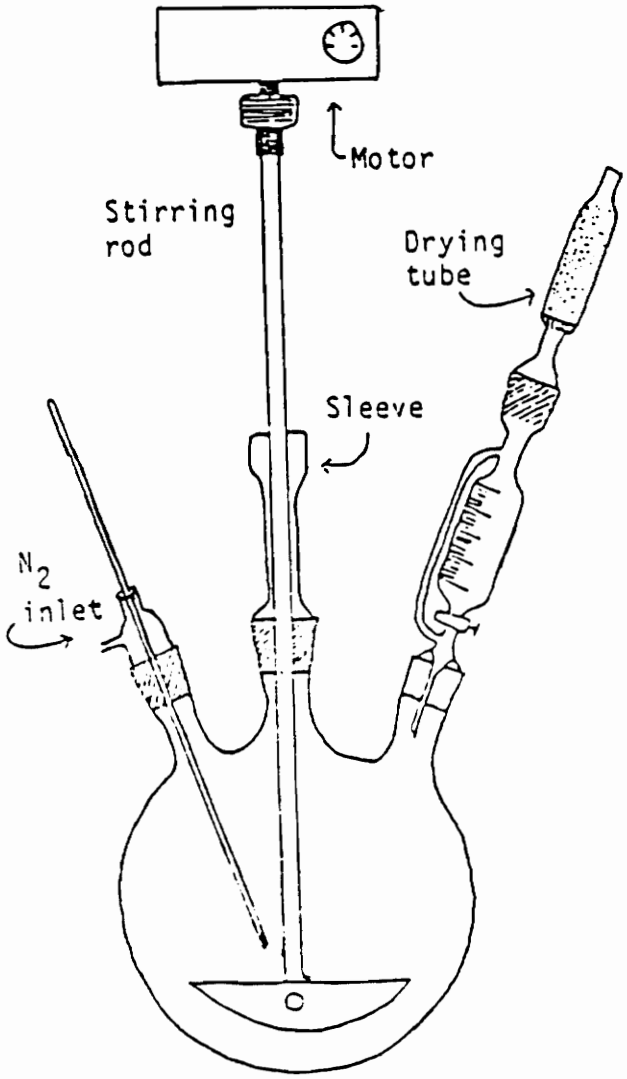

Figure 19. Apparatus used for poly(amic-acid) homopolymer synthesis

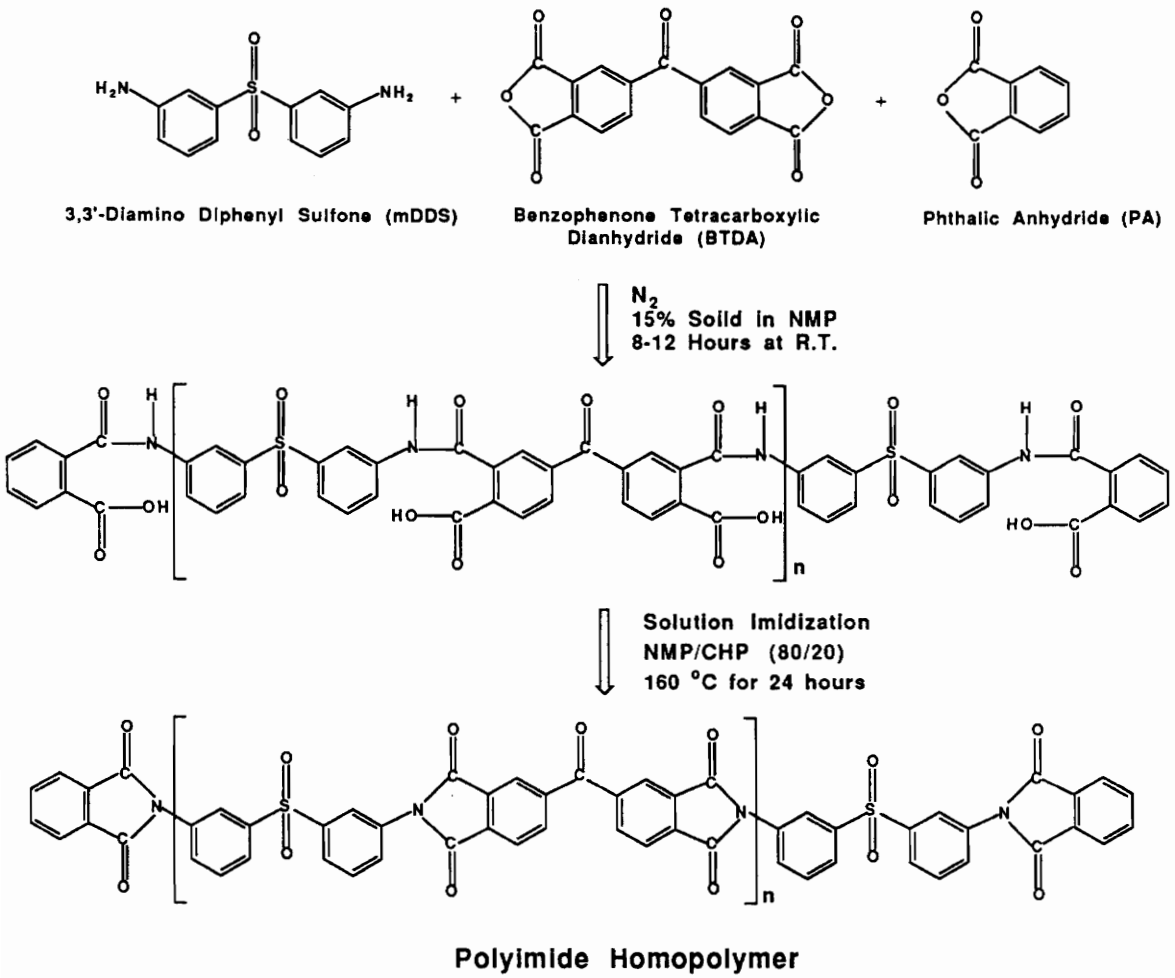

Figure 20. Synthetic scheme for polyimide homopolymer

minated poly(dimethyl-siloxane) oligomers at room temperature under the nitrogen flow. The different solubility characteristics of siloxane oligomers and diamine monomers resulted in the utilization of a solvent mixture of Tetrahydrofuran (THF) and N-methylpyrrolidone (NMP) to provide homogeneous solution mixture and thus homogeneous copolymerization. The segmented copolymers were only prepared from BTDA+mDDS+PDMS. Aminopropyl poly(dimethyl-siloxane) oligomers with a number average molecular weight of 1551 g/mole was added to have incorporations of 10, 20, and 30% by weight. The molecular weight was also controlled to 20,000, 30,000 and 40,000 g/mole by adding the desired amount of phthalic phthalic anhydride (Table 13). The same apparatus (Figure 19) but with an additional funnel was used for the segmented copolyimide synthesis.

The synthesis of poly(amic-acid-siloxane) segmented copolymers was started by dissolving BTDA in the mixture of distilled NMP and THF. After complete dissolution of BTDA, PDMS in THF was added dropwise via an addition funnel, which was rinsed with THF. The solution was allowed to react further for 10 to 15 minutes before the addition of PA and a second diamine, m-DDS. The addition of m-DDS changed the solution to a dark orange color and exhibited about 10 °C of exotherm. The reaction turned from dark orange to a golden yellow solution in approximately 10 minutes. The final solids content of the reaction solution was 15% in a mixture of NMP and THF (50:50). Finally, the reaction was allowed to proceed for 8-12 hours at room temperature under nitrogen flow and constant stirring. The golden colored poly(amic-acid-siloxane) solution was subjected to cyclodehydration to form poly(imide-siloxane) segmented copolymers. The reaction scheme of poly(imide-siloxane) segmented copolymers is shown in Figure 21.

3-1-6 Solution Imidization

Cyclodehydration of poly(amic-acid)s and poly(amic-acid-siloxane)s can be carried out in three ways; solution imidization, thermal imidization and microwave processing. However, in

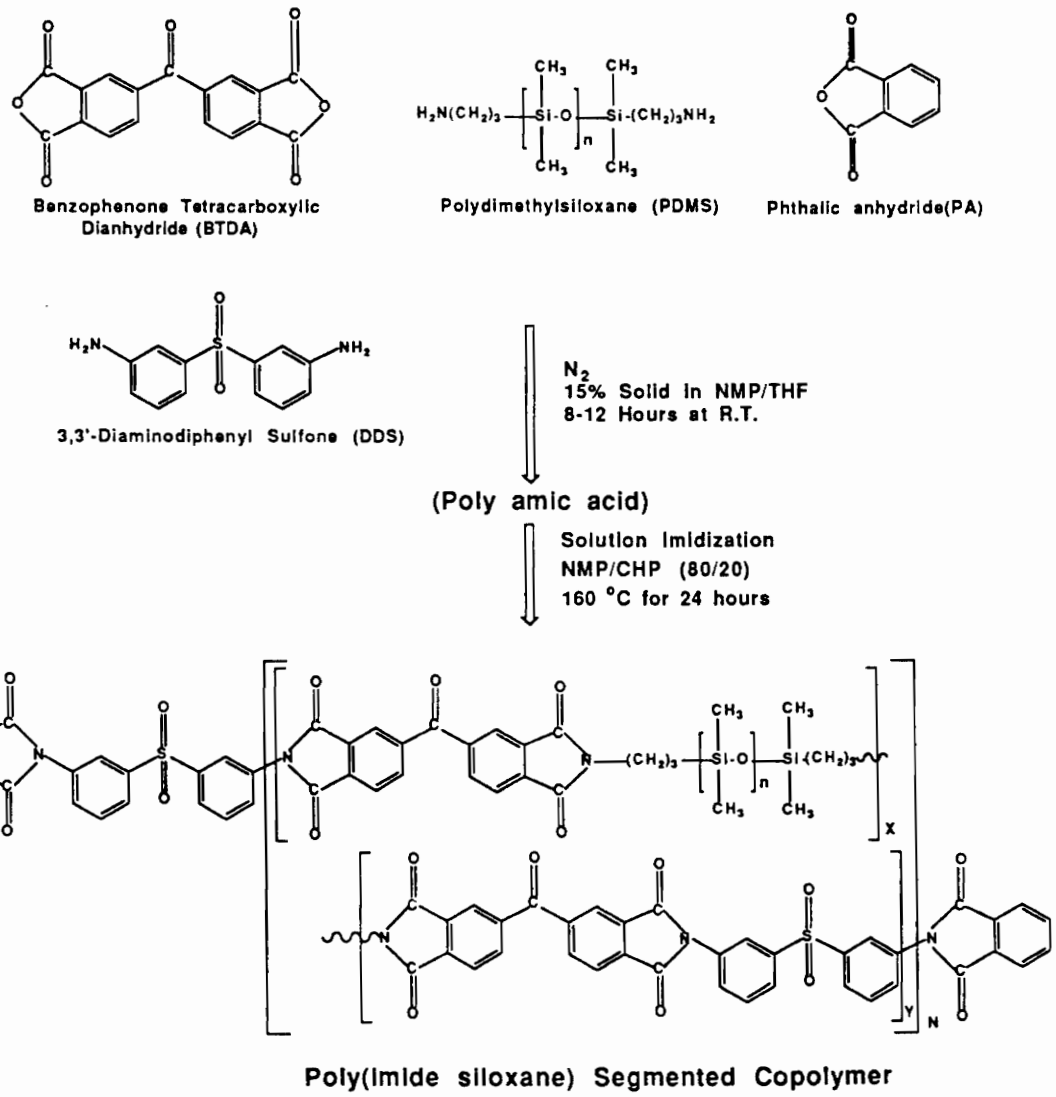

Figure 21. Synthetic scheme for poly(imide-siloxane) segmented copolymer

this study, a solution imidization technique was exclusively utilized since this method was found to be highly versatile to obtain thermoplastic polyimide homopolymers and poly(imide-siloxane) segmented copolymers [213-215]. The poly(amic-acid) was transferred to a new apparatus; a four necked round bottom flask containing CHP which was preheated to 160 °C with oil bath and equipped with nitrogen gas inlet, thermometer, Dean-Stark trap, condensor, drying tube and mechanical stirrer (Figure 22). Imidization was carried out at 15% solids concentration in a mixture of NMP and CHP (80:20 by volume) at 160 °C for 24 hours under nitrogen flow and constant stirring.

The CHP acts as an azeotroping solvent and effectively removes the water of imidization from the reaction solution driving the reaction to completion without hydrolyzing the poly(amic-acid). During imidization, a small amount of water is condensed on the dean stark trap for the homopolyimide while THF is also condensed in the copolymer case. A new technique, which is a so called, "one-pot" process was also developed in our laboratory laboratory [158]. An azeotroping agent, DCB, was added to poly(amic-acid) solution upon the completion of the reaction and the imidization was carried out under the same conditions but with 10 % by volume of DCB. At the completion of imidization, the polymer solution was cooled to room temperature and isolated into a water/methanol mixture (25:75). Well dried polymer powder was stored in a glass bottle until needed.

3-1-7 Characterization

The completion of imidization of poly(amic-acid) was confirmed by FTIR, Nicolet MX-1, with KBr pellets. The confirmation of solution imidization was made by monitoring the appearance of imide bands at 1778 and 725 cm^{-1} and the disappearance of the amide band at 1546 cm^{-1}. Intrinsic viscosity measurements were carried out in order to provide relative molecular weights. Intrinsic viscosity was measured in NMP at 25 °C using a Cannon-Ubbelohde

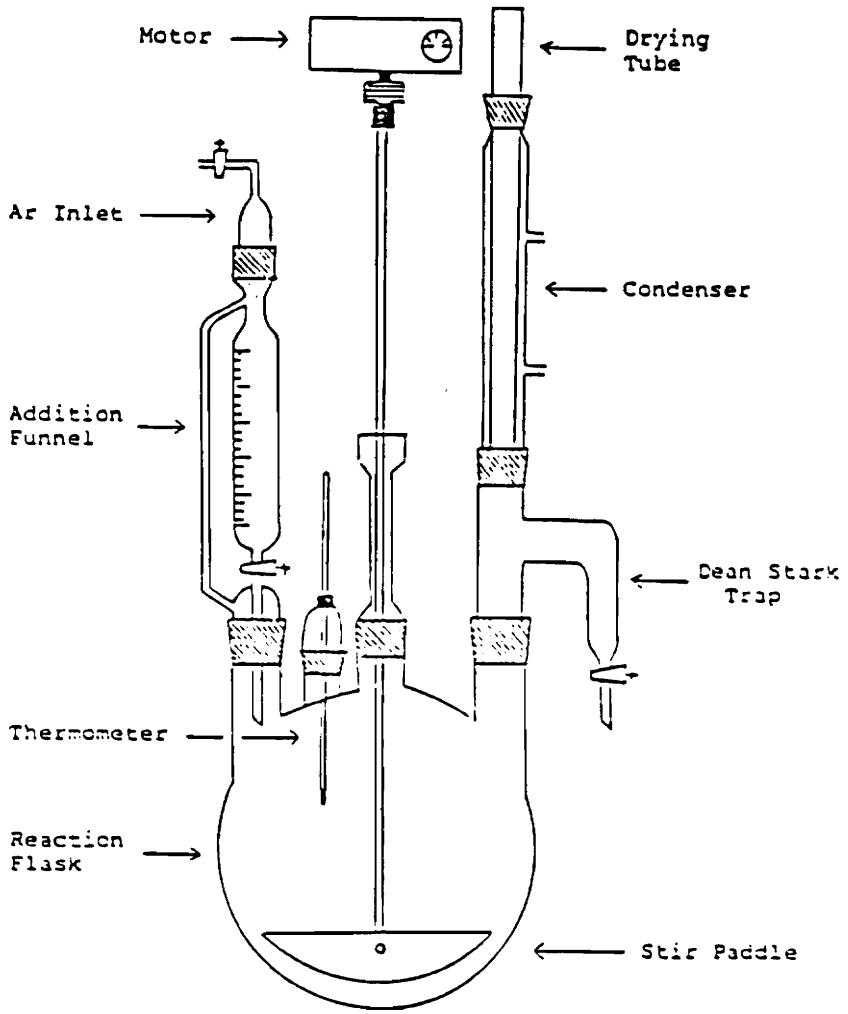

Figure 22. Apparatus used for solution imidization

viscometer. The data were obtained using four different concentrations and extrapolating to zero concentration.

Differential Scanning Calorimetry (DSC) was utilized to determine the upper polyimide glass transition temperatures with DuPont-912 or Perkin Elmer Model DSC-II at 10 °C/minute heating rate. The reported data were obtained from a second scan after heating and fast cooling. The transition temperatures were taken as the mid point of the heat capacity measure.

Thermal Gravimetric Analysis(TGA) was performed on DuPont-915 Thermogravimetric Analyzer in order to determine the relative thermal stabilities and to deduce the residual solvent from the scrim cloth adhesives. The measurements were carried out in air at the flow rate of 10 cc/minute and heating rate of 10 °C/minute. Isothermal scans were also obtained from selected samples.

The relative flow characteristics and softening points were determined by Thermal Mechanical Analyser, Perkin Elmer TMS-2. The scans were carried out utilizing the penetration mode with 10mg probe on compression molded films. The scans were run at 10 °C/minute in air.

3-2 Adhesion investigation with polyimides

3-2-1 Materials

The adhesive bond strength of polyimide homopolymers and segmented copolymers was measured exclusively from single lap shear samples. Two different adherends and a number of polyimides prepared in our laboratory as well as *Ultem*® 1000 were utilized. As listed in Table 14, Ti-6Al-4V alloys and *PEEK*®-graphite composite, APC2/AS4 $[O]_{24}$, were chosen as adherends since the former is a well known material for supersonic aircrafts and the latter is

Table 14. Materials for adhesion study

	Material	Specification	Supplier
Adherend	Ti -6Al-4V	5"x1"x0.005"	NASA LRC
	PEEK®-graphite	4"x1"x0.01"	ICI Fiberite
Adhesive	Polyimide Homopolymers		
	BTDA+mDDS	20k, 30K, 40K, UEC[1]	
	6FDA+pDDS	20K	
	6FDA+pPD	20K	
	Polyimide Copolymers		
	BTDA+mDDS+10%PDMS[2]	20K, 30K, 40K, UEC	
	BTDA+mDDS+20%PDMS	20K, 30K, 40K, UEC	
	BTDA+mDDS+30%PDMS	20K, 30K	
	Ultem® 1000 Polyetherimide		GE
Scrim Cloth	(112 glass fiber fabric)		NASA LRC
Pasa Jell 107[3]			Bancroft Co

1. Uncontrolled molecular weight
2. Poly(dimethyl-siloxane) <Mn>=1551 g/mole
3. 40% nitric acid, 10% combined fluorides, 10% chromic acid, 1% coupler and balance water

a promising material in the aerospace industries. Pasa-Jell 107 was utilized for the surface treatment of Ti-6Al-4V alloys. Scrim cloth, 112-glass fiber fabric treated with γ-APS, was used as a carrier of polyimide and utilized for residual solvent study.

3-2-2 Adherend preparation

3-2-2-1 Surface treatment of Ti-6Al-4V alloys

Ti-6Al-4V coupons, supplied by NASA Langley Research Center, exhibited a very large variation in thickness; eg., anywhere between 45 to 65 mil. Therefore, it was necessary to group them according to their thickness in order to minimize experimental error. Although Pasa-Jell 107 treatment is not the best known technique among the developed methods for the surface preparation of Ti-6Al-4V alloys [194], it is used by many adhesion scientists and was chosen because of its simpleness of treatment and high reproducibility. The grit blasting was also conducted with Trin-mix #4, a mixture of glass beads and aluminum oxide, to remove any contaminant and to increase the surface area. The grit blasted Ti-6Al-4V coupons (5x1″) were dipped into the Pasa-Jell 107 for 15 minutes [194] and washed with running tap water followed by ultrasonic cleaning in tap water and in distilled water for 10 minutes each. After drying at 100 °C for 10 minutes in a vacuum oven, the samples were primer coated to preserve the clean and favorable oxide surface for durable and strong adhesion, then further dried at 150 °C for 30 minutes and stored in a desiccator until needed. The polymer used for primer preparation was the same polymer as the adhesive dissolved in NMP, 10% by weight. All treated samples were packed in a PE bag and stored in a desiccator until needed.

3-2-2-2 Surface treatment of PEEK-graphite composites

Unlike Ti-6Al-4V alloys, there are no widely accepted surface treatment techniques for *PEEK*®-graphite composites as well as for other polymer matrix composites. In this investigation, commercial *PEEK*®-graphite composites friendly provided by ICI Fiberite, were subjected to three methods of surface preparation; 1) wash with acetone and distilled water, 2) grit blasting, and 3) gas plasma treatment. Composite adherends were washed with acetone and distilled water while being brushed with a soft copper brush. It was observed that acetone wetted the composite surface well but the distilled water did not. The grit blasting was carried out with Trin-mix #4, a mixture of glass beads and aluminum oxide. Grit blasted samples were washed with acetone and distilled water and then dried.

The plasma treatment was carried out with a Plasmod instrument at 50W and 13.56 MHz under low pressure of gas (approximately 1 torr) such as oxygen, ammonia, nitrogen or argon. The gases utilized had 99% or higher purity. The plasma treatments were conducted on the washed *PEEK*®-graphite composite samples after 5 minutes of pre-vacuum with a mechanical pump. In order to minimize contamination from the container, quartz instead of glass container was utilized. The treatment time was varied to 1, 2, 5 or 10 minutes. Also, a combination of grit blasting and gas plasma treatment was utilized. All treated adherends for adhesion study were subjected to primer coating directly after the treatment to preserve the surface and dried at 150 °C for 30 minutes. All treated samples were stored in a desiccator until needed. The polymer used for primer preparation was the same polymer as adhesive dissolved in NMP, 10% by weight.

3-2-3 Adhesive preparation

3-2-3-1 Compression molded film adhesives

The film adhesives can be prepared by solution casting or compression molding. Due to the difficulty of obtaining thick films (5-10 mil) and of removing the solvent, the film adhesives were only prepared by compression molding with Pasadena hydraulic press or Tetrahedron smart press. Due to the temperature limitation of the former (600 °F), high Tg polyimides were pressed with Tetrahedron press which can go up to 1000 °F. Well dried polyimide powder was placed between two sheets of Teflon film, ferro-type plates and steel plates. The film was pressed for 10 minutes after allowing 10 minutes under contact pressure in order to allow any moisture and solvent to escape, thereby preventing bubble formation. The compression molding temperatures were optimized by trial and error and could be correlated to the Tg of the polyimides. The pressure and holding times were fixed at 10 klb and 10 minutes, respectively, while the temperatures were varied from 300 to 450 °C depending on the nature of the polyimide. The compression molding temperature (CMT) reported was the lowest temperature at which a clear film was successfully obtained. Although a film thickness of 10-13 mil was desired, it ranged anywhere from 5 to 10 mils. Therefore, it was necessary to stack more than one layer of film to achieve 10 to 13 mil thick adhesives.

3-2-3-2 Scrim cloth adhesives

The scrim cloth adhesives have been also utilized to investigate the effect of residual solvent on the adhesive bond strength as well as flow properties. Previously, the scrim cloth has found wide application in polyimide adhesion due to insolubility and infusibility of early days polyimides. However, in this study, scrim cloth adhesives were utilized strictly for the ease of controlling the residual solvent. Scrim cloth, 112-glass fiber fabric treated with γ-APS, was

dried at 100 °C for 30 minutes prior to coating of 10% polyimide solution in NMP. Scrim cloth adhesives having thickness of 10-13 mil was obtained by repeatedly applying and drying at 50 °C for 20-30 minutes. Then, they were dried at 100 °C for 24 hours and at 150, 200, 250 or 300 °C for additional 2 hours, and stored in a desicator until needed.

The amount of residual solvent was deduced from weight loss (at 400 °C) in dynamic TGA. Since fully imidized polyimides were evaluated, it was expected that the weight loss was only from solvents. A relative measurement of melt viscosity was also investigated by pressing a scrim cloth adhesive (1 x 1 cm) at 350 °C under load of 10,000 lb for 10 minutes. The expanded area was reported as % flow, which is average of four trials.

3-2-4 Bonding preparation of single lap shear samples

3-2-4-1 Ti-6Al-4V alloy adherend

Single lap shear specimens were prepared from Ti-6Al-4V alloys and compression molded polyimide films or scrim cloth adhesives (about 10-13 mil thick). Two samples were made simultaneously to minimize the experimental error. Single lap shear samples (1/2" overlap) were prepared by sandwiching the film adhesive or scrim cloth adhesive between the treated Ti-6Al-4V adherends as shown in Figure 23. The bonding conditions were optimized by varying the bonding temperature (300-450 °C) under fixed holding time 30 minutes and pressure of either 200 psi (1.38 MPa) for BTDA+mDDS based polyimides or 500 psi (3.44 MPa) for 6FDA+pDDS and 6FDA+pPD based polyimide. The samples were heated from room temperature to 280 °C under contact pressure at a heating rate of around 8 °C/minute, then pressure of 200 or 500 psi was applied. Samples were further heated to 350, 360, 390 or 420 °C at a heating rate of 8 °C/minute and were held for 30 min, followed by air cooling to room temperature under pressure. The general bonding procedure is shown in Figure 24.

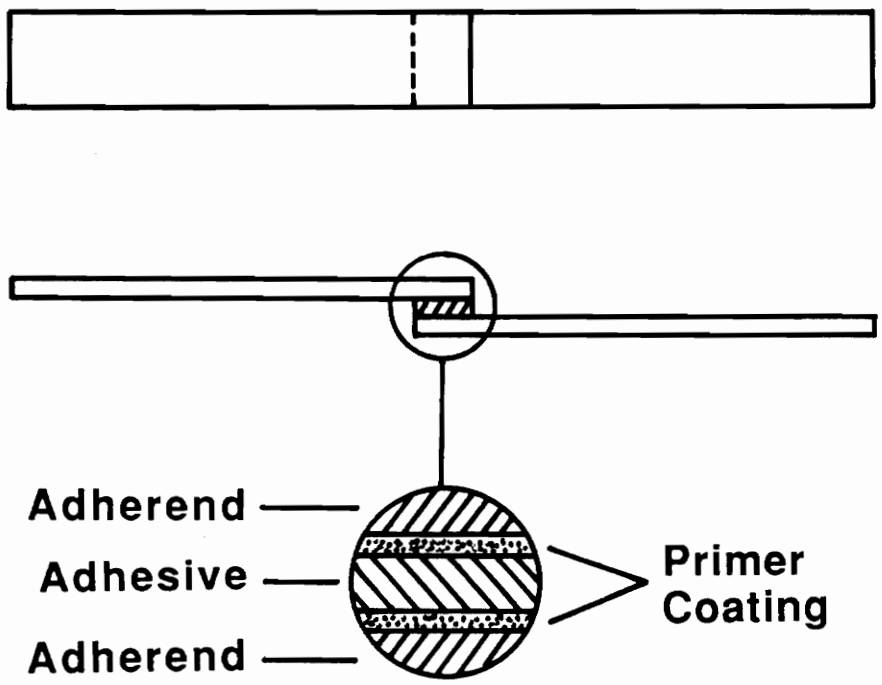

Figure 23. Preparation of single lap shear sample

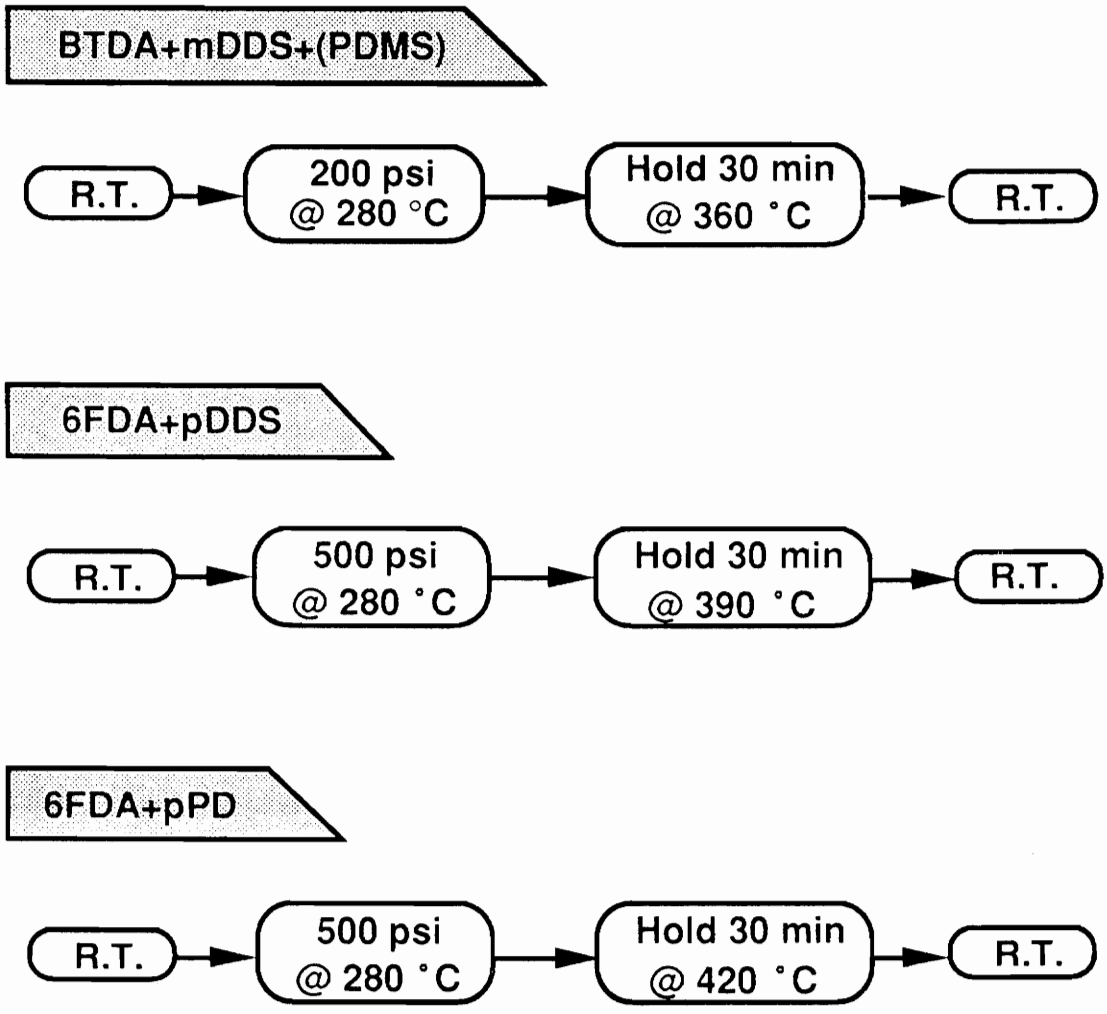

Figure 24. Bonding procedure for polyimides

3-2-4-2 *PEEK-graphite composite adherend*

The bonding temperature was optimized for poly(imide- 30%siloxane) segmented copolymer and *Ultem®* 1000 by varying the temperature from 300 to 360 °C. It was found that the highest bonding temperature without appreciable permanent deformation of *PEEK®*-graphite composite under 200 psi was 340 °C due to the thermal characteristics of *PEEK®* polymer (Tg:145 °C, Tm:345 °C). The single lap shear samples were also prepared from the surface treated *PEEK®*-graphite composite adherend and compression molded film adhesives with 1/2" overlap. The bonding process was begun by heating from room temperature to 280 °C under contact pressure. As soon as the temperature reached 280 °C, 200 psi was applied and further heating took place up to 310 °C for *Ultem®* 1000 or 340 °C for poly(imide-30%siloxane) segmented copolymer. After holding for 30 minutes, the samples were cooled to room temperature under pressure. All samples were stored in an atmospheric condition until the bond strength measurement.

3-2-5 *Testing of single lap shear samples*

Single lap adhesive samples were tested with Instron Model 1123 at a crosshead speed of 0.05"/minute. The adhesive bond strength was measured at room temperature, 100, 150, 200, 250 or 300 °C according to the ASTM D-1002. For the elevated temperature tests, environmental chamber with temperature control (Instron-3116) was used. 15 minutes was allowed to equilibriate the temperature of samples before each test. An average adhesive strength of four or more samples is reported. Some of the tested samples were analyzed by XPS in order to investigate the failure mode.

3-3 Stress-strain analysis

3-3-1 Materials

The stress-strain test is one of the simple means of measuring mechanical properties of materials. In order to correlate the polyimide structure to adhesive bond strength, as well as mechanical properties, the stress-strain measurements were conducted on polyimide homopolymers and poly(imide-siloxane) segmented copolymers prepared in our laboratory. *Ultem*® 1000 and *Kapton*® film were also analyzed for comparison purpose.

3-3-2 Sample preparation

All polyimides were compression molded to afford a film having thickenss of 5 to 10 mil except *Kapton*® polyimide which was obtained as a thin film. Dog-bone type samples were punched with a die of ASTM D-638 Type-V. Samples were punched randomly from compression molded film to minimize direction effect. The dimensions of dog-bone samples are listed in Figure 25. Around 10 dog-bone samples were prepared from 5 to 10 mil thick films since ASTM recommends to test at least 5 samples.

3-3-3 Testing

The data were collected at room temperature, 100, 150 and 200 °C, sometimes at 250 °C at a cross-head speed of 0.05"/min. Due to the time limitation of Instron (20 minutes), very highily extensible samples, especially at elevated temperatures, had to be tested at higher cross-head speed (0.1"/minutes) so as to avoid loss of data. The samples tested at this strain rate were poly(imide-20%siloxane) (20,000 g/mole) at 250 °C, poly(imide-20% siloxane) (40,000

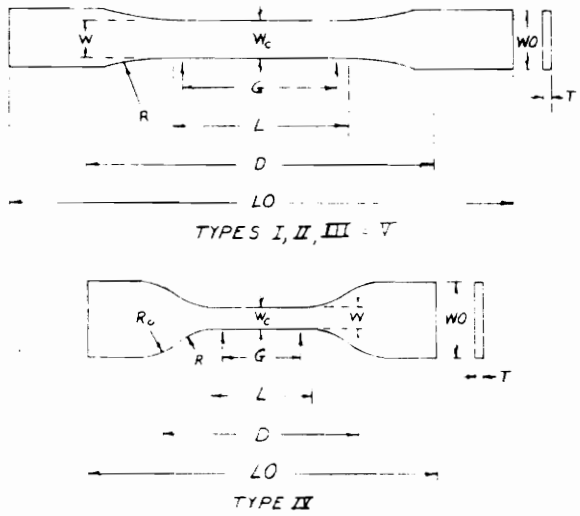

Specimen Dimensions for Thickness, *T*, mm[D]

Dimensions (see drawings)	7 or under		Over 7 to 14 incl.	4 or under		Tolerances
	Type I	Type II	Type III	Type IV[G]	Type V[I]	
W—Width of narrow section[A,B]	13	6	19	6	3.18	±0.5[G,I]
L—Length of narrow section	57	57	57	33	9.53	±0.5[I]
WO—Width over-all, min[E]	19	19	29	19	...	+6.4
WO—Width over-all, min[E]	...	...	...	...	9.53	+3.18
LO—Length over-all, min[F]	165	183	246	115	63.5	no max
G—Gage length[C]	50	50	50	...	7.62	±0.25[I]
G—Gage length[C]	...	...	...	25	...	±0.13
D—Distance between grips	115	135	115	64[H]	25.4	±5
R—Radius of fillet	76	76	76	14	12.7	±1[I]
RO—Outer radius (Type IV)	...	...	...	25	...	±1

Specimen Dimensions for Thickness, *T*, in.[D]

Dimensions (see drawings)	0.28 or under		Over 0.28 to 0.55 incl.	0.16 or under		Tolerances
	Type I	Type II	Type III	Type IV[G]	Type V[I]	
W—Width of narrow section[A,B]	0.50	0.25	0.75	0.25	0.125	±0.02[G,I]
L—Length of narrow section	2.25	2.25	2.25	1.30	0.375	±0.02[I]
WO—Width over-all, min[E]	0.75	0.75	1.13	0.75	...	+0.25
WO—Width over-all, min[E]	...	...	...	...	0.375	+0.125
LO—Length over-all, min[F]	6.5	7.2	9.7	4.5	2.5	no max
G—Gage length[C]	2.00	2.00	2.00	...	0.300	±0.010[I]
G—Gage length[C]	...	...	...	1.00	...	±0.005
D—Distance between grips	4.5	5.3	4.5	2.5[H]	1.0	±0.2
R—Radius of fillet	3.00	3.00	3.00	0.56	0.5	±0.04[I]
RO—Outer radius (Type IV)	...	...	...	1.00	...	±0.04

Figure 25. Dimensions of stress-strain samples

g/mole) and poly (imide-30% siloxane) (20,000 and 30,000 g/mole) at 200 °C, and *Ultem®* 1000 and *Kapton®* polyimide at all test temperatures. The same environmental chamber was utilized as used in adhesion test. The test was conducted after 15 minutes of waiting time to equilibriate the temperature. Although it was not expected to obtain an accurate strain and modulus since strain gauge was not used, a reasonable qualitative comparison among the tested samples could be still be made.

3-4 Surface characterization of PEEK-graphite composites

3-4-1 X-ray photoelectron spectroscopy (XPS)

X-ray photoelectron spectroscopy (XPS) is a well known surface analysis technique, which can provide information of elemental change and binding energy shifts. XPS was utilized for most of the *PEEK®*-graphite samples and for some of the Ti-6Al-4V samples to investigate the failure mode. The samples were analyzed by XPS, Perkin Elmer 5300, with magnesium K-α X-ray source at 250 mW and the take off angle of 90 degree. The reproducibility was confirmed by analyzing two or three samples from each condition. In order to reduce the exposure time to air, the plasma treated samples were transferred in an argon filled bottle as XPS utilized was not equipped with in situ plasma treatment. The chemical changes were deduced from the atomic concentration change and binding energy shift from the deconvolution of C1s peaks. Since XPS provides a relative percentage of atomic concentration, the ratios of oxygen and nitrogen to carbon were taken to minimize the experimental error. A deconvolution was not attempted on the O1s peaks because of complexity.

3-4-2 Scanning electron microscopy

The morphology of modified samples of *PEEK*®-graphite composites and Ti-6Al-4V alloys was also studied by Scanning Electron Microscopy (SEM), ISI-SX-40, at 10 or 15 KV. All samples were coated with gold-palladium to minimize the charging problem and thus to achieve a good resolution.

3-4-3 Contact angle measurement

The advancing contact angle of deionized water was measured on Rame-Hart goniometer. A deionized water drop (10 μl) was placed on the composite surface by a syringe and the sessile contact angle was measured under atmospheric conditions right after the plasma treatment. More than three drops were tried and the results were averaged.

Chapter IV. Results and Discussions

4-1 Characterization of polyimide homopolymers and poly(imide-siloxane) segmented copolymers

4-1-1 FT-IR study

All polyimide homopolymers and poly(imide-siloxane) segmented copolymers utilized in this study were prepared by a traditional two step process; eg. poly(amic-acid) synthesis followed by cyclodehydration to afford the polyimide. The cyclization step utilized a solution imidization technique developed in our laboratory [152]. The completion of imidization was confirmed by FTIR, Nicolet MX-1, utilizing imide bands observed at 1778, 1360 and 725 cm^{-1} and dissappearance of the amide band at 1535 cm^{-1}. Figure 26 shows a representative FTIR spectrum of the polyimide homopolymer from BTDA-mDDS (20,000 g/mole); other polyimides exhibited similar spectra.

Thermal imidization is often conducted at 300-400 °C, where chain extension and /or side reactions can result in insoluble infusibe polyimides [152,153]. Therefore, it is common to em-

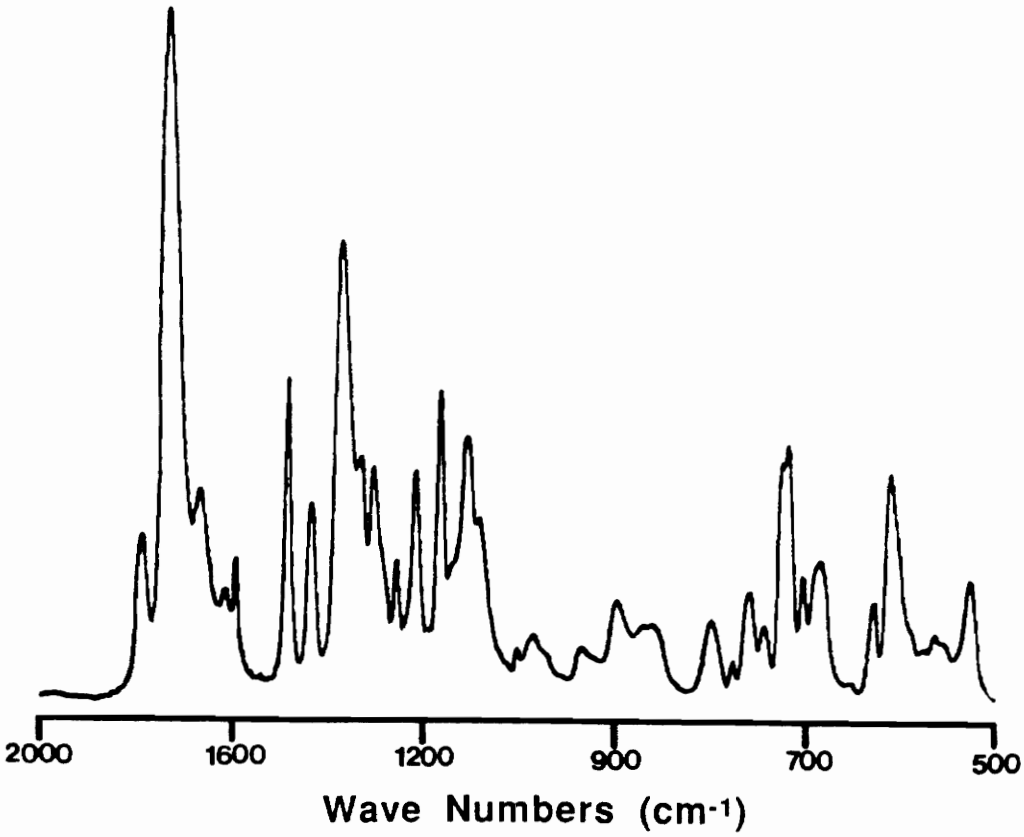

Figure 26. FTIR of polyimide homopolymer form BTDA-mDDS (20,000 g/mole)

ploy poly(amic-acid)s instead of fully imidized polyimides. However, since solution imidization was employed at the moderate temperature (160 °C) and non-reactive end groups were achieved with an end capping agent in this investigation, absolutely true thermoplastic polyimides have been successfully obtained even with the fully cyclized polyimides. This eliminates several inherent problems such as insolubility, infusibility and/or water evolution during processing.

4-1-2 Intrinsic viscosity measurement

Intrinsic viscosity measurement is a simple and inexpensive technique, and thus, is often utilized to obtain relative molecular weights of polymers provided that they are soluble in some solvent. The intrinsic viscosity can be related to the viscosity average molecular weight by the well known Mark-Houwink equation, $[\eta] = KM_v^a$. Since polyimides prepared in this investigation showed a good solubility in a high polar solvents such as NMP, the intrinsic viscosity measurements of polyimide homopolymers and poly(imide-siloxane) segmented copolymers were carried out to provide relative molecular weights, as well as to check the success of molecular weight control with non-reactive end-groups.

As listed in Table 15, intrinsic viscosities measured in NMP at 25 °C indicate that controlling the molecular weights of the polyimides was successful. As the target molecular weight increased, or as the amount of incorporated phthalic anhydride (PA) decreased, higher intrinsic viscosities were obtained. The intrinsic viscosities of uncontrolled molecular weight (1:1 stoichiometric reaction) polymers are exceptionally higher than those of controlled molecular weights, which correlates with poor flow and thus poor processability of high molecular weight polyimides. The intrinsic viscosity results do not indicate whether the theoretical molecular weight was obtained. However, studies indicates that the actual molecular weight determined by end group analysis in protin NMR is apporximately same as the target molecular weight [221] demonstrating that the method utilized in this investigation is very effective for molecular

Table 15. **Characteristics of polyimide adhesives**

Polyimide Adhesive	<Mn>	[η][1]	Tg(°C)[2]	DT(°C)[3]	CMT(°C)[4]
BTDA-mDDS	20K	0.21	259	550	340
	30K	0.26	265	545	350
	40K	0.39	263	560	380
	UEC[5]	0.95	266	565	N/A
BTDA-mDDS-10%PDMS	20K	0.27	248	550	340
	30K	0.29	248	550	340
	40K	0.40	249	555	350
	UEC	0.56	250	550	370
BTDA-mDDS-20%PDMS	20K	0.20	231	530	320
	30K	0.39	228	530	330
	40K	0.43	236	530	330
	UEC	0.92	236	525	350
BTDA-mDDS-30%PDMS	20K	0.21	209	510	300
	30K	0.24	218	505	310
6FDA-pDDS	20K	0.31	259	550	340
6FDA-pPD	20K	0.34	345(360)6	500	390

1. NMP at 25 °C
2. Measured by DSC, 10 °C/min., in 2nd scan
3. Degradation Temperature (10% weight loss in air)
4. Compression Molding Temperature (at 10klb, for 10 min)
5. Unendcapped (1:1 stoichiometric reaction)
6. Measured by DMTA

weight control of polyimides. Although it was expected that siloxane incorporation would affect the intrinsic viscosity of polyimides, no significant change was observed from siloxane incorporation as shown in Table 15.

4-1-3 Glass transition temperature determination

The upper glass transition temperatures of polyimide homopolymers and poly(imide-siloxane) segmented copolymers were measured by DSC and DMTA on the compression molded films (Table 15), and were found to be a function of molecular weight and chain rigidity as expected. The upper glass transition temperatures increased with the stiffness of polyimide backbone and molecular weight, but decreased with siloxane incorporation. Thus, the polyimide homopolymer from BTDA-mDDS (20,000 g/mole) exhibited a Tg of 259 °C and increased slightly with molecular weight, while the 10% and 20% siloxane copolymer (20,000 g/mole) had Tg values of 248 and 231 °C as shown in Figure 27. However, even the poly(imide-30%siloxane) copolymer exhibited a fairly high Tg, 209 °C. A slight increase of Tg with molecular weight is due to the increased chain entanglements, resulting in better strength retention at high temperature, while the incorporation of siloxane segments decreased it by imparting chain flexibility. Thus, a portion of the siloxane segment is miscible with the polyimides. Very high glass transition temperatures exhibited by these polyimides make them suitable for aerospace or electronic applications.

The lower glass transition temperatures of poly(imide-siloxane) segmented copolymers were not measured but the reported values [153] fall in the range of -106 to -123 °C. It was also found [153] that the lower glass transition temperatures from the siloxane domains were not detectable unless around 20 weight percent or more was incorporated, and that they depended on the molecular weight and amount of the siloxane. The upper glass transition temperatures also varied with the molecular weight of siloxane oligomer. In fact, as the molecular weight of siloxane increases, so did Tg, which is consistent with an enhanced micro-

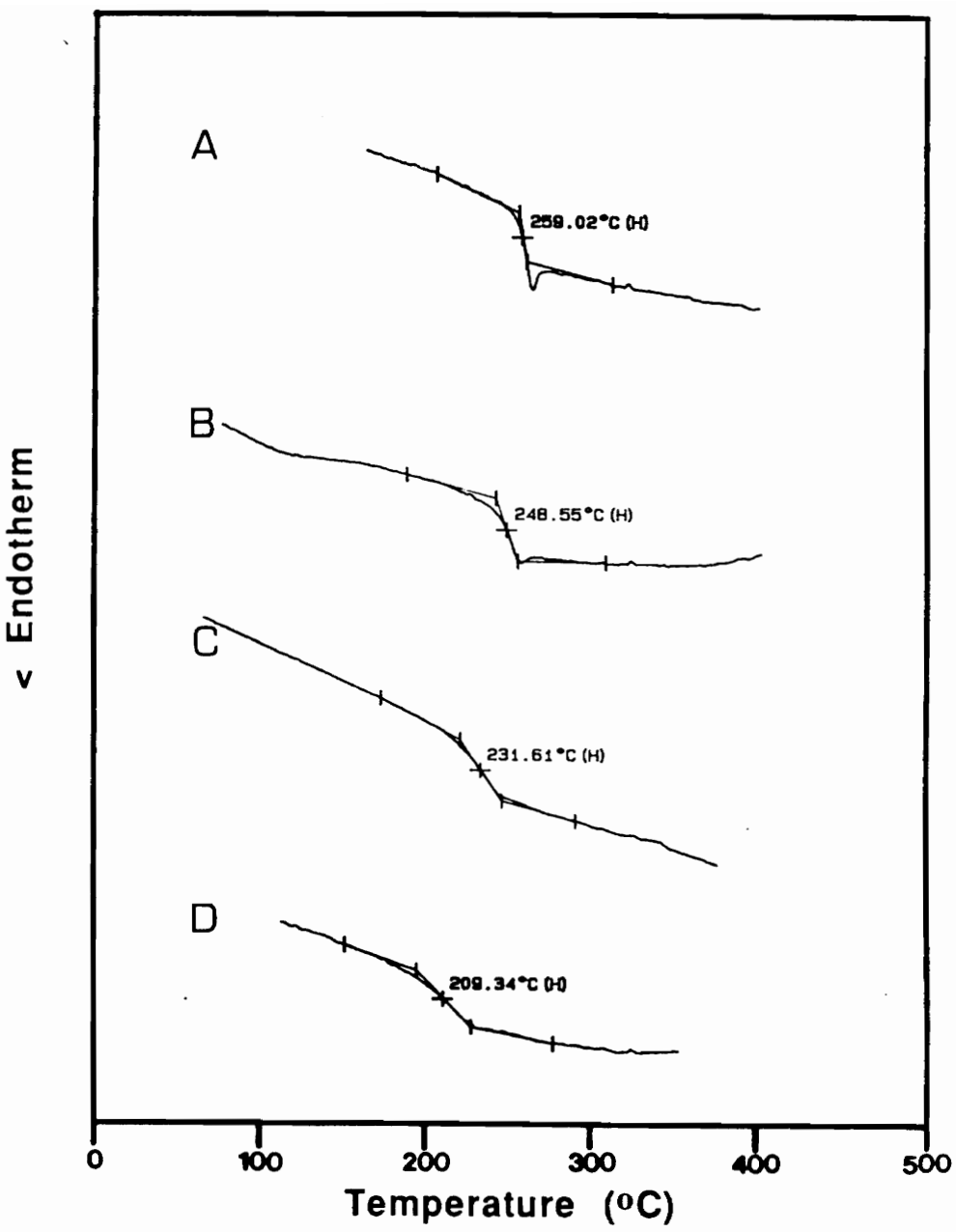

Figure 27. DSC of polyimide homopolymer and poly(imide-siloxane) copolymers (20,000 g/mole): a) Homopolyimide, b) 10%-siloxane copolyimide, c) 20%-siloxane copolyimide, d) 30%-siloxane copolyimide

phase separation as reported by York [222]. Therefore, it is recommended that the molecular weight and amount of siloxane incorporation has to be chosen carefully for a desired application. For example, a partially mixed phase may show lower moisture absorption.

4-1-4 Thermal Stability

The thermal stabilities of polyimide homopolymers and poly(imide-siloxane) segmented copolymers were estimated by thermogavimetric analyzer (TGA) in an air atmosphere either dynamically or isothermally. All samples were prepared by compression molding well dried polyimide powder. The isothermal TGA was carried out at 360 °C for 120 minutes on the polyimide homopolymer from BTDA-mDDS and its copolymers whose number aververage molecular molecular weights were about 30,000 g/mole (Figure 28). While heating to 360 °C (which took around 15 minutes) approximately 1% weight loss was detected in all samples, which might be due to the loss of adsorbed water. The homopolymer exhibited less than 2% weight loss in that condition, but it is believed that the actual weight loss at 360 °C for 2 hours in air was approximately 1% owing to adsorbed water. As the amount of siloxane incorporation increased, the weight loss also increased. The total weight loss of poly(imide-30%siloxane) segmented copolymer (30,000 g/mole) was approximately 7%, while 10% and 20% copolymers showed 2.5% and 3.5%, respectively. It is believe that aliphatic linkages in siloxane chains are responsible for increased weight loss. The isothermal TGA indicated that the thermal stabilities of polyimide homopolymers and poly(imide-siloxane) segmented copolymers under such severe conditions are excellent.

The polyimide homopolymers exhibited excellent high temperature stability without any weight loss until 500 °C in dynamic TGA, as depicted in Figure 29. All poly(imide-siloxane) copolymers also maintained good thermal stability, but degradation occurred at lower temperature. However, the char yield increased as the siloxane content increased. The char yield was proportional to siloxane content, suggesting that silicate-type structure was the

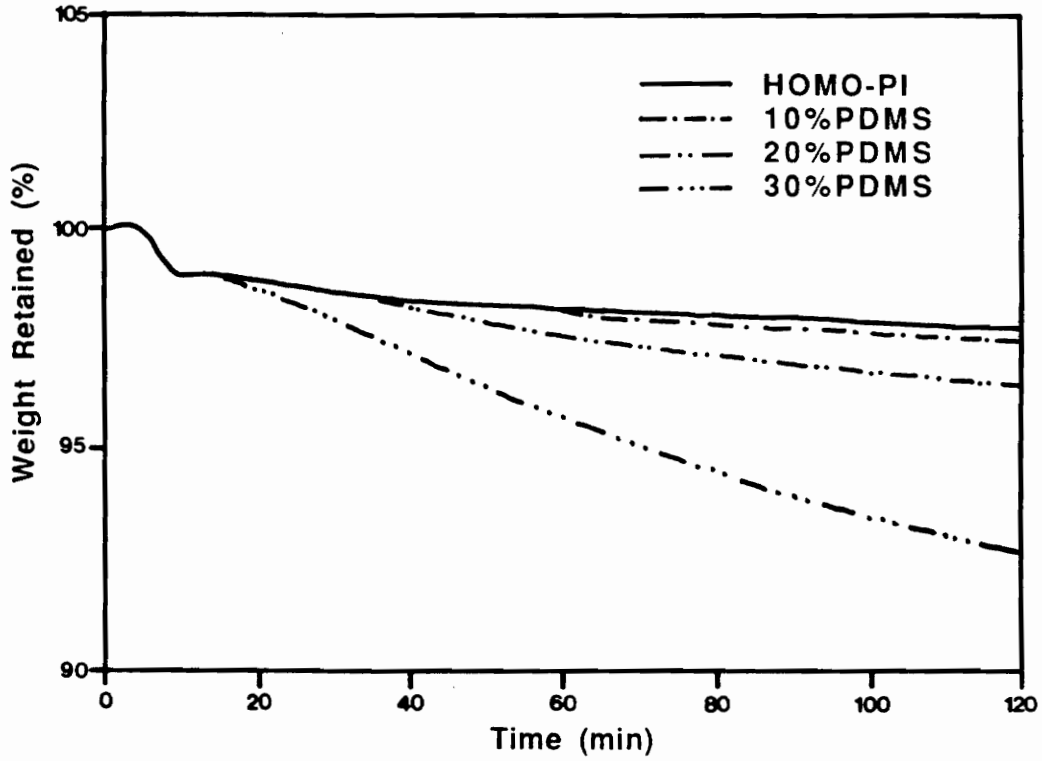

Figure 28. Isothermal TGA of polyimide homopolymer and poly(imide-siloxane) copolymers from BTDA-mDDS (30,000 g/mole) at 360 °C

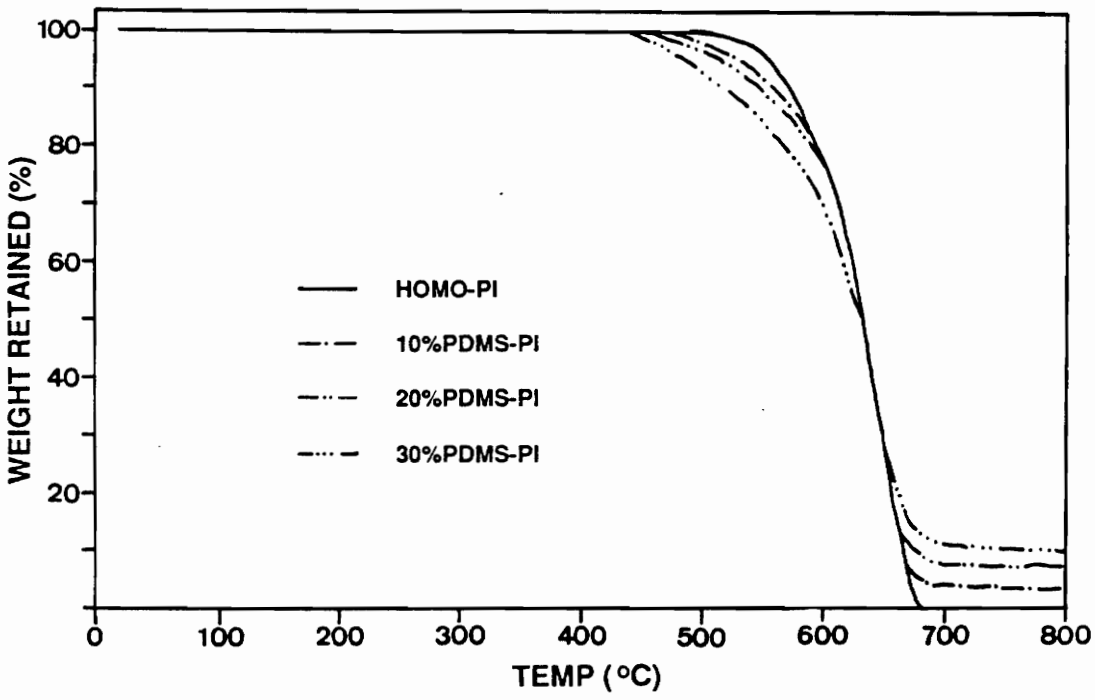

Figure 29. Dynamic TGA of polyimide homopolymer and poly(imide-siloxne) copolymers (20,000 g/mole)

principal degradation product in an air atmosphere [6,153]. The study by Maudgal and St. Clair [154] revealed that the siloxane incorporation exhibited two step degradation process but other observations were the same as ours. The degradation between 400 and 450 °C was believed to be due to the scission of aliphatic linkages in the siloxane segments leaving a relatively stable aromatic structure which degrades around 500 to 550 °C [154]. The two step degradation was possibly due to the larger portion of aliphatic linkages in their study since they utilized siloxane monomers instead of oligomers.

4-1-5 Thermo-mechanical analysis

The glass transition temperatures of polymers are often measured by thermo-mechanical analyzer (TMA) which can be used to measure the penetration depth with a probe or expansion with a hanging weight as a function of temperature. Thus, the temperature response obtained by TMA is similar to a thermo-mechanical spectrum. As indicated in Figure 30, no measurable penetration was detected, until a certain temperature range associated with Tg was reached and then a sharp penetration occurred. Since the stiffness of polymers changes significantly in the glass transition region, the inflection temperature corresponds closely to the Tg measured by other methods such as DSC. However, only glassy and Tg regions were observed because the samples were too thin to allow a long enough time to observe the entire mechanical of spectrum. Note that the curves are offset for clairty and that they represent a range of controlled number average molecular weight values which are all phthalimide end capped along with an "unend-capped" (UEC) high molecular weight control.

The inflection temperatures of polyimides obtained from TMA were a function of molecular weight and siloxane incorporation. As already seen from the DSC results , the inflection temperatures increased with molecular weight and decreased with siloxane incorporation. The penetration rates above Tg were a strong function of molecular weight, which controls the chain entanglements and thus flow behavior. The uncontrolled molecular weight of polyimide

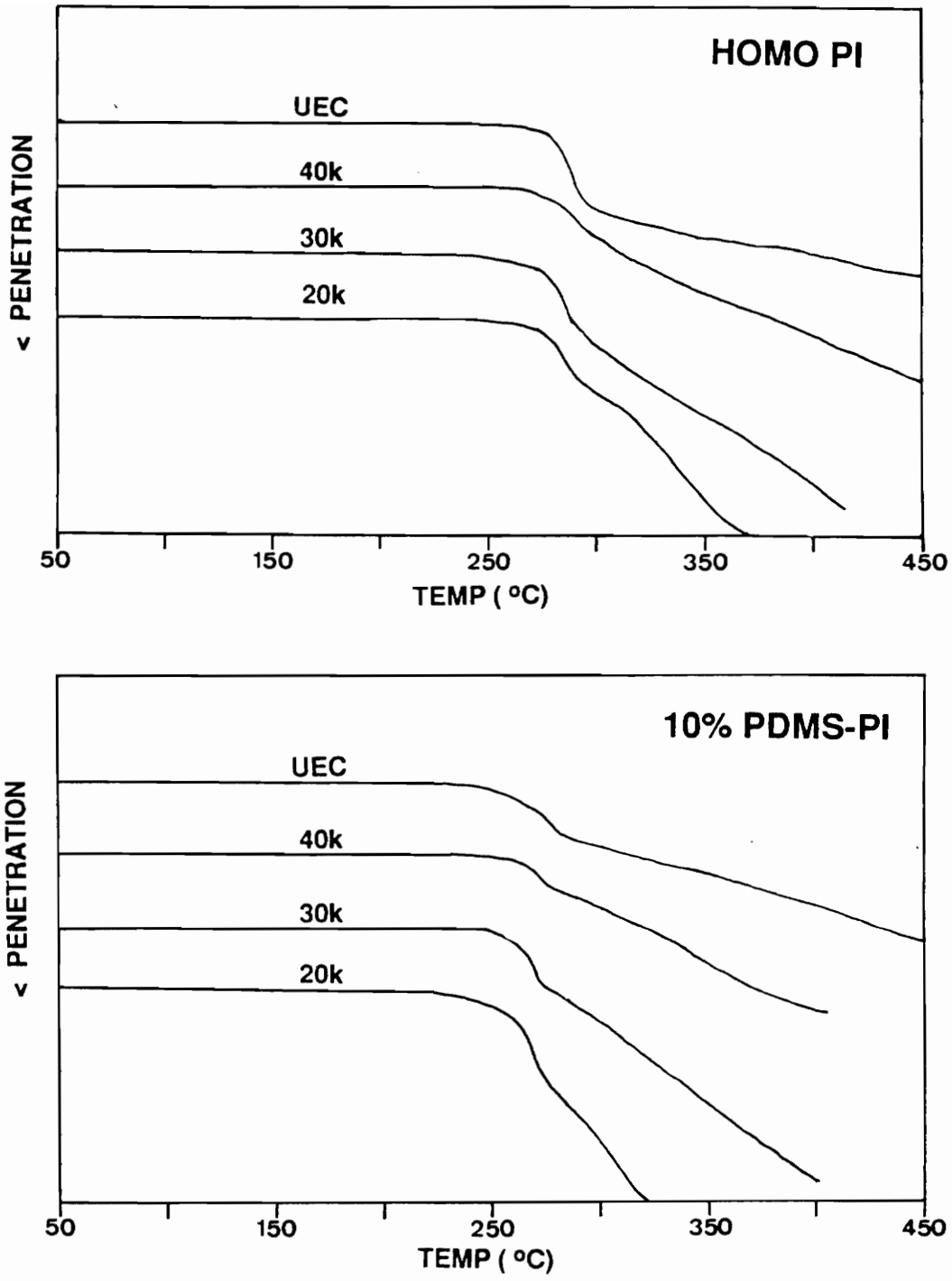

Figure 30. TMA of polyimide homopolymers and poly(imide-siloxane) copolymers

homopolymer and poly(imide-siloxane) segmented copolymers exhibited very slow penetration above the glass transition temperatures which may also reflect continued reaction or "chain extension" at these high temperatures. As the molecular weight decreased, the penetraion rate became higher indicating ease of flow. The molecular weight dependence of the penetration rate in TMA indicates that the molecular weight control of polyimides was successful and is consistent with the intrinsic viscosity results. It also shows how important the molecular weight control is on the flow behavior and provides strong evidence of improved processability of lower molecular weight polyimides. The applicability of these observations to structural adhesive bonding is quite clear.

4-1-6 Compression molding temperature

Since most adhesives were prepared by compression molding in a hot press, the compression molding temperatures can be related to flow behavior of polyimides. The compression molding temperature (CMT) was determined by systematically varying the temperature by 10 °C under a fixed load (10,000 lb) and holding time (10 minutes). The reported values are the lowest temperature at which a clear amber colored films were obtained without any obvious degradation. As expected from the glass transition temperatures measured by DSC and flow behavior by TMA, the compression molding temperatures (CMT)s were also a function of molecular weight and siloxane content, but they are approximately 100 °C above the Tg of the polymer. CMTs increased slightly with molecular weight but decreased rather dramatically with siloxane incorporation (Table 15). However, no film could be obtained from the homopolyimide (BTDA-mDDS) of uncontrolled molecular weight. This might be due to poor flow, with high chain rigidity and chain extension occurred before flow. The capability of compression molding demonstrates that the end capped and polyimides prepared via controlled number average molecular weight with end capping in this study are highly processable.

4-1-7 Effect of polyimide structure

As demonstrated in the previous sections, the techniques developed in our laboratory, such as solution imidization and molecular weight control with non reactive end groups resulted in a soluble, processable thermoplastic polyimides. Therefore, it was attempted to prepare high Tg polyimides with para-substituted monomers such as pDDS and pPD via these new techniques. The hexa-fluoro dianhydride (6FDA) instead of BTDA was utilized as the dianhydride since fluorine containing polyimides have superior thermo-oxidative stability, lower dielectric constants and better solubility. The molecular weight of polyimide was controlled to 20,000 g/mole since it turned out to be the optimum for good flow and good mechanical properties.

The polyimides were characterized by FTIR, DSC, DMTA, TGA and intrinsic viscosity measurement. The characteristics of polyimides are listed in Table 15 together with those of BTDA-mDDS polyimide. The polyimides from 6FDA exhibited good solubility in a number of solvents such as NMP, THF and CH_2CL_2. The solution imidization technique was again successful in obtaining fully cyclized polyimide as confirmed by FTIR as shown in Figure 31. The molecular weight control was monitored by measuring the intrinsic viscosity of polyimides in NMP at 25 °C. The intrinsic viscosity from 6FDA based polyimides were slightly higher than that from BTDA-mDDS polyimide, possibly due to the stiffer backbone from para-linkage.

The glass transition temperatures of polyimides from 6FDA- pDDS and 6FDA-pPD were 325 and 345 °C, respectively. As expected, polyimide from 6FDA-pPD showed higher Tg of 360 °C by DMTA than that by DSC (Figure 32). The thermal stability of 6FDA based polymers measured by dynamic TGA in air was similar to that of BTDA-mDDS polyimide. Although 6FDA-based polyimides exhibited higher Tgs than BTDA-mDDS polyimide, it was still possible to obtain good films by compression molding.

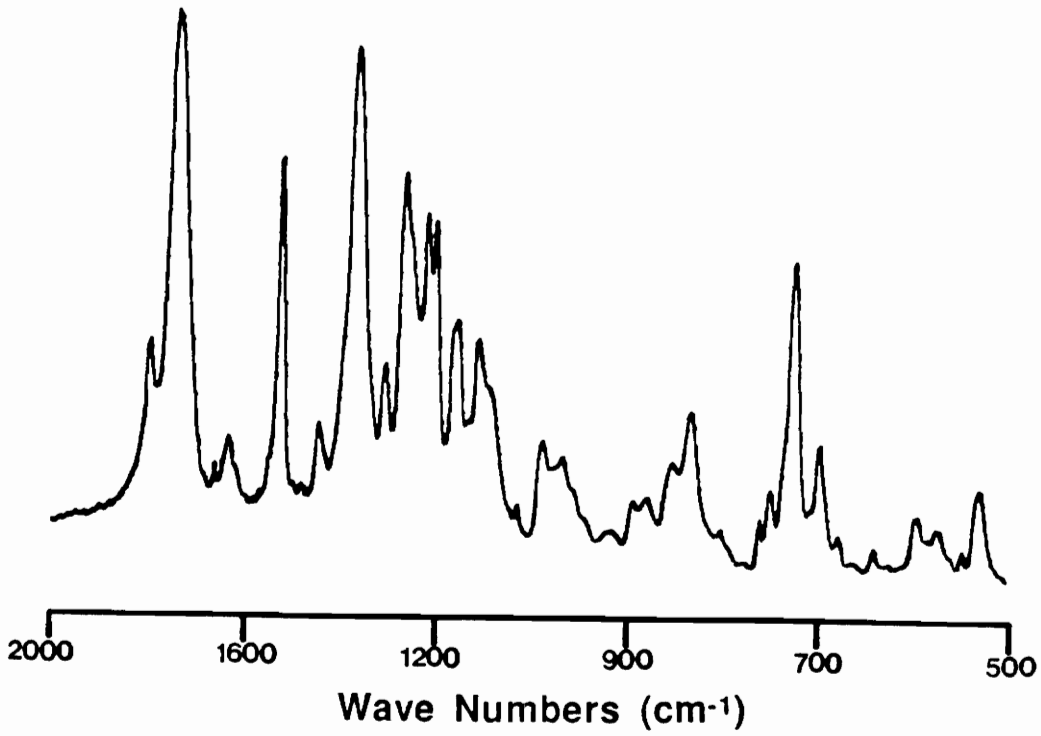

Figure 31. FTIR spectrum of polyimide from 6FDA-pPD

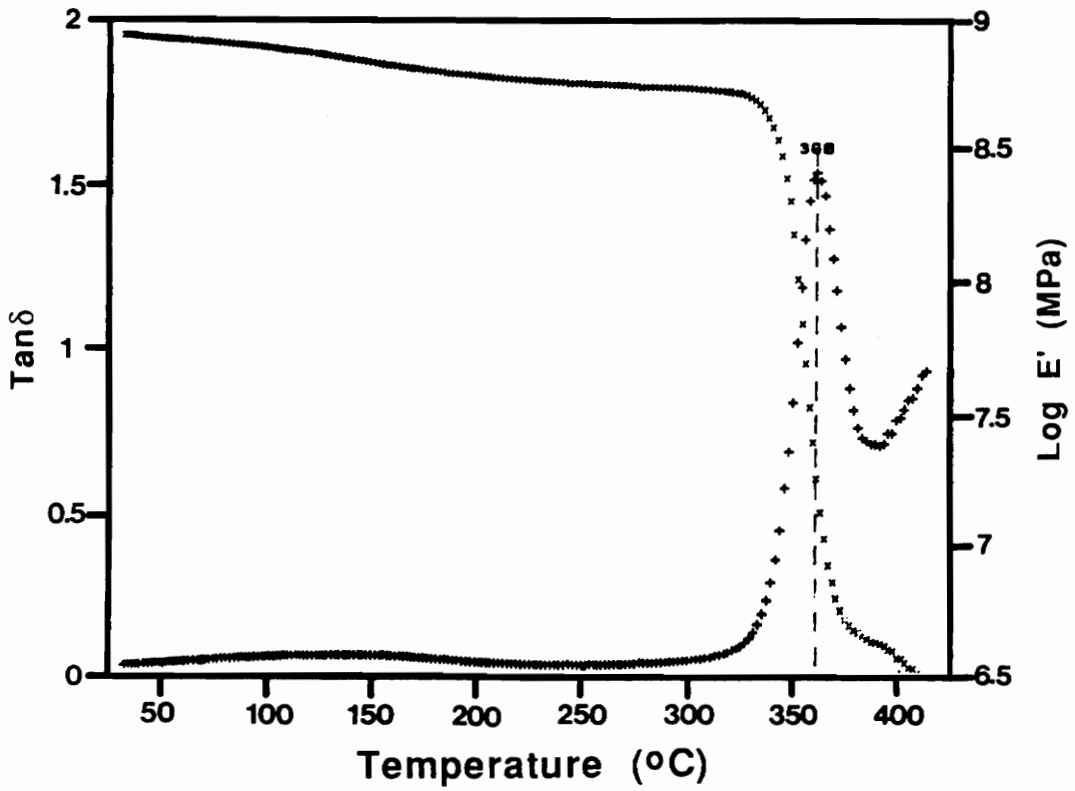

Figure 32. DMTA of polyimide from 6FDA-pPD (20,000 g/mole)

4-2 Mechanical properties of polyimides

In order to provide a better understanding on adhesive bond strength of polyimide homopolymers and poly(imide-siloxane) segmented copolymers, mechanical properties were measured via stress-strain testing as a function of molecular weight, siloxane content and test temperatures. *Ultem®* 1000 and *Kapton®* polyimide controls were also tested for comparison purposes. The tests were conducted according to ASTM D-638 and all dog-bone type specimens were prepared from compression molded films (5-10 mil thick) with ASTM D-638 type V die. However, *Kapton®* is not a thermoplastic and was supplied as a thin film. More than 5 samples were analyzed and averaged. Since strain gauge was not available, absolute moduli data were not generated, but relative comparison of mechanical properties were still useful.

4-2-1 Effect of molecular weight

As expected, the mechanical properties of polyimide homopolmers and poly (imide-siloxane) copolymers were found to be a function of molecular weight. In this research, the molecular weight of polyimides was controlled to afford 10,000 20,000, 30,000 and 40,000 (g/mole) together with uncontrolled molecular weight. However, since the molecular weight of 10,000 (g/mole) was too brittle to prepare film adhesive, that was excluded. According to Waldbauer [222], the critical molecular weight of polyimide for chain entanglement falls in the molecular weight of 15,000 to 20,000 (g/mole), which is consistant with observation in this study.

The polyimide homopolymer (20,000g/mole) exhibited tensile strength of 10.4 ksi (71.7 MPa), tensile modulus of 300 ksi (207 MPa) and 5.9% elongation. The tensile strength and strain of polyimide homopolymer increased significantly with molecular weight (17.7 ksi and 7.5% with 40,000 g/mole), while the apparant tensile modulus did not vary significantly (313 ksi with 40,000 g/mole) at room temperature as indicated in Figure 33. Compared with well known

polyimide, LARC-TPI, which has tensile strength of 19.7 ksi, modulus of 540 ksi (obtained with a strain gauge) and 4.8 % elongation [140], polyimide homopolymers demonstrated good mechanical properties with the advantage of good processability. Since strain gauge was not employed in this measurement, the tensile modulus is probably 30-50% lower than the absolute values, which will be discussed in detail later.

The lowest molecular weight (20,000 g/mole) used was at or above the critical range of molecular weight for good mechanical properties, otherwise a large change would have been observed. As the molecular weight increased, more chain entanglements were generated resulting in improved mechanical properties, but the increase was not great.

The effect of molecular weight on the stress-strain behavior was also conducted at 200 °C. Although the thermal energy increased ductility and decreased strength, the effect of molecular weight on the trend of mechanical properties was simillar to that at room temperature (Figure 33). Tensile strength increased slightly from 6.5 ksi with 20,000 g/mole to 9.0 ksi with 40 ,000 g/mole at 200 °C, while tensile modulus did not change. Tensile strain, however, increased from 8.7% with 20,000 g/mole to 16.7% with 40,000 g/mole. Once again, increased chain entanglement is responsible for increasing mechanical properties with molecular weight.

4-2-2 Effect of polydimethylsiloxane segment incorporation

Siloxane incorporation into polyimide backbone increases chain flexibility, which influences ductility and bond consolidation, and results in improved adhesive bond strength. The stress-strain behavior of polyimide homopolymers and poly(imide-siloxane) copolymers with molecular weight of 30,000 g/mole is depicted in Figure 34 and summarized in Figure 35. Polyimide homopolymer showed a tensile strength of 13 ksi, modulus of 283 ksi and 6% elongation. As siloxane incorporation was increased, the tensile strength increased to 14.3

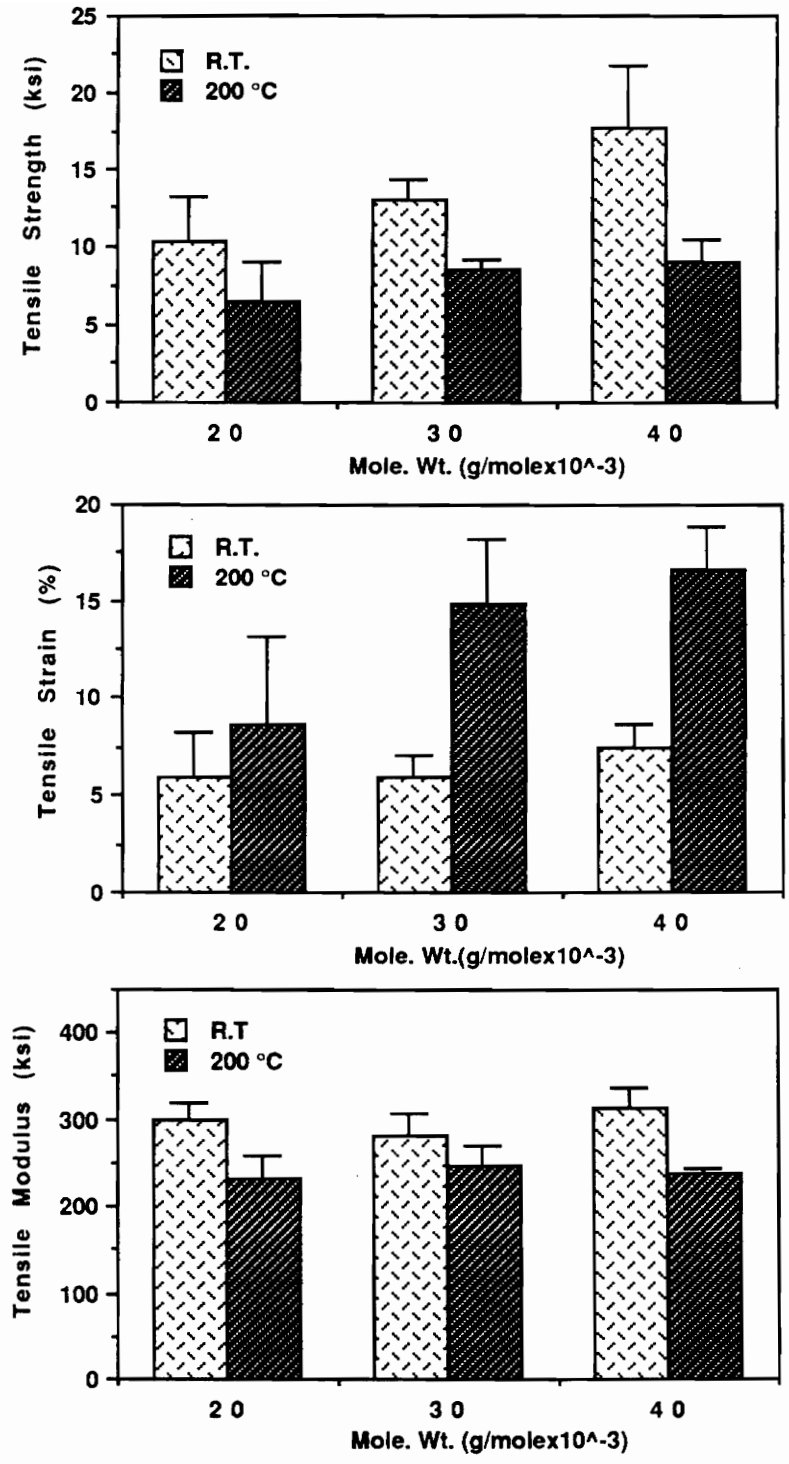

Figure 33. Effect of molecular weight on stress-strain behavior of homopolyimide

ksi with 10% siloxane, and then decreased to 13.2 and 9.9 ksi with 20% and 30% siloxane incorporation, respectively.

Tensile strain increased with siloxane incoporation while the tensile modulus decreased slightly with it. As indicated in Figure 13 and 14, the tensile strength and modulus increased with strain rate or decreased with test temperature, while the tensile strain exhibited an opposite trend to strength since polymers are viscoelastic materials. Since siloxane incorporation lowered tensile strength and modulus, and increased tensile strain, it has the same effect as decreasing the strain rate or increasing the test temperature. As the strain rate decreased, less force was required to move the chains a given distance or for a given time period resulting in lowered strength and modulus but higher strain at break.

Due to high chain stiffness and chain entanglements, polyimide homopolymers have little room to move before being anchored by entanglement points so that polymer chains are broken at low strain but high strength. A small amount of siloxane (eg 10%) incorporation slightly improved the chain flexibility. The improved strength is believed to be resulted from slightly enhanced ductility of the polymer. In general, very rigid chains are not very extensible and results in brittle fracture. Since 20% and 30% siloxane incorporated copolymers had more chain mobility, they resulted in higher strain but lower strength. Thus, siloxane incorporation had the similar effects as decreasing the strain rate.

The tensile strength of the polyimides containing 20% and 30% siloxane at 200 °C was measured at a strain rate of 0.1″/minutes due to the so high elongation of these polyimides instead of 0.05″/minutes which used for polyimide homopolymer and poly(imide-10% siloxane) copolymers. Although it was expected a slight change of mechanical properties, no appreciable change was not observed. The tensile strength decreased linearly with siloxane incorporation while the tensile modulus decreased exponentially at 200 °C. The tensile strain, however, increased exponentially with siloxane incorporation at 200 °C; from 14% with polyimide homopolymer to 212% with 30% siloxane copolymer, while tensile strength and

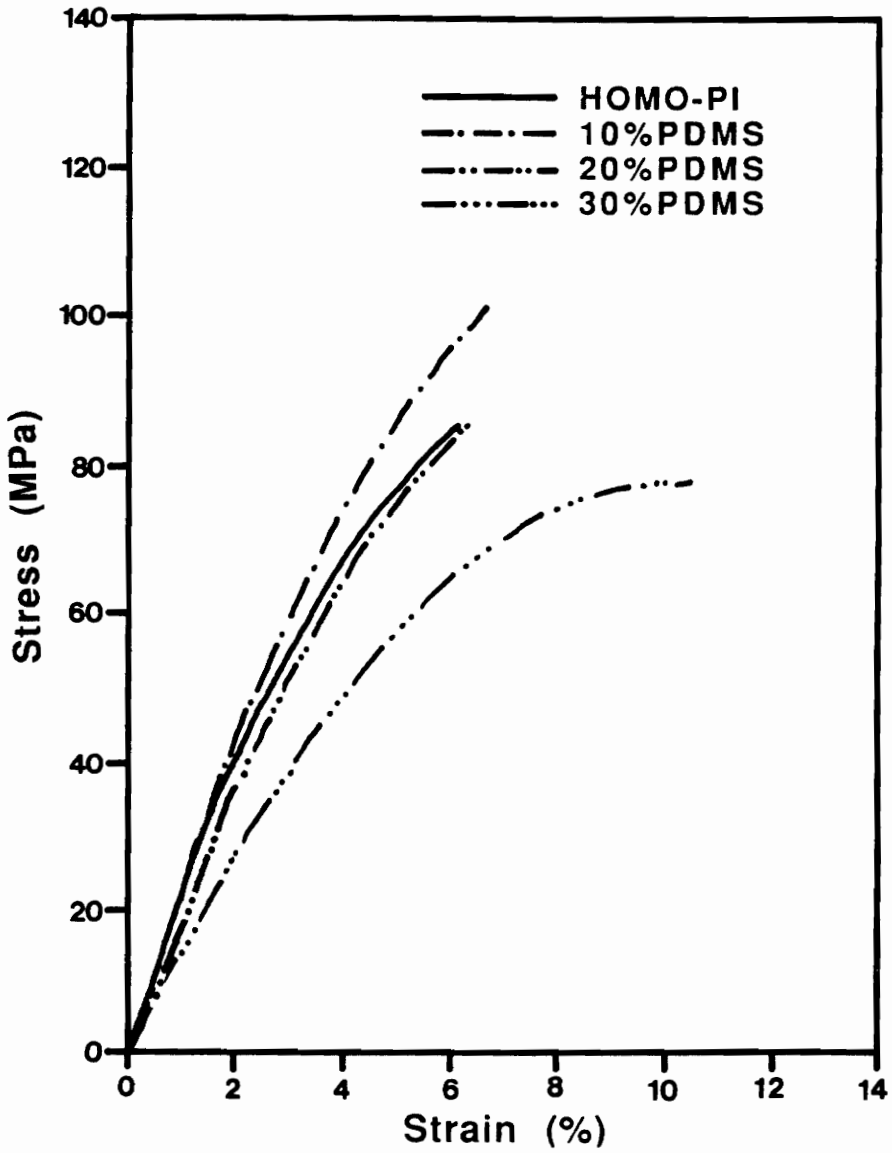

Figure 34. Stress-strain behavior of polyimide homopolymer and poly(imide-siloxane) copolymers (30,000 g/mole) at ambient temperature

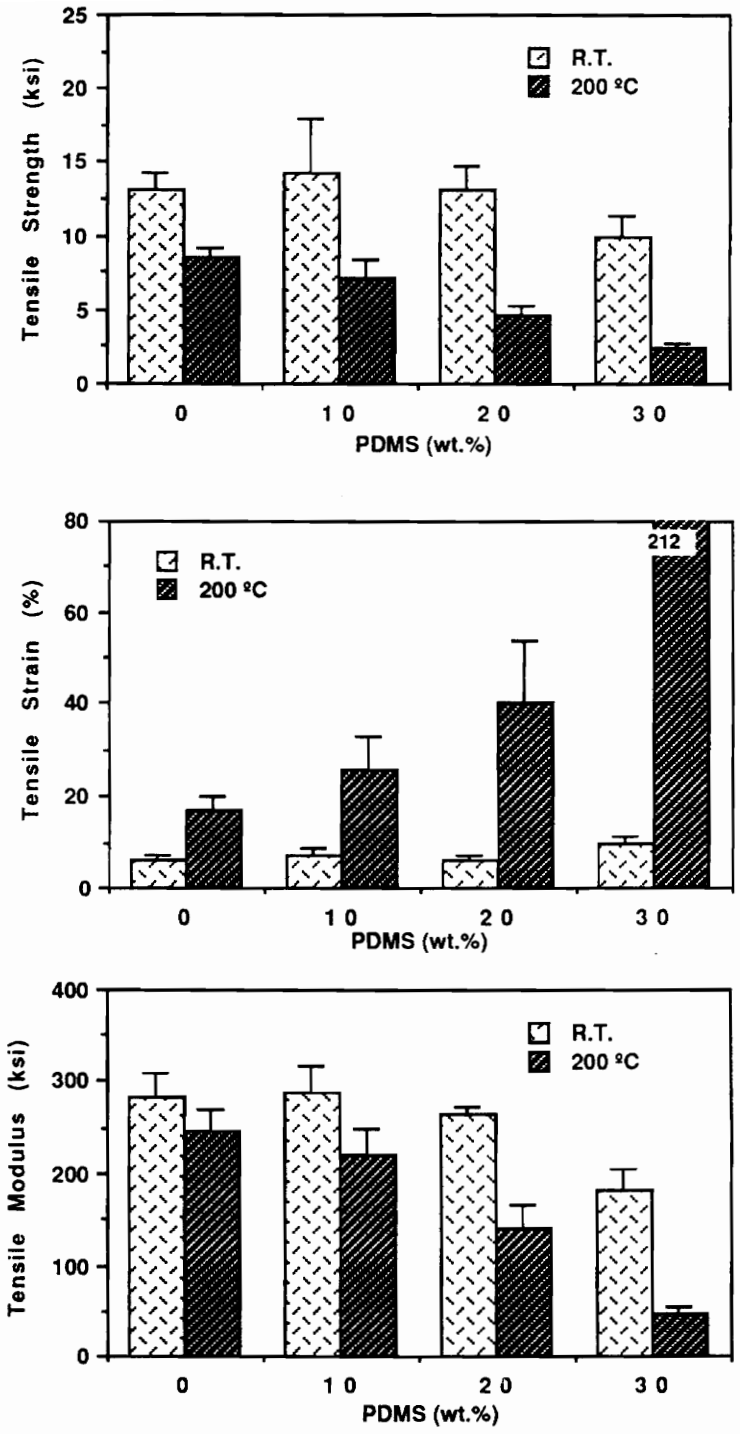

Figure 35. Effect of siloxane block (<Mn> = 1550 g/mole) incorporation on the stess-strain behavior of polyimides

modulus decreased rapidly. Due to increased free volume by siloxane incorporation as well as thermal energy, the polymer chains had high mobility and were less resistant to applied external force, which resulted in reduced strength and modulus.

4-2-3 Effect of test temperature

Test temperature has a tremendous effect on the mechanical behavior of polymers and also on adhesive bond strength. The thermal energy provided by test temperature increases the free volume of polymer chains, resulting in enhanced chain mobility, increased ductility but decreased strength. Due to the time limitation of Instron (20 minutes), very highily extensible samples, especially at elevated temperatures, had to be tested at higher cross-head speed (0.1"/minutes) so as to avoid loss of data. The samples tested at this strain rate were poly(imide-20%siloxane) (20,000 g/mole) at 250 °C, poly(imide-20% siloxane) (40,000 g/mole) and poly(imide-30% siloxane) (20,000 and 30,000 g/mole) at 200 °C, and *Ultem*® 1000 and *Kapton*® polyimide at all test temperatures.

The stress-strain behavior of polyimide homopolymers and poly(imide-siloxane) segmented copolymers of 30,000 g/mole molecular weight are shown in Figure 36, which is similar to Figure 14. The mechanical properties are summarized in Figure 37. In general, polyimides exhibited loss of strength and modulus, but gain of ductility with temperature. The tensile strength of homopolyimides and copolyimides decreased approximately linearly with temperature with the exception of some unusually low strength homopolymer samples at room temperature. The latter is mainly due to their brittle premature failure processes. Therefore, as the temperature increased, enhanced ductility by thermal energy did not decrease tensile strength of polyimide homopolymer but actually improved the values to a more normal level (Figure 37).

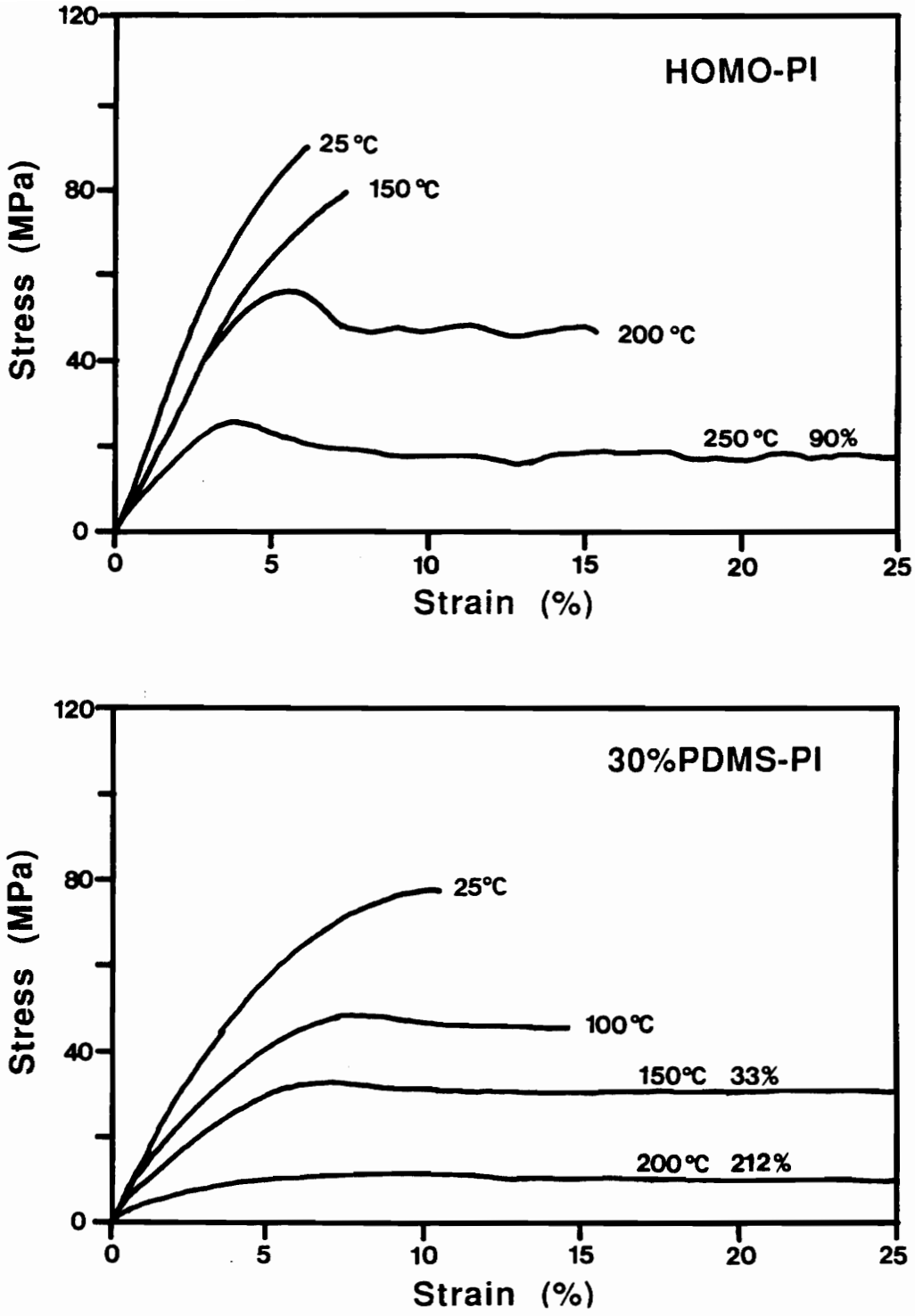

Figure 36. Stress-strain behavior of polyimide homopolymer and poly(imide-30%siloxane) copolymers as a function of temperature

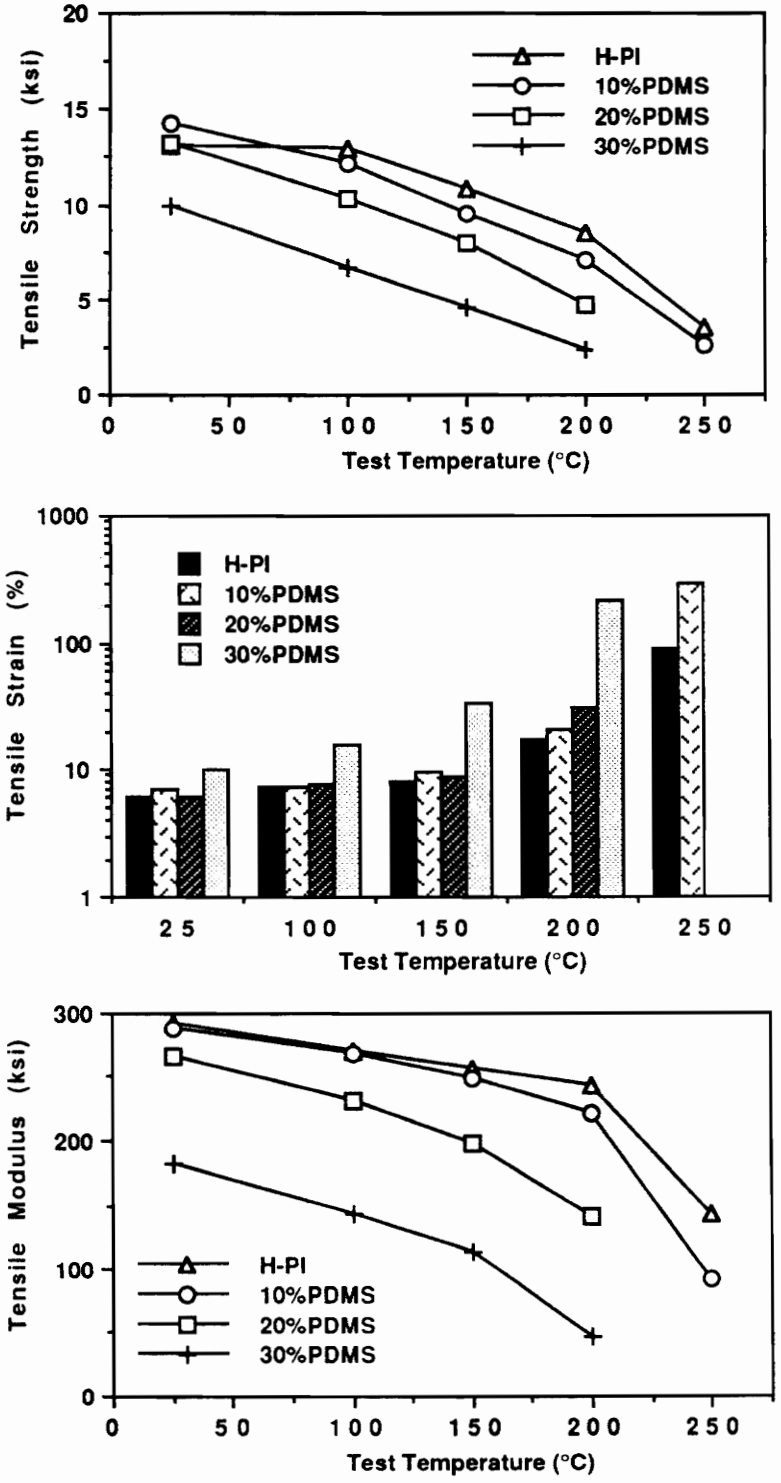

Figure 37. Effect of test temperature on the stress-strain behavior of polyimides homopolymer and poly(imide-siloxane) copolymers

As expected, the tensile strain increased almost exponentially with test temperature. Thus, polyimide homopolymer exhibited 6%, 14% and 91% of tensile strain at 25°C, 200 °C and 250 °C, respectively, while 30% siloxane copolymers showed 10%, 33% and 212% at room temperature, 150 and 200 °C, respectively. As the test temperature approached the Tg of the polymer, tensile strain increased dramatically due to large increase of free volume around Tg. The tensile modulus exhibited similar trend as strength. Polyimide homopolymer and 10% siloxane copolymer showed a slight decrease of tensile modulus with temperature until 200 °C then abrupt decrease thereafter as the test temperature approached the Tg of the polymer. Figure 38 also clearly demonstrated the effect of siloxane on the tensile properties. The retention of tensile strength and modulus decreased with siloxane content.

The relationship between test temperature and molecular weight of the 10% siloxane copolymers is shown in Figure 38. Tensile strength varied with molecular weight at room temperature, but the difference became negligible as temperature increased. Tensile modulus did not show a major variation, while tensile elongation exhibited a large change with molecular weight in the temperature range of 100 and 250 °C. At room temperature and 100 °C, the molecular weight variation did not result in any difference (negligible mobility) due to the somewhat brittle nature of polyimide. In the range of 100 to 250 °C, enhanced free volume by thermal energy was not very large and polymer chains had limited mobility (medium mobility). Thus, an effect of molecular weight was detected in this temperature range. However, at 250 °C, due to the excessive ductility by temperature, all polyimides did not show the dependence of strength and stiffness on molecular weight.

4-2-4 Polyimide structure

Strain-stress measurements were also carried out on the high Tg (360 °C) polyimide based on 6FDA-pPD. Commercial polyimides such as *Ultem*® 1000 and *Kapton*® were also subjected to measurement so as to provide an idea on the precision and accuracy of data generated

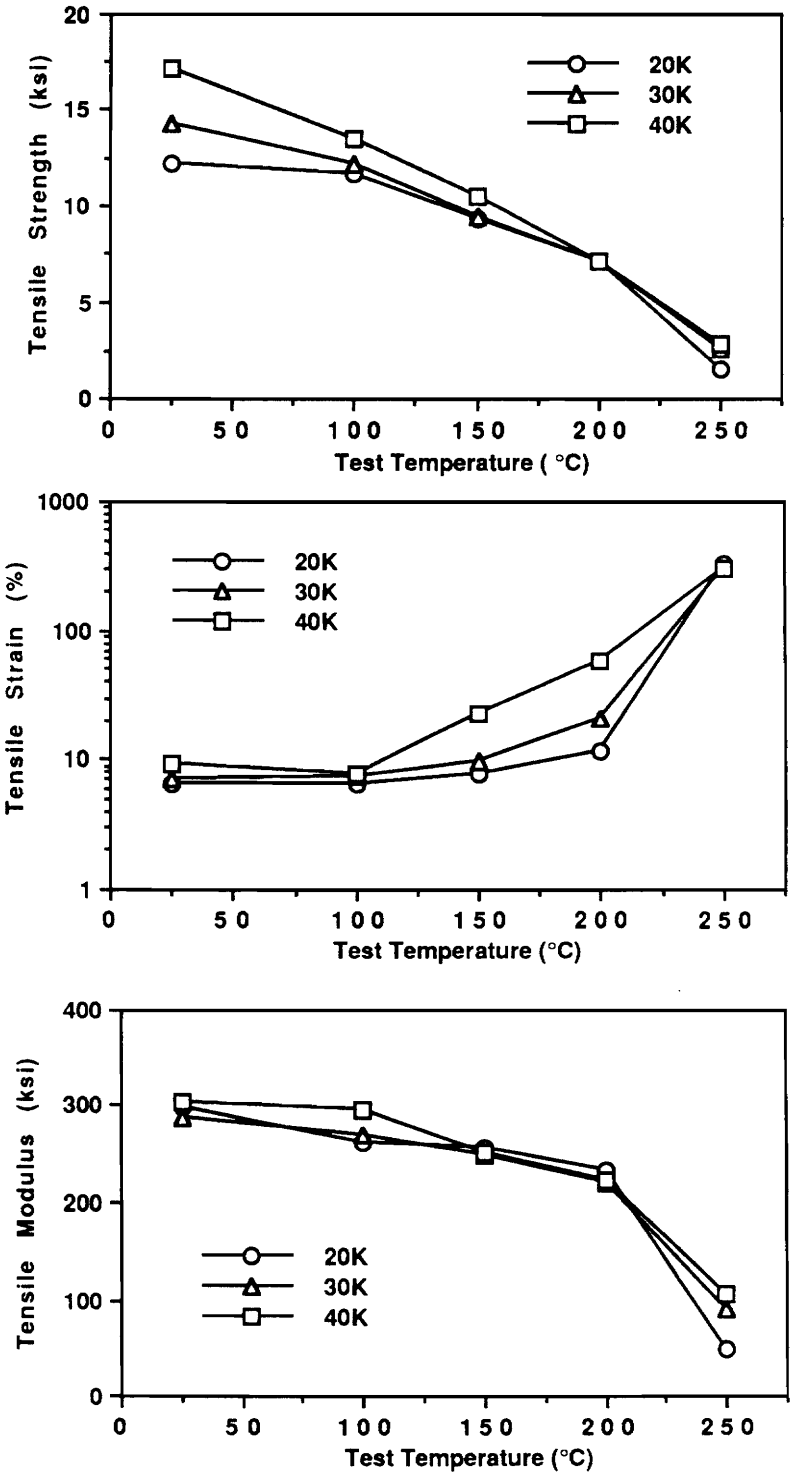

Figure 38. Effect of test temperature and molecular weight on the stress-strain behavior of poly(imide-10% siloxane) copolymers

without the use of strain gauge, as well as to compare with polyimides prepared in this laboratory. The mechanical properties of polyimide derived from 6FDA was measured at a strain rate of 0.05"/minute while that of *Ultem*® 1000 and *Kpton*® polyimides were collected at 0.1"/minute.

The mechanical properties from strain-stress tests on all polyimides are summarized in Table 16 together with polyimide from BTDA-mDDS. Stress-strain behavior of polyimide derived from 6FDA-pPD, *Ultem*® 1000 and *Kpton*® polyimides are also shown in Figure 39. *Ultem*® 1000 exhibited clear yield phenomena while *Kapton*® showed stick-slip at high temperature tests. As expected, commercial oriented film *Kapton*® provided the highest tensile strength followed by 6FDA-pPD, BTDA-mDDS and *Ultem*® 1000. The reported tensile strength of *Kapton*® was 25 ksi and our measured value was 23 ksi, while by comparison the polyimide from 6FDA-pPD had a tensile strength of 21 ksi. Considering that *Kapton*® film is believed to have chain orientation, affect the ultimate strength tests are probably comparable. All samples demonstrated decreasing tensile strength with temperature as expected.

The highest tensile strain was obtained by *Ultem*® 1000, around 100% which was higher than the reported value of 60% [140], while *Kapton*® exhibited 70% which was very close to the reported value. The high Tg polyimide based on 6FDA-pPD, showed 15% tensile elongation, which was less than those of commercial polyimides but higher than the BTDAmDDS system. The tensile strain of these polymers did not vary significantly with temperature up to 250 °C. However, polyimide from BTDA-mDDS (20,000 g/mole) showed an abrupt increase of tensile strain at 250 °C, since the test temperature was near the Tg of the polymer. The lower moduli values reflects that our experiments did not use the strain gauges.

The polyimide from BTDA-mDDS (20,000 g/mole) exhibited highest tensile modulus (300 ksi) followed by 6FDA-pPD (293 ksi), *Ultem*® 1000 (241 ksi) and *Kapton*® (195 ksi), and decreased with temperature. Compared to the reported tensile modulus of *Ultem*® and *Kapton*®, which were 430 ksi, the measured values were lower by 44% and 55%, respectively, which can be

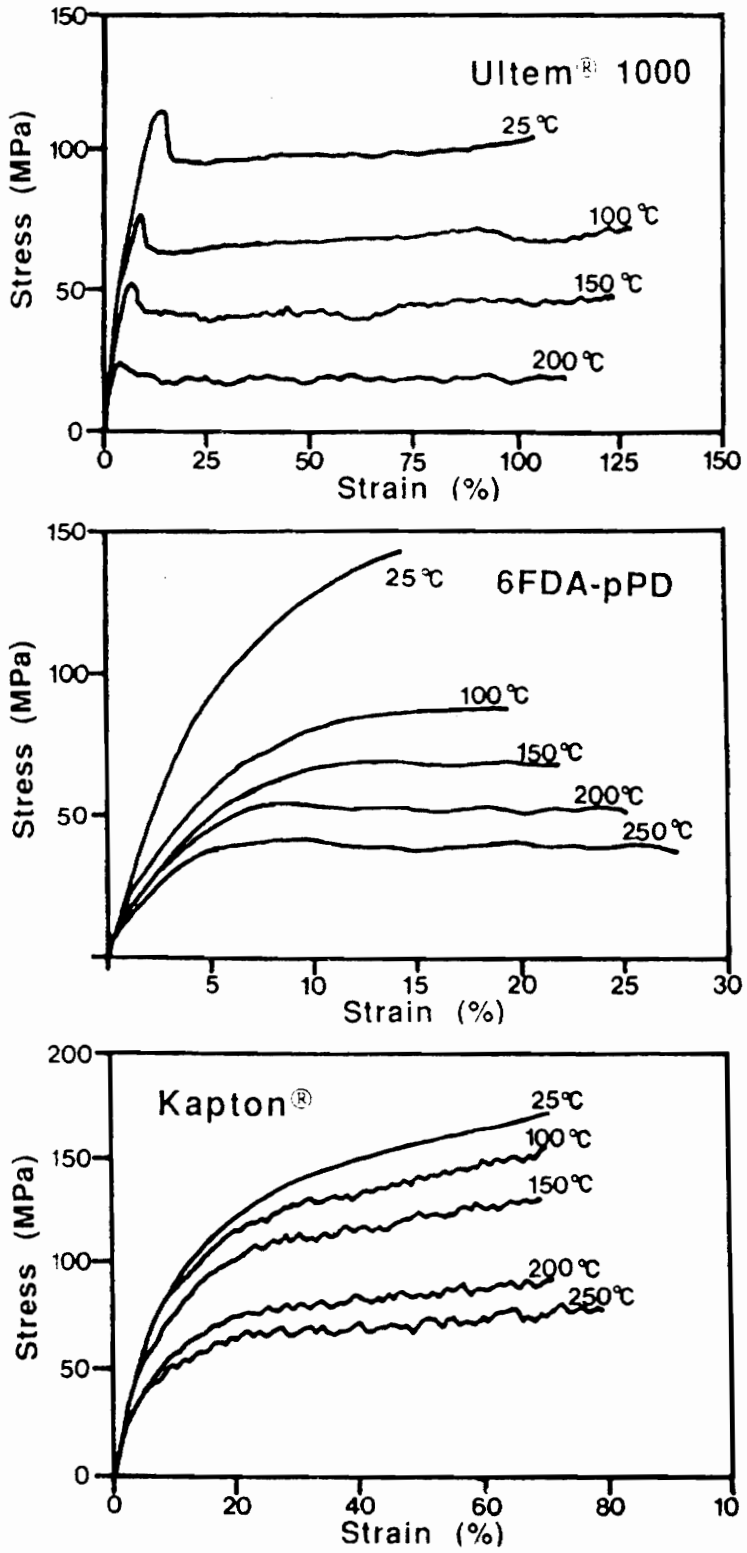

Figure 39. Stress-strain behavior of polyimide from 6FDA-pPD, Ultem and Kapton as a function of temperature

Table 16. Mechanical properties of polyimide by stress-strain.

		BT-mDDS	6F-pPD	Ultem®	Kapton®	LARC-TPI
σ	M	17.7	20.7(8.4)	16(3.4)	23(8.4)	
(ksi)	R			15.2	25(17)	19.7
ε	M	7.5	15(28)	105(113)	71(68)	
(%)	R			60	70(90)	4.8
E	M	313	293(162)	241(136)	241(155)	
(ksi)	R			430	430(260)	540

M : MEASURED R: REPORTED, ( ) : AT 200 °C

attributed to the fact that strain gauge was not utilized. In the range of 100 °C to 250 °C, the polyimide of BTDA-mDDS showed excellent tensile modulus retention while others also showed similar values, around 200 ksi, thus demonstrating excellent potential for high performance structure.

4-3 Adhesion study of Ti-6Al-4V alloys

The adhesive bond performance of polyimide homopolymers and poly(imide-siloxane) segmented copolymers was investigated as a function of molecular weight, siloxane incorporation and test temperatures. The prime requirements for a strong, durable adhesive bond formation are good bond consolidation and good mechanical properties of adhesives. The bond consolidation is controlled by parameters such as chain rigidity, molecular weight, residual solvent, siloxane incorporation, plasticizers, and bonding conditions (especially bonding temperature). The mechanical properties are also a function of these factors and additionally test temperature. High strength and high strain (ductility) are desirable mechanical properties. Unfortunately, it is difficult to optimize both characteristics since they are often mutually exclusive.

4-3-1 Ti-6Al-4V alloy adherend

As-received Ti-6Al-4V alloy adherends were sand blated and treated with Pasa Jell 107 which is widely utilized surface treatment agent for strong and durable adhesive bond formation with polimides. As shown in Figure 40, as-received samples were relatively flat with some strip-like mark from manufacturing. However, sand blating resulted in very rough surface. Although the main purpose of sand blasting was cleaining, it also increased surface roughness, which is good for adhesion. As expected, Pasa Jell 107 treatment did not change surface

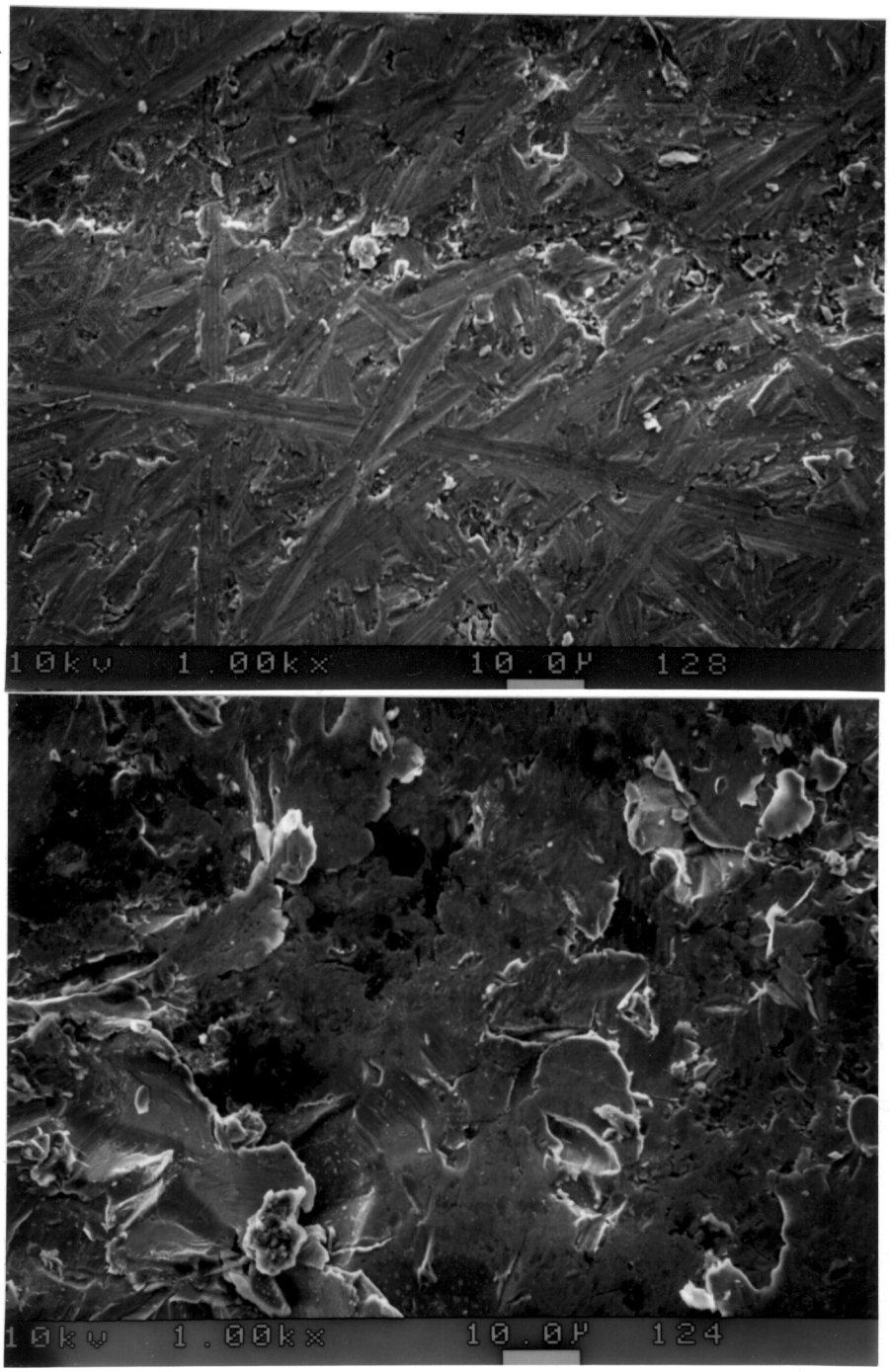

Figure 40. SEM micrographs of as-received and sand blated/Pasa Jell 107 treated Ti-6Al-4V alloy adherends

morphology of Ti-6Al-4V alloy adherend since Pasa Jell treatment removes old titanium oxide and then froms new titanium oxide for strong durable bond formation. Although surface modification of adherend was one of important areas of research, it was not investigated in this study.

4-3-2 Bonding condition optimization

In order to achieve maximum adhesive bond strength, good flow and optimum bond line thickness are essential [73, 219]. Both of these characteristics are governed by interrelated bonding conditions such as melt stability, temperature, pressure and time. Therefore, it is essential to optimize these conditions in order to achieve good flow and optimum adhesive layer thickness and thus maximum adhesive bond performance. In this investigation, adhesive bond thickness was not optimized but an attempt was made to afford the thickness of 0.02-0.04″ and most of samples fell in this range. The effect of excess adhesive on the edge of adhesive bond was not carefully investigated. However, the initial adhesive thickness (0.01-0.014) and size (approximately 1.25″x0.75″) were controlled to minimize the experimental variation and thus error. The size and shape of excess adhesive (spew fillet) looks same for all samples and the shape of spew fillet was not idel type. Therefore, it was assumed that the effect of spew fillet was negligible on the adhesive bond strength.

Since the adhesive bond strengths depend slightly on applied pressure and widely utilized autoclave systems can afford only around 300 psi (2.07 MPa), 200 psi (1.38 MPa) was chosen for these polyimides derived from BTDA-mDDS. The holding time may also have a significant effect on the adhesive bond strength. After exploration studies which varied the holding time from 10 to 30 minutes, 30 minutes appeared to be optimum. As expected, the bonding temperature plays a critical role in the flow of adhesives and thus adhesive bond performance.

The bonding temperatures were optimized for the homopolyimides and poly(imide-siloxane) copolymers with controlled molecuar weight of 20,000 and 30,000 g/mole and uncontrolled molecular weight by varying the temperature from 340 to 370 °C. These polyimide homopolymers exhibited a maximum adhesive bond strength from 370 °C bonding, while the uncontrolled molecular weight of 10% and 20% siloxane copolymers showed maximum adhesive bond strengths at 360 and 350 °C, respectively, as shown in Figure 41. However, some degradation of polyimide homopolymer and 10% siloxane copolymer was observed at 370 °C bonding as evidenced by the darkening of the adhesive. Further analysis of 10% and 20% siloxane copolymers at 350 and 360 °C demonstrated that 360 °C was the optimum temperature. Finally, 360 °C bonding was chosen for the adhesion study of all polyimides based on BTDA-mDDS system in order to facilitate data comparison easier.

4-3-3 Effect of molecular weight

Since most physical properties of polymers, such as mechanical properties and flow behavior are function of molecular weight, it is expected that the adhesive bond strengths also depend on the molecular weight of the adhesive. If the polymer chains are very stiff as in most polyimides, controlling the molecular weight is even more critical for good bond consolidation The goal was to find a molecular weight range where good processability as well as good mechanical properties could be obtained. The mechanical property measurement via stress-strain test indicated that the lowest molecular weight (20,000 g/mole) in this study was at or above the critical molecular weight for good mechanical properties.

As depicted in Figure 42, the adhesive bond strengths decreased with molecular weight of polyimide homopolymers and poly(imide-siloxane) segmented copolymers, despite the enhanced mechanical properties with molecular weight (Figure 33). This is due to the decreased flow during bonding from increased melt viscosity which reduced the bond consolidation. The polyimide homopolymers having molecular weights of 30,000 and 40,000 g/mole showed very

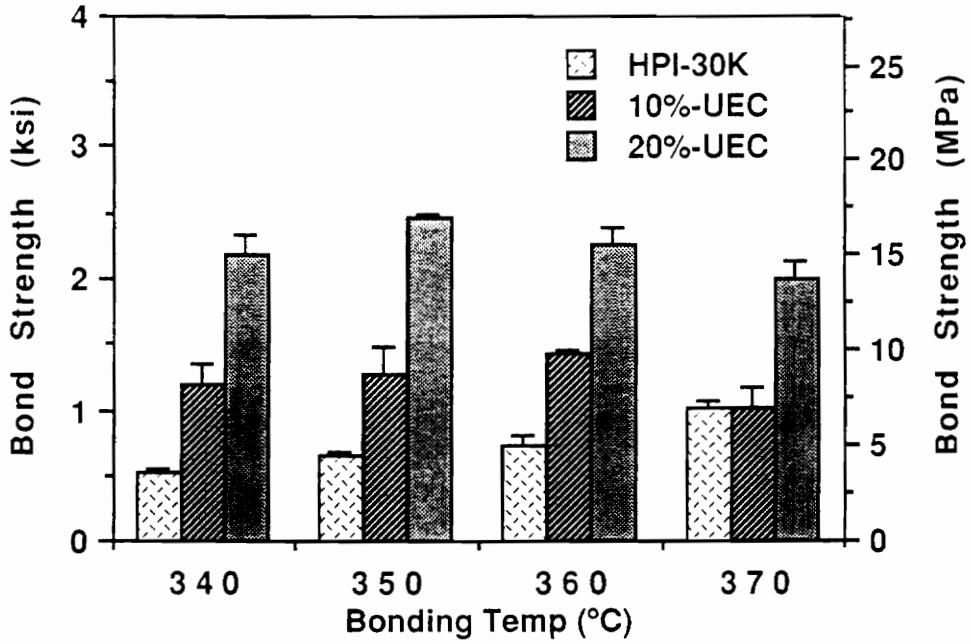

Figure 41. Effect of bonding temperature on the adhesive bond strength of polyimide homopolymers and poly(imide-siloxane) segmented copolymers

low adhesive bond strengths at room temperature (723 and 768 psi) as well as at 200 °C (655 and 623 psi), while polyimide homopolymer with a molecular weight of 20,000 g/mole exhibited 1680 psi (11.6 MPa) at room temperature and 2820 psi (19.5 MPa) at 200 °C. Despite the lower mechanical properties at 200 °C. the adhesive bond strength of homopolyimide (20,000 g/mole) was actually higher at 200 °C than at room temperature, which may seem somewhat unusal. However, this may be explained by the brittle-ductile transition behavior of the polyimides.

The high molecular weight polyimide (30,000 and 40,000 g/mole) did not have good bond consolidation due to a high chain entanglements in combination with high extent of chain rigidity, resulting in a low adhesive bond strengths both at room temperature and at 200 °C. However, the lower molecular weight systems produced fair bond consolidation despite the high chain rigidity. This was anticipated from the difficulty in compression molding of these samples. The dependence of adhesive bond strength on the molecular weight became less as the siloxane incorporation and/or test temperature increased as observed in mechanical property measurement (Figure 33 and 42).

Despite the enhanced mechanical properties with molecular weight, the adhesive bond strength decreased due to reduced flow, resulting from increased melt viscosity. Since adhesive bond strength is a function of not only molecular weight but also bond consolidation, increased viscosity hindered bond consolidation, resulting in reduced adhesive bond strength. Previous investigation [10,216] on the effect of molecular weight on the adhesive properties produced somewhat controversial results. Tsuji et. al. [216] have reported that peel strength of polyethylene film with a rubbery polyisobutylene adhesive exhibited a maximum with molecular weight. The reason for a low peel strength with high molecular weight was suggested to be interfacial failure, resulting from poor flow, which is exactly the same conclusion we have reached. However, a study by Sancaktar and co-workers [10] indicated that adhesive bond strength of rigid polyimide from BTDA+mDDS increased with molecular weight. However, the range of molecular weight in the latter study was so narrow (17,400 to 19,700 g/mole)

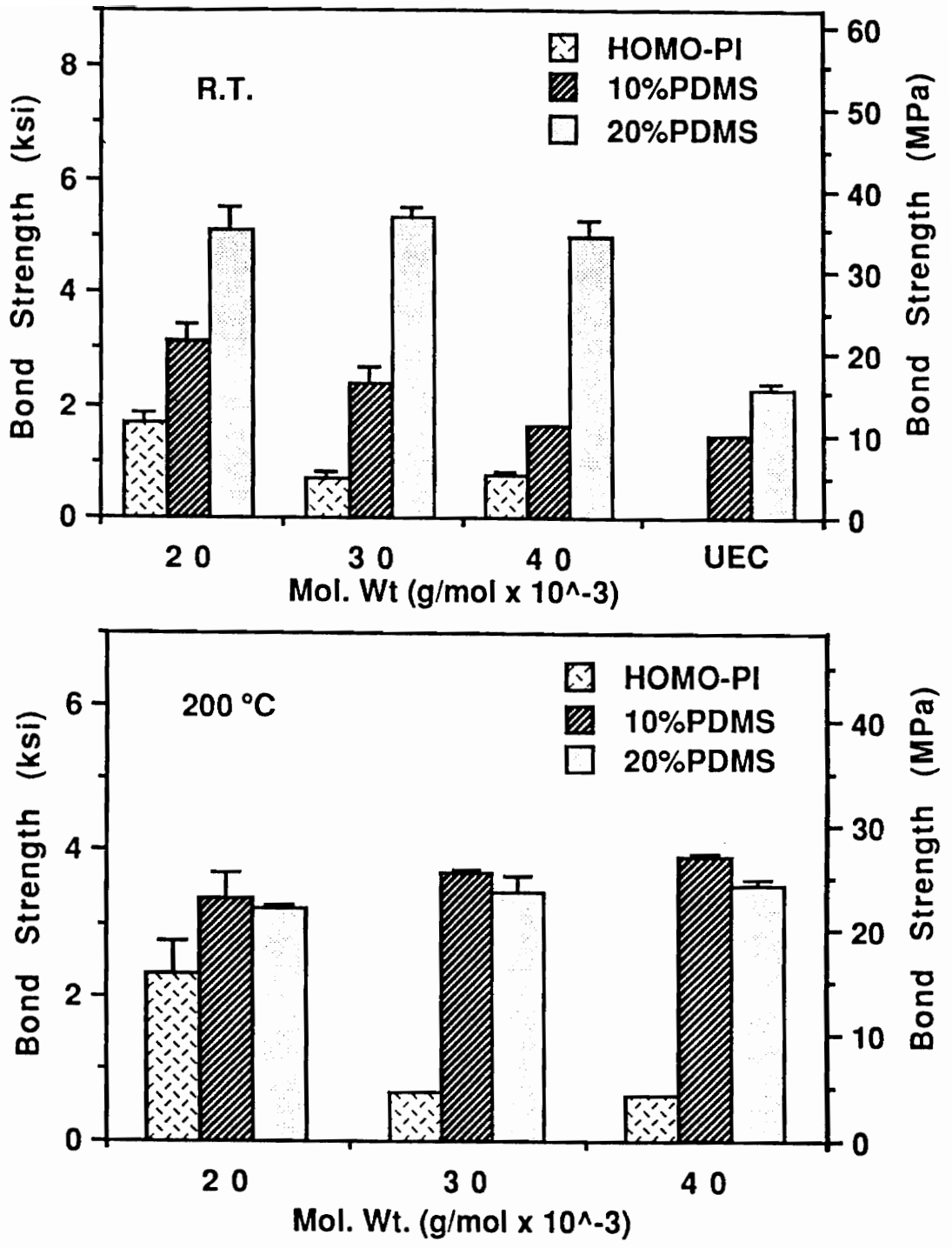

Figure 42. Effect of molecular weight on the adhesive bond strength of polyimide homopolymers and poly(imide-siloxane) copolymers (BTDA-mDDS): a) at R.T. and b) at 200 °C test

that the trend reported is probably meaningless. In addition, the utilization of scrim cloth during the bond formation may have a profound effect on the trend of adhesive bond strength with molecular weight as discussed later.

4-3-4 Polyimide-siloxane segmented copolymers

Due to the inherent flexibility of siloxane oligomers, siloxane incorporation increases chain flexibility of polyimides and thus affect other properties such as the glass transition temperature, ductility, flow behavior and thermal stability. The adhesive bond strength of polyimides increases almost linearly with siloxane incorporation in the room temperature test, as shown in Figure 43. The adhesive bond strength of 1680 psi (11.6 MPa) was obtained from polyimide homopolymer (20,000 g/mole), while the same molecular weights of 10%, 20% and 30% copolymers showed adhesive bond strengths of 3140 psi (21.7 MPa), 5134 psi (35.4 MPa) and 7316 psi (50.5 MPa), respectively. The latter values appear to be truly remarkable.

The adhesive bond strength increased linearly with siloxane incorporation at room temperatures, while the tensile modulus and strength increased with 10% siloxane and then decreased with 20% and 30% siloxane content (Figure 38), with tensile strain increasing only slightly. Therefore, the improved adhesive bond strength with siloxane incorporation is due to the enhanced ductility (strain) and bond consolidation. It can be seen from these results that the tensile strength is certainly not the only factor on adhesive bond strength and that strain and bond consolidation are also very important. However, siloxane incorporation beyond 30-40% probably would not improve adhesive bond strength even at room temperature because of low mechanical strength of elastomer-like polyimides [9], probably because co-continuous or even phase inverted morpholgies would be observed.

At 200 °C, the adhesive bond strength increased with 10% siloxane and then decreased with further incorporation (Figure 43), which is the same trend as that of tensile strength at room

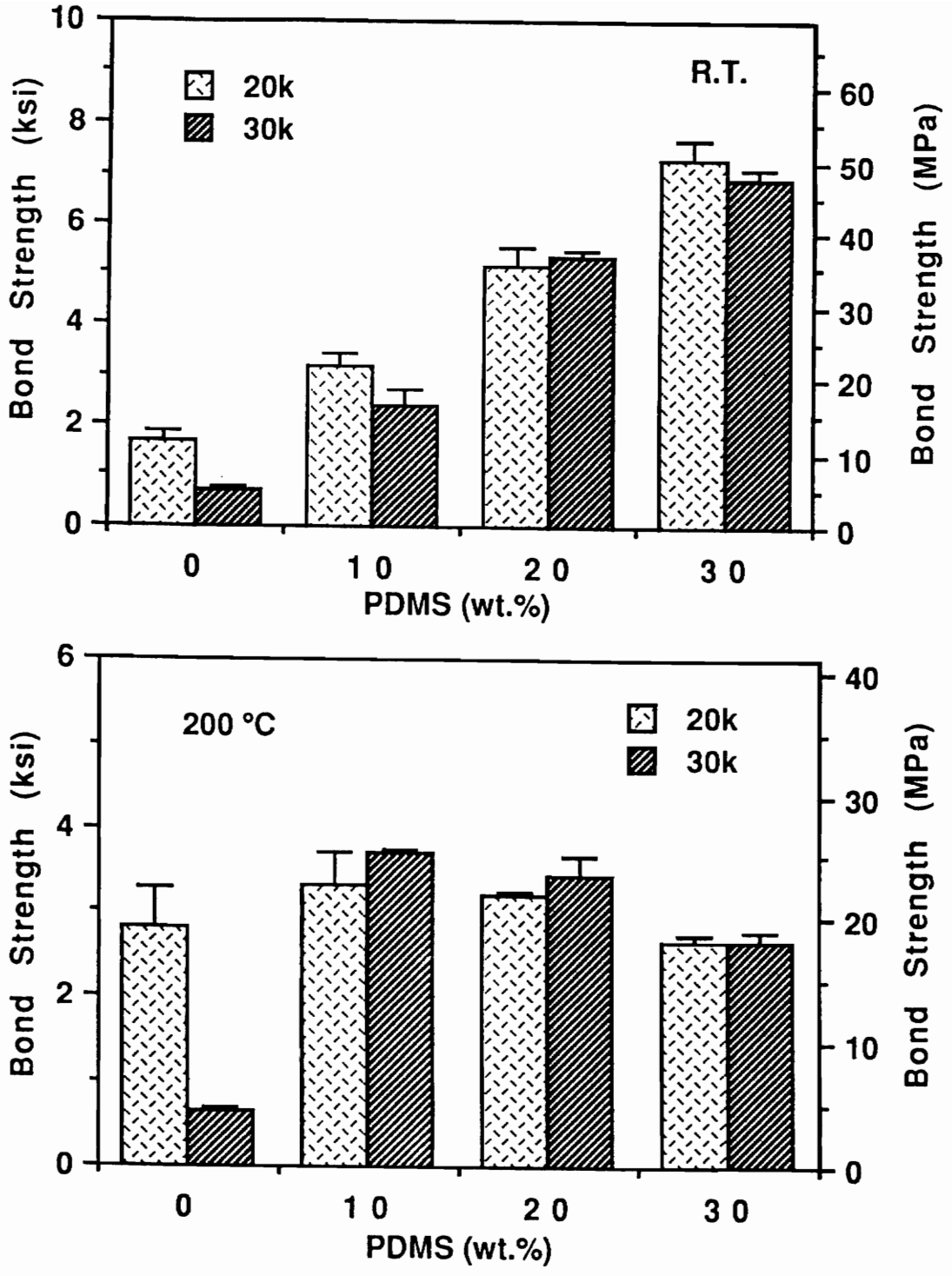

Figure 43. Effect of siloxane incorporation on the adhesive bond strength of polyimide: a) at R.T. and b) at 200 °C test

temperature (Figure 34), while tensile strength and modulus decreased with siloxane content at 200 °C (Figure 35). A optimum adhesive bond strength with 10% siloxane incorporation at 200 °C was due to increased strength and ductility. In part, the improvement of adhesive bond strength should be credited to enhanced bond consolidation by siloxane incorporation, although quantitative relationships are not clear. Higher incorporation of siloxane (eg. 20% and 30%), however, reduced strength and modulus appreciably while largely increasing strain at 200 °C. In this case, the strength was perhaps too low, and ductility was too high to afford maximum adhesive bond strength, despite good bond consolidation. Therefore, it is believed that the strength (modulus) and strain (ductility) should be in a certain range to achieve maximum adhesive bond strength. Since mechanical properties are a strong function of siloxane and test temperature while bond consolidation is a function of siloxane and bonding conditions, care should be exercised to achieve optimum combination of strength and ductility for a given applications.

Siloxane incorporation reduced the dependence of adhesive bond strength on molecular weight (Figure 42). The poly(imide-10%siloxane) copolymers clearly showed the dependence of adhesive bond strength on the molecular weight. However, the adhesive bond strength of poly(imide-20%siloxane) copolymers did not vary significantly among molecular weights of 20,000, 30,000 and 40,000 g/mole with the exception of the samples which had uncontrolled molecular weight. The decreasing adhesive bond strength with increasing molecular weight resulted from increased chain entanglements, which inhibit the flow and bonding of the adhesives. As the siloxane incorporation increased, enhanced chain flexibility reduced the difference of chain entanglement among molecular weights (20,000-40,000 g/mole), resulting in similar adhesive bond strength. This effect was not significant in the 10% siloxane copolymers but was important in the 20% and 30% siloxane copolymers.

In the literature, the effect of siloxane incorporation on acetylene terminated network and thermoplastic polyimides have been reported [16,154]. Cured acetylene terminated oligomeric polyimide [16] showed increased adhesive bond strength with siloxane incorporation while a

pseudo-thermoplastic polyimide from BTDA-DBP [154] resulted in decreased adhesive bond strength. The former system is a rather brittle network polyimide having low ductility. Siloxane incorporation enhanced ductility, resulting in increased adhesive bond strength. In the latter study, one should note that scrim cloth adhesives were utilized, which were dried at 100 °C for 1/ 2 hours and might contain contain a significant amount of solvent [20]. Moreover, the polyimide was not end-capped and was probably not melt stable. These studies demonstrated that ductility and residual solvent are also important factors on adhesive bond strength. Our investigation of the effect of residual solvent on the bond strength will be discussed in section 4-3.

4-3-5 Effect of test temperature

As mentioned in the previous sections, siloxane segment incorporation enhances not only the bond consolidation but also ductility, resulting in improved adhesive bond strength. However, the test temperature does not affect bond consolidation, but rather influence flow and hence basic mechanical properties of polyimide adhesives. With increasing test temperature, the rigidity and strength of the polymer decreases while its ductility increases as observed from mechanical property measurement (Figure 37), which has a profound effect on the adhesive bond strength. The addition of a plasticizer would no doubt make this system more complicated.

As the test temperature increased, the adhesive bond strength of polyimide homopolymers and poly(imide-siloxane) segmented copolymers showed distinctive features, depending on the siloxane content (Figure 44). The adhesive bond strengths of homopolymer and poly(imide-10% siloxane) copolymer exhibited a maximum at 200 and 150 °C, respectively, while those of 20% and 30% siloxane copolymers were good at ambient temperature but decreased with test temperatures. On the other hand, the adhesive bond strengths of polyimide homopolymer (20,000 g/mole) which was relatively low at room temperature 1680 psi (11.6

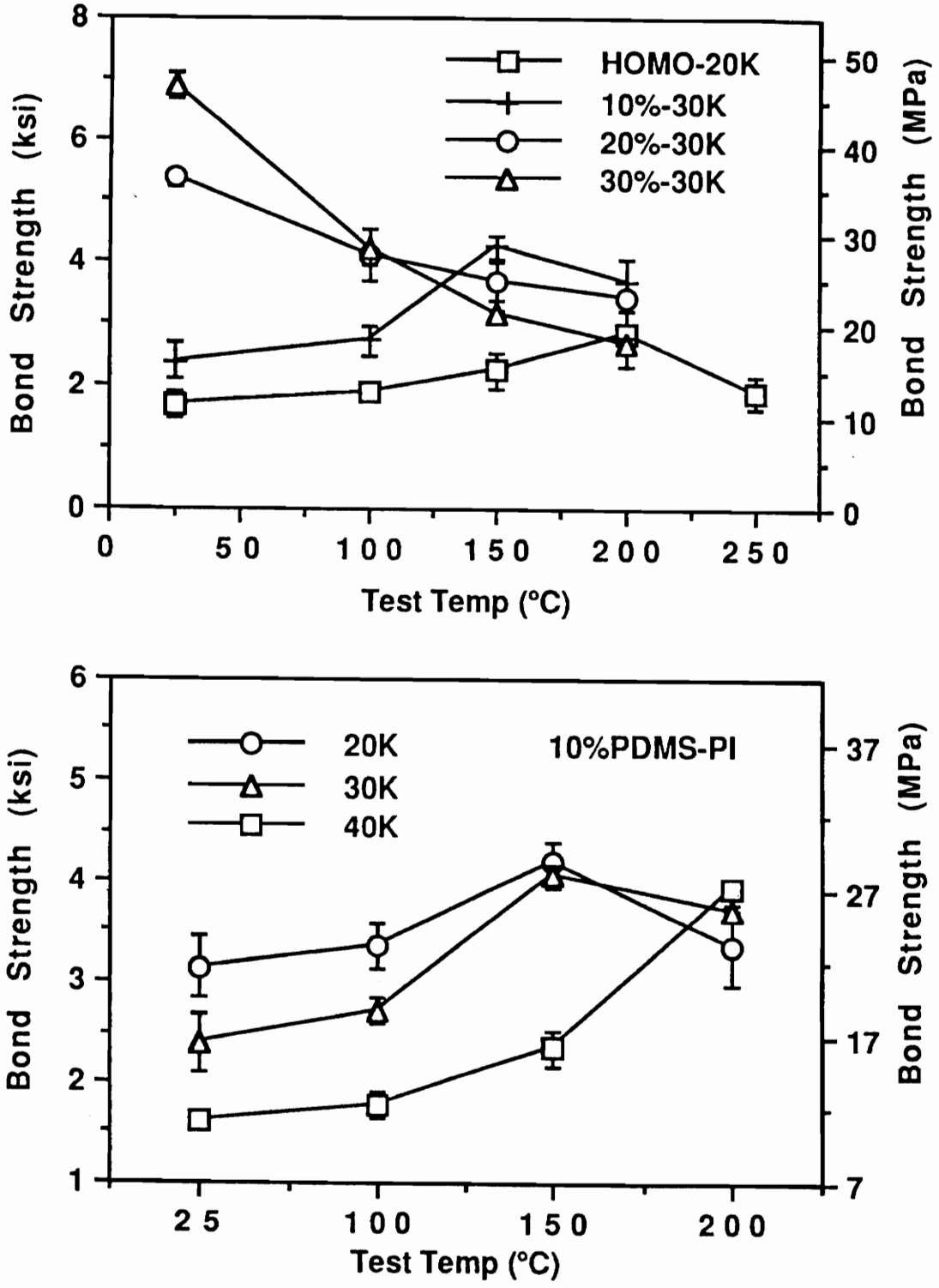

Figure 44. Effect of test temperature on the adhesive bond strength of polyimides

MPa) increased to 2820 psi (19.5 MPa) at 200 °C but decreased to 265 psi at 300 °C. Even at 250 °C, the adhesive bond strength was the same as that obtained at room temperature test. Clearly, this reflects behavior below and above Tg, which is about 265 °C. The poly(imide-10% siloxane) copolymers (30,000 g/mole) exhibited a maximum at 150 °C (21.7 at room temperature to 29 MPa at 150 °C) and also showed a higher adhesive bond strength at 200 °C than at room temperature.

Further analysis of 10% siloxane copolymers showed an interesting trend depending on the molecular weight of the polymer, as shown in Figure 44. The maximum adhesive bond strength was obtained at 150 °C from copolymer which had the molecular weights of 20,000 and 30,000 g/mole, and at 200 °C from the material with a molecular weight of 40,000 g/mole. The high molecular weight adhesive (40,000 g/mole) is more extensively entangled and thus had a better retention of strength at high temperature, resulting in better adhesive properties at 200 °C, which was evidenced by high elongation. Thus, provided good bond consolidation is obtained, higher molecular weight can result in better adhesive bond performance at high temperatures.

Since the adhesive bond strengths are governed by not only ductility but also the stiffness and strength of the adhesive, maximum adhesive bond strengths are obtained from optimum combination of these two factors. However, if one of these factors is lower or higher than it should be, the adhesive bond strength would be lower than the maximum. It is not so simple to obtain the optimum combination of these factors because they are mutually exclusive and are function of many factors such as siloxane content, test temperature, and plasticizer. Only two factors, siloxane incorporation and test temperatures, have been examined here.

Polyimide homopolymers are often brittle in nature due to their high chain rigidity which is derived from connected aromatic rings in the backbone. Rheological consideration may produce poor bond consolidation and brittle, rigid molecular structure may produce low adhesive bond strength at room temperature. However, as the test temperature is increased,

enhanced ductility can first increase the adhesive bond strength, although eventually a decrease is again observed as Tg is approached or even exceeded. The optimum combination of strength and ductility was obtained around 200 °C, below which polyimides had high strength but low ductility, and above which they gained high ductility at the price of losing stiffness and strength as the test temperature approached the Tg of polyimide.

The incorporation of the poly-dimethyl-siloxane segment enhanced ductility without a significant loss of strength (Figure 37), which is one of the major contribution to the improved adhesive bond strength at room temperature. As the test temperature increased, the 10% siloxane copolyimides became ductile, resulting in an increased adhesive bond strength relative to the homopolyimide. The initial higher ductility of poly(imide-10%siloxane) copolymers exhibited a maximum adhesive bond strength at lower temperature (150 °C). Obviously, the adhesive bond strength is lower due to the low strength above 150 °C. The adhesive bond strength of the 20% and 30% siloxane copolymers (30,000 g/mole) were remarkably high at room temperature (5350 and 6893 psi) and decreased with test temperature to 3440 and 2666 psi at 200 °C, respectively. They seemed to have an optimum combination of strength and ductility at or below room temperature. Therefore, only decreasing trend was observed. With this trend, 40% siloxane incorporation might result in optimum combination at temperatures far below room temperature and would probably exhibit a somewhat lower adhesive bond strength at room temperature as has been observed [9, 153].

The stress-strain analysis indicated that tensile strength and modulus decreased with temperature while strain increased; the effect of temperature was noted to be much greater than that of siloxane incorporation. However, the adhesive bond strength of polyimide homopolymer and 10% siloxane copolymer exhibited a maximum at 200 °C and 150 °C, respectively, while 20% and 30% siloxane copolymers showed a maximum values at room temperature. The tensile strength and strain values for maximum adhesive bond strength was 8.5 ksi - 13.9% (200 °C) for polyimide homopolymer, 9.5 ksi - 9.7% (150 °C) for 10% siloxane copolmer, 13.2 ksi - 6.2% (room temperature) for 20% copolymer and 9.9 ksi - 10% (room

temperature) for 30% copolymer. All polyimides except the 20% siloxane copolymer exhibited very simillar tensile strength and strain values, which well support the proposed model. The reason for the off-values of homopolyimide and 20% siloxane copolyimide is possibly due to the discrete measurement of mechanical properties and adhesive bond strength. Therefore, the possible temperature for maximum adhesive bond strength was little lower than 200 °C for homopolyimide, while that for 20% siloxane copolymer fell between room temperature and 100 °C. There seemed to be an optimum combination of tensile strength and strain for the maximum adhesive bond strength, although maximum adhesive bond strength varied with the efficiency of bond consolidation.

4-3-6 Comparison with previous literature studies

In the literature, the adhesive bond strengths of polyimides at room temperature reportedly range from 3,000 to 5,000 psi [13,18-20] and decrease with test temperature similar to the trends observed herein with 20 and 30% siloxane copolymers. The different results obtained in this study can be explained both by the bond consolidation capability and brittle-ductile behavior of the polyimide, which are a function of siloxane content, residual solvent and test temperature. The additional factors are the effect of scrim cloth itself, unremoved low molar mass species and residual poly(amic-acid). In the previous investigations, scrim cloth utilized probably because of the poor flow behavior of early polyimides [12], which were prepared by coating poly(amic-acid) solution on the scrim cloth and drying at around 175 °C. It has been reported that the full imidization was accomplished at 250 °C [12], which indicates that 175 °C might not have achieved 100% conversion of poly(amic-acid) to polyimide. The remaining solvent (residual solvent), unconverted poly (amic-acid) and low molar mass species could be expected to enhance bond consolidation and ductility, resulting in high adhesive bond strength at room temperature. However, in high temperature tests, scrim cloth adhesives lose strength rapidly due to the plasticization effect from residual solvent and low molar mass

species. In order to clarify this phenomena, studies invetigating the effect of residual solvent on the adhesive bond strength were conducted and are discussed in section 4-4.

4-4 Effect of residual solvent on adhesion behavior

As is well understood, mechanical properties as well as flow behavior are strong functions of additives such as plasticizers [107]. The most common plasticizer is the solvent remaining in the adhesives, which is usually unintentionally. In adhesion studies of polyimides, scrim cloth adhesives with poly(amic-acid) have been commonly utilized. The scrim cloth helps to control the adhesive thickness and provides an escape route for volatiles during "cure". Since the scrim cloth adhesives are usually dried at 175 °C for 1 to 3 hours [13,19-20], there could well be significant amount of residual solvent, as reported by Dezern & Young [12]. Although the residual solvent in the adhesive plays a very important role in the evaluation of adhesive bond strength, very few studies have been conducted. Thus, it was considered important here to attempt to correlate the amount of residual solvent with adhesive bond performance both as a function of test temperature and siloxane incorporation.

4-4-1 Residual solvent determination

Traditional scrim cloth adhesives were utilized for the residual solvent study since they can help control the amount of residual solvent in an adhesive. The scrim cloth adhesives were prepared from fully imidized, isolated and redissolved polyimide solution in NMP. The utilized polyimides were end-capped polyimide homopolymer and poly(imide-siloxane) segmented copolymers based on BTDA-mDDS whose molecular weight was 20,000 g/mole. The amount of residual solvent was controlled by drying at different temperatures and was determined by measuring the weight loss at 400 °C in dynamic TGA for all scrim cloth adhesives (Table 17).

The weight loss was also measured after bonding for some adhesives to correlate the effect of bonding temperature with the residual solvent. Since fully imidized polyimides were utilized, it was assumed that the weight loss measured at 400 °C was mainly from the residual NMP solvent.

The residual solvent (weight loss) was a function of drying temperature and siloxane content as shown in Figure 45. The homopolyimide scrim cloth adhesive dried at 100 °C for 12 hours (HSC100) showed about 9% weight loss while that dried at 300 °C (> Tg) for 2 hours, HSC300, showed less than 1%. As the scrim cloth adhesive drying temperature increased, the residual solvent could more easily escape due to the increased free volume. However, at a given scrim cloth drying temperature the residual solvent decreased with siloxane incorporation, which is attributed to enhanced chain flexibility and diffusivity by siloxane incorporation. The residual solvent in the scrim cloth adhesives HSC200 was also measured after bonding at 310, 330 and 350 °C and was found to be less than 1% in general, regardless of the previous drying temp eratures. Despite less than 1% residual solvent from different bonding temperatures, the adhesive bond strength can be very different, which will be discussed later.

It was also reported by Dezern and Young [12] that the volatile content of the scrim cloth adhesive decreased with scrim cloth drying temperature. However, since poly(amic-acid) precursors instead of fully cyclized polyimides were used in their study, a direct comparison was meaningless due to the fact that their volatile fragment was a mixture of solvent and water from the imidization. In the literature, 175 °C drying is widely used, which still has around 9% volatiles, according to Dezern and Young [12], which is slightly higher than our observation. The difference could be due to the water from imidization, in their case.

Table 17. Nomenclature of scrim cloth adhesives as a function of drying condition

SC 100	:	At 100 °C for 12 hours
SC 150	:	At 100 °C for 12 hours, then 150 °C for 2 hours
SC 200	:	At 100 °C for 12 hours, then 200 °C for 2 hours
SC 250	:	At 100 °C for 12 hours, then 250 °C for 2 hours
SC 300	:	At 100 °C for 12 hours, then 300 °C for 2 hours

H: Homopolyimdes

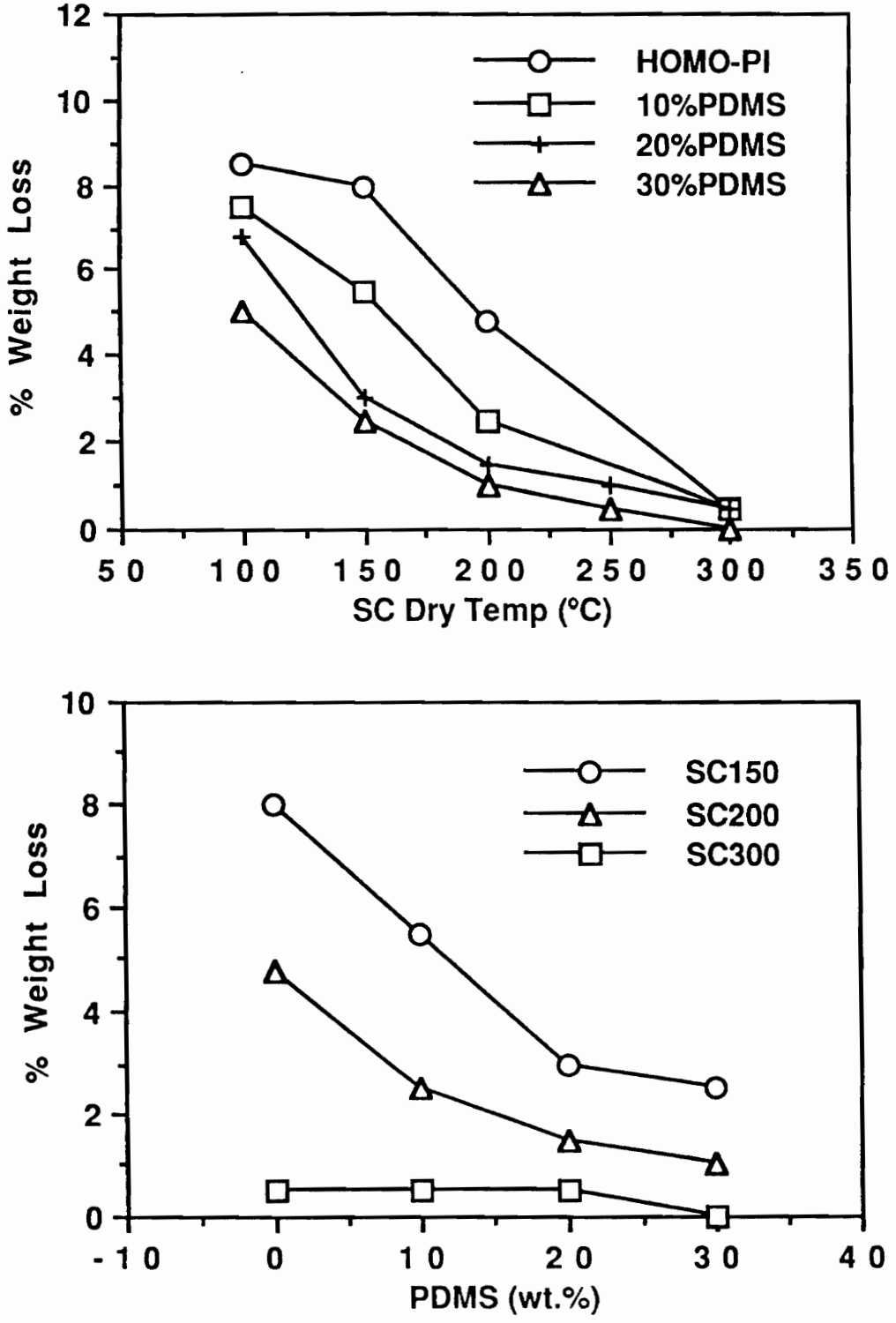

Figure 45. Effect of scrim cloth adhesive drying temperature on the residual solvent measured by TGA

4-4-2 Flow behavior of scrim cloth adheives

The flow or rheological behavior is one of the vital indicators of bond consolidation and is a function of a number of factors such as temperature, time, pressure and plasticizer. The flow properties were measured by pressing a scrim cloth adhesive (1cmx1cm and 10-13 mil thick) at 350 °C, under 10,000 lb load for 10 minutes and expressed as % area expansion. The reported values are the average of four trials. As shown in Figure 46, % flow decreased with scrim cloth drying temperature which is consistent with the decreased residual solvent as seen in Figure 45 and the observations by Dezern and Young [12]. Scrim cloth adhesive based on a homopolyimide dried at 150 °C (HSC150) showed about 460% flow, but those dried at 200 and 300 °C (HSC200 and HSC300) showed only 180 and 80%, respectively.

Although it was found that flow was enhanced by siloxane incorporation and residual solvent, the combined effect was not simply additive, since the siloxane incorporation enhanced flow but lowered the level of residual solvent which eventually decreased the total flow. Thus, the flow enhancement by 10% siloxane incorporation was much smaller than flow reduction by decreased residual solvent. However, further incorporation of siloxane showed increased flow behavior despite the decreased residual solvent. As the scrim cloth drying temperature increased, the flow became insensitive to siloxane content (Figure 46). The scrim cloth dried at 300 °C for 2 hours, SC300, showed only a slight dependence of siloxane on flow, which clearly demonstrated that flow is a function of residual solvent.

4-4-3 Bonding temperature optimization

The effect of bonding temperature on adhesive bond strength was investigated with scrim cloth adhesives based on homopolyimide (20,000 g/mole) which were dried at 100 °C for 12 hours and an additional 2 hours at 150, 200 or 300 °C. The bonding pressure (200 psi) and time

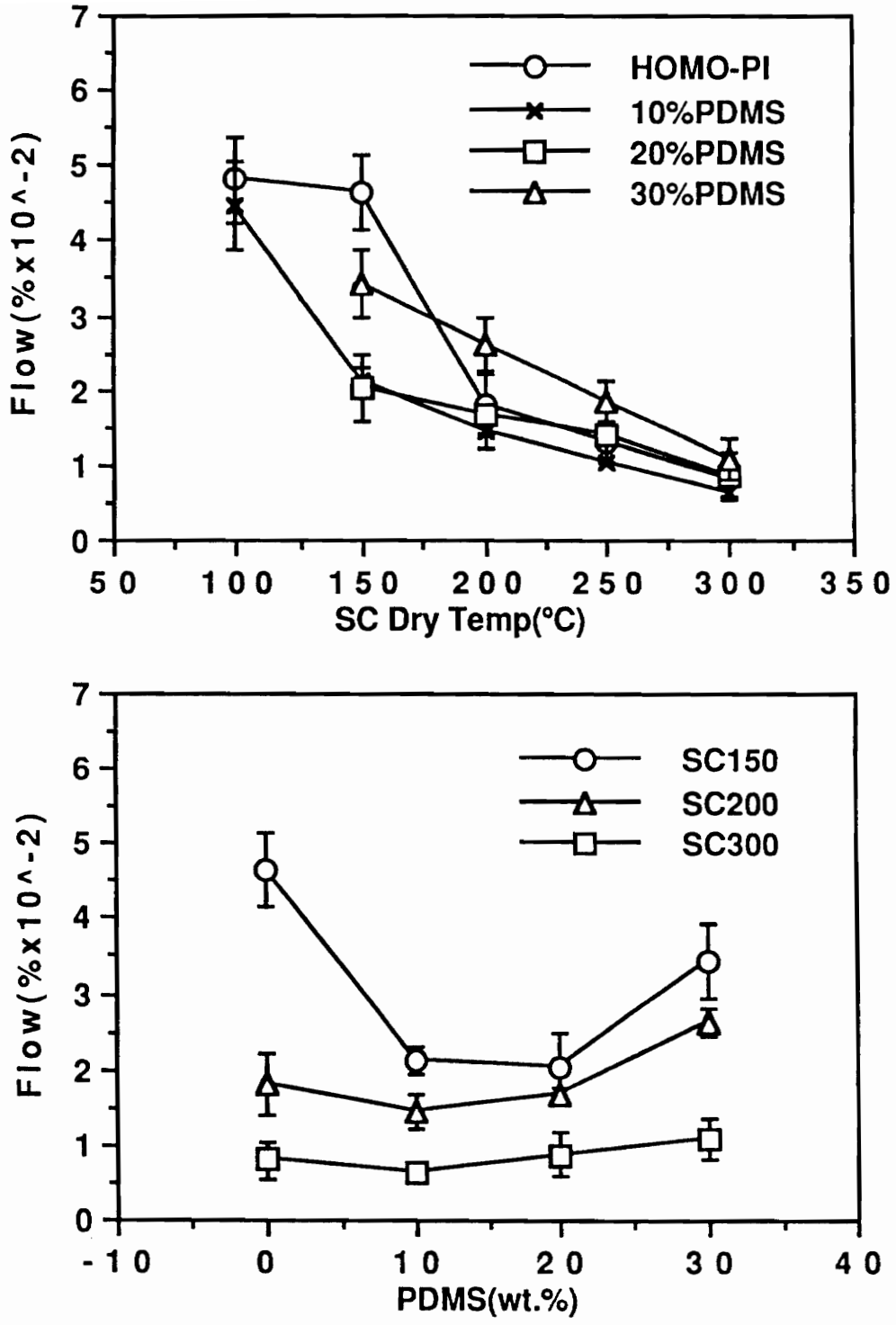

Figure 46. Effect of scrim cloth adhesive drying temperature and siloxane incorporation on the flow behavior of scrim cloth adhesives

(30 min) were fixed while the bonding temperature was varied from 290 to 350 °C. Since bond consolidation is a function of temperature and residual solvent, it was expected that bond strength would vary and thus, it seems appropriate to optimize bonding temperature. As indicated in Figure 47-A, a maximum adhesive bond strength at room temperature was obtained at 330 °C bonding, regardless of the scrim cloth drying temperatures. The region below 330 °C bonding, where lower bond strength was obtained due mainly to the reduced bond consolidation and partially to the brittle nature of the polyimide, is considered as the consolidation control region. The bond strength was also lower despite the relatively good flow in the upper region, because of the brittle nature of the adhesive resulting from the loss of residu alsolvent. This second region is called the ductility control region. At 330 °C bonding, these two conditions were at an optimum, resulting in a maximum bond strength.

However, the adhesive bond strengths of the scrim cloth adhesive at 200 °C increased with bonding temperatures and were similar regardless of the scrim cloth drying temperatures, with exception of the scrim cloth dried at 300 °C (HSC300). The latter exhibited much lower bond strength, as shown in Figure 47-B. Therefore, 350 °C bonding was chosen for later investigation. The adhesive bond strength at 200 °C was higher than those obtained in the room temperature test and the increment depended on the scrim cloth drying temperature, bonding temperature (residual solvent and bond consolidation). The highest increase was observed from SC 300 at 350 °C bonding (85%) and the lowest from SC100 at 290 °C bonding (5%). The former had a fairly good bond consolidation but the brittle adhesive resulting in low adhesive bond strength at room temperature but high strength at 200 °C due to enhanced ductility.

On the other hand, SC100 that had a large amount of residual solvent exhibited the highest adhesive bond strength at room temperature. Only a small increase in adhesive bond strength was achieved at 200 °C because the remaining residual solvent after bonding reduced the strength of the adhesive and lowered the overall adhesive bond strength. These results indicate that the scrim cloth adhesives contained some residual solvent, which was a function of the scrim cloth drying and bonding temperature.

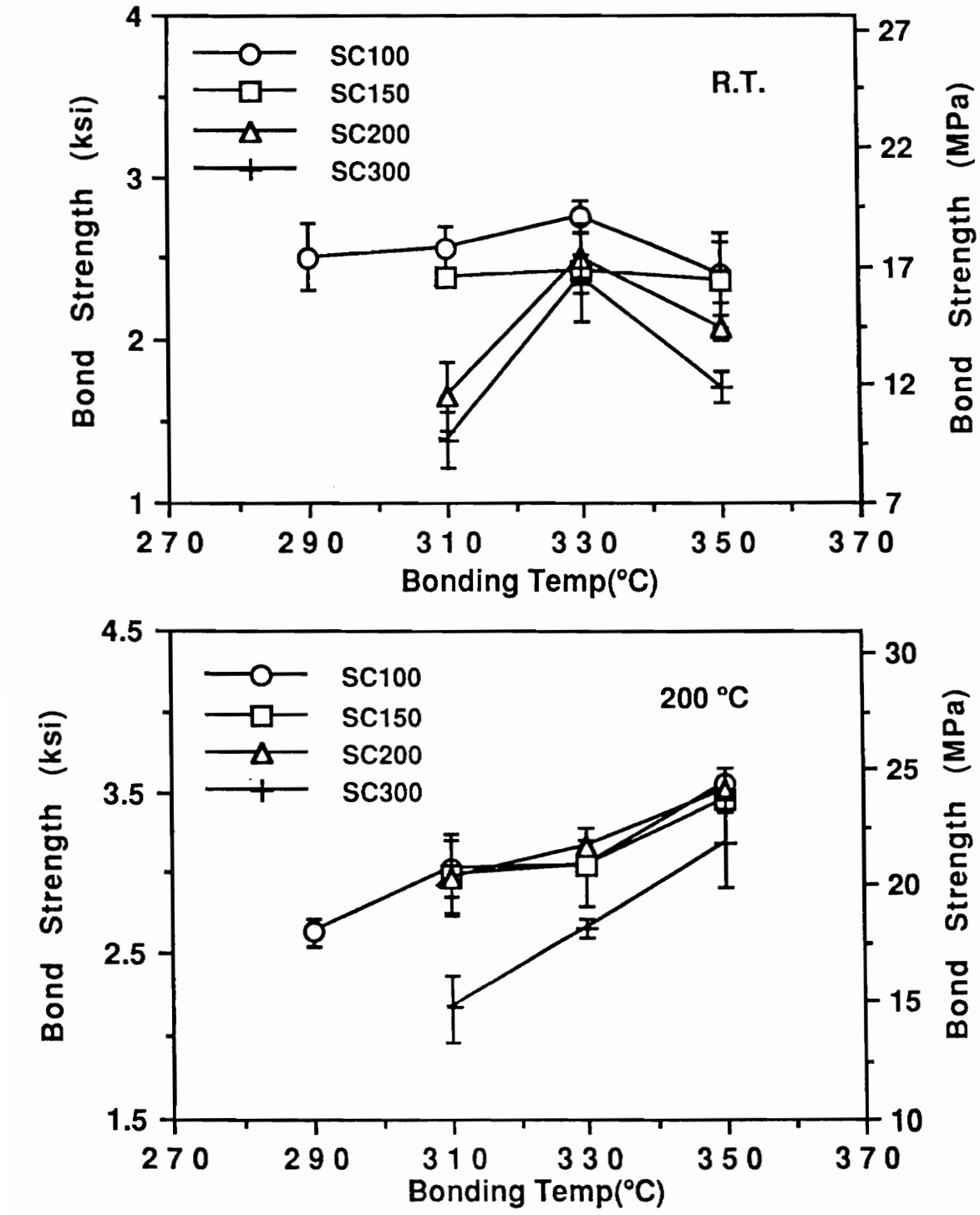

Figure 47. **Effect of bonding temperatures on the adhesive bonding of scrim cloth adhesives:** a) at R.T. and b) at 200 °C test

A distinct adhesive bond performance can be attributed to the brittle-ductile behavior of polyimides. As the bonding temperature increased, the adhesive lost more residual solvent, and could become brittle. Consequently, room temperature test results demonstrated low bond strength, but at 200 °C, enhanced ductility of the adhesive was obtained without detracting from strength thus allowing for higher adhesive bond strength. If, however, the adhesive bonds were tested at even higher temperature (eg. 300 °C), a much lower adhesive bond strength was obtained due to the loss of stiffness and strength above Tg.

4-4-4 Influence of scrim cloth adhesives drying temperature

It was already observed that the flow behavior and the residual solvent are a function of the scrim cloth drying temperature. Since bond consolidation is a decisive factor in adhesive bond strength, it was expected that the adhesive bond strength would decreased with scrim cloth drying temperature. In room temperature tests, the adhesive bond strength of the polyimide homopolymer decreased slightly with scrim cloth drying temperature as reported [12] (Figure 48-A). The scrim cloth dried at 100 °C (HSC100) and at 150 °C (HSC150) showed similar adhesive bond strength (approximately 2400 psi at room temperature) which was expected, but that dried at 300 °C (HSC300) showed about 1700 psi. The adhesive bond strengths at 200 °C did not vary with scrim cloth drying temperatures and were higher than those at room temperature by 45 to 85 %. As the scrim cloth drying temperature increased, the reduced flow and hence bond consolidation by lowered residual solvent resulted in a decreased adhesive bond strength at room temperature. At 200 °C, the previously brittle adhesive became ductile, resulting in increased bond strength. Therefore, almost constant adhesive bond strength from all scrim cloth adhesives were observed at 200 °C. The enhancement of the adhesive bond strength by the test temperature was greater as the scrim cloth drying temperature increased.

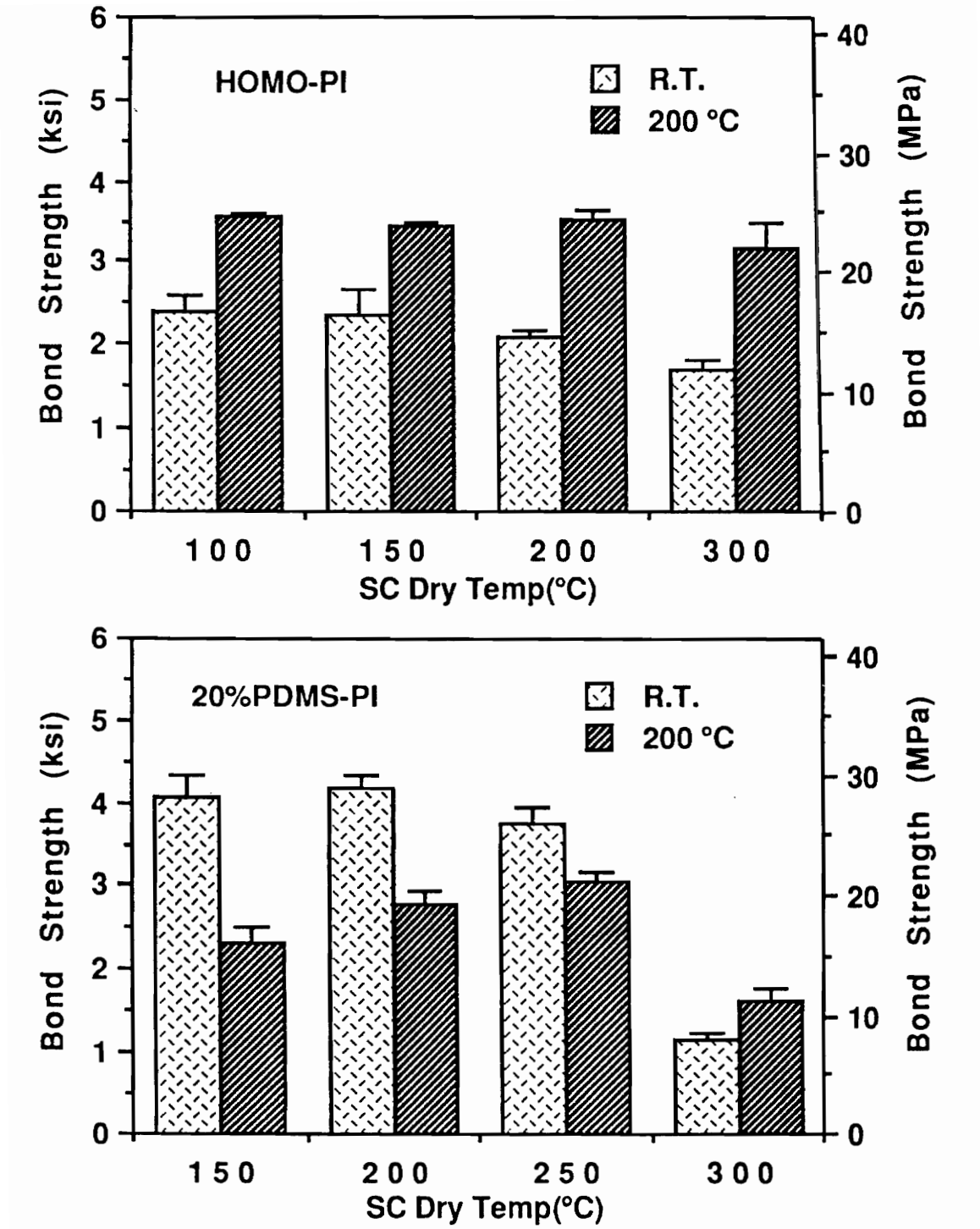

Figure 48. Effect of scrim cloth drying temperatures on the adhesive bond strength

Adhesive bond strength of poly(imide-20% siloxane) copolymer at room temperature was not a function of scrim cloth drying temperature with the exception of SC300, where the scrim cloth drying temperature of 250 °C exhibited a maximum adhesive bond strength at 200 °C (Figure 48-B). This is the same trend as the molecular weight effect previously shown in Figure 42. As the scrim cloth drying temperature increased, less residual solvent remained, resulting in a more brittle adhesive. This system exhibited enhanced adhesive bond strength at 200 °C, with the exception of SC300 as shown in Figure 48-B. As expected, the adhesive bond strength at room temperature was larger than that at 200 °C, which is consistent with results from film adhesives. The scrim cloth adhesive SC300 behaved differently from others, exhibiting very low adhesive bond strength at 25 °C as well as at 200 °C. It is not clear whether this is due to the reduced residual solvent with the high drying temperature or some combination with possible side reactions, both of which resulted in poor flow and brittle adhesive. However, the possibility of chain extension was ruled out because all polymer chains were end capped with non-reactive end groups.

The different behavior of adhesive bond strength can also be attributed to the brittle-ductile behavior of polyimides. Due to the inherent brittle nature of the polyimide at room temperature, the adhesive bonds undergo brittle fracture, resulting in low adhesive bond strength (ductility control). In the moderate temperature range, the ductility is enhanced and the stiffness and strength are nearly constant, leading to higher bond strength. In the high temperature range, low adhesive bond strength would be obtained due to the high ductility but low stiffness/strength (strength control). The ductility can be enhanced not only by thermal energy but also by siloxane incorporation. Residual solvent which would produce similar effects in principle, but this could be a transient effect. Consequently, the level of siloxane and residual solvent have to be controlled according to the application environment and desired degree of bond consolidation

4-4-5 Effect of siloxane incorporation on adhesive bond strength

As indicated in the flow property section, the combined effect of residual solvent and siloxane incorporation on the adhesive bond strength is not a simple matter, since siloxane incorporation enhances flow but reduces the residual solvent in the adhesive. The effect of siloxane incorporation on bond strength at ambient temperature is shown in Figure 49-A. In general, the adhesive bond strength decreased slightly with 10% siloxane incorporation but increased with further incorporation (20% and 30% by weight). The decreased adhesive bond strength of 10% copolymer is mainly due to the reduced flow as indicated in flow property section. The decrease in flow by loss of residual solvent was much larger than enhancement of flow by the 10% siloxane incorporation. However, further incorporation of siloxane increased the adhesive bond strength due to the enhanced bond consolidation and ductility of polyimide despite the reduction of residual solvent. In other words, with higher siloxane content, the effect of enhanced flow and ductility by siloxane incorporation was greater than that lost by reduced residual solvent. SC150 and SC200 exhibited very similar adhesive bond strength regardless of the siloxane content, but SC300 showed lower values compared to SC150 and SC200, due to low bond consolidation.

The bond strength of polyimide copolymers at 200 °C exhibited very different behavior depending on the siloxane content and the scrim cloth drying temperature (Figure 49-B). The scrim cloth adhesives dried at 150 °C for 2 hours (SC150) showed decreasing bond strength with siloxane incorporation. The adhesive bond strength from SC200 decreased with 10% siloxane incorporation, increased with 20% and again decreased with 30%, while that of SC300 decreased with 10% siloxane but increased slightly with further incorporation. All of these phenomena are related to the bond consolidation and brittle-ductile behavior of the polyimide homopolymer or poly(imide-siloxane) segmented copolymer systems. Since SC150 of homopolyimide was ductile due to both residual solvent and elevated temperature (200 °C),

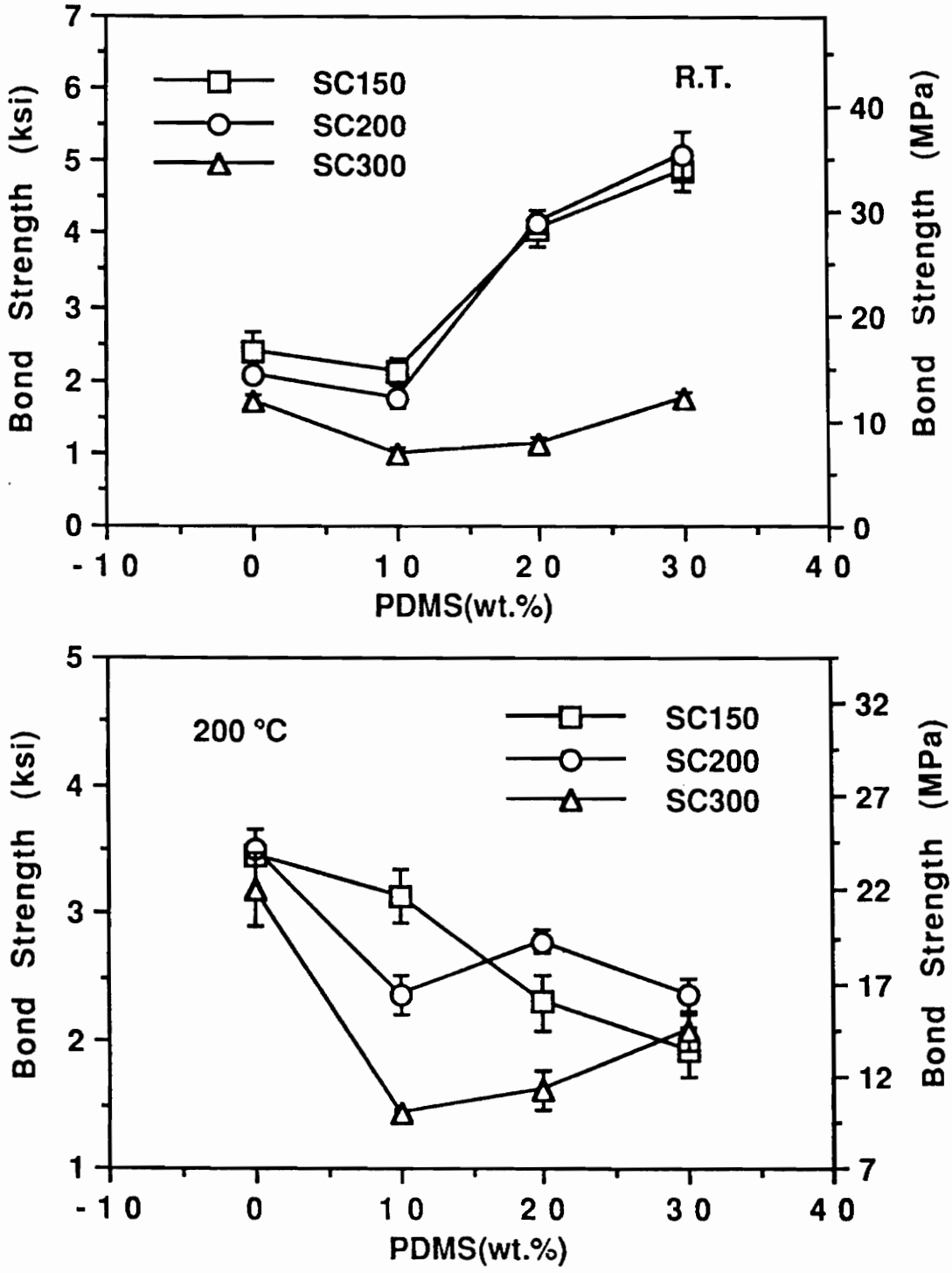

Figure 49. **Effect of siloxane on the adhesive bond strength of polyimide with scrim cloth adhesives:** a) at R.T. and b) at 200 °C test

incorporation of siloxane resulted in lowered adhesive bond strength due to the additional ductility by siloxane incorporation.

The SC300 sample containing very little solvent showed decreased adhesive bond strength with 10% siloxane perhaps due to decreased flow, but exhibited increased adhesive bond strength with 20 and 30% siloxane due to the enhanced flow and ductility. In the case of SC300, ductility was the limiting factor, but for SC150, strength was the limiting factor at 200 °C. The ductility of SC200 homopolyimide at 200 °C was probably close to optimum. With 10% siloxane incorporation, the loss of residual solvent led to poor flow resulting in lowered adhesive bond strength. However, 20% siloxane incorporation enhanced flow as well as ductility, leading to increased increased adhesive bond strength. Finally, adhesive bond increased adhesive bond strength. Finally, adhesive bond strength decreased with 30% siloxane incorporation because of loss of stiffness and strength despite good bond consolidation.

As expected, the adhesive bond performance of copolyimides at 200 °C was a function of siloxane content and bond consolidation (Figure 49). In general, the poly(imide-10% siloxane) segmented copolymer as well as polyimide homopolymer showed higher bond strength at 200 °C than at room temperature while 20% and 30% siloxane copolyimides showed higher bond strength at room temperature. At 200 °C test, the 10% siloxane incorporation enhanced ductility but did not reduce strength, resulting in higher bond strength, while 20% and 30% siloxane copolyimides had high ductility but low strength which led to low adhesive bond strength. An exception, however, was SC300 sample which showed similar bond strength at 200 °C and at room temperature. This may be attributed to reduced bond consolidation resulting from the very low level of residual solvent.

4-4-6 Comparison of scrim cloth adhesives with film adhesives

The adhesive bond strengths of scrim cloth adhesives were compared with those of film adhesives in order to elucidate the effect of residual solvent on the adhesive bond strength of polyimide homopolymers and poly(imide-siloxane) copolymers. All film and scrim cloth adhesives were prepared from polyimides having a molecular weight of 20,000 g/mole, and the scrim cloth adhesives were dried at 150 °C for 2 hours and bonded at 350 °C for 30 minutes. Although the optimum bonding temperature for film adhesives was 360 °C, 350 °C bonding was utilized for the scrim cloth adhesives since 360 °C bonding showed a significant amount of degradation as evidenced by the darkening of the adhesives.

The scrim cloth adhesives of polyimide homopolymer exhibited higher adhesive bond strength at room temperature and 200 °C than film adhesives, while poly(imide-siloxane) copolymers demonstrated lower values with scrim cloth adhesives as depicted in Figure 50. At ambient temperature, the improved adhesive bond strength of scrim cloth adhesive (2370 psi) from polyimide homopolymer compared with film adhesive (1680 psi) was due to the enhanced bond consolidation, which resulted from a significant amount of residual solvent (8%) and partially due to the absence of fluorine on the surface of film adhesive. Since film adhesives were prepared by compression molding with *Teflon®* sheets, they contained around 10% of fluorine on the surface, which reduced the adhesion and thus the adhesive bond strength.

As the siloxane incorporation increased, the film adhesive showed a faster increase of adhesive bond strength than the scrim cloth adhesives. Since the 20% and 30% siloxane copolymers were able to provide good bond consolidation without any assistance from residual solvent, further enhancement of bond consolidation did not occur in scrim cloth systems of 20% and 30% siloxane copolymers. However, a small amount of remaining solvent after bonding enhanced ductility, leading to high extensibility (too low strength), which generated lower adhesive bond strength in the scrim cloth system relative to that of the film. Even a

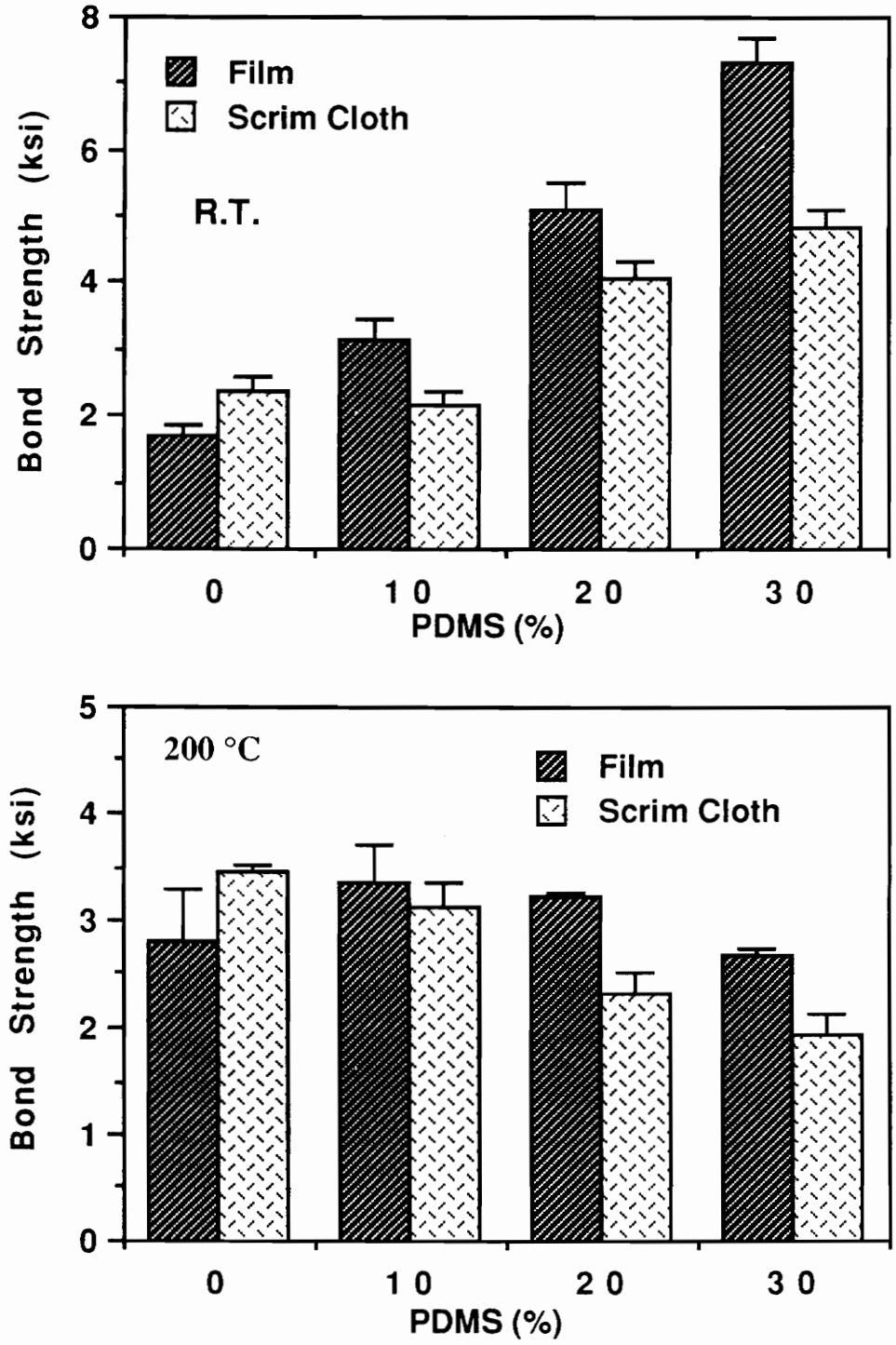

Figure 50. Comparison of adhesive bond strength from scrim cloth adhesive with that from film adhesives

small amount of residual solvent became critical as siloxane incorporation increased and as the test temperature increased.

The scrim cloth adhesives of polyimide homopolymers exhibited higher adhesive bond strength at 200 °C than the film adhesive, while siloxane copolymers showed the opposite trend. The higher adhesive bond strength of scrim cloth adhesives from the polyimide homopolymers at 200 °C is due to increased bond consolidation. The adhesive bond strength of film adhesives increased with 10% siloxane incorporation and decreased with further incorporation at 200 °C, while that of scrim cloth adhesives decreased with siloxane incorporation as shown in Figure 50. In other words, the maximum adhesive bond strength with film adhesive was obtained with the 10% siloxane copolymer, while that with the scrim cloth adhesive was obtained with polyimide homopolymers. Therefore, it is believed that the residual solvent shifted the maximum adhesive bond strength peak to a lower siloxane content (10% to 0%) due to extra ductility by residual solvent.

The comparison of adhesive bond strength of scrim cloth adhesives with that of film adhesives did not provide in full detail the effect of residual solvent on the adhesive bond strength. Although it was expected that the scrim cloth adhesive of the homopolyimide would show high adhesive bond strength (for example 3000-4000 psi) at ambient temperature which would decrease with test temperature, this was not observed. The probable cause is utilization of fully cyclized polyimide which provided much less bond consolidation than poly(amic-acid). Another possibility is that high bonding temperature (350 °C) and long holding time (30 minutes) removed most of the residual solvent and produced brittle adhesives, as evidenced by increased adhesive bond strength of polyimide homopolymer and poly(imide-10% siloxane) copolymer at 200 °C .

In the literature [12, 13, 20], however, poly(amic-acid) has been exclusively utilized and relatively low bonding temperatures (310-330 °C) and short holding time (5-15 minutes) were employed. This procedure may have left a fair amount of residual solvent, which may have

produced ductile adhesives. Brittle adhesives shown lower adhesive bond strength at 25 °C than the ductile adhesives. However, the former exhibited maximum adhesive bond strength with test temperature while the latter showed a significant decrease of adhesive bond strength. Therefore, if lower bonding temperature and shorter holding time had been employed, we might have observed the same trend as that reported in the literature. An additional factor to be considered is the presence of low molar mass species whose effect is believed to be similar as that of the residual solvent. There should be some low molar mass species in scrim cloth adhesive since the poly(amic-acid) utilized was not isolated. However, all polyimides utilized in this study were isolated in a mixture of water and methanol, and no or very little low molar mass species were expected to remain in these polyimide.

4-5 Effect of polyimide structure on adhesion behavior

The polyimides derived from 6FDA exhibited excellent mechanical properties and very high glass transition temperatures with good processability even after full imidization. Therefore, it seemed appropriate to evaluate the adhesive bond strength of these polyimides with Ti-6Al-4V alloys to compare with the adhesive bond strength of polyimides from BTDA-mDDS.

4-5-1 Bonding condition optimization

The optimization of bonding condition is a very important step for maximum adhesive bond strength. Under a fixed holding time (30 minutes), the bonding temperature and pressure were varied, but capable minimum bonding pressure was 500 psi due to limitation of the hot press utilized. For the polyimide from 6FDA-pDDS, the bonding temperature was varied from 380 to 420 °C, and 390 °C was chosen for later use as shown in Table 18. The bonding temperature as well as bonding pressure were varied for polyimide from 6FDA-pPD. In the tem-

perature range of 390 to 450 °C, the maximum adhesive bond strength (which was unfortunately less than 500 psi) was obtained at 420 °C bonding. Although, higher bonding pressure (5,000 psi) was employed, only a slight improvement was obtained (Table 18). As expected from high glass transitions of 6FDA based polymers, the optimum bonding temperatures were higher than that of BTDA -mDDS polyimide.

4-5-2 Adhesive bond strength of high Tg polyimides

The effect of structural modification of polyimide on the adhesive bond strength is shown in Figure 51. The polyimide from 6FDA-pDDS exhibited relatively low adhesive bond strength (755 psi) at room temperature, which is mainly due to the poor bond consolidation from high chain rigidity. As the test temperature increased, the adhesive bond strength increased slightly in 200 °C (790 psi) and 250 °C test (860 psi) but increased greatly in 300 °C test (2167 psi). It was expected that the adhesive bond strength would decrease with further increases of test temperature (eg. 350 °C) due to loss of strength, since Tg of this polyimide is 323 °C. The adhesive bond strength of polyimide from 6FDA-pPD was very low (480 psi) at room temperature and increased with test temperature to 1287 psi in the 300 °C test. It is believed that the adhesive bond strength would increase a little more with test temperature (eg. 330 °C) but eventually would decrease due to the loss of strength as test temperature approaches the Tg of polyimide (345 °C).

Compared with the polyimide from BTDA-mDDS, polyimides from 6FDA exhibited much lower adhesive bond strength at room temperature but higher adhesive bond strength at 300 °C, which is extraordinary. Once again, increasing adhesive bond strength with test temperature is explained by the brittle-ductile behavior of polyimide. Due to their inherent high chain rigidity, 6FDA based polyimides exhibited high brittleness and poor flow resulting in low adhesive bond strength. As test temperature increased, enhanced ductility by thermal energy resulted in increased adhesive bond strength. These results demonstrated that the high

Table 18. Effect of bonding temperature and pressure on the adhesive bond strength of 6FDA-pPD and 6FDA-pDDS polyimides

	6FDA-pDDS	6FDA-pPD	
Bonding Temp. (°C)	500 PSI	500 PSI	5,000 PSI
380	730±75	-	-
390	755±29	392± 37	-
400	751±110	448±25	508±45
410	-	393±30	402±41
420	237±50	481±42	501±48
430	-	441±37	-
450	-	128±22	-

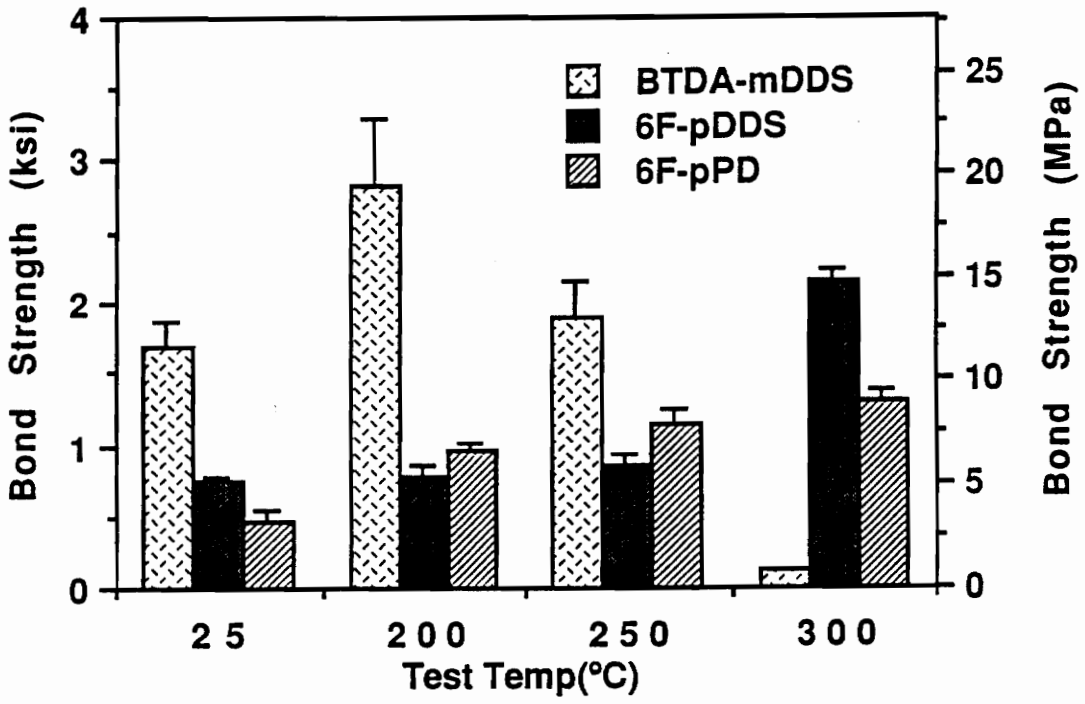

Figure 51. Effect of polyimide structure on the adhesion behavior of polyimides

temperature adhesive bond performance can be improved by structural modification of polyimide.

As expected from mechanical properties which demonstrated decreased tensile strength and modulus with temperature while increased tensile strain with temperature up to 250 °C, the adhesive bond strength of polyimide from 6FDA-pPD increased with test temperature until 300 °C, which is explained by slightly increased strain in that temperature range. Even at 300 °C, strength retention was very high while strain was slightly enhanced. Therefore, it was concluded that the optimum combination of strength and ductility had not been reached yet but it would be at around 330 °C, since the Tg of this polyimide is 345 °C.

4-5-3 Effect of residual solvent on the adhesive bond strength

In order to demonstrate the effect of residual solvent and thus the brittle-ductile behavior of high Tg polyimides, adhesive bond strength was determined with scrim cloth adhesive of polyimide from 6FDA-pPD. The scrim cloth adhesive was prepared as described earlier and dried at 150 °C for 2 hours. The adhesive bond strength was measured at room temperature, 200, 250 and 300 °C as shown in Figure 52. The adhesive bond strength with test temperatures of 200 °C and 250 °C but decreased with 300 °C. This was different from that of the film adhesive which demonstrated increasing adhesive bond strength with test temperatures. As expected, the scrim cloth adhesive exhibited higher adhesive bond strength than film adhesive at 25 °C and similarly at 200 and 250 °C, but showed lower values at 300 °C test. This is attributed to the presence of a small amount of residual solvent in the scrim cloth adhesives, which enhanced bond consolidation, resulting in improved adhesive bond strength in R.T. test.

However, since test temperature of 300 °C imparted sufficient ductility by itself, additional contribution from residual solvent led to too high ductility, thereby lowering the adhesive bond strength of scrim cloth adhesive sive at 300 °C. Therefore, the film adhesives containing no

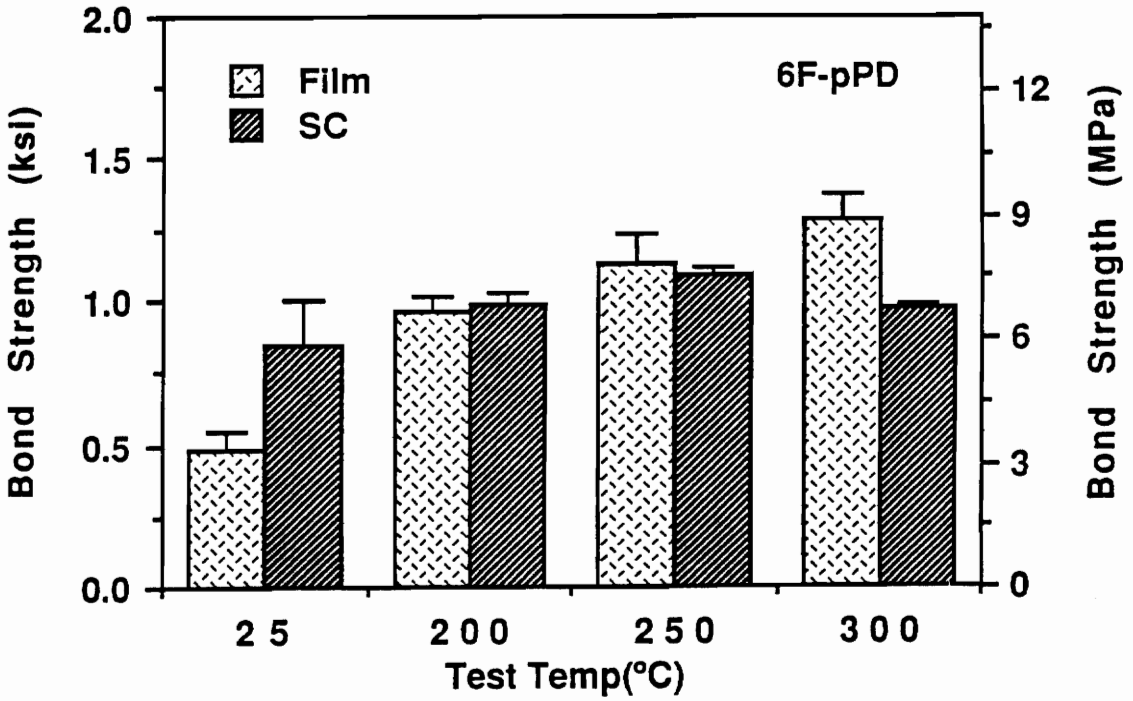

Figure 52. Effect of scrim cloth adhesive on the adhesive bond strength of high Tg polyimides

residual solvent resulted in higher adhesive bond strength than scrim cloth adhesives at 300 °C. This is exactly the same phenomena observed in the residual solvent study of BTDA-mDDS polyimides. It might also be said that the residual solvent moved the maximum adhesive bond strength peak from 300 °C to 250 °C, which was the same trend shown in Figure 44, 48, and 50. These results indicated that whatever enhances the ductility of adhesives, the maximum adhesive bond strength moves to a lower level. It was also proven that the residual solvent has tremendous effect on the adhesive bond performance of polyimides, and the highest adhesive bond strength could be obtained at room temperature if there is a right amount of residual solvent.

4-6 Failure mode analysis of adhesive bonds

The adhesive bond failure modes should be mentioned whenever adhesive bond strengths are explained in order to provide a better understanding of the adhesive bond performance and/or the goodness of surface treatment, especially in a durability test. Therefore, it was attempted to correlate the adhesive bond strength with failure modes. Two major failure modes are cohesive and adhesive failure (or interfacial failure); the former stands for failure within the adhesives while the latter indicates failure between the adhesive and the adherend. Unless it was clearly a cohesive failure by visual inspection, X-ray photoelectron spectroscopy (XPS) was utilized to determine the actual failure mode. The failure modes found in this study were a function of test temperature and bond consolidation which is controlled by the molecular weight, siloxane content, residual solvent and polyimide structure.

4-6-1 Failure modes of polyimide film adhesives from BTDA-mDDS

The failure modes were determined by visual inspection and when necessary by XPS. XPS analysis was conducted on the adhesive and adherend side as well as Pasa Jell treated Ti-6Al-4V adherend, primer coated Ti-6Al-4V adherend, compression molded film and scrim cloth adhesives. The XPS results from selected samples are shown in Table 19. Surface analysis of Pasa Jell 107 treated Ti-6Al-4V adherend detected Ti (9.3%), Si (15.8%) and F (1.8%). It is believed that silicon was derived from the sand blasting treatment while fluorine is from Pasa Jell whose constituents are 40% nitric acid, 10% combined fluorides, 10% chromic acid, 1% coupler and balance water. As expected, the theoretical calculation indicates that polyimide homopolymer contained 74.4% carbon, 17.8% oxygen, 5.1% nitrogen and 2.6% sulfur while the cast film did not have Ti or fluorine but contained nitrogen (5.7%), sulfur (1.6%) and silicon (0.5%); the first two elements are from polyimide itself while the latter may be a contaminant. However, the compression molded film showed more than 20% of fluorine, and a small amount of nitrogen (2.1%) and sulfur (0.95%). The lower concentration of nitrogen and sulfur is due to the predominating flurone in the surface layer.

The decision on failure modes was made based on the detection of titanium, sulfur and nitrogen since titanium is a major constituent of Ti-6Al-4V adherend while the polyimide of BTDA-mDDS contained sulfur and nitrogen. The fluorine may also have come from the *Teflon®* sheet used in compression molding and provided an additional information. However, the silicon did not play an decisive role, since it either came from the polyimide copolymers, grit blaster and/or contamination unless binding energies of this element is carefully determined. The failure mode of the polyimide from BTDA-mDDS was a function of molecular weight, siloxane content and test temperature as shown in Table 20. Adhesive failure between primer coating and the adhesives (mode AA) was dominant for polyimide homopolymers and poly(imide-10%siloxane) copolymers, while 20 and 30% siloxane copolymers exhibited cohesive failure in general. The polyimide homopolymer having molecular weight of 20,000 g/mole

Table 19. XPS results of failure analysis

		C	O	Ti	Si	F	N	S
Ti 6/4 (Pasa Jell treated)		28.68	44.43	9.3	15.81	1.78	--	--
H-PI (20k)	Cast Film	72.19	19.97	--	0.51	--	5.69	1.64
	SC Adhesive	73.89	18.23	--	0.92	--	4.79	2.17
	CM Film	60.69	7.89	--	--	27.97	2.10	0.95
	Calculation	74.4	17.8	--	--	--	5.1	2.6
H-PI, Film	Film Side	66.84	22.95	--	--	2.49	5.38	2.34
(150 °C)	Ti Side	63.26	25.95	--	--	3.95	4.68	2.16
HSC300	SC Side	61.52	32.20	--	1.42	--	3.28	1.58
	Ti Sice	58.02	37.37	--	1.08	--	3.77	1.76
HSC100	SC Side	57.89	31.82	--	2.11	--	4.31	1.84
	Ti Side	59.97	31.31	--	1.86	--	4.84	2.01
10%PDMS	Cast Film	58.72	26.53	--	10.77	--	2.89	1.10
	SC Adhesive	69.23	19.82	--	5.17	--	3.99	1.80
	CM Film	57.48	18.02	--	4.95	6.04	2.56	0.94
10% PDMS	Ti Side	61.72	27.49	--	1.51	2.90	4.53	1.85
(Film Adh)	Film Side	60.05	27.36	--	2.80	3.15	4.94	1.70
10%PDMS	Ti Side	67.97	20.69	--	3.47	--	5.49	2.38
(SC100)	SCSide	67.51	20.85	--	5.56		4.21	1.87
10%PDMS	Ti Side	66.33	21.49	--	3.91		5.81	2.46
(SC300)	SC Side	61.95	23.91	-	7.39	--	4.57	2.17
6FDA-pPD	CM Film	49.78	4.68	--	--	43.62	1.92	--
	SC Adhesive	71.75	11.35	--	1.19	11.40	4.32	--
6FDA-pPD	Ti Side	32.35	40.02	10.88	3.44	11.40	1.92	--
(150 °C)	Film Side	56.41	22.77	1.92	2.04	11.47	4.40	--
6FDA-pPD	Ti Side	27.08	39.69	9 05	4.62	13.01	2.13	--
	SC Side	65.54	13.11	1.22	2.01	15.25	3.86	--
SC Itself	C:29.75, O:40.51, Si:17.86, N:3.08, S:0.72, Ca:2.53, Ba:0.06, Al:3.94							

exhibited a layered failure in 300 °C test as shown in Figure 53, but the interpretation of this is not clear.

The surface analysis of the adhesive and Ti-6Al-4V adherend side of samples from polyimide homopolymer (20,000 g/mole) tested at 150 °C showed similar atomic concentration of O, C, F, N and S on both sides (Table 19). This may lead to the conclusion that it is a cohesive failure. However, the detection of fluorine on both sides indicated that this could be an interfacial failure between the primer coating and film adhesive since fluorin was only on film adhesive. If this is true cohesive failure, fluorine should not be detected on both sides, and it should be very low in concentration if it represents adhesive failure between the titanium oxide and primer coating. All conclusion on the failure mode was made based on such analysis. Interfacial failure also indicated that bond consolidation was not good as predicted from low adhesive bond strength. The poly(imide-10% siloxane) copolymers (20,000 g/mole) generally exhibited the same failure mode as the polyimide homopolymer (Table 19). The XPS analysis of poly(imide-10%siloxane) copolymers tested at 150 °C showed the same trend as for the polyimide homopolymer (20,000 g/mole). The only difference was an increased silicon content, due to the siloxane and more random adhesive failure at 200 °C.

With higher siloxane content, the locus of failure changed from AA mode (between adhesive and primer coating) to cohesive failure, which is attributed to increased chain flexibility resulting in enhanced ductility and bond consolidation. The ideal cohesive failure (CI) (Figure 53) was dominant for 20% siloxane copolymer with the exception of the uncontrolled molecular weight (UEC) samples which exhibited adhesive failure between primer coating and adhesives (AA type). Also at 200 °C, all 20% siloxane copolymers showed a random type adhesive failure due to enhanced ductility. On the other hand, poly(imide-30% siloxane) copolymer produced all cohesive failure mode. In the lower test temperature region, an ideal type cohesive failure was observed while in the upper region, random distribution of adhesive on both sides was obtained. The failure mode is thus directly related to adhesive bond strength; generally cohesive failure resulted in better adhesive bond performance. In general,

Table 20. Summary of failure mode of film adhesive from BTDA-mDDS polyimide

		Testing Temperature (°C)			
		R.T.	100	150	200
Homo-PI	20k	AA	AA	AA	AA
	30K	AA	-	-	AA
	40K	A A	-	-	AA
10%PDMS	20K	AA	AA	AA	AR
	30k	AA	AA	AA	AR
	40K	AA	AA	AA	AR
	UEC	AA	-	-	-
20%PDMS	20K	CI	CI	CI	AR
	30K	CI	CI	CI	AR
	40K	CI	CI	CI	AR
	UEC	AA	-	-	-
30%PDMS	20K	CI	CI	CR	CR
	30K	CI	CI	CR	CR

AA: Adhesive Failure between adhesive and primer coating

AR: Random distribution of adhesive on both side

CI : Ideal cohesive failure

CR: Random cohesive failure

R.T.: Room Temperature

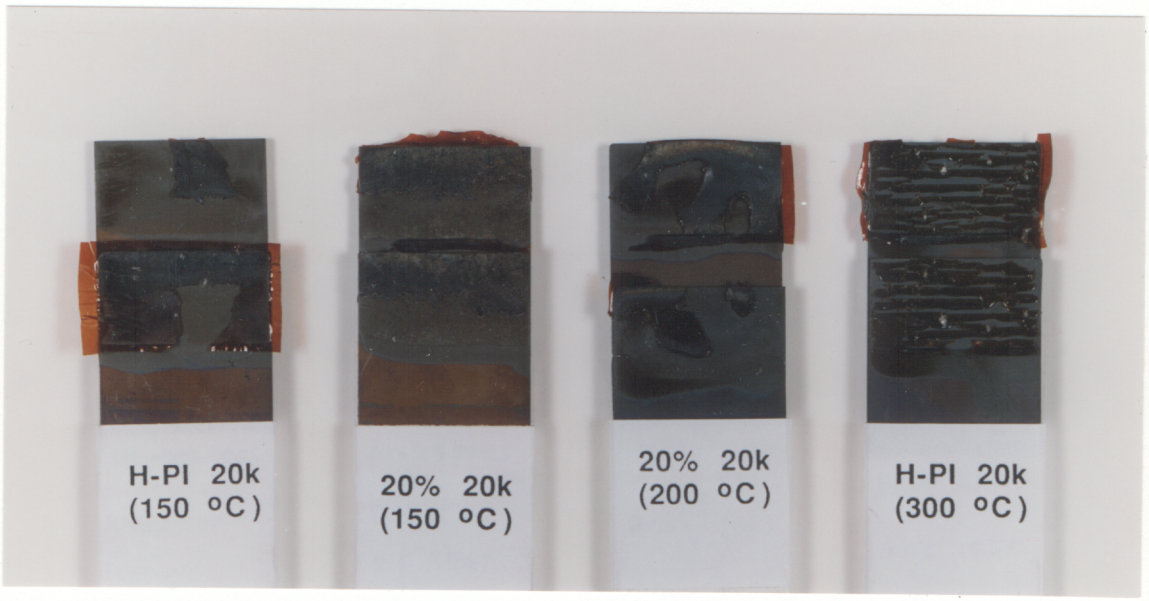

Figure 53. Examples of failure mode of film adhesive from BTDA-mDDS polyimide: a) adhesive, b) ideal-cohesive, c) random-cohesive, d) layered failure

good bond consolidation leads to high adhesive bond strength and thus cohesive failure, while poor bond consolidation associated with high chain rigidity and/or high molecular weight (viscosity) generated poor bond consolidation and resulted in interfacial failure and low adhesive bond strength. However, the failure mode depends not only on polymer characteristics but also on surface preparation as discussed earlier.

4-6-2 Failure mode of polyimide scrim cloth adhesives

The presence of residual solvent improved adhesive bond strength for 25 °C and moderate temperature tests, which was attributed to enhanced bond consolidation and ductility. As a result, it was expected that scrim cloth adhesives would exhibit either cohesive or mixed failure rather than interfacial failure. Although a number of samples seemed to show adhesive failure, XPS analysis indicated all cohesive failure. Therefore, failure modes were labeled as CA, CM and CC which stand for cohesive type adhesive failure, cohesive type mixed failure and cohesive type cohesive failure, respectively and they are shown in Figure 54. In general, the failure mode changed from CA to CM and to CC with siloxane incorporation due to the enhanced bond consolidation and ductility. The CA failure mode was dominant for polyimide homopolymers and CM for poly(imide-10 %siloxane) copolymers, while CC mode was observed with poly(imide-30%siloxane) copolymers. Scrim cloth adhesive dried at 300 °C exhibited slightly different failure mode from other scrim cloth adhesives, which is believed to be from very low residual solvent. But no major difference was noticed between the 25 °C test and 200 °C tests (Table 21).

According to the XPS analysis of scrim cloth adhesives from polyimide homopolymer (HSC300 and HSC100), the actual failure may have occurred at the interface of polyimide and scrim cloth, which was evidenced by increased intensity of silicon on both sides, compared with those from cast film and scrim cloth adhesives. Since scrim cloth (E-glass) is composed of 52.4 % SiO_2, 14.4% Al_2O_3 and Fe_2O_3, 17.2% CaO, 4.6% MgO and 10.6% Ba_2O_3, the enhanced

Table 21. Summary of failure mode of scrim cloth adhesive from BTDA-mDDS polyimide

		Failure Mode			
		Homo-PI	10%PDMS	20%PDMS	30%PDMS
SC100	R.T.	CA	CM	-	-
	200 °C	CA	CM	-	-
SC150	R.T.	CM	CM	CC	CC
	200 °C	CM	CM	CM	CC
SC200	R.T.	CA	CM	CC	CC
	200 °C	CM	CM	CM	CC
SC250	R.T.	-	-	CC	CC
	200 °C	-	-	CM	CC
SC300	R.T.	CA	CA	CM	CM
	200 °C	CA	CA	CM	CC

CA: Failure between scrim cloth and polyimide
CM: Failure between scrim cloth and polyimide, but random distribution of scrim cloth on both side
CC: Failure between scrim cloth and polyimide, even disribution of scrim cloth on both side (mirror image)

R.T.: Room Temperature

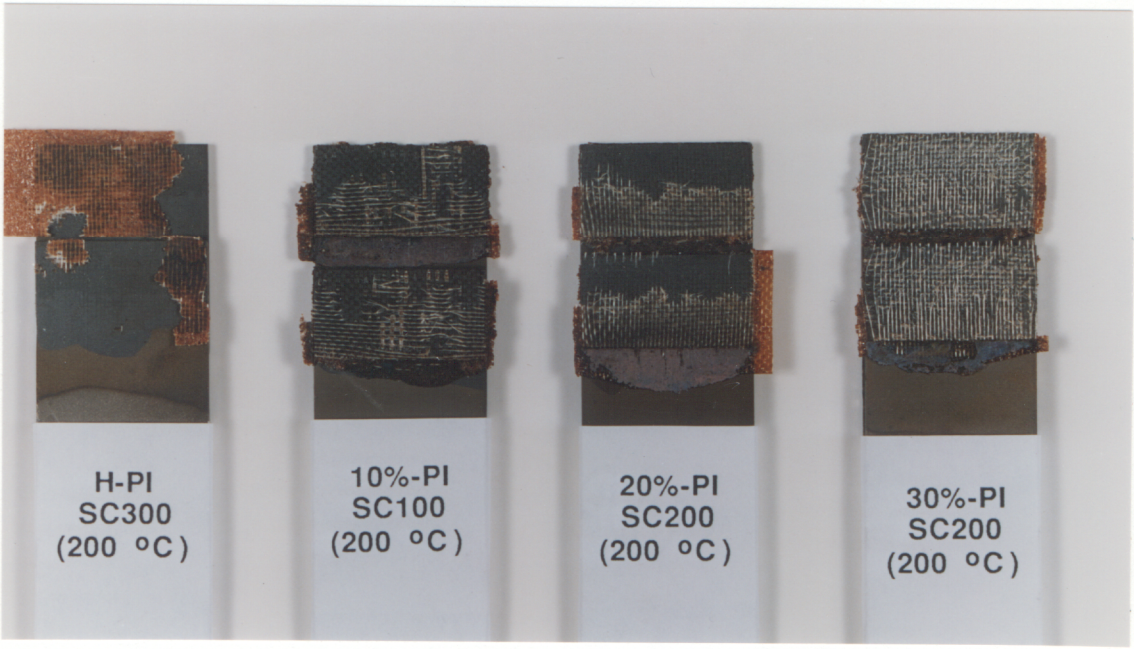

Figure 54. Examples of failure mode of scrim cloth adhesive of homopolyimide: a)adhesive-cohesive, b)mixed-cohesive, c)ideal-cohesive, d)cohesive-cohesive

intensities of silicon is believed to be derived from scrim cloth. Therefore, it was concluded that the failure occurred between polyimide and scrim cloth, resulting in a small amount of scrim cloth transfer to the Ti adherend side. The CM failure mode, which looked like mixed mode but was cohesive, occurred in the scrim cloth with uneven distribution of scrim cloth on each side. The CC mode, cohesive failure of the scrim cloth itself, was not analysed by XPS. In thid mode, the scrim cloth was seen on both side of the samples, as in a mirror image.

4-6-3 Effect of pc mide structure on failure mode

The structural modification of polyimides resulted in very low adhesive bond strength at room temperature. Basically, the failure mode for high Tg polyimides was interfacial failure between primer coating and Ti oxide indicating poor bondability. XPS analysis of the polyimide film adhesive from 6FDA-pPD (Table 19) showed a similar concentration of fluorine on both sides but higher concentration (11%) of Ti on the Ti side and low Ti (2%) on the adhesive side. The nitrogen concentration was high (4.4%) on the adhesive side but low (1.9%) on the Ti side. The carbon and oxygen on Ti side were almost the same as those on Pasa Jell treated Ti adherend. Therefore, it was concluded that interfacial failure occurred between Ti oxide and polyimide primer coating. In the scrim cloth adhesive case, the atomic concentration of all elements were the same as film adhesive case. The interfacial failure of 6FDA based polyimide adhesives may be from fluroine in polyimide. Therefore, it is recommended to find or develope proper surface treatment for these polyimides.

4-7 Proposed model

It has been observed that the adhesive bond strength of polyimides either exhibited a maximum at some temperatures or decreased with test temperature (Figure 44, 47, 48, 50, 51, 52).

In the former case (Figure 51), as the Tg of polyimide increased, a maximum adhesive bond strength was obtained at higher temperature. The value determined was smaller, which is due likely to decreased adhesive bond consolidation. In the latter case, the adhesive bond strength decreased with temperature and lower Tg polyimide showed higher values at 25 °C. The question arises what if temperature decreased further ? Would adhesive bond strength keep increasing ? To put it another other way, would tensile strength and modulus keep increasing with decreased temperature while tensile strain keep decreasing ? The answer is obviously no, otherwise a tremendous research effort would have not been carried out to improve the cryogenic material properties. As the temperature decreased, molecular motion becomes smaller and the material would become more brittle in nature. With this in mind, there should be a temperature which provide an optimum combination of strength and ductility (strain), which would result in maximum adhesive bond strength observed in Figure 55.

Due to inherently brittle nature of the high Tg polyimides at room temperature, adhesive bonds undergo brittle fracture, resulting in low adhesive bond strength (ductility control) as indicated in Figure 56. In the moderate temperature range, the ductility is slightly enhanced while the strength decreased slightly, leading to improved adhesive bond strength. In the high temperature range, low adhesive bond strength would be obtained due to high ductility but low strength (strength control) (Figure 56, top)). The ductility can be enhanced not only by thermal energy but also by rubber, eg. siloxane incorporation and residual solvent.

As observed, increased chain stiffness of the polyimide shifted the maximum adhesive bond strength peak to higher temperature while siloxane incorporation moved it to a lower temperature. Therefore, it is proposed that factors which increase chain stiffness move the point of maximum adhesive bond strength to higher temperature and vice versa as indicated in Figure 56 (bottom). The common softening agents are plasticizers such as low molar mass species, residual solvent and rubber(eg. siloxane). Thus, maximum adhesive bond strength could be obtained at lower temperature with less chain stiffness and/or more plasticizers, while it can also be achieved at higher temperature with rigid chain.

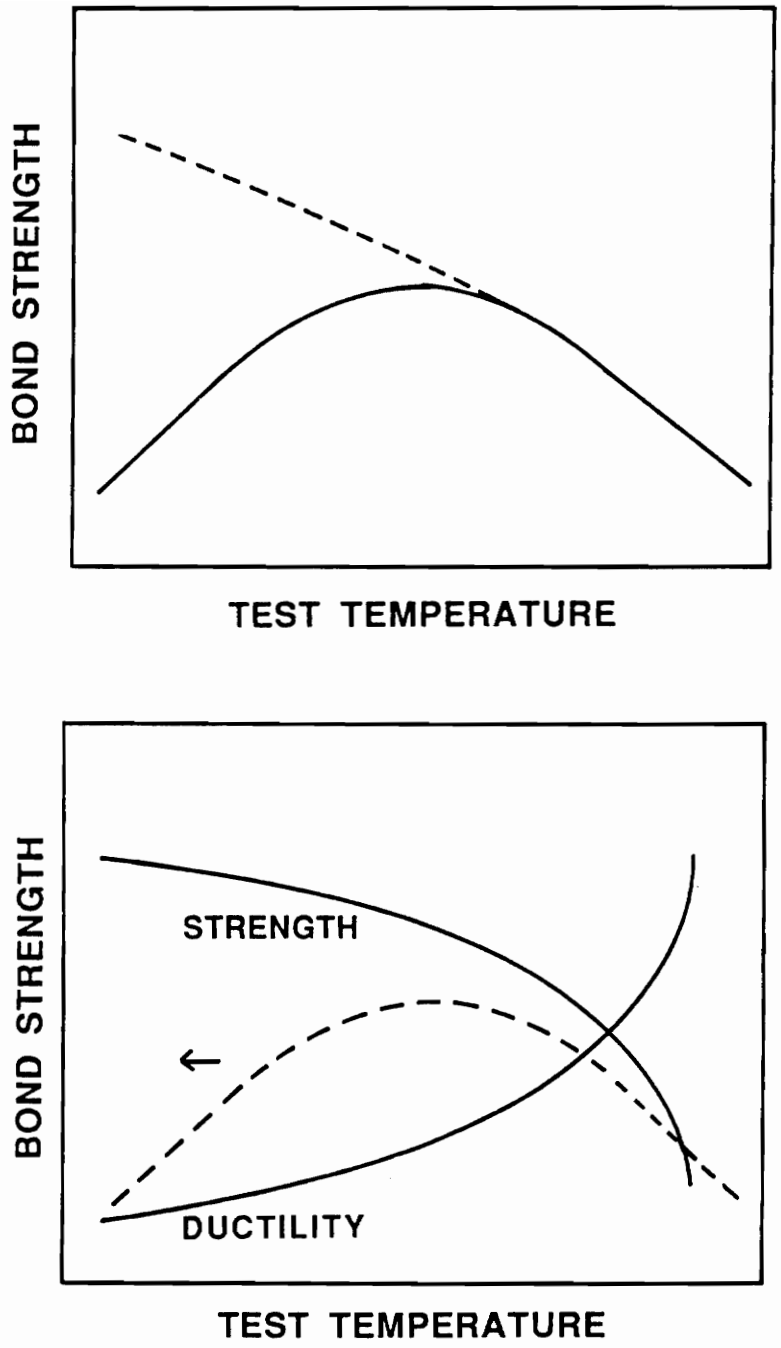

Figure 55. A possible model for the relationship between strength, ductility and bond strength at a given strain rate

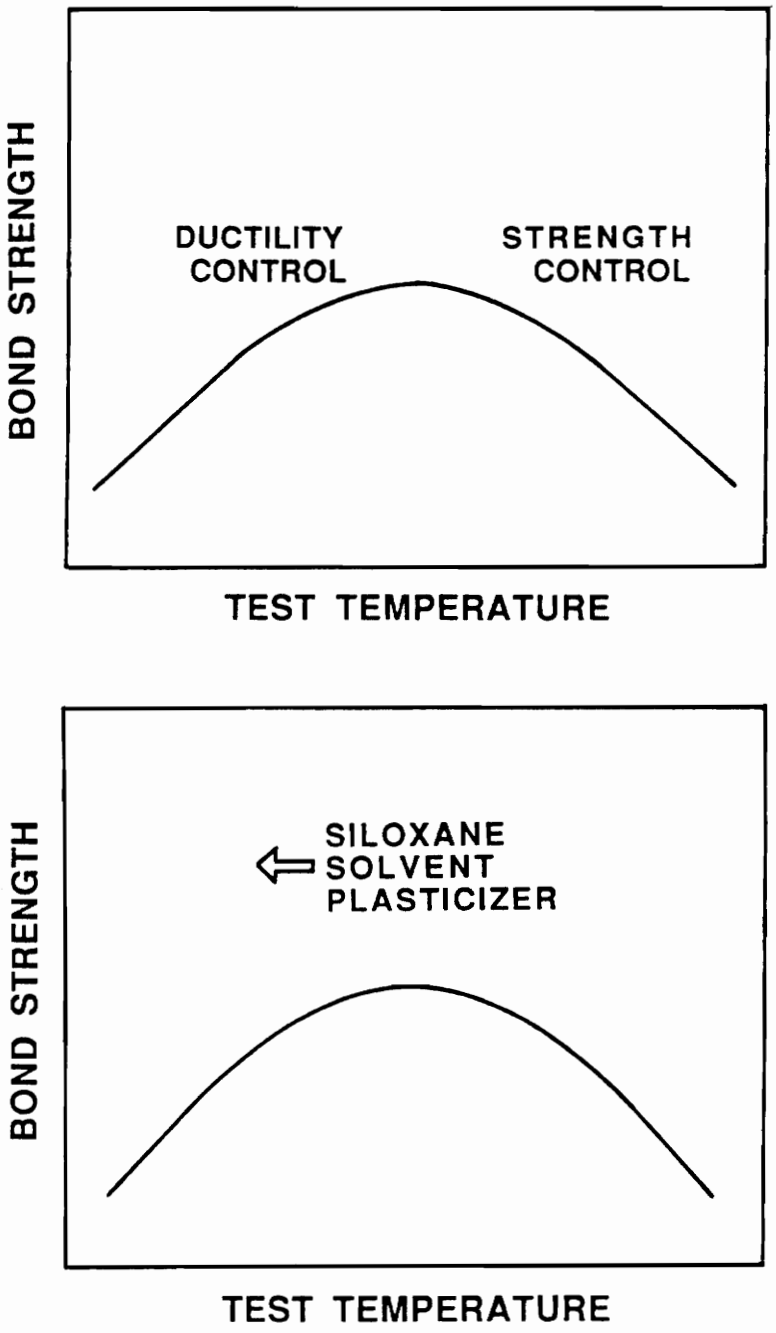

Figure 56. Proposed model for adhesive bond strength variation with test temperature at a given strain rate

However, most of previous studies in the literature have not observed increasing adhesive bond strength with test temperature, which can be explained by considering the nature of the polymer and the presence of "unintentional" plasticizers. In most adhesion studies of polyimides, scrim cloth adhesives have been widely utilized due to the insoluble and infusible nature of many polyimides. In general, scrim cloth adhesives were prepared by brush coating unisolated poly(amic-acid) on E-glass fabric, called scrim cloth and dried at 175 °C. It was found that these scrim cloth adhesives contained a fair amount of residual solvent and unconverted poly(amic-acid) and also possibly low molar mass species, all of which enhanced bond consolidation resulting in high adhesive bond strength (3,000 to 5,000 psi) at room temperature.

Decreased adhesive bond strength with test temperature indicated that the scrim cloth adhesive contained plasticizer(s), which was supported by lower Tg of scrim cloth system even after bonding (when compared with the film adhesive). Another evidence was that aging bonded samples at high temperature (eg 204 °C) for long period of time (500 -10,000 hours) lowered the adhesive bond strength at ambient temperature, but improved adhesive bond strength at elevated temperatures. It is believed that aging removed the residual solvent and/or trapped water in the scrim cloth adhesive, or induced chain extension reactions, or both. All of these decreased the ductility of adhesives, resulting in lower adhesive bond strength at ambient temperature, but enhanced values at elevated temperatures such as 204 °C. A fair amount of residual solvent and low molar mass species provided highly ductile scrim cloth adhesive, resulting in high adhesive bond strength at ambient temperature. As the test temperature increased, the adhesive bond strength decreased since ductility provided by thermal energy and by plasticizers was excessive leading to low strength but high strain. Therefore, it is believed that maximum adhesive bond strength would have been obtained at or below ambient temperature in the previous literature studies. Thus, only the upper portion of the whole curve was observed in the early studies. In certain cases, the presence of plasticizer may be desirable; eg., very high chain stiffness polyimides such as 6FDA-pPD

polyimide which has high viscosity and very poor bond consolidation and needs "plasticizer" to enhance bond consolidation and thus adhesive bond strength.

4-8 Adhesion study of PEEK-graphite composite

Polymeric composites have been used increasingly for military, aerospace, sporting goods and automobile applications due to their superior properties relative to ceramic or metallic materials, such as high specific strength and specific modulus, high corrosion resistance and design flexibilities. One of the major obstacles for wide application is joining difficulty. Adhesive bonding, as opposed to mechanical fastening, has been in creasingly utilized for composite joining. In order to achieve strong and durable adhesive bonding, proper surface treatments and good adhesives are vital requirements. In this section, the adhesive bond performance of *PEEK*®-graphite composite with a poly(imide-30%siloxane) segmented copolymer and with *Ultem*® 1000, commercial poly(ether imide), was investigated as a function of surface treatments such as treatment. The treated composite surface was characterized by XPS, SEM and contact angle measurement, and the results were correlated to adhesive bond performance.

4-8-1 Bonding temperature optimization

In order to achieve maximum adhesive bond performance, bonding temperature was optimized under fixed load of 200 psi and holding time of 30 minutes. The bonding temperature was varied from 290 to 340 °C for *Ultem*® 1000 and from 330 to 360 °C for poly(imide-30% siloxane) copolymer as indicated in Table 22. The "welding" adhesion of *PEEK*®-graphite composite themselves provided 6800 psi at 360 °C bonding, while values of 1540 and 800 psi at 340 and 350 °C bonding were observed, respectively. However, a problem existed from

Table 22. **Bonding temperature optimization of PEEK-graphite composite**

	Bonding Temperature (°C)						
	300	310	320	330	340	350	360
NO ADHESIVE				0	880	1542	6800
PEEK® (P45)				0	--	850	--
PI-30%PDMS				609	1332	2147	--
Ultem® 1000	2712	3089	3127	2972	2802	--	

1. severe deformation at 360 °C bonding and slight deformation at 350 °C
2. surface only washed with water and acetone (no primer, no sand blasting)

deformation of the composite at 350 and 360 °C bonding temperatures since *PEEK®* has Tg of 145 °C and Tm of 345 °C. As expected, poly(imide-30%siloxane) segmented copolymer exhibited 2140 psi in 350 °C bonding, with slight deformation of *PEEK®*-graphite composite, and 1332 psi in 340 °C bonding without any deformation. Therefore, 340 °C was chosen for the investigation. On the other hand, bonding temperature was varied from 290 to 340 °C for *Ultem®* 1000. Although high adhesive bond strength was obtained at 310 and 320 °C bonding, 310 °C was chosen for later studies. Acetone washed *PEEK®* composites were utilized for the adhesion of poly(imide-30%siloxane) copolymer while sand blasted adherends were utilized for *Ultem®* 1000.

4-8-2 Effect of surface treatment on adhesive bond strength

The adhesive bond strength of *PEEK®*-graphite composite increased with grit blasting, and further with gas plasma treatment as shown in Figure 57. A combination of grit blasting and gas plasma treatment was also desirable. The adhesive bond strength with the poly(imide-30%siloxane) copolymer increased to 3263 psi when treated with grit blasting, which is approximately a 250% enhancement compared to the acetone washed control (1332 psi). The adhesive bond strength improvement by grit blasting may be attributed to increased surface area as well as the cleaning effect. Primer coating of grit blasted *PEEK®*-graphite composite with the same polymer as the adhesive further increased adhesive bond strength (3845 psi), indicating that the primer coating may act as a desirable binder between composite, and chopped fiber and matrix resin. *Ultem®* 1000 exhibited slightly higher adhesive bond strength (2000 psi) with acetone washed samples than poly(imide-30%siloxane) segmented copolymer. However, adhesive bond strength with *Ultem®* 1000 increased slightly with grit blasting, and a combination of grit blasting and primer coating, but the values were still lower than with the poly(imide-30%siloxane) segmented copolymer.

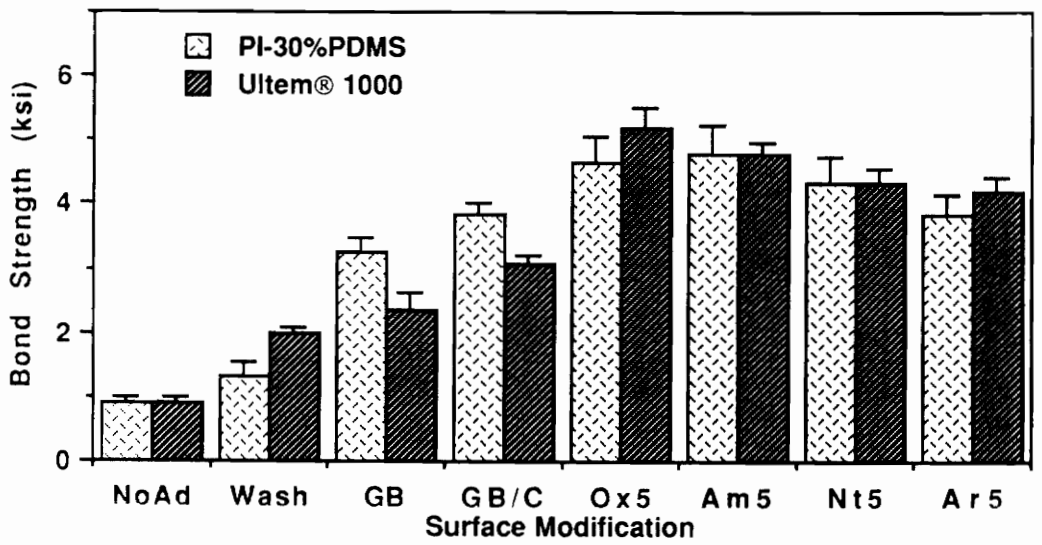

Figure 57. Effect of surface treatment on the adhesive bond strength of PEEK-graphite composite with poly(imide-30%siloxane) copolymer and Ultem 1000:
NoAd: no adhesive used
Wash: washed with acetone and distilled water
GB: grit blasted (no primer coating)
GB/C: grit blasted and primer coated
Ox 5: oxygen plasma treatment for 5 minutes
Am 5: ammonia plasma treatment for 5 minutes
Nt 5: nitrogen plasma treatment for 5 minutes
Ar 5: argon plas ma treatment for 5 minutes

Gas plasma treatments with oxygen, ammonia, argon and nitrogen improved adhesive bond performance of poly(imide-30% siloxane) segmented copolymer and *Ultem*® 1000 even further ! Oxygen and ammonia plasma treatments exhibited very similar adhesive bond strength of almost 5000 psi. Argon and nitrogen plasma showed slightly inferior adhesive bond performance but was still over 4000 psi. Although argon gas plasma was not expected to improve adhesive bond strength since argon is an inert gas, the effect was the same as that by nitrogen gas plasma. *Ultem*® 1000 adhesives also exhibited a similar trend and values of adhesive bond strength as poly(imide-30%siloxane) segmented copolymer. As widely accepted, the improved adhesive bond strength by gas plasma treatment is due to the "cleaning" effect and induced functional group(s) on composite adherend which form either chemical bonds or strong specific interactions, for example "acid-base interaction", to adhesives.

Further analysis of gas plasma treatment on adhesive bond strength indicated that the variation of treatment times (2, 5 and 10 minutes) did not show a significant change in adhesive bond strength of *PEEK*®-graphite composite (Figure 58 and 59). However, a combination of grit blasting and plasma treatment resulted in increased adhesive bond strength by around 1000 psi compared to plasma treatment only. The additional improvement could be credited to increased surface area by grit blasting. Although grit blasting improved adhesive bond strength greatly, it is not highly recommended for high precision purposes since it is a destructive method. All plasma treated and grit blasted samples exhibited cohesive failure mode, which is consistent with that observed with the Ti-6Al-4V adherend. However, simple acetone washed samples showed adhesive failure between the primer coating and "composite failure was never observed.

Although *PEEK*® has been known to be miscible with *Ultem*® 1000 but not with poly(imide-30%siloxane) segmented copolymers derived from BTDA- mDDS-PDMS [217], the adhesive bond performance of these materials did not very strongly discriminate between these two samples. Gas plasma treatments such as oxygen, ammonia, argon and nitrogen used in this study, have been believed to provide active free radicals species to the exposed

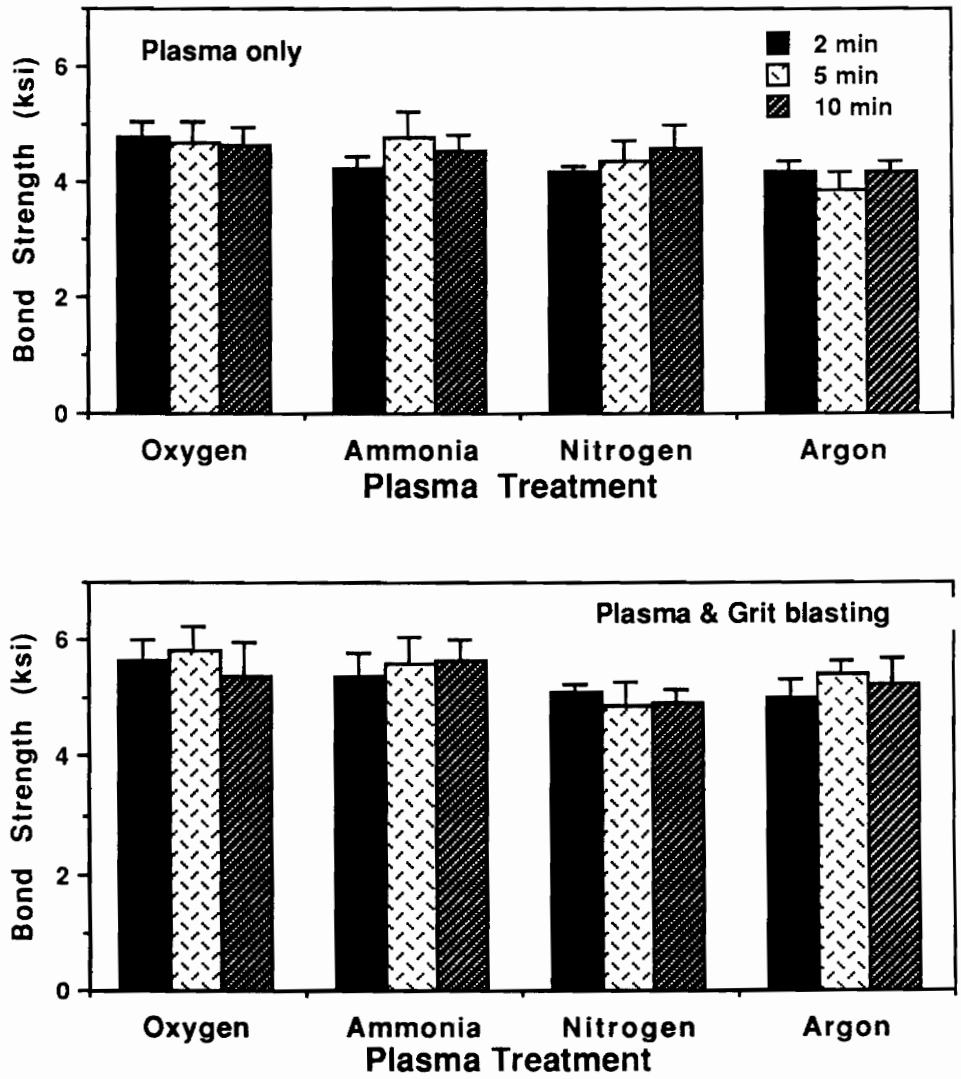

Figure 58. Effect of treatment time of gas plasma and a combination of gas plasma and grit blasting on adhesive bond strength with polyimide copolymer

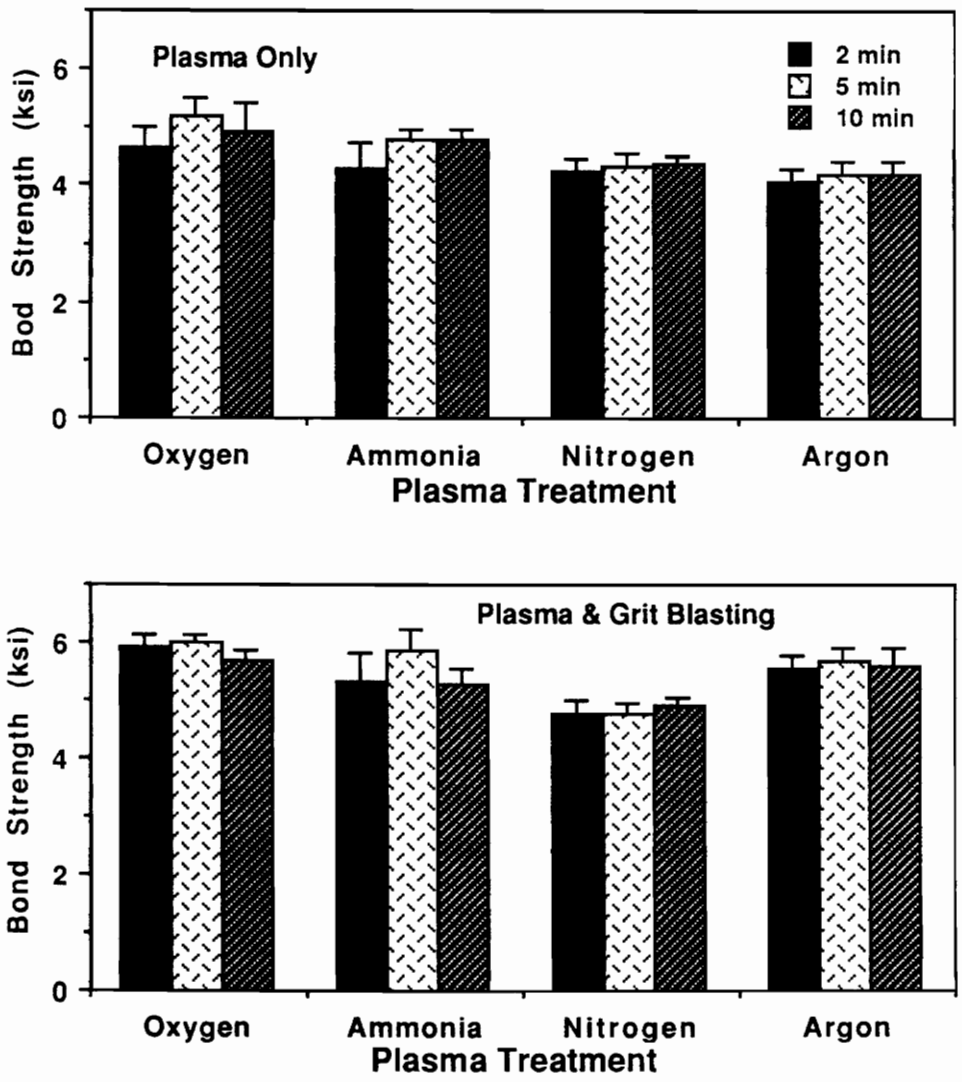

Figure 59. Effect of treatment time of gas plasma and a combination of gas plasma and grit blasting on adhesive bond strength of Ultem 1000

surfaces [21], which is considered to be responsible for enhancing bond performance. Studies [177], however, have indicated that plasma treatment and grit blasting did not improve bond performance of *PEEK*®-graphite composite. The deviation might be due to the primer coating utilized in this investigation, which preserved the active, clean surface and introduced strong bonds between fractured fibers and matrix resin and adhesives.

It was observed that a white, porous film formed on the composite while primer coating of *Ultem*® 1000 was being dried at room temperature. This film melted around 140 °C and finally provided a clear coating. However, the adhesive bond strength was much higher for samples which did not form a white film. It is strongly believed that the film forms a weak boundary layer, and is promoted by water in *Ultem*® solution. No indication of film formation was detected from the poly(imide-30%siloxane) copolymer.

4-8-3 Surface analysis of treated PEEK-graphite composite

Our XPS instrumentation is not currently equipped with in situ plasma treatment. Thus, it was impossible to measure the surface change from the treatments without brief exposure of the sample to air. The surface analysis data are summerized in Table 23. Washed and split samples showed a similar atomic concentration (86% carbon, 13% oxygen), while grit blated samples exhibited higher oxygen content and additional nitrogen and silicon. It is belived that nitrogen is from fiber and silicon is from glass bead of blaster. Washed *PEEK*®-graphite composites contained apporoximately 1% fluroine on their surface which is from mold release agent. The compression molded *PEEK*® film, however, showed around 11% fluorine, which was completely etched by oxygen plasma treatment of one minute. Ammonia plasma did not etched out fluorine but rather atomic concentration of fluorine seemed to increase.

The atomic concentration ratios of oxygen to carbon and to nitrogen are shown in Figure 60. Oxygen plasma treatment showed the highest O/C ratio followed by argon, nitrogen and am-

Table 23. Summary of surface analysis of PEEK-graphite composites

		C	O	F	N	Si	Na
PEEK Film		79.3	9.3	11.4	-	-	-
Washed	85.7	13.4	0.9	-	-	-	
Split	86.8	13.2	-	-	-	-	
Grit Blasted		76.9	18.1	-	1.5	3.4	-
O_2 Plasma	2 min.	63.7	34.1	-	0.7	1.1	0.4
	5 min.	66.7	31.7	-	0.5	0.7	0.4
	10 min.	65.7	32.3	-	0.2	1.1	0.7
NH_3 Plasma	2 min.	80.3	13.9	-	4.9	0.8	0.1
	5 min.	79.8	13.0	-	6.0	1.0	0.2
	10 min.	82.1	12.4	-	4.3	1.0	0.2
N_2 Plasma	2 min.	69.4	28.3	-	0.9	1.2	0.2
	5 min.	69.4	28.3	-	1.1	0.9	0.3
	10 min.	68.9	27.8	-	2.5	0./7	0.1
Ar Plasma	2 min.	72.8	25.4	-	0.7	1.0	0.1
	5 min.	72.8	24.8	-	1.0	1.4	-
	10 min.	74.2	24.0	-	1.1	0.7	-
NH_3 Plasma	2 min.	72.9	8.2	13.3	4.5	-	-
(PEEK film)	5 min.	78.2	8.6	8.3	4.6	-	0.3
	10 min.	75.6	6.5	12.4	5.0	-	0.5
O_2 Plasma	2 min.	67.7	31.4	0.7	0.2	-	-
(PEEK film)	5 min.	68.5	30.6	-	0.9	-	-
	10 min.	65.6	32.9	-	1.5	-	-
O_2 Plasma	2 min.	86.8	13.2	-	-	-	-
(Split)	5 min.	64.4	33.8	-	1.3	0.1	0.4
	10 min.	64.9	31.8	-	1.3	-	2.0

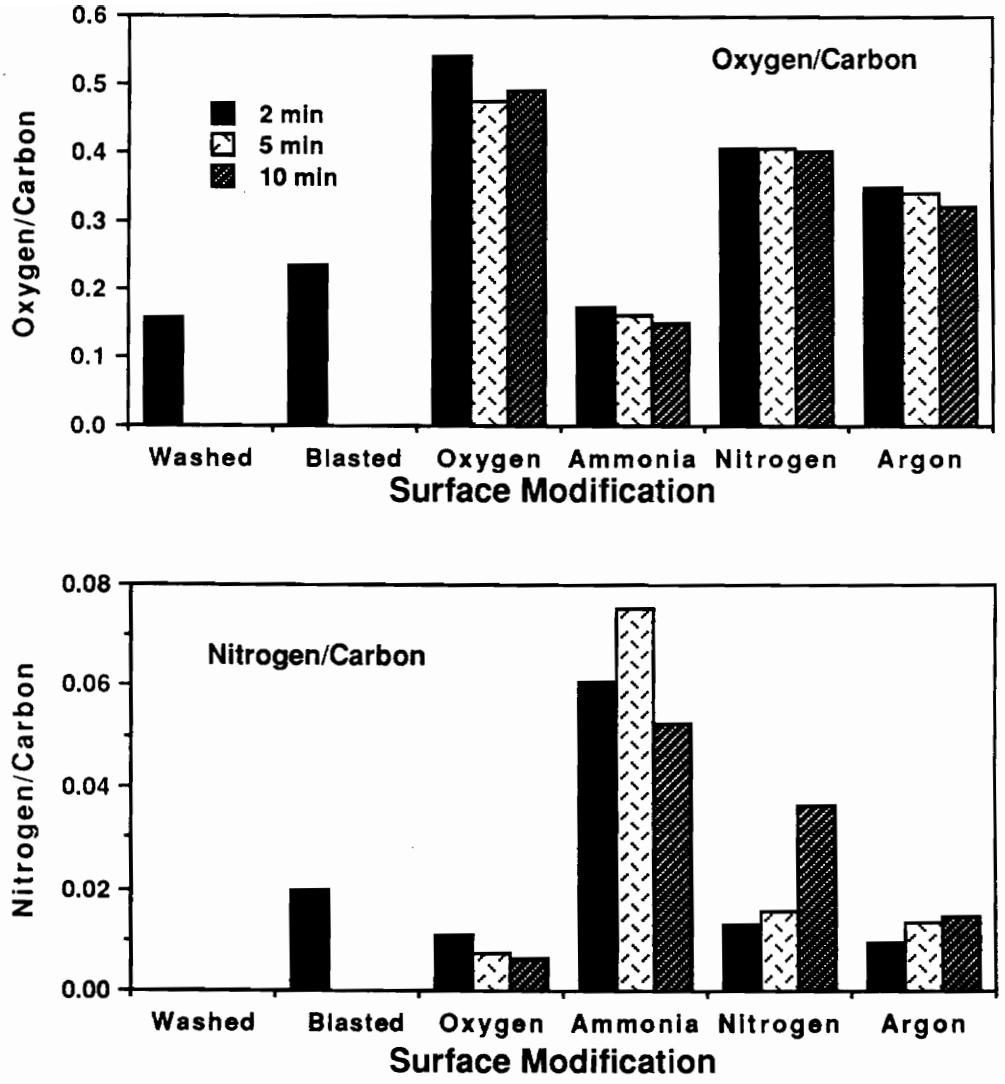

Figure 60. Atomic concentration ratio change by surface treatments in XPS analysis

monia plasma treatment. Although ammonia plasma treatment increased O/C value slightly, it exhibited the highest N/C ratio followed by nitrogen, argon, and oxygen plasma treatment. The ammonia plasma treatment increased only the nitrogen concentration while oxygen, argon and nitrogen plasmas increased the oxygen content, compared to the simple acetone washed and grit blasted samples. As can be seen in Figure 60, the O/C ratio decreased slightly with treatment time while N/C ratio showed a mixed trend depending on the gas utilized. However, in general, the treatment time did not seem to have a major effect on the chemical concentration and thus the adhesive bond strength. It is believe that the increased O/C ratio and/or N/C ratio by the gas plasma treatment could be attributed to the induced functional group or groups which improved adhesive bond performance by formation of "chemical" bond(s).

Deconvolution of C1s peaks was conducted to provide a better idea about adhesive bond strength improvement due to the gas plasma treatments and grit blasting. The washed sample and split sample exhibited four peaks at the binding energy at 285, 286.7, 288 and 291.6 eV, which corresponds to C-C, C-O, C=O bonds and a satellite peak from the aromatic rings of *PEEK*® [21,31] as shown in Figure 61. However, the grit blasted sample showed an additional small peak at 289.5 eV which may correspond to O-C=O bond. This additional peak could have been introduced by carbon fiber [218] which has been sized and contained impurities. The oxygen plasma as well as nitrogen and argon plasma enhanced the intensity of peaks corresponding to C-O, C=O and O-C=O bond. The intensity of deconvoluted peaks were very similar from one plasma to another.

However, the ammonia plasma showed only three peaks at 285, 286.5 and 288 eV possibly corresponding to C-C, C-N and C=O bonds together with a very weak satellite peak. The peak at 286.5 eV could be a mixture of C-O and C-N bonds [25]. The diminishing intensity of the satellite peak from ammonia plasma treatment might be due to the transformation of aromatic rings to some other forms, but this is not clear. Although the atomic ratio of oxygen to carbon was not changed much by ammonia plasma, a fairly large additional peak at 288

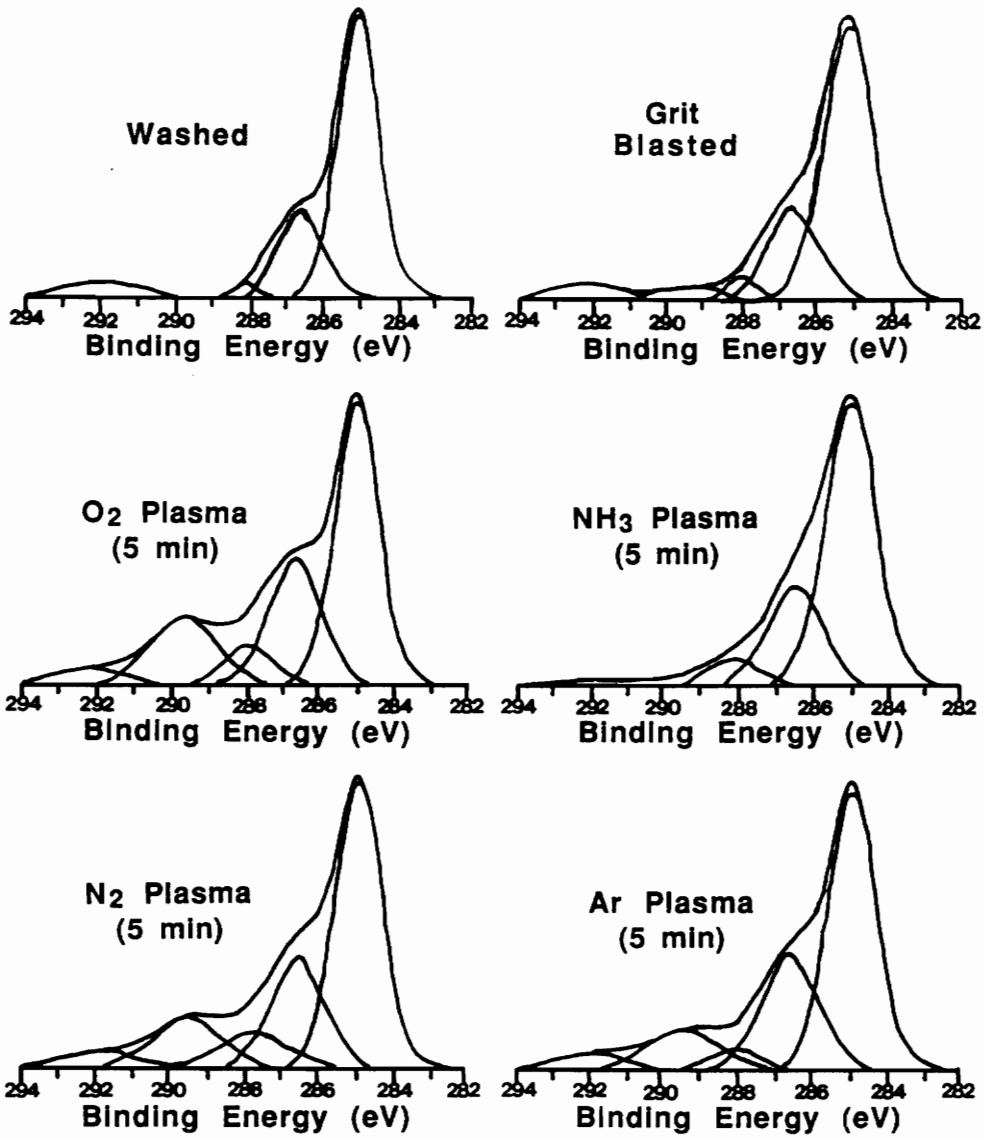

Figure 61. Deconvolution of C1s peaks of surface treated PEEK-graphite composite

eV was observed and the peak shift was confirmed by deconvolution of the C1s peak. The deconvolution exercise indicated that the bond strength increase by grit blasting could be attributed to an increased surface area and in part to a O-C=O bond, while that by plasma treatments to O-C=O as well as C=O bond, with the exception of the ammonia plasma which could be due to C-N bond and to C=O bond.

The deconvolution of O1s peaks was not attempted due to the high complexity (Figure 62). The washed samples showed two distinct peaks corresponding to C=O (532 eV) and C-O (534 eV), while the grit blasted sample exhibited a mixture of two or three peaks, possibly from the glass bead and aluminium oxide used for grit blasting that was left on the surface. The peak from SiO_2 was at 533 eV whie that from Al_2O_3 at 531.6 ev. The plasma treatment of oxygen, nitrogen and argon showed the same O1s peak. As indicated in C1s peak, plasma treatment raised the peak intensity of C-O, C=O and O-C=O. However, in O1s peaks, O=C peak shifted to a higher binding energy position with the disappearance of the shoulder. Therefore, it is believed that a new O=C peak was introduced by plasma treatment, at around 532 eV. On the other hand, ammonia plasma treatment displayed a broad O1s peak. In the deconvolution of C1s peak, the second peak rose at slightly lower binding energy (286.5) indicating a mixture of C-O and C-N peak. Thus, it is believed that the intensity of C-O peak did not change but the increased peak intensity of C=O and lowered binding energy of C-O peak resulted in a broad O1s peak. In this respect, C1s peaks corresponded well to O1s peaks. Therefore, newly introduced C-O=O peaks and enhanced peak intensity of C=O and C-O should be responsible for the improved adhesive bond strength by plasma treatment of oxygen, argon and nitrogen.

4-8-4 Topology change by surface treatment

All treated samples were subjected to SEM analysis to detect any topology change. The surface of washed samples were relatively smooth and flat (Figure 63), except for the small

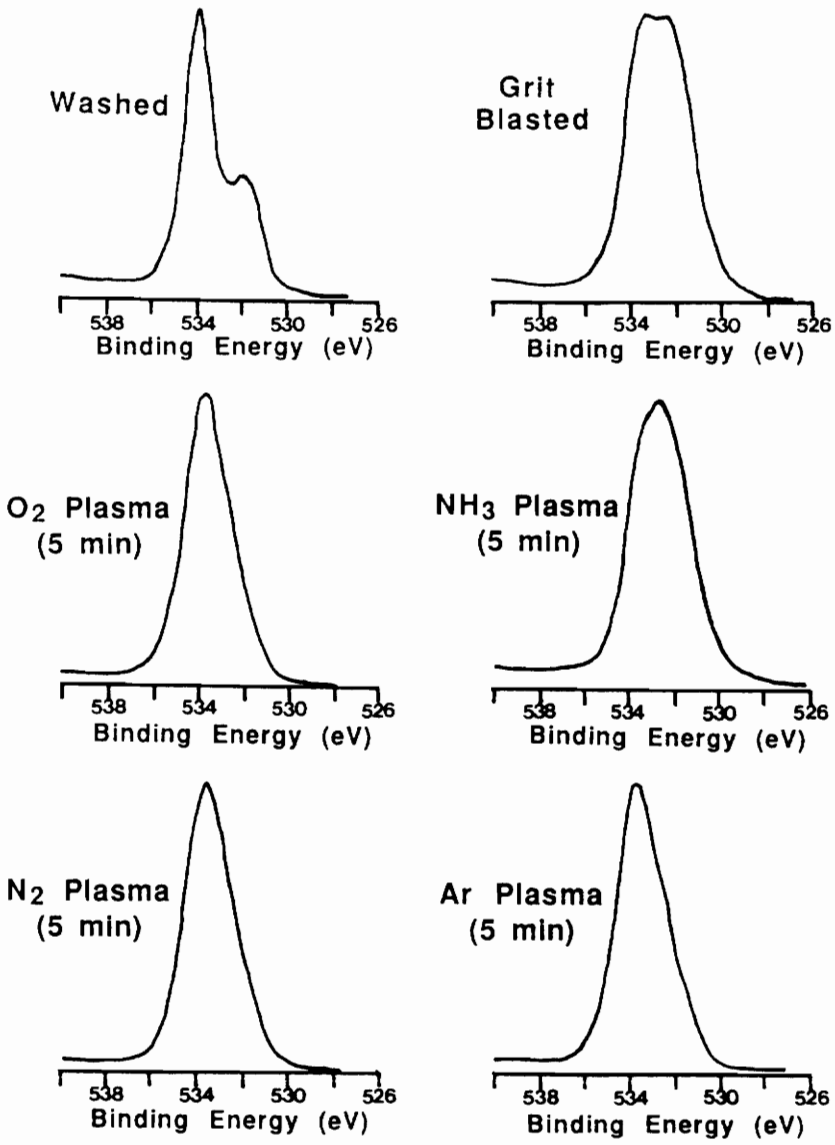

Figure 62. O1s peaks of surface treated PEEK -graphite composites

portions of exposed fibers and defects. Grit blasting, however, removed the top layer of matrix resin (around 2-3 mil) and left broken fibers and matrix resin pieces ! Therefore, improved adhesive bond strength by grit blasting could be explained by the increased surface area and cleaning effect since *PEEK*®-graphite composite had around 1% of fluorine on the surface, which might be from a release agent. Additional improvement was obtained by primer coating, which used the same polymer as adhesive dessolved in NMP, indicating that chopped fiber and matrix resin pieces formed a weak boundary layer, unless a primer coating was applied. Therefore, it is concluded that primer coating act as a binder between the composite and the resin and fiber fragments. Slight preferential etching was observed from oxygen plasma treatment of 5 and 10 minutes, but no difference was detected from the samples treated by other gas plasmas even though the treatments enhanced bond strength greatly (Figure 63). Therefore, it is believed that the enhancement of bond performance can be attributed mostly to the active species induced by plasma treatment rather than surface roughness.

4-8-5 Contact angle measurement

The contact angle measurement is another useful technique to investigate the effect of surface treatment. The contact angles measured with double distilled water by sessile drop method showed a different trend from that of XPS and adhesive bond strength (Figure 64). Washed and grit blasted samples gave 73 and 72 degree contact angles, respectively, although grit blasting enhanced adhesive bond strength greatly. As a result, it can be said that improved adhesive bond strength is mainly due to increased area and partially to a cleaning effect. The contact angles of plasma treated samples corresponded well to the oxygen content in the XPS results. The samples from oxygen plasma treatment showed the lowest contact angle while those from ammonia plasma treatment resulted in the highest one, but these showed better adhesive bond strength than argon and nitrogen plasma treated samples.

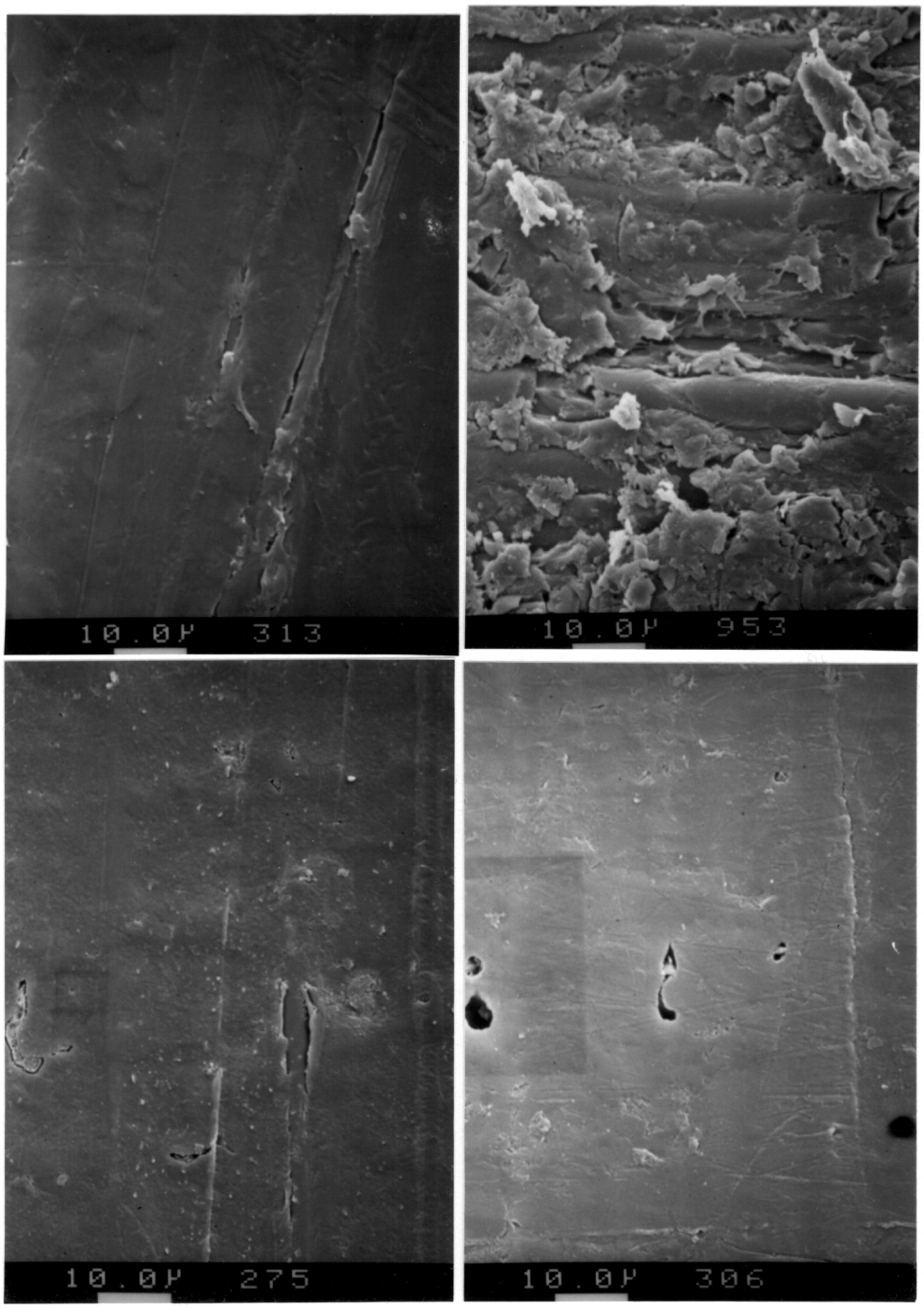

Figure 63. SEM micrographs of PEEK-graphite composites: AS: as received, GB: grit blasted, OP5: oxygen plasma 5 min, AmP5: ammonia plasma 5 min.

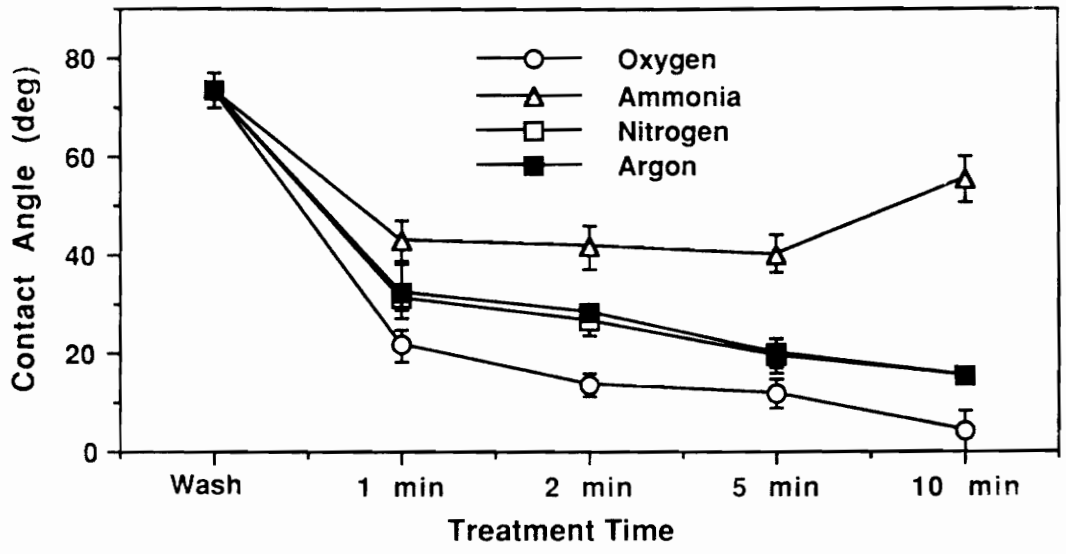

Figure 64. Effect of surface treatment on the water contact angle of PEEK-graphite composites

Thus, the contact angle was believed to be a function of only the oxygen functional group(s). Argon and nitrogen plasma treated samples exhibited approximately the same contact angles for all measurements corresponding well to the results from XPS analysis and adhesive bond strength. The contact angle measurements correspond well to adhesive bond strength results with the exception of ammonia plasma treatment which improved adhesive bond strength by introducing oxygen functional group(s) as well as nitrogen functional group(s). The variation of plasma treatment time indicated that one minute treatment might be enough since contact angle decreased only slightly with treatment time, except ammonia plasma for 10 min treatment which could be related to decreased satellite peak.

Chapter V. Summary and Conclusions

Thermoplastically processable high glass transition temperature polyimides were successfully synthesized from a number of appropriate organic or oligomeric diamines (mDDS, pDDS, pPD and PDMS), dianhydrides (6FDA and BTDA) and end capping agent (phthalic anhydride) via solution imidization and molecular weight control. The characterization data by DSC, DMTA, TMA, TGA, intrinsic viscosity measurements and stress-strain tests indicated that polyimides prepared had Tg values, as high as 360 °C, excellent thermal stability and mechanical properties and well controlled molecular weight. FTIR also demonstrated that solution imidization was successful in achieving fully imidized polyimides.

Single lap shear samples were prepared by sandwiching either compression molded film adhesives or scrim cloth adhesives between two Ti-6Al-4V alloys which were treated in Pasa Jell 107 and primer coated with the same polymer as the adhesive. Adhesive bond performance of these polyimides was investigated as a function of molecular weight, test temperature, residual solvent and siloxane incorporation. Adhesive bond strength decreased slightly with increasing molecular weight but increased dramatically with siloxane incorporation. As the

test temperature increased, homopolyimide and 10% siloxane copolymers became more ductile and showed maximum adhesive bond strength at 200 and 150 °C, respectively, while 20% and 30% siloxane copolymers showed decreased adhesive bond strength relative to their very high ambient temperature values.

The polyimides from 6FDA exhibited increasing adhesive bond strength with temperature up to 300 °C. Therefore, an attempt was made to explain the two distinct adhesive bond strength behaviors via the brittle-ductile transition behavior of polyimides. Polyimide homopolymers can be quite brittle at room temperature and thus experience brittle fracture, which results in low adhesive bond strength. As the test temperature increased, enhanced ductility by thermal energy changed the failure mode from brittle to ductile fracture, resulting in increased adhesive bond strength. Adhesive failure between primer coating and the adhesives (mode AA) was dominant for polyimide homopolymers and poly(imide-10%siloxane) copolymers, while 20 and 30% siloxane copolymers exhibited cohesive failure in general. Thus, at a certain temperature, the strength and strain of the adhesive were optimum.

There are several possibilities as to why previous investigators have not observed this phenomenan, which is partially related to residual solvent and low molar mass species. Early investigators utilized poly(amic-acid) via the scrim cloth carrier instead of fully imidized polyimide due to their insolubility and infusibility. The scrim cloth adhesives were prepared by brushing unisolated poly(amic-acid) in highly polar solvent on E-glass fabric which is called scrim cloth, and then drying at 175 °C for several hours. Therefore, the scrim cloth adhesives definitely contained some unconverted poly(amic-acid), a fair amount of residual solvent and some low molar mass species, which all improved flow, and hence the bond consolidation. In the present study, polyimides which were fully imidized and ioslated in water/methanol mixture were utilized in film form and thus no residual solvent or no low molar mass species were expected to remain in the adhesive. This reality led to a study of the effect of residual solvent on the adhesive bond strength of these polyimides.

The adhesive bond strength increased with residual solvent at ambient temperature, but decreased at 200 °C. The behavior was found to be a function of scrim cloth adhesive drying temperature as well as bonding temperature, which indicated that adhesive bond strength is definitely a function of residual solvent. A possible explanation is that the residual solvent as well as low molar mass species enhanced bond consolidation resulting in initially high adhesive bond strength, but at 200 °C, increased ductility occurs which leads to low strength. The enhanced bond consolidation was evidenced by failure modes. All scrim cloth adhesives exhibited cohesive failure occurring between polymer and scrim cloth. In this work, high adhesive bond strength at ambient temperature and decreased adhesive bond strength with temperature was not observed, which is believed to be due to low residual solvent from high bonding temperature and long holding time. However, the effect of residual solvent has been clearly demonstrated.

In order to provide a better understanding of the brittle-ductile transition behavior of polyimides, stress-strain analysis was conducted on polyimides as a function of molecular weight, siloxane content and test temperature, and also on some commercial polyimides for comparison purposes. Polyimide homopolymers and copolymers exhibited excellent mechanical properties and the lowest molecular weight utilized in this study turned out to be at or above the critical value for good mechanical properties and good processability. The tensile strength and modulus decreased with temperature while tensile strain increased. The variation became greater as the temperature increased, which is explained by the brittle-ductile transition behavior of polyimides. Siloxane oligomer incorporation also decreased strength and modulus but increased strain, supporting the ductile-brittle behavior. A careful examination of the stress-strain data indicated that there was an optimum combination of stress and strain which were similar for all polyimides from BTDA-mDDS and was obtained at different temperature, depending on the amount of siloxane incorporation.

The adhesive bonding of polymeric composite materials such as *PEEK*®-graphite composites became increasingly important and thus the adhesive bond performance utilizing

poly(imide-30%siloxane) copolymer and *Ultem*® 1000 was investigated. Surface treatments such as acetone washing, grit blasting and gas plasma etching were employed. The adhesive bond strength was correlated to surface morphology by SEM, chemical changes by XPS and contact angle measurements. The adhesive bond strength of *PEEK*®-graphite composite with poly(imide-30%siloxane) copolymer and *Ultem*® 1000 was greatly improved by grit blasting and further by gas plasma treatment, although the underlying mechanisms are not well understood. The improved adhesive bond strength by grit blasting was believed to be from increased surface area and cleaning effect, while that by gas plasma was from induced the chemical functional group or groups. This was supported by XPS and contact angle measurement. Deconvolution of the C1s peaks indicated that gas plasma treatment not only introduced a new surface structure but also enhanced peak intensity. In general, gas plasma etching by oxygen, nitrogen and argon increased oxygen concentration, while that of ammonia increased nitrogen concentration, both of which are probably responsible for the improved adhesive bond strength. Several conclusions were drawn from above observations:

1. Fully imidized thermoplastic polyimides were sucessfully prepared from a number of diamines and dianhydrides via solution imidization, molecular weight control and siloxane incorporation.

2. Adhesive bond strength increased dramatically with siloxane incorporation, and decreased slightly with molecular weight and stiffer polyimide backbone at ambient temperature.

3. As the test temperature increased, polyimide homopolymer from BTDA-mDDS and poly(imide-10%siloxane) copolymer exhibited maximum adhesive bond strength at 200 and 150 °C, respectively, and poly(imide-siloxane)(20 and 30% by weight) copolymers showed decreased adhesive bond strength. Polyimides from 6FDA-pDDS and 6FDA-pPD demonstrated increasing trend in the test temperature range of ambient temperature to

300 °C. This phenomenan was explained by brittle-ductile transition behavior of the polyimide.

4. Presence of residual solvent increased adhesive bond strength at ambient temperature but decreased it at elevated temperature, indicating that residual solvent enhanced bond consolidation and ductility of the adhesive.

5. Adhesive bond failure mode changed from pure interfacial failure with polyimide homopolymers to cohesive failure with poly(imide-30% siloxane) segmented copolymers, indicating siloxane incorporation as well as residual solvent enhanced bond consolidation.

6. Polyimides prepared in this investigation demonstrated excellent mechanical properties and exhibited good relationship between maximum adhesive bond strength and optimum combination of stress-strain behavior of the adhesives.

7. Poly(imide-30%siloxane) copolymer exhibited excellent adhesive bond performance with *PEEK*®-graphite composite, and grit blasting and gas plasma treatment of oxygen, ammonia, nitrogen and argon showed great potential for further improvement.

Chapter VI. Suggested future studies

Although polyimides prepared in this study demonstrated excellent adhesive bond strength and mechanical properties, there are many possible improvement which could allow for better adhesive bond performance. The polyimides from 6FDA-pPD and 6FDA-pDDS exhibited high glass transition temperature, but poor adhesive bond strength. Therefore, it is suggested to prepare siloxane containing polyimides with 6FDA-pPD and 6FDA-pDDS to afford high glass transition temperature and good processability, since siloxane incorporation has been proven to be beneficial. Another class of polyimides, namely the phosphorous containing flame-resistant polyimides shown below, should be subjected to adhesive bond strength measurement since they are also desirable structural adhesives for aerospace applications.

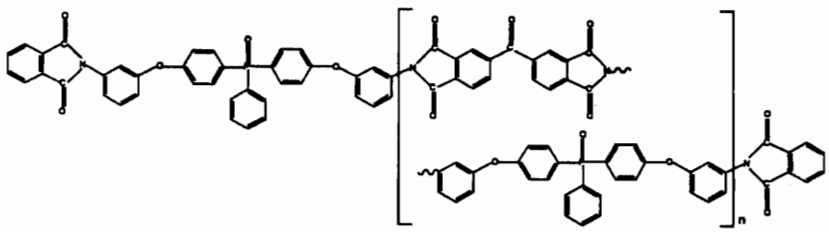

It would also be valuable to compare the adhesive bond strength of polyimide containing perfectly alternating siloxane segments with that of polyimide containing segmented siloxane

block. Scrim cloth adhesives have long been exclusively utilized in polyimide adhesion. However, no study has been conducted on the effect of the scrim cloth itself ! Scrim cloth (E-glass fabric) should have some effect on the adhesive bond strength. A possible speculation is the scrim cloth acts as a reinforcing fabric, as in composite materials. Scrim cloth might provide extra ductility at ambient temperature, since many polyimides are brittle. By contrast, near their Tg, scrim cloth is much more rigid and stronger than polyimide and could act as strengthener. Thus, utilization of scrim cloth adhesive might provide different adhesive bond strength from film adhesive.

Although this study tried to elucidate the effect of residual solvent on the adhesive bond strength, it was not entirely successful. Therefore, it is suggested to evaluate the adhesive bond strength with unisolated and isolated poly(amic-acid) coated scrim cloth adhesive, unisolated and isolated fully cyclized polyimide coated scrim cloth adhesive, and unisolated and isolated fully cyclized polyimide film adhesives. This investigation might clarify the effect of low molar mass species, unconverted poly(amic-acid) and residual solvent on the adhesive bond performance. For clear understanding of brittle-ductile behavior of polyimides, it is desirable to measure adhesive bond strength as well as stress-strain properties at sub-ambient temperatures to see whether a maximum adhesive bond strength or an optimum combination of stress-strain exist. Variation of strain rate would also be valuable.

The durability study has to be carried out with scrim cloth adhesive and film adhesive. If scrim cloth can provide a path for solvent and water generated upon imidization, it is also possible to provide a path for water from outside in the durability test in water. It is surely important to investigate whether scrim cloth is really needed in field applications. Since Pasa Jell treatment of Ti-6Al-4V alloys is not the best surface treatment method, newly developed technique such as acid etching is suggested to achieve better adhesive bond performance.

In the adhesive bond performance of *PEEK*®-Graphite composites, more study has to be carried out to elucidate the mechanism of adhesive bond strength improvement by gas plasma

treatment. As found from XPS analysis, the compression molded film contained a quite amount of fluorine on the surface layer, which was from mold releasing *Teflon*® sheet, and which might reduce the adhesive bond strength. This should be removed before the bonding, possibly by oxygen plasma treatment.

Although poly(imide-30% siloxane) segmented copolymer and *Ultem*®1000 did not show a major difference in adhesive bond strength with *PEEK*®-graphite composites despite the latter is miscible with *PEEK*®polymer, while the former is not, the miscbility and/or compatibility of adhesive with matrix resin of composites might be very important for the adhesive bond performance, especially for long term applications. Therefore, it is reccomended to investigate the miscbility or compatatility of polyimides with *PEEK*®and correlate adhesive bond strength to miscbility results.

Bibliography

1. H. D. Burks and T. L. St. Clair in K. L. Mittal, ed., *Polyimides: Synthesis, Characterization and Applications*, 1, Plenum, NY, 117 (1984)

2. C. Feger, M. M. Khojasteh and J. E. McGrath, ed., *Polyimides: Materials, Chemistry and Characterization,* Elsvier, (1989)

3. D. Wilson, P. Hergenrother and H. Stenzenberger, ed., *Polyimides,* Chapman and Hall, (1990)

4. F. W. Harris, et al., in ref. 1, pp3-14

5. T. L. St. Clair and D. A. Yamaki, in ref. 1, pp99-116

6. C. A. Arnold, D. Chen, Y. P. Chen, J. D. Graybeal, R. H. Bott, T. H. Yoon, B. E. McGrath and J. E. Grath, PMSE Sym. Aero. App. Polym., 9, 25, (1988)

7. C. A. Arnold et al., *SPE Composite Div. Meeting*, Nov. 15-17, Los Angeles, CA., (1989)

8. C. A. Arnold, J. D. Summers, Y. P. Chen, T. H. Yoon, B. E. McGrath, D. Chen and J. E. McGrath, in ref. 2, p69-89

9. R. H. Bott, J. D. Summer, C. A. Arnold, L. T. Taylor, T. C. Ward and J. E. McGrath, *J. Adhesion*, 23, 67, (1987)

10. E. Sancaktar and S. K. Dembosky, *J. Adhesion*, 19, 287, (1986)

11. S. Mall, *J. Adhesion*, 20, 251, (1987)

12. J. F. Dezern and P. R. Young, *Int. J. Adhesion and Adhesive*, 5, 183, (1985)

13. D. J. Progar and T. L. St. Clair, *Int. J. Adhesion and Adhesive*, 6, 25, (1986)

14. D. J. Progar and R. A. Pike, *Int. J. Adhesion and Adhesive*, 8, 25, (1988)

15. A. K. St. Clair and T. L. St. Clair, *Int. J. Adhesion and Adhesive*, July, 249, (1981)

16. S. Maudgal and T. L. St. Clair, *SAMPE Quarterly*, Oct., 6, (1984)

17. D. J. Progar et al., *SAMPE Journal*, Jan/Feb, 53, (1990)

18. D. J. Progar and J. F. Dezern, *J. Adhesion Sci. Tech.*, 3, 305, (1989)

19. D. J. Progar and T. L. St. Clair, *J. Adhesion*, 30, 185, (1989)

20. D. J. Progar and T. L. St. Clair, *J. Adhesion*, 21, 35, (1987)

21. E. M. Silverman and R. A. Griese, *SAMPE Journal*, 25 (5), (1989)

22. V. K. Varadan and V. V. Varadan, *1990 MRS Spring Meeting*, San Fransisco, CA, April, 16-21 (1990)

23. J. Osterndorf and M. J. Bodner, *SAMPE Journal*, 25, 15, (1989)

24. J. M. Siperko and R. R. Thomas, *J. Adhesion Sci. Tech.*, 3, 157, (1989)

25. A. D. Katnani, A. Knoll and M. A. Mycek, *J. Adhesion Sci. Tech.*, 3, 441, (1989)

26. E. M. Liston, *J. Adhesion*, 30, 199, (1989)

27. D. J. D. Moyer, *Ph.D Dissertation*, VPI & SU, (1989)

28. E. M. Silverman and R. A. Griese, *SAMPE Journal*, 25, 34, (1989)

29. G. K. A. Kodokian and A. J. Kinloch, *J. Material Sci. Letters*, 7, 625, (1988)

30. A. J. Kinloch and C. M. Taig, *J. Adhesion*, 24, 291, (1987)

31. B. R. Strohmeier, *J. Vac. Sci. Tech.*, A7, 3228, (1989)

32. A. J. Kinloch, *Adhesion and Adhesives*, Chapman & Hall, New York, (1987)

33. ASTM Standard, V15.06, (1989)

34. R. Thompson, *Adhesive Bonding in Modern Plastics Encyclopedia*, McGraw-Hill Inc., New York, p433, (1984)

35. A. J. Kinloch, *Durability of Structural Adhesive*, Applied Sci. Pub., New York, p15, (1983).

36. K. W. Allen, *J. Adhesion*, 21, 265, (1987)

37. B. O. Bateup, *Int. J. Adhesion & Adhesive*, July, p233, (1981)

38. F. J. Meyer, *Adhesion & Bonding, in Encyclopedia of Polym. Sci. & Eng.*, V1, John Wiley & Son, New York, (1985)

39. L. H. Sharpe, *J. Adhesion*, 29, 1, (1989)

40. A. W. Bethune, *SAMPE J.*, 11(3), 4, (1985)

41. E. M. Boroff and W. C. Wake, *Trans. Inst. Rubber Industry*, 25, 199, (1949)

42. A. J. Kinloch, *J. Matter. Sci.*, 15, 2141, (1980)

43. D. E. Packam, Aspects of Adhesion, D. J. Alner and K. W. Allen, ed., *Transcript Books*, London, (1973)

44. D. Tabor and R. H. S. Winterton, *Proc. Roy. Soc.*, A312, 435, (1969)

45. K. L. Johnson, K. Demdall and A. D. Robert, *Proc. Roy. Soc.*, A324, 301, (1971)

46. S. S. Voyutskii, *Autohesion and Adhesion of High Polymers*, John wiley/Interscience, New York (1963)

47. B. V. Deryaguin and V. P. Smilga, *Adhesion , Fundamentals and Practice*, Mclaren and Son, London, 152 (1969)

48. H. Krupp, *J. Adhesion*, 4, 83 (1972)

49. H. Krupp, *J. Adhesion*, 5, 269 (1973)

50. W. Possart, *Int. J. Adhesion and Adhesives*, 8(2), 77 (1988)

51. C. Kemble, *Adhesion*, D. D. Eley, ed., Oxford Univ. Press, London, 19 (1961)

52. J. R. Huntsberger, *Treatise on Adhesion and Adhesive*, V1, R. L. Patrick, M. Dekker, ed., New York, 119 (1967)

53. A. J. Staverman, *Adhesion and Adhesives*, V1, ed., R. Houwink and G. Salmon, Elsevier, Amsterdam, 9 (1965)

54. W. C. Wake, *RIC Lecture Series*, No4, 1 (1966)

55. F. M. Fowkes, *J. Phys. Chem.*, 66, 66 (1962)

56. F. M. Fowkes, *J. Adhesion*, 4, 155 (1972)

57. A. Larson and W. E. Johns, *J. Adhesion*, 25, 121 (1988)

58. P. J. C. Chappell and D. R. Williams, *J. Adhesion Sci. Tech.*, 4(1), 7 (1990)

59. S. P. Wilkinson and T. C. Ward, *SAMPE Symposium*, 35, 1180 (1990)

60. W. C. Wake, *in Recent Advances in Adhesion*, L. H. Lee, ed., Gordon & Breach, New York (1973)

61. A. N. Gent, *Int. J. Adhesion and Adhesives*, April, 175 (1981)

62. A. N. Gent and R. H. Tobias, *J. Polym. Sci., Polym. Phys. Educ.*, 22, 1483 (1984)

63. J. J. Bikerman, *The Science of Adhesive Joint*, Academic Press, New York (1968)

64. J. Comyn, *Int. J. Adhesion and Adhesives*, 10(3), 161 (1990)

65. H. Schonhorn, *J. Polym. Sci.*, A1, 6, 2343 (1963)

66. E. P. Puelddeman, *J. Adhesion*, 2, 184 (1970)

67. A. Ahagon and A. N. Gent, *J. Polym. Sci.: Polymer Phys. Ed.*, 13, 1285 (1975)

68. R. G. Schmidt and J. P. Bell, *J. Adhesion*, 25, 85 (1988)

69. A. V. Patsis and S. Cheng, *J. Adhesion*, 25, 145 (1988)

70. N. L. Jarvis and W. A. Zisman, *Surface Chem. of Fluorochemicals*, in Encyclo. of Chem. Tech., 2nd ed., V9, Wiley-Interscience, 707 (1966)

71. A. H. Landrok, *Adhesive Tech. Handbook*, Noyes Pub., New Jersey, 31 (1985)

72. I. Skeist, *Handbook of Adhesives*, van Nostrand Reinhold Co., New York, 108 (1977)

73. G. P. Anderson, S. J. Bennett and K. L. Devries, *Analysis and Testing of Adhesive Bonds*, Academic Press, New York (1977)

74. J. Shields, *Adhesive Handbook*, 2nd ed., Newnes-Butterworth, London (1976)

75. S. Mall and G. Ramamurthy, *Int. J. Adhesion and Adhesive*, 9(1), 33 (1989)

76. A. N. Gent, *Rubber Chem. & Tech.*, V47, 202 (1974)

77. R. D. Adams and W. C. Wake, *Structural Joint in Engineering*, New York, Elsvier (1984)

78. A. N. Gent, *J. Polym. Sci.*, Part A-2, 9, 283 (1971)

79. D. W. Aubrey, G. N. Welding and T. Wong, *J. Apply. Polym. Sci.*, 13, 2193 (1969)

80. J. L. Dordon, *in Treaties on Adhesion & Adhesives*, V1, R. L. Patrick, M. Dekker, ed., New York, Ch 8 (1967)

81. N. J. DeLollis, *Adhesive, Adherends, Adhesion*, R. E. Krieger Pub. Co., Huntington, New York (1980)

82. A. N. Gent and S. Y. Kaang, *J. Adhesion*, 24, 173 (1987)

83. A. N. Gent and G. R. Hamed, *Polym. Eng. & Sci.*, 17, 462 (1977)

84. A. N. Gent and G. R. Hamed, *Rubber Chem. Tech.*, 55, 483 (1982)

85. S. A. Hamoush and S. H. Ahamd, *Int. J. Adhesion and Adhesives*, 9(3), 171 (1989)

86. K. M. Liecht and T. Freda, *J. Adhesion*, 28, 145 (1989)

87. S. J. Shaw and D. A. Tod, *J. Adhesion*, 28, 231 (1989)

88. S. Mall, *J. Adhesion*, 20, 251 (1987)

89. M. L. Williams, *J. Appl. Polym. Sci.*, 13, 29 (1969)

90. Y. H. Lai and D. A. Dillard, *J. Adhesion*, 33, 63 (1990)

91. H. D. Conway and J. P. R. Thomsin, *J. Adhesion Sci. & Tech.*, 2(3), 227 (1988)

92. V. M. Sura and R. Rhinehart, *J. Adhesion Sci. & Tech.*, 4(3), 161 (1990)

93. W. Brockmann, *J. Adhesion*, 29, 53 (1989)

94. N. Nakamura, T. Ueda, S. Hosono, and T. Maruno, *Int. J. Adhesion and Adhesives*, 7(4), 209 (1987)

95. C. Matz, *Int. J. Adhesion and Adhesives*, Jan., 24 (1988)

96. J. Comyn, *J. Adhesion*, 29, 121 (1989)

97. P. Cawley and R. D. Adams, *Mater. Evalu.*, 47(5), 558 (1989)

98. G. B. Chapman, *Nondestructive Testing for Quality Assurance of FRP Assemblies*, SAE Tech. Paper Ser. #820226, Warrendale, Pa, Feb. (1982)

99. Y. Bar-Cheon, A. K. Mal and C. C. Yin, *J. Adhesion*, 29, 257 (1989)

100. B. P. Holownia, *Int. J. Adhesion and Adhesives*, 7(1), 25 (1987)

101. A. N. Gent and A. J. Kinloch, *J. Polym. Sci.*, Part A-2, 9, 659 (1971)

102. B. M. Malyshew and R. L. Salganik, *Int. J. Frac. Mech.*, 1, 114 (1965)

103. R. S. Rilin and A. G. Thomas, *J. Polym. Sci.*, 10, 29 (1953)

104. J. J. Benbow and F. C. Roessler, *Proc. Phys. Soc.*, B70, 201 (1957)

105. A. N. Gent and G. R. Hamed, *Rubber Chem. Tech.*, 51, 354 (1978)

106. A. N. Gent and R. P. Petrich, *Proc. R. Soc. London*, A310, 433 (1969)

107. A. Rudin, *The Element of Polymer Sci. and Eng.*, Academic Press Inc., New York, 422 (1982)

108. P. M. Hergenrother, *Chemtech*, Aug, 496 (1984)

109. N. A. De Bruyne, *U. S. Patent #2499134*, (1950)

110. P. Shlack, *U. S. Patent #2136928*, (1936)

111. H. Vogel and C. S. Marvel, *J. Polym. Sci.*, 50, 511 (1961)

112. G. P. de Gaudermaris and B. J. Sillon, *J. Polym. Sci.*, B-2, 203 (1964)

113. J. K. Stille and J. R. Williams, *J. Polym. Sci.*, B-2, 209 (1964)

114. P. M. Hergenrother and H. H. Levine, *J. Polym. Sci.*, A-1 (5), 1453 (1967)

115. W. M. Edward, *U. S. Patent #3179614 & 3179634*, (1965)

116. A. L. Endrey, *U. S. Patent #3179631 & 3179633*, (1965)

117. M. Kushner, *SAMPE J.*, 26(5), 7 (1990)

118. F. Swanson, *Polym. Eng. & Sci.*, 17(2), 122 (1977)

119. C. Strobech, *Int. J. Adhesion and Adhesive*, July, 225 (1990)

120. D. M. Brewis, J. Comyn, S. T. Tredwell, *Int. J. Adhesion and Adhesives*, 7(1), 30 (1987)

121. P. Mani, A. K. Gupta, A. S. Krishnamoorthy, *Int. J. Adhesion and Adhesives*, 7(3), 157 (1987)

122. M. Snir, S. Wassenman, H. Dodiuk, and S. Kenig, *J. Adhesion*, 27, 175 (1989)

123. N. Bianchi, F. Garbassi, R. Pucciariello and G. Romano, *Int. J. Adhesion and Adhesives*, 10(1), 19 (1990)

124. H. Dodiuk, A. S. Kenig, *Int. J. Adhesion and Adhesives*, 8(3), 159 (1988)

125. E. C. Millard, *Elev. Temp. Resist. Adhes. in Adh. Bond. of Al. Alloys*, E. W. Thrall and R. W. Shannon, ed., Marcel Dekker Inc., Ch8 (1985)

126. L. H. Lee, *Int. J. Adhesion and Adhesives*, 7(2), 81 (1987)

127. S. H. Goodman, *Epoxy Resins in Handbook of Thermoset Plastics*, S. H. Goodman, ed., Noyes Pub., New Jersey, 132 (1986)

128. E. C. Millard, *Epoxy Adhesives in Adh. Bonding of Al. Alloys*, E. W. Thrall and R. W. Shannon, ed., Marcel Dekker Inc., NY, Ch7 (1985)

129. L. V. McAdams and J. A. Gannon, *Epoxy Resins in Encyclopedia of Polymer Sci. & Eng.*, V6, 322 (1985)

130. J. K. Gilham, *Cure and Properties of Thermosetting Polymers in Structural Adhesives*, A. J. Kinloch, ed., Elsevier, New York, p1 (1986)

131. H. Jozavi and E. Sancaktar, *J. Adhesion*, 29, 233 (1989)

132. H. Jozavi and E. Sancaktar, *J. Adhesion*, 27, 143 (1989)

133. S. J. Shaw and D. A. Tod, *J. Adhesion*, 28, 231 (1989)

134. A. Lee and G. B. McKenna, *Polym. Eng. & Sci.*, 30(7), 431 (190)

135. H. Dodiuk, S. Kenig and I. Liran, *J. Adhesion*, 31, 203 (1990)

136. A. J. Kinloch, *Rubber Toughened Thermoset Polymers, in Structural Adhesives*, A. J. Kinloch, ed., Elsevier, New York, 127 (1986)

137. A. J. Kinloch, *Rigid-Particulate Reinforced Thermoset Polymers, in Structural Adhesives*, A. J. Kinloch, ed., Elsevier, NY, 163 (1986)

138. New Product, *Adhesive Age*, June, 8 (1990)

139. J. C. Hedrick, *Ph.D Dissertation*, VPI & SU (1990)

140. F. A. King and J. J. King, *Engineering Thermoplastics*, Marcel Dekker Inc., New York (1985)

141. N. Adrova, M. Bessnov, L. Laivis and A. Radakov, *Polyimides: A new Class of Thermally Stab. Polym.*, Techonic Pub. Co., Stamford, CT (1970)

142. M. T. Bogert and R. R. Renshaw, *J. Amer. Chem. Soc.*, 30, 1135 (1980)

143. L. W. Frost and I. Kesse, *J. Appli. Polym. Sci.*, 8, 1039 (1964)

144. R. J. Angle, *U. S. Patent 3282898* (1966)

145. F. G. Gay and C. E. Bert, *J. Polym. Sci.*, 6 1935 (1968)

146. V. L. Bell, *U. S. Patent 4094862* (1978)

147. P. M. Hergenrother and S. J. Havens, *J. Polym. Sci.*, A27, 1161 (1989)

148. A. K. St. Clair and T. L. St. Clair in *Polym. for High Tech. Elect. and Photonics*, M. J. Bowden and S. Turner, ed., ACS 437 (1987)

149. F. E. Rogers, *U. S. Patent 3356648* (1967)

150. H. D. Burks, T. L. St. Clair and D. J. Progar, *in Rec. Adv. in Polyimide Sci. and Tech.*, D. W. Weber and M. R. Gupta, ed., SPE, 150 (1987)

151. R. H. Bott, J. D. Summer, C. A. Arnold, L. T. Taylor, T. C. Ward and J. E. McGrath, *SAMPE J.*, July/August (1987)

152. J. D. Summer, *Ph.D. Dissertation*, VPI & SU, Blacksburg, VA (1988)

153. C. A. Arnold, *Ph.D. Dissertation*, VPI & SU, Blackburg, VA (1989)

154. S. Maudgal and T. L. St. Clair, *Int. J. Adhesion and Adhesives*, 4(2), 87 (1984)

155. T. Takakoshi, *Advanced Polymer Sci.*, 94 (1990)

156. C.A. Arnold, J.D. Summer, Y.P. Chen, T.H. Yoon, B.E. McGrath, D. Chen and J. E. McGrath, *Polyimide: Mat., Chem. & Char.*, Elsevier (1989)

157. T. H. Yoon, C. A. Arnold and J. E. McGrath, *SAMPE Symposium*, 35, 1892 (1990)

158. R. O. Waldbauer, M. E. Rogers, C. A. Arnold, G. A. York and J. E. McGrath, *SAMPE Symposium*, 35, 97 (1990)

159. N. Bilow, A. L. Landis, L. J. Miller, *U. S. Patent 3845018* (1974)

160. A. O. Hanky and T. L. St. Clair, *Int. J. Adhesion and Adhesives*, 3(4), 181 (1983)

161. H. R. Lubowitz, *U. S. Patent 3528950* (1970)

162. A. K. St. Clair and T. L. St. Clair, *Int. J. Adhesion and Adhesives*, July, 249 (1981)

163. K. C. Brinker and I. M. Robinson, *U. S. Patent 2895948*, June (1959)

164. H. A. Bogel and C. S. Marvel, *J. Polym. Sci.*, 50, 511 (1961)

165. D. J. Progar, T. L. St. Clair and H. Burks, *SAMPE J.*, Jan/Feb, 53 (1990)

166. R. M. Baucon and J. M. Marchello, *SAMPE Q.*, July, 14 (1990)

167. D. Hull, *An Intro. to Composite Materials*, Cambridge Univ. Press (1981)

168. K. K. Chawla, *Composite Materials*, Spinger-Verlag, New York (1987)

169. F. P. Gerstle, Jr., *Composite in Encyclopedia of Polym. Sci. & Eng.*, John Wiley & Sons, V3, 776 (1985)

170. G. S. Deutsch, *SAMPE Symposium*, 23, 34 (1978)

171. R. J. Diefendorf, W. C. Stevens and S. H. Chen, *Fiber Producers*, 16 (1979)

172. R. J. Diefendorf and E. Tokarsky, *Polym. Eng. & Sci.*, 15, 150 (1975)

173. A. Shindo, Rep. Osaka, *Ind. Res. Insti.*, No317 (1961)

174. L. K. English, *Mater. Eng.*, 102, 32 (1985)

175. H. Stenzenberger, *Bismaleimides in Struct. Adhesives*, A. J. Kinloch, ed., Elsevier, New York, p77 (1986)

176. S. Y. Wu and A. M. Schuler, *19th SAMPE Tech. Conf.*, 277 (1987)

177. S. Y. Wu, *SAMPE Symposium*, 35, 846 (1990)

178. B. R. Strohmeier, *J. Vac. Sci. Tech.*, A7, 3228 (1989)

179. J. R. Hollaban and A. T. Bell, *Tech. and Appl. of Plasma Chemistry*, John Wiley & Sons, New York (1974)

180. T. Kasemura, S. Ozawa and K. Hattori, *J. Adhesion*, 33, 34 (1990)

181. H. Gleich, R. M. Criens, H. G. Mosle and U. Leute, *Int. J. Adhesion and Adhesives*, 9(2), 88 (1989)

182. J. R. Vinson, *Polym. Eng. & Sci.*, 29(19), 1325 (1989)

183. J. R. Vinson, *Polym. Eng. & Sci.*, 29(19), 1332 (1989)

184. V. K. Stokes, *Polym. Eng. & Sci.*, 29(19), 1310 (1989)

185. R. P. Wool, B. L. Yuan and O. J. McGarel, *Polym. Eng. & Sci.*, 29(19), 1340 (1989)

186. M. N. Watson and M. G. Murch, *Polym. Eng. & SCi.*, 29(19), 1382 (1989)

187. A. B. Strong, D. P. Johnson and B. A. Johnson, *SAMPE Q.*, Jan., 38 (1990)

188. J. Barksdale, *Titanium, its Occurrence, Chem. and Tech.*, Ronald Press, New York (1966)

189. G. Lutjering, U. Zwicker and W. Bunk, *Titanium: Science & Tech.*, Deutsche Gesellschaft fur Metallkunde, Germany (1985)

190. H. E. Boyer and T. L. Gall, ed., *Metals Handbook*, ASM, 9th ed., V3, 353 (1989)

191. R. A. Wood and R. J. Favor, *Titanium Alloys Handbook*, Metals and Ceramics Information Center (1972)

192. R. M. Brick, A. W. Pense and R. B. Gorden, *Struct. and Prop. of Eng. Materials*, 4th ed., McGraw Hill, New York (1977)

193. K. W. Allen, H. S. Alsalim and W. C. Wake, *J. Adhesion*, 5, 153 (1974)

194. A. Mahoon, *Titanium Adherends, Durability of Struct. Adhes.*, A. J. Kinloch, ed., Applied Sci. Pub., New York, 255 (1983)

195. H. M. Cerafield, D. K. Shaffer, S. L. Vandoren and J. S. Ahearn, *J. Adhesion*, 29, 81 (1989)

196. D. P. Peters, E. A. Ledbury, C. L. Hendricks and A. G. Miller, *SAMPE Symposium*, 27, 940 (1982)

197. J. D. Venables, *J. Mater. Sci.*, 19, 2431 (1984)

198. A. C. Kennedy, R. Kohler and P. Poole, *Int. J. Adhesion and Adhesives*, 3, 133 (1983)

199. J. A. Filbey, J. P. Wightman and D. J. Progar, *J. Adhesion*, 20, 283 (1987)

200. J. L. Cotter and A. Mahoon, *Int. J. Adhesion and Adhesives*, 2, 47 (1982)

201. D. J. Progar, *J. Adhesion Sci. Tech.*, 1, 135 (1987)

202. J. D. Venables, *Applied Surface Sci.*, 3, 88 (1979)

203. B. M. Ditchek, *SAMPE Symposium*, 25, 12 (1980)

204. J. A. Filbey and J. P. Wightman, *J. Adhesion*, 28, 1 (1989)

205. K. W. Allen, S. H. Alsalin, *J. Adhesion*, 6, 229 (1974)

206. C. Matz, *Int. J. Adhesion and Adhesives*, 8(1), 17 (1988)

207. M. Natan and J. D. Venables, *J. Adhesion*, 15, 125 (1983)

208. *Structural Adhesives*, National Materials Advisory Board ed., Marcel Dekker Inc., New York, 40 (1976)

209. J. W. Verbicky, Jr., Polyimides, *Encyclopedia of Polymer Sci. and Eng.*, V12, John Wiley & Sons, New York, 364 (1985)

210. J. E. McGrath, P. M. Sormani, C. S. Elsbernd, S. Kilic, *Makromol. Chem., Macromol. Symp.*, 6, 67 (1986)

211. D. D. Perrin, W. L. F. Armarego and D. R. Perrin, *Purification of Laboratory Chemicals*, Pergamon Press, New York (1980)

212. G. Odian, *Principles of Polymerization*, 2nd ed., John Wiley & Son, New York, 113 (1981)

213. J. D. Summer, C. A. Arnold, R. H. Bott, L. T. Taylor, T. C. Ward and J. E. McGrath, *SAMPE Sympo.*, 32, 613 (1987)

214. J. D. Summer and J. E. McGrath, *Polym. Prep.*, 28(2), 230 (1987)

215. E. S. Moyer, *Ph.D. Dissertation*, VPI & SU, Blacksburg, VA 91989)

216. T. Tsuji, M. Masuoka dn K. Nakao, *in Adhesion and Adsorption of Polymers*, L. H. Lee ed., Plenum Pub., New York (1980)

217. J. C. Hedrick, C. A. Arnold and J. E. McGrath, *SAMPE Symp./Exhibition*, 35, 82 (1990)

218. R. S. Farinato, S. S. Kaminski and J. L. Courter, *13th Adhesion Society Annual Meeting*, Savannah, GA, Feb. 18-21 (1990)

219. D. Broek, *Elementary Engineering Fracture Mechanics*, Martin Nijhoff Pub., Boston, p232 (1987)

220. R. D. Adams and J. A. Harris, *Int. J. Adhesion and Adhesives*, 7(2) 69 (1987)

221. R. O. Waldbauer, M. E. Rogers, C. A. Arnold, G. A. York, Y. Kim and J. E. McGrath, *Polymer Preprint*, 31(2), 432, (1990)

222. G. A. York, R. O. Waldbauer, C. A. Arnold, M. E. Rogers, and J. E. McGrath, *SAMPE Symposium*, 35(1), 579, (1990)

Appendix A. Complexity of adhesive bond formation using ill-defined polyimides

As is well understood, the molecular weight control with non reactive end groups is carried out to afford true thermoplastic polyimides with good processabilities as well as good mechanical properties by preventing or minimizing the chain extension reactions which could occur during the processing. However, the importance of molecular weight control with non reactive end groups was not appreciated until recently. Thus, most investigators utilized either polyimides from 1:1 stoichometric reaction or those from off-stoichiometric reaction to afford controlled molecular weight, but with reactive end groups.

In the early stage of this research, the importance of molecular weight control with non reactive end groups was not appreciated. Thus, the polyimides from 1:1 stoichiometric reaction were utilized for the adhesion study with Ti-6Al-4V alloys and soon we realized processing difficulties, which led to development of new techiques such as molecular weight control with non reactive end groups. This approach together with solution imidization and siloxane in-

corporation resulted in highly processable true thermoplastic polyimides. Therefore, an attempt has been made to describe the how ill-defined polyimide systems affect the adhesive bond strength.

The polyimides utilized in preliminary investigation were prepared from BTDA and m-DDS and sometimes additional siloxane oligomers (1550 g/mole). All synthetic reactions were carried out in 1:1 stoichiometric balance. As expected, polyimides exhibited high Tg and moderate intrinsic viscosity, but relatively low adhesive bond strength as shown in Table 24. The low adhesive bond strength of homopolyimides is possibly due to the poor processability and poor ductility resulted from the chain extension reaction (or reactions) during bonding process and film preparation. However, the siloxane copolyimides of 10 and 20 wt.% siloxane exhibited also relatively low adhesive bond strength, which certainly indicates that the chain extension reaction had occured during bonding and/or compression molding. Another strong evidence of chain extension reaction was insolubility of polyimides in NMP solvent after compression molding. Even polyimides isolated and dried in a vacuum oven at 150 °C for over night exhibited only marginal solubility in NMP. Another supporting evidence of chain extension reaction is obtained from high temperatrue aging study, which demonstrated that aging at 200 °C reduced the adhesive bond strength at 200 °C. The possible explanation is that the aging promoted chain extension reaction, resulting in highly brittle adhesive and thus lowered adhesive bond strength.

The unsatisfactory adhesive bond strength of polyimdes inspired our group to develop new techniques such as molecular weight control with non reactive end groups to afford true thermoplastic polyimides.

Table 24. Characteristics and adhesive bond strength of ill-defined polyimide adhesives

Polyimide	[η]	Tg (°C)	Adhesive Bond Strength (psi) R.T.	200 °C
Homopolymer	0.35	262	1825	3772
10% Copolymer	0.46	247	2603	3683
20% Copolymer	0.44	228	3403	3223

Vita

Tae-Ho Yoon was born in Chung Nam, Korea on September 16, 1957. He graduated from Chung Nam National University in Dae-Jeon, Korea, in February 1980 where he earned his B.S. degree in Metallurgical Engineering.

After serving as a lieutenant in the Korea Army for three years, he came to Virginia Polytechnic Institute and State University in January, 1985 for his graduate study. He completed his master's degree in Materials Engineering in July, 1987.

During his Ph.D. work under the supervision of Dr. James E. McGrath, he married Regina H. Kim in August, 1988, and became a father of Peter Yoon in April, 1991.

Tae-Ho Yoon